Arenberg Doctoral School for Science, Engineering and Technology
Faculty of Engineering Science
Department of Architecture
Architectural Engineering Division
Kasteelpark Arenberg 1 box 2430, 3001 Heverlee, Belgium
www.architectuur.kuleuven.be
www.website.kuleuven.be

Tam NGUYEN VAN

KU LEUVEN

ARENBERG DOCTORAL SCHOOL
FACULTY OF ENGINEERING SCIENCE

MANAGING COST AND QUALITY OF LARGE SCALE HOUSING PROJECTS

Managing Cost and Quality of Large Scale Housing Projects

Tam NGUYEN VAN

Promoters:
Prof. Dr. ir .arch. Frank De Troyer
Prof. Dr. Nguyen Hieu Trung

Dissertation presented in partial fulfilment of the requirements for the degree of Doctor of Engineering Science (PhD): Architecture

November 2017

NOVEMBER 2017

MANAGING COST AND QUALITY OF LARGE SCALE HOUSING PROJECTS

Tam NGUYEN VAN

Promoter:
Prof. Dr. ir. arch. Frank De Troyer

Co-promoter:
Prof. Dr. Nguyen Hieu Trung

Examination Committee:

Prof. Dr. ir. Jean Berlamont
Prof. Dr. ir .arch. Frank De Troyer
Prof. Dr. Nguyen Hieu Trung
Prof. Dr. ir. arch. Bruno De Meulder
Prof. Dr. Ma. arch. Kelly Shannon
Prof. Dr. ir. arch. Mattias Schevenels
Prof. Dr. Ir. arch. Sigrid Reiter

Dissertation presented in partial fulfilment of the requirements for the degree of Doctor of Engineering Science (PhD): Architecture

November 2017

Doctoraatsproefschrift aan de faculteit Ingenieurswetenschappen van de K.U.Leuven

Uitgegeven in eigen beheer, Tam Nguyen Van, Arenberg Doctoraatsschool, W. de Croylaan 6, 3001 Heverlee, België

PREFACE

First of all, I am grateful to all the jury members for revising this dissertation and providing valuable comments and corrections to improve the thesis. Their knowledge on different specific aspects of the integrated research was crucial to attain the final results.

To my promoter, Prof. Frank De Troyer, I would like to express my deepest gratitude for his endless patience and enthusiasm along with his motivation during my studies.I am grateful for sharing his knowledge and experience with me. I thank Prof.F. De Troyer, for his daily advice, support and friendship. To my co-promoter, Prof.Nguyen Hieu Trung, I would like to thank for giving me ideas and comments related to urban planning knowledge and supporting data from Vietnam.

I would like to thank my assessors, Prof. Kelly Shannon and Prof. Bruno De Meulder, for giving fantastic ideas and comments on my research from the beginning. They were willing to provide knowledge related to Vietnam situation. Special thanks to Prof. Kelly Shannon for recommending me to do PhD research at KU Leuven.

I would like to thank the Department of Architecture, Urbanism and Planning (ASRO) for giving me opportunities to do this research. Financial support from the Vietnamese Government, working facilities at KU Leuven and finance from promoter's research projects are gratefully acknowledged.

Many thanks to all my colleagues for great atmosphere and the inspiring discussions. To Prof. Karen Allacker, Damien and Ayu, thank you for your collaboration during my research. My special thanks to Dr. Nguyen Anh Tuan, Faculty of Architecture, Danang University of Technology, who kindly gave many instructions of GenOpt for optimization.

And last but not least, I would like to thank my family and friends. My wife, Hong Giang always brings the sunshine to me in difficult moments. She always keeps a warm family atmosphere. I thank my sons, Hien Nhan and Tri Nhan, you effort a lot at school with new language, Dutch. The daily grown-up and laughter of sons are also my motivation to overcome big challenges in Leuven.

CONTENTS

PREFACE i

CONTENTS iii

ABSTRACT ii

SAMENVATTING iii

LIST OF ACRONYMS ix

CHAPTER 1 INTRODUCTION 1

CHAPTER 1 INTRODUCTION 1

1.1 Background 3

1.2 Housing issues in Vietnam 4
1.2.1 Fast industrialisation 4
1.2.2 Rural urban migration and population growth 4
1.2.3 Two housing processes: large scale housing projects (LSHP) and small scale individual developments 5
1.2.4 Repetition of types 6
1.2.5 Identifying problems 6

1.3 Requirement of simple tools for early design stages 7

1.4 Research Objectives 8
1.4.1 General Objectives 8
1.4.2 Specific objectives 8

1.5 Research questions 9

1.6 Research hypotheses 10

1.7 Outline of the research 10

CHAPTER 2 STUDY AREAS 13
2.1 Introduction 15
2.2 Economic and demographic evolution 15
2.2.1 GDP per capita of Vietnam 15
2.2.2 Population growth 16
2.2.3 Rural – urban migration 16
2.2.4 Family size 18
2.2.5 Development pools (schooling, job opportunities and the supply of goods and services) 19
2.2.6 Public private partnerships for housing projects 20
2.3 Natural context (Cantho City but similar throughout the entire region) 21

2.3.1 Foundation: sedimentation in the river 21
2.3.2 Climate: temperature, relative humidity, solar radiation and wind 22
2.4 Cantho's housing context 32
2.4.1 Rural types 32
2.4.2 Small scale individual developments: apartments, terraced, detached 33
2.4.3 Large scale housing projects 35
2.4.4 Urban forms 36
2.4.5 Materials and technologies for buildings 37
2.4.6 Street types, squares and public life 37
2.5 Cut and fill and river sand for sustainable urban development 38

CHAPTER 3 METHODOLOGY 41

3.1 Introduction 43

3.2 The element method for cost control 44

3.3 Life cycle costing (LCC) 46
3.3.1 General description of life cycle costing 46
3.3.2 Discount rate 47
3.3.3 Inflation rate 47
3.3.4 Nominal versus real discount rate 48
3.3.5 Growth rate 48

3.4 Multi-objective optimization model: Pareto front in case of multi-objectives 49

3.5 Latin Hypercube Sampling method to select design options for sensitivity 49

3.6 Sensitivity analysis and selecting a sensitivity analysis method 50
3.6.1 Sensitivity analysis 50
3.6.2 Selecting a sensitivity analysis method this study 52

CHAPTER 4 SIMPLE MODELS FOR PREDESIGN PHASE OF LARGE SCALE HOUSING PROJECTS 55

4.1 Large scale housing projects 57
4.1.1 Hierarchy of design decision processes in large scale housing projects 57
4.1.2 Street pattern and technological solutions 58

4.2 Typologies abstracted from observed developments 60

4.3 Illustration of model approach of the different types 63
4.3.1 Terraced house 63
4.3.2 Apartment 67
4.3.3 Detached house 69
4.3.4 Greens, water areas and filling soil 72

4.4 Typical materials and technologies 74

4.5 Conclusions 74

CHAPTER 5 FOUNDATION COST 77

5.1 Introduction 79

5.2 Foundation types 80
5.2.1 Shallow and small wood piles 80
5.2.2 Small pile 81
5.2.3 Large pile 81

5.3 Assumptions and Standards 82
5.3.1 Building height 82
5.3.2 Soil properties 83
5.3.3 Building layout 83
5.3.4 Pile foundation approach 83
5.3.5 Input parameters 84

5.4 Analysis of methodology 84
5.4.1 Optimal cost per ton capacity of pile foundations 85
5.4.2 Fundamental frequency (building period) 87
5.4.3 Loads upon foundation 89
5.4.4 Correction factor to shear lag effect of the reinforced concrete rigid frame 97

5.5 Results and Analysis 100
5.5.1 Cost optimal piles for five locations at Cantho 100
5.5.2 Wind load as a function of building height 101
5.5.3 Seismic load as a function of building height 103
5.5.4 Lateral loads transfer to pile foundations 104
5.5.5 Foundation cost integrated with building height and land costs 105

5.6 Sensitivity analysis 107

5.7 Parameter study and rules of thumb 108

5.8 Conclusions 109

CHAPTER 6 MARKET VALUE 113

6.1 Introduction 115

6.2 Literature review 115
6.2.1 The problem of location and land 115
6.2.2 Housing preferences 116

6.3 Conceptual model 116
6.3.1 Diminishing marginal utility functions of housing preferences 116
6.3.2 Multi-Attribute Utility theory 116
6.3.3 Overview of approach 119

6.4 Data collection methods (Deriving preferences from the web data and test for small scale plot) 119
6.4.1 Data source selecting 119
6.4.2 Data collection 120

6.5 Attribute selection 121

6.6 Developed tool for capturing information 121
6.6.1 Explicitly reported parameters 121
6.6.2 Multiple exponential regression analysis 122

6.7 Deriving utility functions 123

6.8 Deriving visual conclusion for stakeholders 124
6.8.1 Visual reference information to make decision for designer 124
6.8.2 Visual reference information to make decision for developers 126
6.8.3 Visual reference information to make decision for customers or users 127
6.8.4 Visual reference information to make decision for policy makers 127

6.9 Sensitivity analysis 128

6.10 Conclusions 129

CHAPTER 7 COMFORT AND COSTS 133

7.1 Introduction 135

7.2 Thermal comfort in built environments 135

7.3 Predicted Mean Vote (PMV) and Adaptive Thermal Comfort (ATC) approach 136
7.3.1 Predicted Mean Vote (PMV) approach 136
7.3.2 Adaptive Thermal Comfort (ATC) 137

7.4 Dynamic heat balance of the EnergyPlus simulation tool 138
7.4.1 Heat balance 138
7.4.2 Building energy simulation programs and EnergyPlus 139

7.5 Multi-zone Airflow Network model 140

7.6 Surrogate models to obtain the wind pressure coefficient (Cp) 140
7.6.1 Surrogate models 140
7.6.2 Wind pressure coefficient (Cp) 141
7.6.3 Cp meta-model based on Cp Generator TNO for terraced houses 143
7.6.4 Meta-model Cp based on the meta-model Cp of M. Grosso for a detached house and apartment 154
7.6.5 Cp values based on Grosso's model for detached and Semi-detached house 156
7.6.6 Approximation formulas to calculate wind pressure coefficients (detached and Semi-detached house) 157
7.6.7 Approximation formulas to calculate wind pressure coefficients (Apartment) 159

7.7 Strategies for comfort (dynamic schedule and user behaviour) 162
7.7.1 Comfort evaluation and strategy based on dynamic schedules for ventilation and cooling 162
7.7.2 Strategy based on dynamic schedules for ventilation and cooling 162

7.8 Life Cycle Cost: Parameters in EnergyPlus 163

7.9 Urban forms, geometry and materials of housing types 164
7.9.1 Terraced house geometry 164
7.9.2 Detached house geometry 165
7.9.3 Apartment geometry 166
7.9.4 General options for material 167

7.10 Results and discussions 167
7.10.1 Case study for terraced house: Varying all selected parameters with fixed building North 167
7.10.2 Energy consumption in case of different orientations for terraced house 169
7.10.3 Case study for detached house: Varying all selected parameters 171
7.10.4 Case study for apartment unit at the middle of the building 174
7.10.5 Case study for apartment unit at bottom, middle and top of building 177

7.11 Rules of thumb for design 179

7.12 Conclusions 179

CHAPTER 8 OPTIMISATION OF PASSIVE DESIGN FOR THERMAL COMFORT IN A HOT AND HUMID CLIMATE 183

8.1 Selection of optimization method 186
8.1.1 Exponential growth of optimization methods 186
8.1.2 Optimization programs selected for energy use and life cycle cost of buildings 186
8.1.3 Concepts behind optimization algorithms 187

8.2 The integration of the sub models 195
8.2.1 Links between models 195
8.2.2 Optimization algorithm setting 197
8.2.3 Optimization process 198

8.3 A graphical post processing of the simulation results 199
8.3.1 Pareto front in case of life cycle cost and initial cost 199
8.3.2 Parallel Coordinates 199

8.4 Results of optimisation 200
8.4.1 Terraced houses: Parameters, Results and Discussions 200
8.4.2 Detached house: Parameters, results and discussions 212
8.4.3 Apartment: Parameters, Results and discussions 223

8.5 Comparison of the three housing types 232
8.5.1 Comparison including land and infrastructure 232
8.5.2 Comparison without land and infrastructure 232
8.5.3 Comparison of energy use of three housing types 233

8.5.4 Energy use for fans and cooling depending on acceptable PMV levels 234
8.5.5 Overhang, urban layout and orientations 235

8.6 Findings throughout three housing types 236

8.7 Conclusions regarding the methodology 237

CHAPTER 9 CONCLUSIONS AND FURTHER RESEARCH 241

9.1 Original contributions of the thesis 243
9.1.1 Integration of sub models for cost and quality 243
9.1.2 Model for cost-optimal-pile foundations 243
9.1.3 Model predicting market value 244
9.1.4 Model predicting energy consumption 244
9.1.5 Model for life cycle costing including cost optimisation 245

9.2 Limitations of the models in this thesis 245
9.2.1 Limited integration of quality aspects 245
9.2.2 Limited to column and beam structures 245
9.2.3 Limitation of the thermal comfort model 246
9.2.4 Limitation of objective function 246
9.2.5 Future work 246

APPENDIX A 247

APPENDIX B 253

LIST OF TABLES AND FIGGURES 267

PUBLICATIONS 279

Abstract

The economic development, the population growth and the rural-urban migration create a huge demand on the Vietnamese housing market. At the same moment there is a growing purchasing power, but proposals have to be elaborated within strict budget constraints. Developers, avoiding risks and striving to maximize profit, supply in most cases very stereotype units. The government would like to stimulate the development of the housing stock in a sustainable way but has limited resources.

The basic aim of this research is to develop a simulation tool that is adaptable to specific requirements and expandable in order to come to a win-win-win situation: better quality for end users within budget, opportunities to implement a social policy and reasonable profits required for mobilising private funding.

The starting point is the element method for cost control from sketch design to detailed design. The method is expanded in three ways: (1) better estimating from the first sketch on of land cost and costs for pile foundation for high-rise building in soft soil condition of the Mekong delta, (2) taking into account preferences of end users (renters or buyers) derived in a semi-automatic way from selected internet advertising (3) achieving thermal and light comfort via decision on different scale levels from urban clustering and orientation, over building layout up to material selection. For this last point two original contributions are elaborated: (a) the development of a surrogate model for predicting pressure coefficients (Cp) used to estimate air flow exchange via natural ventilation. (b) the implementation of an “Energy Management System” (EMS) to simulate, via a dynamic modelling, the occupant behaviour to minimize energy use as much as possible with passive means. In a final step the optimization process of life cycle costs is elaborated by coupling a general optimisation software (“GenOpt”) with dynamic energy and light simulations (“EnergyPlus”) linked to the meta model for estimating costs of pile foundation for high rise buildings in soft soil conditions. The graphical representations of the results of the optimisation can support in the early design phase developers, designers, users and policy makers to come to better solutions.

Due to the modular implementation, in the future many expansions are possible: other climatic contexts, new soil conditions, different economic price levels and predictions, urban and dwelling typologies from another culture, other registered preferences, etc.

Samenvatting

De economische ontwikkeling, de bevolkingsgroei en de migratie naar de steden heeft een grote vraag gecreëerd op de Vietnamese woningmarkt. Op hetzelfde ogenblik is er een groeiende koopkracht, maar voorstellen moeten uitgewerkt worden binnen strikte budgetbeperkingen. Projectontwikkelaars, risikoschuw en op zoek naar winst, leveren meestal erg steriotype wooneenheden. De overheid wil graag de evolutie in een meer duurzame richting stimuleren, maar beschikt over beperkte middelen.

Het fundamentele doel van dit onderzoek is om een simulatietool te ontwikkelen aanpasbaar aan specifieke noden en uitbreidbaar om te komen tot een win-win-win situatie: betere kwalteit voor eindgebruikers binnen hun budget, mogelijkheden om een sociale politiek uit te werken en aanvaardbare winsten om privee middelen te mobiliseren.

Startpunt is de elementenmethode om bouwkosten te beheersen van schetsontwerp to gedetailleerd ontwerp. De methode is verder aangevuld in drie richtingen: (1) beter schatten van kosten voor grondverwerving en paalfunderingen in de alluviale gronden van de Mekong delta vanaf de eerste schetsen, (2) rekening houden met voorkeuren van eindgebruikers (huurders en kopers) afgeleid van webaankondigingen in een semi-automatische procedure, (3) bereiken van thermisch en visueel comfort via beslissingen op verschillende schaalniveaus gaande van stedelijke schakelingen en oriëntatie, over gebouw lay-out tot keuze van materialen. Wat dit laatste punt betreft werden er twee originele bijdragen geleverd: (a) de ontwikkeling van een metamodel om drukcoëfficiënten te voorspellen (Cp) gebruikt om natuurlijke ventilatie te schatten, (b) het implementeren van een “Energie Management Systeem” (EMS) om, via dynamisch modelleren, het gebruikersgedrag te simuleren om energieverbruik te minimaliseren door zo veel mogelijk passieve middelen te gebruiken. In een laatste stap werden een optimalisatie procedure uitgewerkt voor levenscycluskosten door algemene optimalisatiesofrware (“GenOpt”) te linken met dynamische energie- en lichtberekeningen met inbegrip van het metamodel voor kostenschatting van paalfunderingen voor hoogbouw in een alluviale vlakte. De grafische voorstelling van de resultaten van het optimalisatieproces kan in de vroege ontwerpfase projectontwikkelaars, ontwerpers, gebruikers en beleidmakers ondersteunen om tot betere beslissingen te komen.

Door de modulaire aanpak zij meerder doorontwikkelingen in de toekomst mogelijk: ander klimaatomstandigheden, andere bodemkenmerken, ander prijsniveaus en kostenvoorspellingen, andere stedelijke- en woontypologieën, andere geregistreerde voorkeuren, …

LIST OF ACRONYMS

ATC	Adaptive thermal comfort
Cp	Wind pressure coefficient value
CPT	Cone penetration test
EC	Energy cost
EMS	Energy management system in EnergyPlus software
FC	Foundation cost
GDP	Gross domestic product
IC	Initial construction cost
LCC	Life cycle cost
LSHP	Large scale housing project
OPC	Operational cost: Energy cost and maintenance cost
PAD	Plan area density or building density in urban area
PMV	Predicted mean vote, thermal comfort
PP	Purchasing power
PPD	Predicted Percentage of Dissatisfied
PPP	Public private partnership
PV	Present value
SA	Sensitivity analysis
SPT	Standards penetration test
SRC	Standardized regression coefficient
TMY	Typical Meteorological Year
WLA	Whole life appraisal

CHAPTER 1 INTRODUCTION

Table of Contents

1.1	**Background**	**3**
1.2	**Housing issues in Vietnam**	**4**
1.2.1	Fast industrialisation	4
1.2.2	Rural urban migration and population growth	4
1.2.3	Two housing processes: large scale housing projects (LSHP) and small scale individual developments	5
1.2.4	Repetition of types	6
1.2.5	Identifying problems	6
1.3	**Requirement of simple tools for early design stages**	**7**
1.4	**Research Objectives**	**8**
1.4.1	General Objectives	8
1.4.2	Specific objectives	8
1.5	**Research questions**	**9**
1.6	**Research hypotheses**	**10**
1.7	**Outline of the research**	**10**

1.1 Background

Cost estimation in housing projects can be divided into initial cost (IC) and life cycle cost (LCC). LCC includes initial, maintenance and operational cost. In most cases the initial cost can be estimated during the early design phase to detail design phase. In order to estimate the operational cost designers need to develop building performance simulations to estimate energy and maintenance cost. Physical characteristics of the dwelling units, user behaviour and local climate are significant input parameters that are integrated in the building performance models. In addition, soil condition, wind and seismic properties together with building layout impact on cost of foundation and structure elements. Hence, such aspects should be considered at the early design phases.

Housing quality is a complicated issue and related to different expectations such as culture, local climate and income level. Housing quality criteria system can be different to meet the demands of different organizations such as governmental departments, agencies or future inhabitants. Good quality housing requires adequate hydrothermal and acoustic behaviour, structural durability, basic infrastructure systems, pleasant environment and accessibility to workplaces [1] [2] [3]. As a consequence, housing quality is the result of choices on different levels: from material scale over construction elements up to neighbouring level. Some criteria are imposed by design codes, for instance, daylight level, ventilation rate and thermal comfort. These criteria can be used as reference rules for designers.

High industrialization and urbanisation rates generate high pressure on the housing demand and overloaded infrastructure systems. In Vietnam many small and large scale housing projects have been developed to meet the high housing demand. The large scale housing projects combine mostly three housing types: terraced units, detached units, apartments. The housing projects have some problematic characteristics: high housing density, limited green areas, no water areas (ponds, canals, rivers, etc.) as well as no recreational or public spaces. These projects often miss certain qualities: thermal comfort, day light comfort, economic efficiency, social and environmental characteristics. Many urban issues and high energy use for thermal comfort and light are often very difficult to solve in future if certain basic options are fixed. Designers without appropriate engineering tools and profit-oriented developers can play critical roles in the early design phases.

Innovation in building design can involve an engineering approach to architecture and focus upon the technical aspects which include structural systems and building physics at

the building and urban levels. These elements are tackled in a multidisciplinary setting in order to assess and improve the overall performance, sustainability and cost of buildings. Optimization models are tools to solve those issues through an integrated approach. Searching for appropriate design alternatives (considering multiple scales) at the early design phases is often a challenge and comprises an extremely complex and time consuming processing. A model by which to manage cost and quality, using an integrated approach, can be helpful in order to satisfy the profitable, affordable and sustainable goals of stakeholders of large scale housing projects (LSHP).

1.2 Housing issues in Vietnam

1.2.1 Fast industrialisation

Vietnam is a developing country with one of the highest industrialisation rates in the world. The Vietnamese economy experienced a rapid structural transformation, which is reflected in the shift of its sectorial composition and employment. In the year 2000, almost 65.3% of all workers were employed in the field of agriculture. A substantial shift occurred between 2000 and 2007 whereby the industrial sector, provided 19.2% of the employment (Table 1.1).

Table 1.1 Distribution of employment by sector, 2000 - 2007 (%)

Year	2000	2001	2002	2003	2004	2005	2006	2007
Agriculture (%)	65.3	64	62	59.7	57.9	56.7	54.7	52.2
Industry (%)	12.4	13.9	14.7	16.4	17.4	17.9	18.3	19.2
Services (%)	22.3	22.1	23.3	23.9	24.8	25.4	27	28.6
Total (%)	100	100	100	100	100	100	100	100

Source: Ministry of Labour-Invalids and Social Affairs: Labour and employment survey (various years).

1.2.2 Rural urban migration and population growth

The jobs and living conditions offered in cities have attracted increasing amounts of young people. They often move from rural areas to urban areas and to the residential areas of industrial zones. In the period between 1999 and 2009, the average population growth rate was 1.2% per annum while urban growth was 3.4% per year and counted only 0.4% per year in rural areas [4]. The increasing housing units generated an overloaded infrastructure systems. The housing demand generated many small and large scale housing projects. Natural and artificial canals have been narrowed or filled with river sand in order to allow for newly built up areas. This has led to an increase in the number of urban floods when heavy rain and high tide coincide. Other consequences of urban migration are the ‘heat island effect’ and the reduction of natural ventilation in recently built urban areas.

1.2.3 Two housing processes: large scale housing projects (LSHP) and small scale individual developments

Apart from the small scale individual housing developments, which are responsible for a great proportion of the supply (Figure 1.1), large scale housing projects are very common in Vietnam (Figure 1.2). The LSHP can provide a large number of housing units but some issues, related to the cost and to the quality, are challenges for developers, designers and users. If the developers are tempted to reduce the quality very significantly in order to reduce initial cost. As consequence, there is a real risk that they will not be able to find a market.

Figure 1.1 Typical Small private housing projects.

Figure 1.2 Typical large scale housing projects in Cantho city.

1.2.4 Repetition of types

Almost all of the large scale housing projects have been developed by private developers either as new projects or as support for resettlement where parts of cities have been reconstructed to improve urban environments. The ubiquitous poor quality, in terms of thermal comfort, high energy use and urban flooding can become very difficult to correct in the long run.

1.2.5 Identifying problems

A characteristic of the Mekong Delta area is a warm/hot, humid climate and "*soft soil conditions*". The cost of buildings' foundations represent a major part of the total construction cost, particularly for middle or high rise buildings. The small residential buildings are usually built without professional consultations. Even worse the large scale housing projects are sometimes developed without appropriate studies being undertaken at all. Developers try to maximize profits, rather than looking into the affordability for its occupants and their reasonable expectations of comfort. The indoor environments can be sub-standard and lead invariably to high energy use which is necessary in order to obtain comfort.

Buildings generate high energy cost, for cooling and lighting, are very common in urban areas. Recently, developers have also introduced the "Tube" house with narrow width and very long depth, in order to reduce infrastructural cost and to maximise the profit. This has come at a significant cost for future residents in terms of their comfort. These characteristics normally are fixed in the early design phase. Consequently, the life cycle cost (LCC) of housing units may increase as a direct outcome of the money saved in initial construction phase. In some cases, the profit returned to the developers results in the passing on of higher operational costs to the users in the long run.

The housing prices are based on the preferences users. They consider the characteristics of buildings which include: location, housing type, urban layout and infrastructure systems. Housing prices are an essential element in generating reasonable profits for developers with respect to both affordability and willingness to pay. Hence, understanding housing preferences and selecting the most appropriate housing type and the urban characteristics becomes significant factors in the early design phases.

1.3 Requirement of simple tools for early design stages

Choices made during the early phases affect strongly the end results [5]. In order to balance cost and quality of housing projects, intuition and experience are not always sufficient for architects and designers to make appropriate decisions. Software tools such as the Building Information Model (BIM) are used more and more to the contribution of architects and engineers, developers, contractors and many more participants in the process.

BIM was defined by international standards as “shared digital representation of physical and functional characteristics of any built object which forms a reliable basis for decisions”, ISO 29481-1:2010(E). BIM is the process of generating and managing digital representations of the building's physical and functional characteristics to facilitate the exchange of information [6]. In the case BIM is used in a process including energy prediction, the central BIM-data model is used for the automatic preparation of the building energy model for various energy simulation tools like: eQUEST, EnergyPlus, TRANSYS, Ecotect and Green Building Studio and Modelica-based tools [7]. In the BIM approach the same model is used to feed different programs to analyse life cycle cost, structural stability or other aspects. Tools are developed to read data from BIM and convert to input files for the energy performance, structure analysis and optimization processes.

In principle it would be possible to build a BIM model to capture geometry and physical characteristics, (1) to send it to a CFD model to calculate wind pressure coefficient, (2) and then send information to a program to do energy calculation with comfort constraints, (3) to do structural calculation (4) to send the information to a cost calculating program doing the life cycle cost and then controlling all these exchanges by a program (5) searching an optimum. Since the geometry is relatively simple for the different schematic layouts in an exploration of sketch design alternatives, it was much simple to organize those exchanges directly.

1.4 Research Objectives

Based on the above, the overall aims of this research are elaborated in the sections which follow and comprise the work's general and specific objectives.

1.4.1 General Objectives

The first research objective is to develop a general and expandable approach for the optimisation of design choices. The second objective concerns testing the models using provisional data. Detailed data acquisition of case-specific-data lies beyond the scope of this thesis.

The global aim of this research is to balance occupant's preferences and life cycle cost (LCC) of dwellings of large scale housing projects at the early design stage. Mekong Delta context in Vietnam is used as a starting point to test tools. In other countries, users should adapt weather data, soil properties and housing typologies. This dissertation cannot, of course, cover all aspects of the housing projects. Instead, it focuses on significant aspects that challenge architects and engineers: soft soil condition, life cycle cost and climate responsive design strategies for thermal and light comfort.

1.4.2 Specific objectives

1.4.2.1 Expandable model based on element method for cost control in the case of large scale housing projects

Flexible models for cost control are elaborated, based on different scales (material, work section, element, building and urban scale) and the applicability to different dwelling types (terraced housing, detached housing, apartment, commercial building) as well as public spaces and infrastructure. Life cycle costing (including inflation and interest) has also been integrated.

1.4.2.2 Foundation cost

The cost model includes the foundation cost in view of the Mekong Delta's soft soil condition. This model can also be applied to different soil conditions. The unit cost per ton capacity (based on the optimal use of piles) and the building's geometry are the major parameters integrated in the model in order to evaluate the cost of the foundation.

1.4.2.3 Market value

Predicting price is another crucial aspect of the modelling which is important to real estate developers in order to assess profitability. Housing preferences are used to derive a regression function for estimating the willingness to pay for residential land and/or dwelling.

1.4.2.4 Comfort and cost

Costs for thermal and light comfort, reaching a defined minimum are integrated into the life cycle cost model. The relationship between multiple levels (from material to building geometries and urban form) are integrated as well as for operational as initial cost.

1.4.2.5 Optimisation

Optimization models, based on fundamental geometrical aspects, will be elaborated in order to apply the process of optimisation from different viewpoints (end users, developers and authorities).

1.5 Research questions

Question 1: Design decisions, in the current manner of operating, are taken in consecutive phases which are as follows: urban planning, global architectural layout and engineering/detailing. How can the element method, help to control the cost on different scale levels and different design phases?

Question 2: How, in soft soil conditions, do the cost of foundation and land price influence the building's overall cost?

Question 3: Is it possible to elaborate a model which would predict the "willingness to pay" for given dwelling units, based on web information concerning the selling price of housing types and their characteristics?

Question 4: How can the cost of energy for residential buildings be minimized, through the use of design alternatives, in a hot and humid climate?

Question 5: Can the result of the aforementioned models ("Cost", "Willingness to pay" and "Comfort") be integrated into an optimization tool to support design decisions in the early phases? Or is it possible, based on detailed simulations, to formulate "design guidelines for sketch design"?

1.6 Research hypotheses

Hypothesis 1: High rise buildings, including foundation cost, can offer affordable housing units in mass housing projects.

Hypothesis 2: "Willingness to pay" for characteristics of housing units, urban patterns and locations are crucial factors and play a key role in the determination of housing prices on the market.

Hypothesis 3: Comfort and cost of energy use, throughout an entire housing service's lifetime, can be evaluated and design decision can be adjusted during the early design stages and in conjunction with the initial construction cost.

Hypothesis 4: Optimisation tools are useful in integrating the planning, architecture and engineering design stages.

1.7 Outline of the research

This dissertation contains nine chapters and each chapter is briefly sketched below.

Chapter 1 describes the research topic, defines its objectives, proposes hypothesises and provides the outline of the dissertation.

Chapter 2 focuses on four aspects of the areas under study. Firstly, the geographic context of Vietnam and Cantho city are briefly explored. Secondly, the economic and demographic evolution is capitulated in order to understand the research areas' situation. Thirdly, the natural context is summarized in terms of its soft soil properties and hot, humid climate. The final part presents common approach to housing, from the building level to the neighbourhood level.

Chapter 3 examines the general contours of the methodology selected for this dissertation which concerns the data collection as well as the cost modelling.

Chapter 4 elaborates a cost model for large scale housing projects which is based on models selected from a variety of cases ranging from detached housing, terraced housing, apartments and public areas. All of these sub-models are structured and begin with the design parameters selected for elements, buildings characteristics and urban layouts which are relevant in the early design stages.

Chapter 5 describes the foundation cost model for pile foundation of mid-rise buildings in soft soil conditions. This model considers the width, depth and height of the buildings, the land cost and the soft soil properties.

Chapter 6 analyses the housing preferences through the use of web data but other data sources have also been used where available.

Chapter 7 analyses the thermal comfort, daylight and natural ventilation. For the model, two sub models are developed in detail: wind pressure coefficients (Cp) prediction and the Energy Management System (EMS), simulating the dynamic behaviour of inhabitants based on experienced thermal comfort.

Chapter 8 proposes and evaluates an optimization tool. This chapter also brings all the sub models together into one model for use in analysing large scale housing projects.

Chapter 9 summarizes the different results this dissertation has uncovered. It also outlines the work's limitations and suggests various avenues for further research.

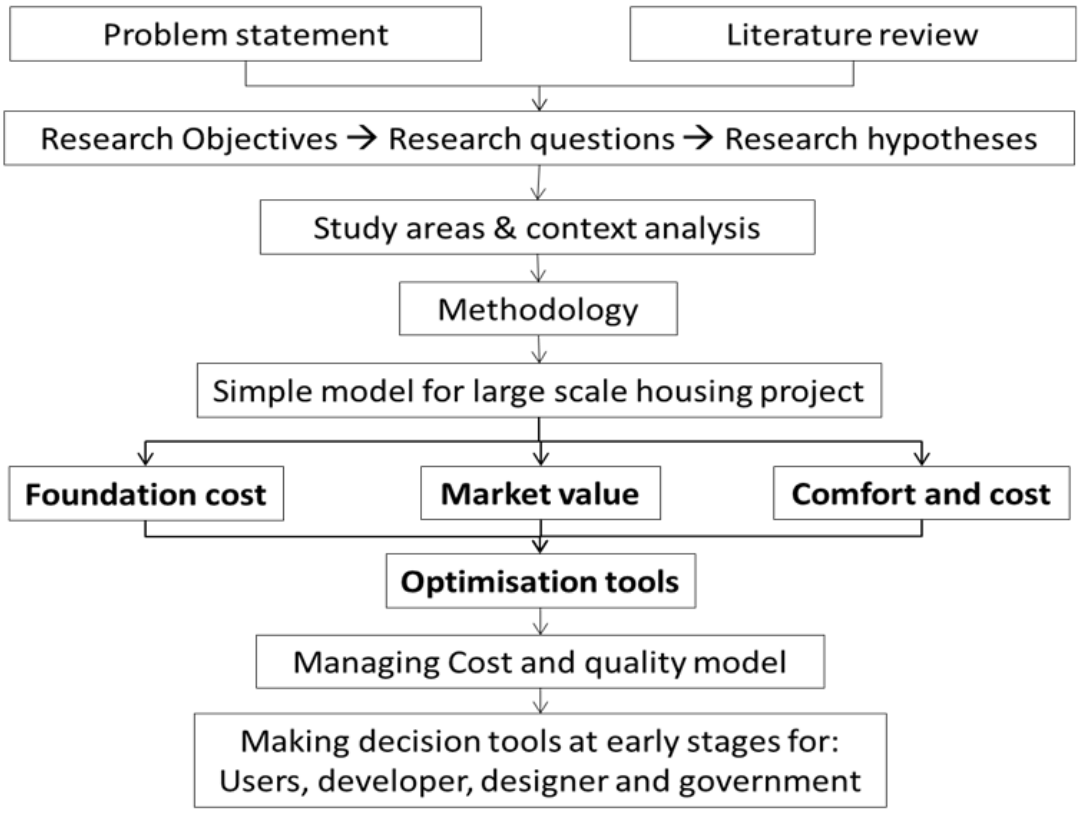

Figure 1.3 The dissertation structure.

REFERENCES

[1] R. Imrie, Accessible Housing: Quality, disability and Design, Taylor & Francis, 2006.

[2] B.J. Franklin, Discourses of Design: Perspectives on the Meaning of Housing Quality and ?Good? Housing Design, Hous. Theory Soc. 18 (2001) 79–92.

[3] M. Cousins, Design quality in new housing: learning from the Netherlands, Taylor & Francis, 2009.

[4] General Statistics Office, Vietnam, Vietnam population and housing census 2009 - Age-Sex Structure and Marital Status of the Population in Vietnam, 2011.

[5] U. Bogenstätter, Prediction and optimization of life-cycle costs in early design, Build. Res. Inf. 28 (2000) 376–386.

[6] C. Eastman, P. Teicholz, R. Sacks, K. Liston, BIM Handbook: A Guide to Building Information Modeling for Owners, Managers, Designers, Engineers, and Contractors, Second Edition, John Wiley & Sons, Inc., Hoboken, New Jersey, 2011.

[7] W. Yan, M. Clayton, J. Haberl, W. Jeong, J.B. Kim, S. Kota, J.L.B. Alcocer, M. Dixit, Interfacing BIM with Building Thermal and Daylighting Modelling, in: 2013: pp. 3521–3528.

CHAPTER 2 STUDY AREAS

This chapter introduces four aspects of the area under examination.

Firstly, a brief introduction of the geographical contexts of Vietnam and Cantho city are described in greater detail.

Secondly, the economic and demographic evolution is briefly pictured.

The third section summarizes the natural context: soft soil properties and hot, humid climate conditions.

The final section concerns the current housing approach and describes at the building level as well as at the neighbourhood level.

Table of Contents

2.1	**Introduction**	**15**
2.2	**Economic and demographic evolution**	**15**
2.2.1	GDP per capita of Vietnam	15
2.2.2	Population growth	16
2.2.3	Rural – urban migration	16
2.2.4	Family size	18
2.2.5	Development pools (schooling, job opportunities and the supply of goods and services)	19
2.2.6	Public private partnerships for housing projects	20
2.3	**Natural context (Cantho City but similar throughout the entire region)**	**21**
2.3.1	Foundation: sedimentation in the river	21
2.3.2	Climate: temperature, relative humidity, solar radiation and wind	22
2.4	**Cantho's housing context**	**32**
2.4.1	Rural types	32
2.4.2	Small scale individual developments: apartments, terraced, detached	33
2.4.3	Large scale housing projects	35
2.4.4	Urban forms	36
2.4.5	Materials and technologies for buildings	37
2.4.6	Street types, squares and public life	37
2.5	**Cut and fill and river sand for sustainable urban development**	**38**

2.1 Introduction

Vietnam is located in Southeast Asia and stretches from 9° to 23° North latitude and 102° to 110° East longitude. The country has 331,212 square kilometres and has 3,200 km coastline. The Vietnamese population has been estimated to be 85.8 million, ranking third in all of Southeast Asia and 13th in the world. Approximately 30% of the population lives in urban areas.

Cantho is located in the centre of the Mekong Delta, has 1,214,000 inhabitants and comprises 1,409 square kilometres. It is quite far from Phnom Penh (200 km), Ho Chi Minh City (169km) and the East Sea (75km). Cantho has the highest density river network in all of Vietnam. The average elevation is about 0.8 to 1.0 meters above sea level. This low elevation means that a great deal of sand is required to lay the foundation for new housing and infrastructure projects to reach the necessary safety level of between 2.5 and 2.7 meters.

2.2 Economic and demographic evolution

2.2.1 GDP per capita of Vietnam

The World Bank estimated the GDP per capita of Vietnam for the year 2012 to be 1,755 US and ranked 57th out of 191 countries. The gross domestic product was 15,582 million US dollars. Over the past 10 years GDP has increased continuously; see Figure 2-1 and has led to the generation of increasingly high rates of housing demand in urban areas throughout Vietnam.

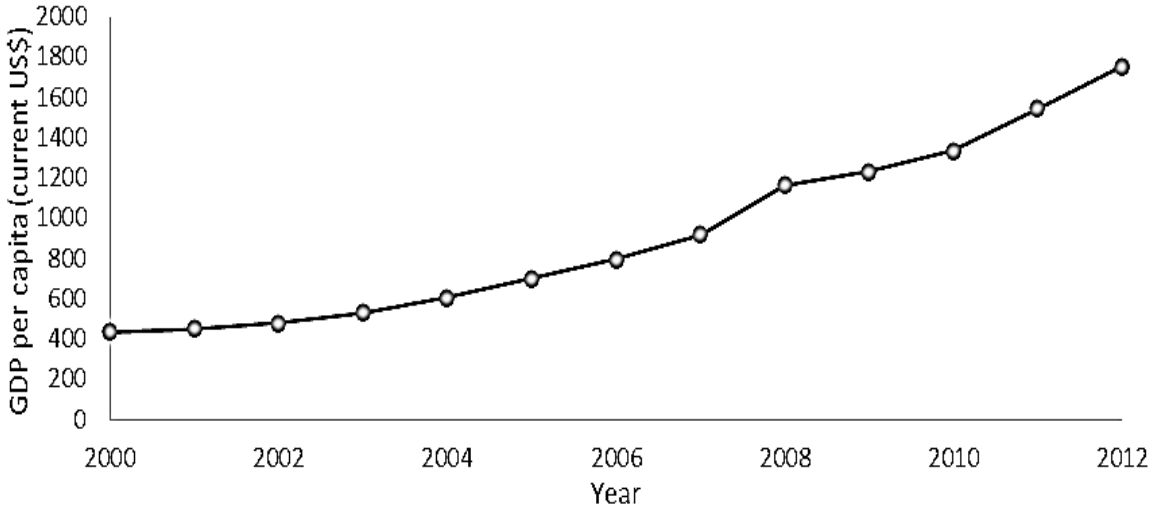

Figure 2-1 GDP per capita (current US$) of Vietnam which has an average growth rate of 13.3%, source of World Bank, 2015).

2.2.2 Population growth

Alongside the increase in GDP, the population increase is another significant factor behind high housing demand, Figure 2-2. In the period between 1999 and 2009, the average population growth rate was 1.2% per annum while urban growth rose at 3.4% per annum and rural growth rose by only 0.4% per annum [1].

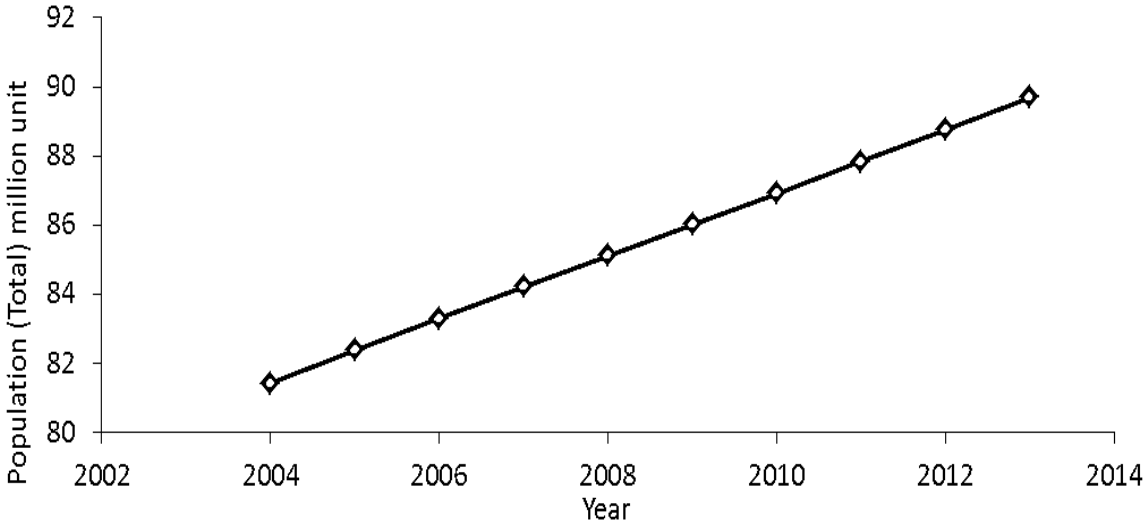

Figure 2-2 Total population of Vietnam. Source: World Bank, 2014.

2.2.3 Rural – urban migration

Jobs and the living conditions in cities have attracted young people from rural areas to urban areas. This increases housing demand and generates an overload of strain upon the infrastructure systems. This process occurs very quickly in the Mekong Delta area; the urbanization process in the Southern area at Cantho city from between 2003 and 2017 as shown in Figure 2-3. The housing demand has generated many small and large scale housing projects. Problematic issues in those projects include high housing density, limited green areas, no ponds, canals or other water surfaces and few or small public spaces. Some large scale housing projects have no educational, commercial or recreational facilities. This new population leads to a heavy burden being placed upon existing infrastructure systems. Natural and artificial canals have been narrowed or filled in with river sand for new built up areas because of their low surface level. Even after the filling was completed it only lead to ranges of between 1 and 1.5 meters above sea level, compared to 2.7 meters which is considered to be the safe level. Other problematic issues the urban environment are the heat island effect as well as natural ventilation reduction.

The development of South Cantho as of 28 August, 2003

The development of South Cantho as of 08 December, 2008

The development in South Cantho as of 23 January, 2017

Figure 2-3 Illustrating the urbanization progress of the South area of Cantho city using Google Earth from 2003 to 2017.

2.2.4 Family size

In Vietnam, households with 4 or fewer members are very common (with an average of 72% throughout the entire country) especially in urban areas where the figure rises to 76% [2], Figure 2-4. The average household size declined drastically from 4.82 people in 1989, to 4.51 people in 1999 and to 3.78 in 2009. This reduction is similar to other rural and urban areas [1], Figure 2-5. Another analysis shows that most Vietnamese families are modest in size, comprising four to six members [3].

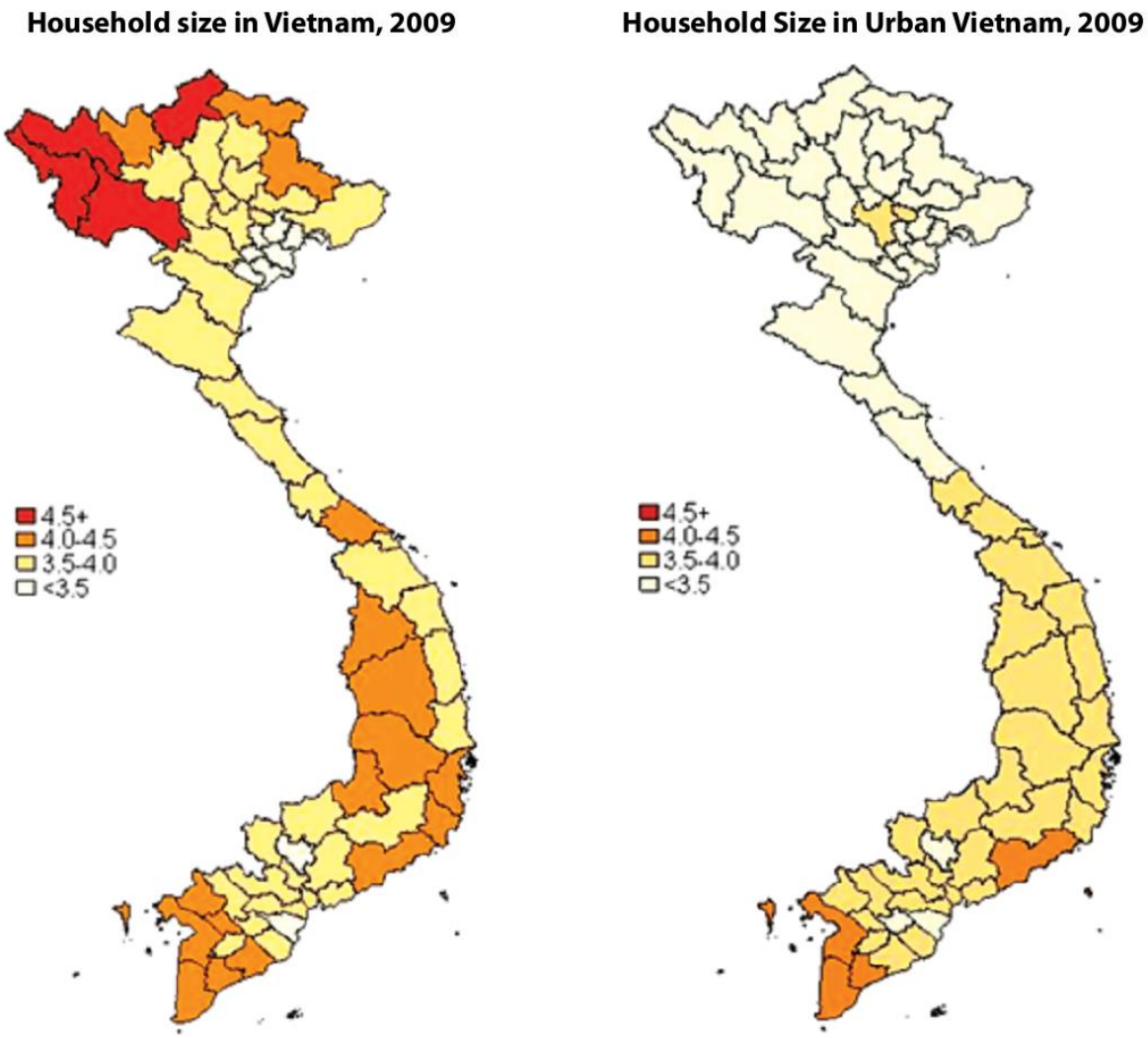

Figure 2-4 Map of household size by province in Vietnam, 2009 [2]

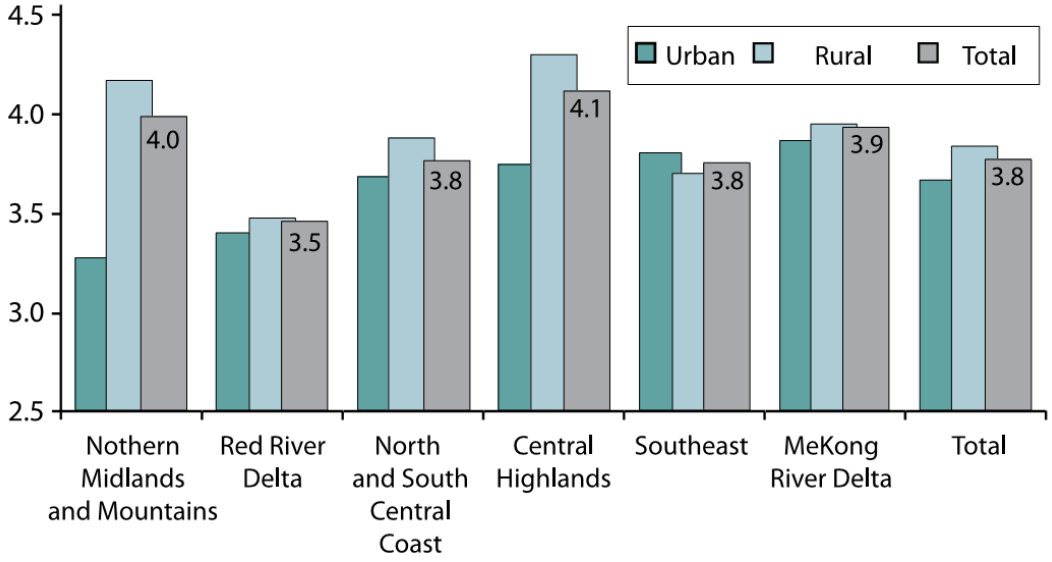

Figure 2-5 Household size by region in Vietnam, 2009, [1]

2.2.5 Development pools (schooling, job opportunities and the supply of goods and services)

Large scale housing projects have generally been developed in conjunction with public and/or private services (school, health care, sport and commercial utilities), infrastructure systems and housing units (Figure 2-6). Housing unit types consist of terraced houses, detached houses and apartments.

Figure 2-6 Typical structure of a new large scale housing project (Construction company Number 8 (CIC8) Viet Nam, http://cic8.com.

2.2.6 Public private partnerships for housing projects

Public private partnership (PPP), as a new approach to new LSHP, has been widespread in many developments in South-East Asia and has become an effective way through which to strive for better value for money in delivering infrastructure projects [4]. Infrastructure developments play a crucial role in economic development and reducing poverty [5]. Infrastructure systems have traditionally been supported by the government. However, the increasing demands for developing new infrastructure and maintaining of existing infrastructure, requires a large financial investment and these financial needs cannot be met by public funding alone. PPP delivery has become a solution for issues of funding by mobilizing private sector funds into infrastructure investment [6]. Private participation is able to maximize the productivity and efficiency of given operations, through innovative ideas and their high-level of management skill, which results in the improvement of higher quality services and the reduction of service cost compared to public sector provisions (ADB, 2008). The positive and negative factors of PPP projects in Singapore have been analysed by Bon-Gang and his research group [7].

The research into PPP for low-income housing in Vietnam was carried out by Quy [8]. The five factors, which have been based on extensive literature review and expert verification, which influences the success of PPP in low-income housing development include (1) government supports for private participations, (2) government taxation on private parties, (3) subsidies for low-income groups, (4) target group policy control and (5) the tenure system.

Apart from housing projects for resettlement, newer and large scale housing projects which would provide housing through the free market should also be considered. The benefits to the three main partners (including users, developers and the government) should strive to a "*Win-Win-Win*" situation, as shown in Figure 2-7. The users are willing and able to pay for their houses in terms of initial, operational and maintenance costs in line with quality standards of living. The profit is the driving force for developers and they are the ones who have to negotiate with the city's municipality for subsidies or for a better tax programs for particular projects at specific locations.

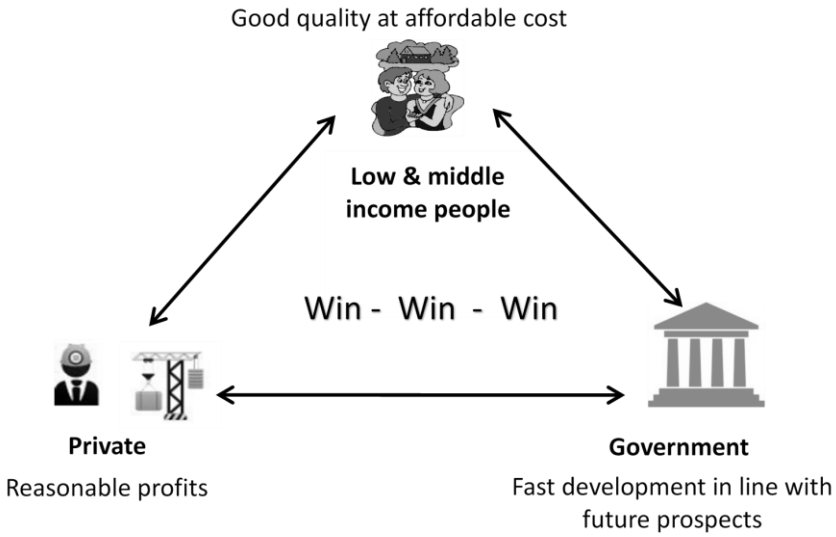

Figure 2-7 The win–win–win approach to public private partnerships.

Public-Private Partnerships for infrastructure development, including transportation, electricity and energy projects, have worked well for local and foreign investors. However, real estate and large scale housing projects have experienced difficulties depending on their specific situation. These difficulties involve, first, the need for large land resources which always generates conflict with local people, regarding compensation and resettlement issues primarily. Secondly, housing price depends on mobility, affordability and a design which is in respecting cultural traditions.

The PPP model for housing, (striving for win-win-win for government, developers and users) can hopefully stimulate collaboration in order to solve this situation. Firstly, the government can control provisions for public infrastructure, such as parks and roads by which to connect new large scale housing projects to the city centre. Secondly, subsidies, a reduction in tax rates, social interest rates and land acquisition rules can offer good strategic points by which to help developers eke out reasonable profits in free housing market situations. Third, developers have the budget, technology and management skills necessary to carry out projects of this sort. Finally, users' finance, based on housing project progress, can also generate financial resources.

2.3 Natural context (Cantho City but similar throughout the entire region)

2.3.1 Foundation: sedimentation in the river

Vietnam's Mekong delta is located downstream from the Mekong Rivers. This delta has been formed by sedimentation from the river and the land increases in size at Camau province by about 80 m every year. In fact, an extremely soft muddy clay layer, with a

thickness of between 10m and 20m, is added to the coastal line per year. The thickness and other properties are different in different locations along the river bed. The cost of building foundations is often higher for this reason.

2.3.2 Climate: temperature, relative humidity, solar radiation and wind

2.3.2.1 Overview of the climate of Vietnam

The whole territory of Vietnam is situated in the tropics which leads to high annual average temperature and solar radiation. Over half of Vietnam is covered in mountains and highlands. This geographical composition, combined with the trade wind, creates plenty of rain and which leads to an average rainfall of between 1000 and 3000mm per year. The result is a humid climate which has an average humidity of between 77% and 87%.

The Köppen-Geiger classification in Figure 2-8 is quite appropriate for the different climate zones in Vietnam because of the length from North to South and complex geography [9]. In the North and the South areas the rainy season falls in the summer; the climate of the middle area has a different pattern, compared to the two others, with a rainy season in winter and hot Föhn winds and tropical storms in the summer. In the Mekong Delta area, the average temperature is higher than Red River Delta due to 12° latitude difference. The weather of Hanoi and Cantho are analysed in the sections which follow and their analysis is based on the Typical Meteorological Year (TMY) weather data available.

There are two main tropical monsoon climate regions, based on the Vietnam Building Code, [10]. The North region (from 16° to 23° North latitude) has a tropical monsoon climate with the cold winter while the South region (from 8° to 16° North latitude) has a typical monsoon climate with a high average temperature and a rainy period between May and October and a dry period between November and April.

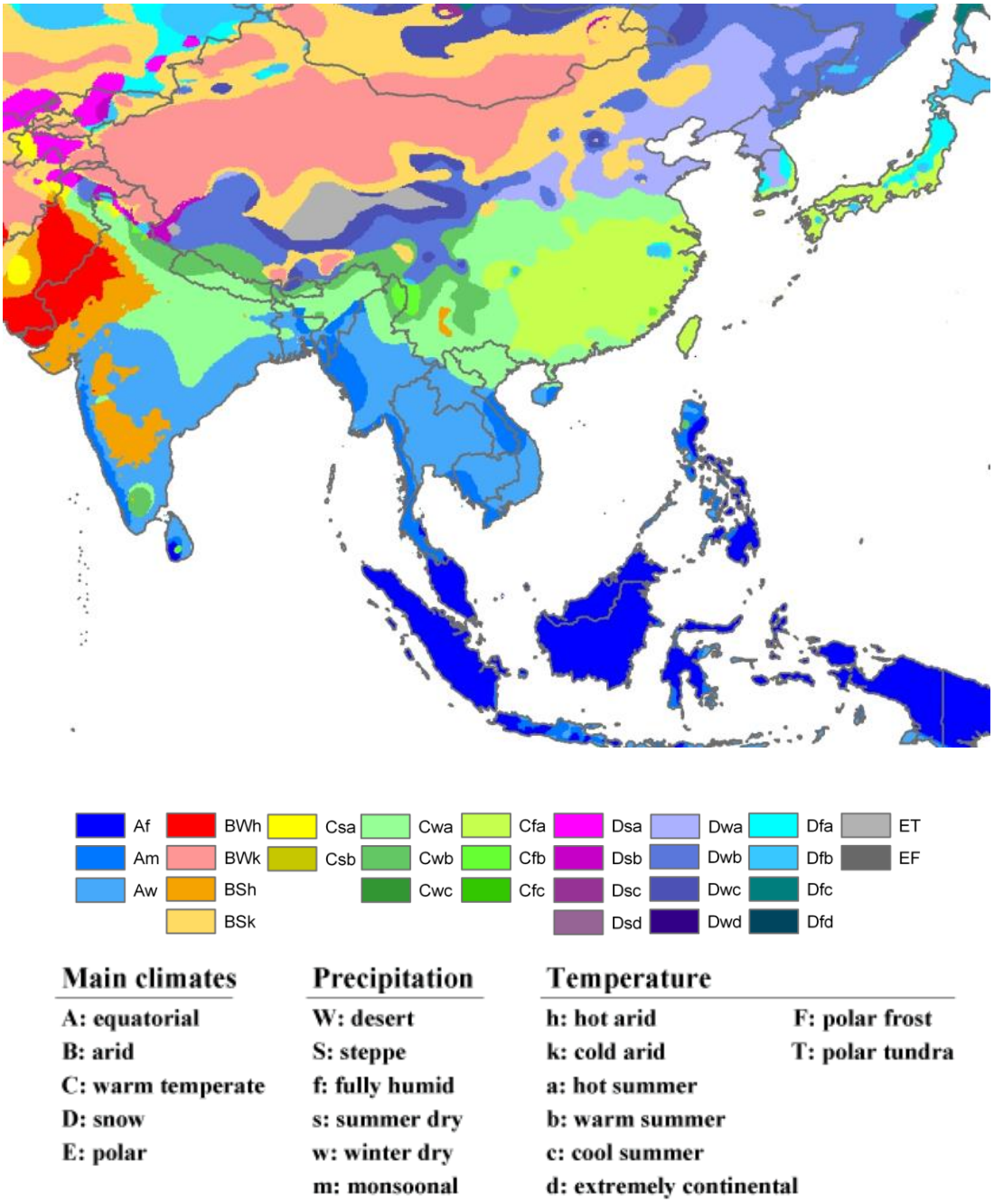

Figure 2-8 Köppen-Geiger climate classification map of Asia [9]

2.3.2.2 Weather data Based on Typical Meteorological Year (TMY)

Some weather data sources can be used for energy simulations. The Typical Meteorological Year (TMY) weather data is based on long-term average statistics over 30 years of hourly data taken at the same location. While they are not suitable for designing systems to meet the worst-case conditions occurring at any given location, they do represent typical rather than extreme conditions. In this study, commercial weather data from Weather Analytics

have been interpolated in order to simulate energy consumption for comfort [11]. These data have been interpolated using existing Meteorological Stations which are close to the location being analysed.

The U.S. Department of Energy's TMY data (2015) for Hanoi and Bangkok have been analysed to compare them with TMY data interpolated from Weather Analytics for Cantho. Extreme temperatures in Cantho vary between 25°C and 36°C and average out at about 28°C. The average relative humidity is between 70% and 80% and its range increases between January and April, the dry season (Figure 2-9). These natural conditions generate uncomfortable hours unless the occupants intervene. However, the wind (or force air movement) can increase the number of thermal comfort hours.

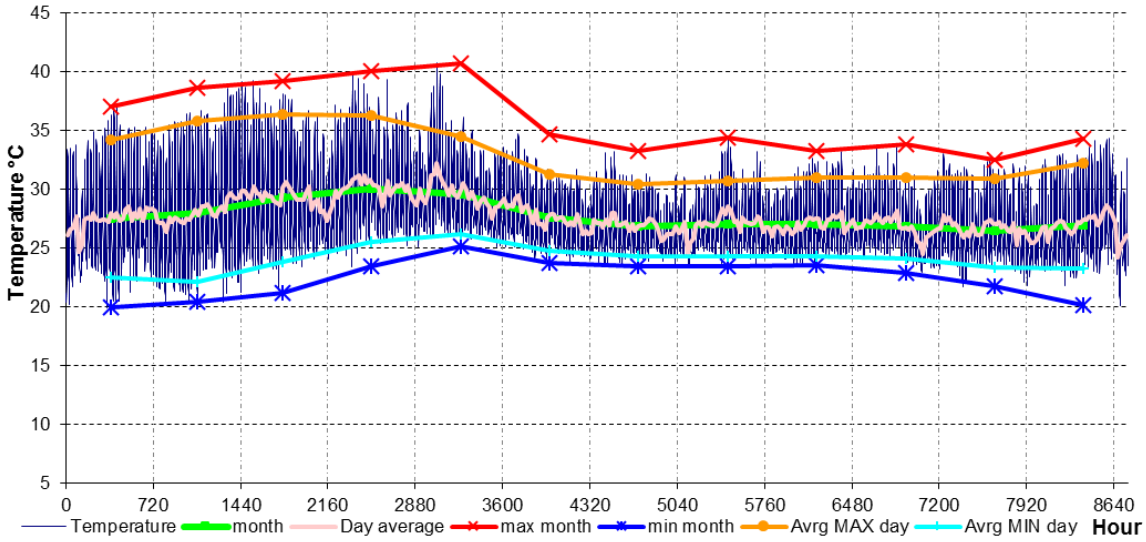

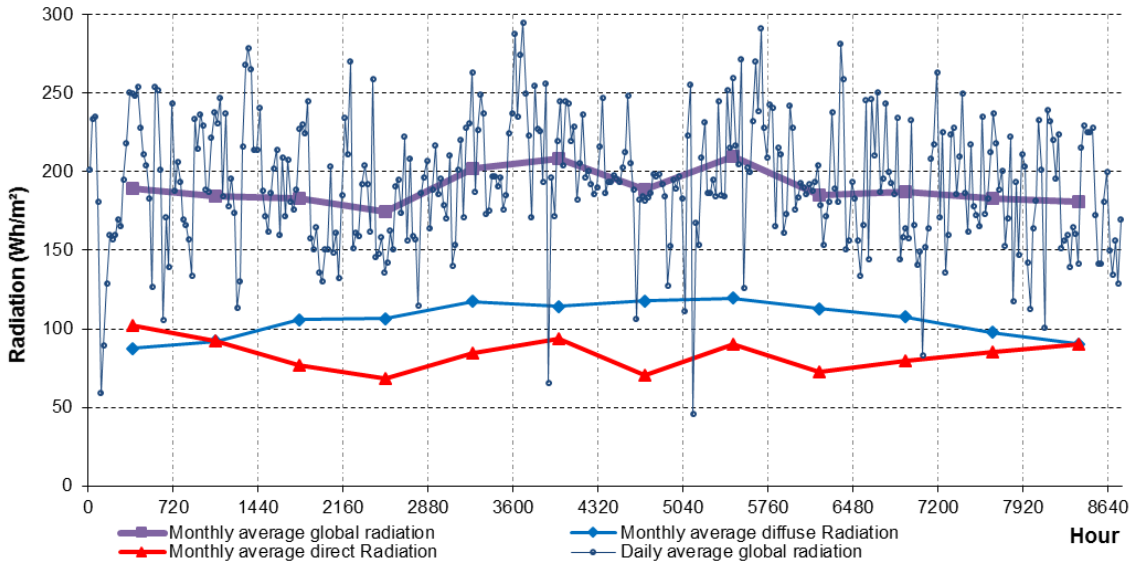

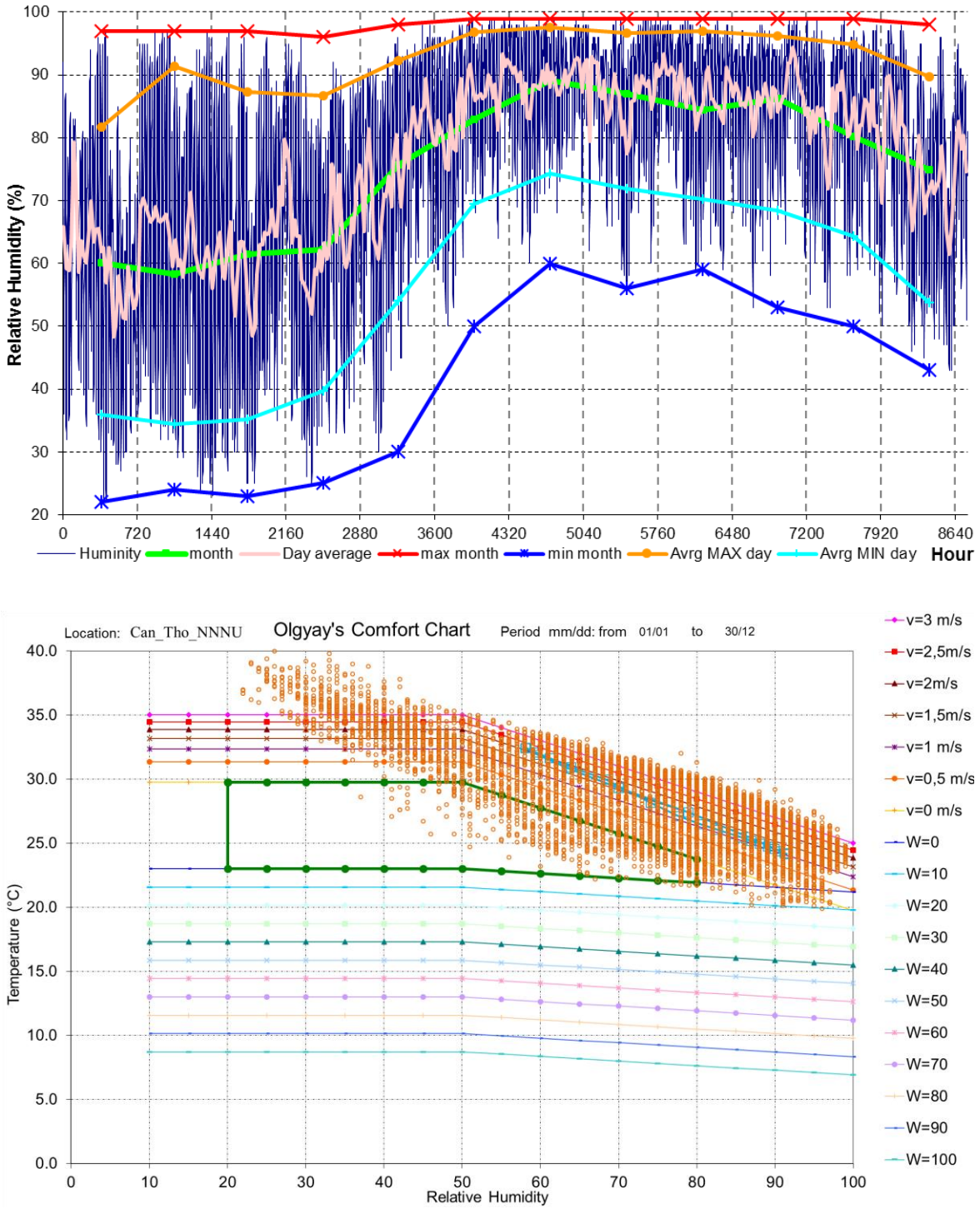

Figure 2-9 *Cantho's temperature at Cantho city, relative humidity, radiation and Olgay' Comfort chart, TMY.*

Bangkok's extreme temperatures also vary from between 22°C and 38°C, with an average of about 28°C. The average relative humidity ranges from 50% to 90% and this range increases between January and April, the dry season (Figure 2-10).

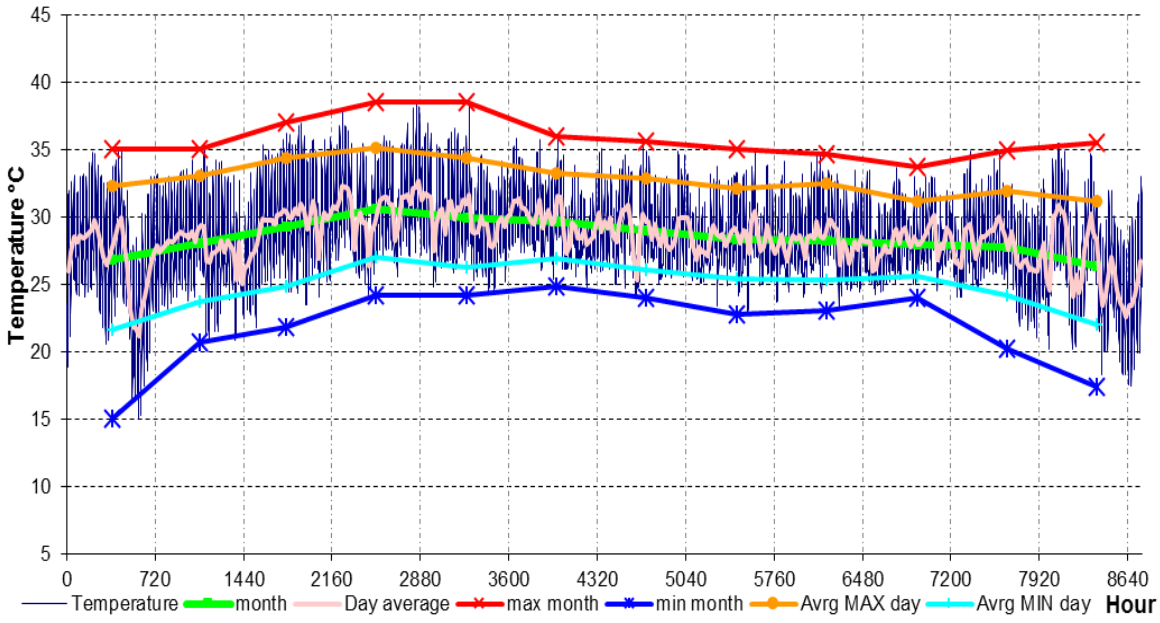
Temperature °C
45
40
35
30
25
20
15
10
5
0
720
1440
2160
2880
3600
4320
5040
5760
6480
7200
7920
8640
Temperature
month
Day average
max month
min month
Avrg MAX day
Avrg MIN day
Hour

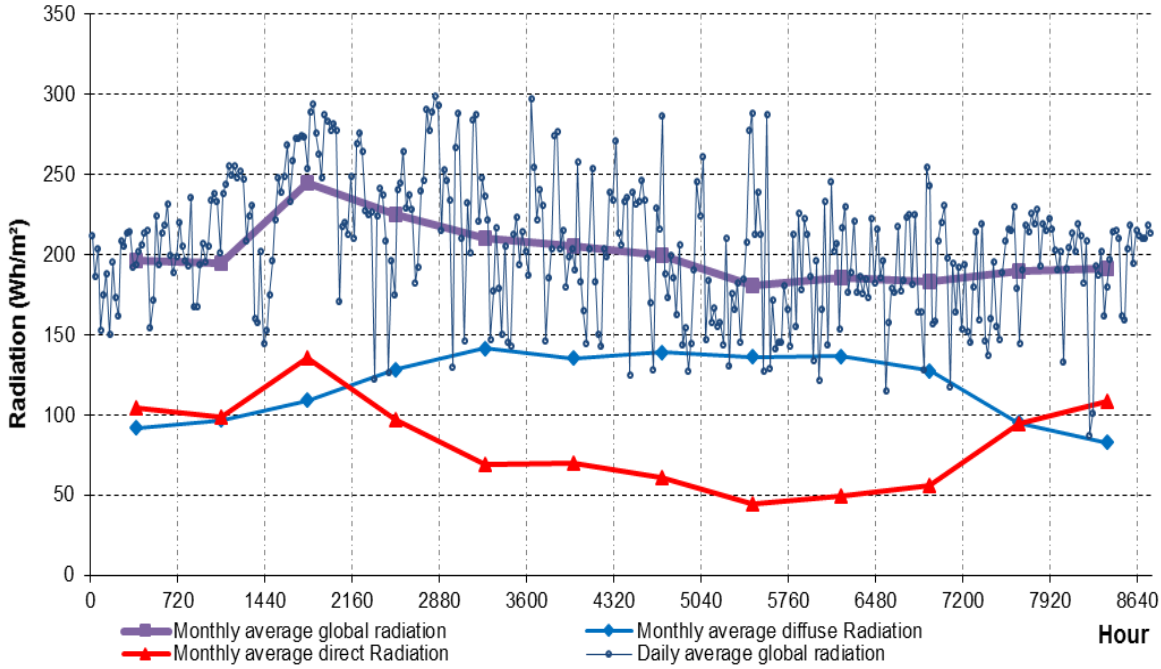
Radiation (Wh/m²)
350
300
250
200
150
100
50
0
0
720
1440
2160
2880
3600
4320
5040
5760
6480
7200
7920
8640
Monthly average global radiation
Monthly average direct Radiation
Monthly average diffuse Radiation
Daily average global radiation
Hour

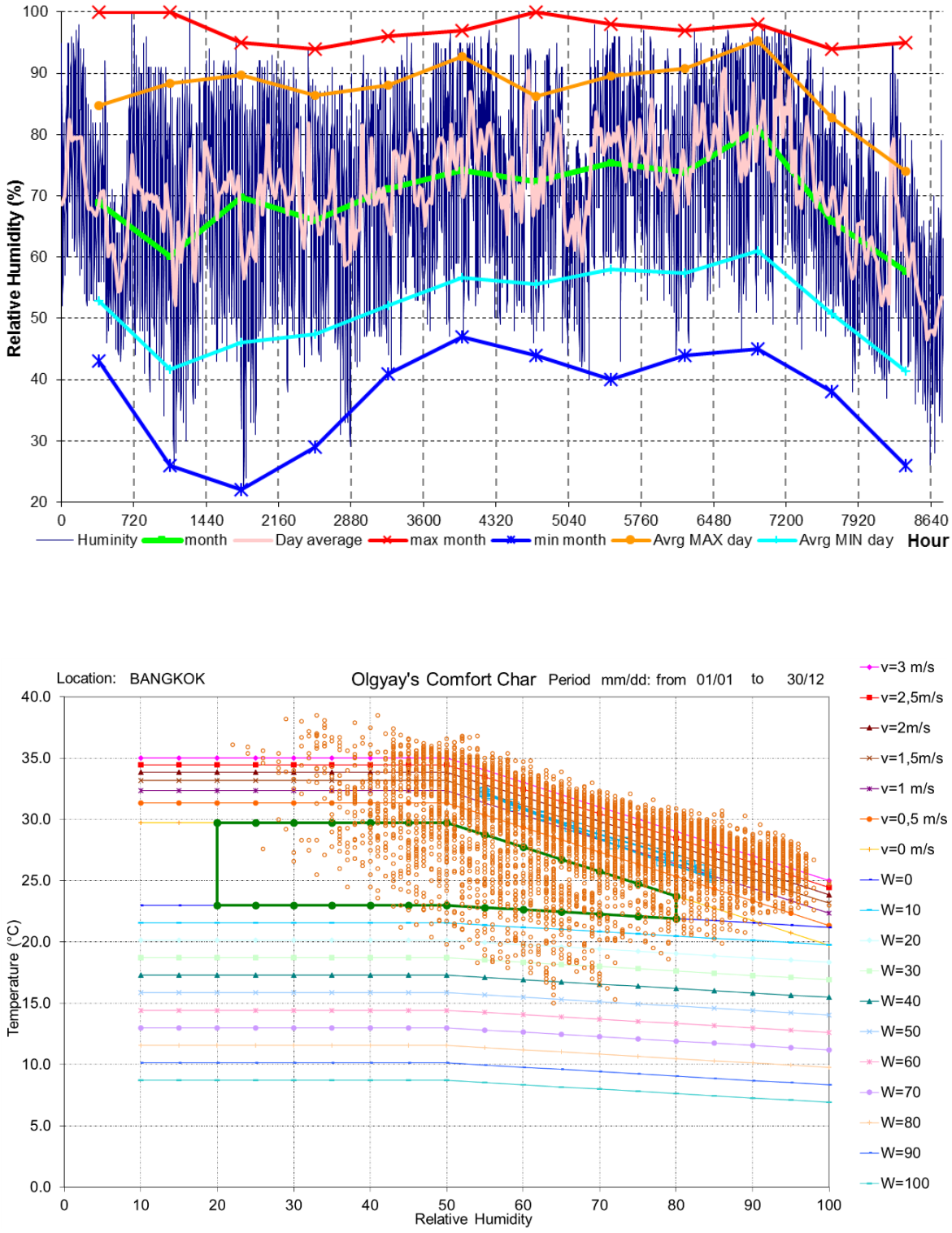

Figure 2-10 Bangkok's temperature hourly, relative humidity, radiation and Olgay' Comfort chart, TMY.

For Hanoi, the temperature range is between 10°C and 35°C, it has 80% relative humidity and there are four distinguishable seasons (Figure 2-11). A low capacity heating system

has to be employed during the winter time. A cooling system is also a required during summer time.

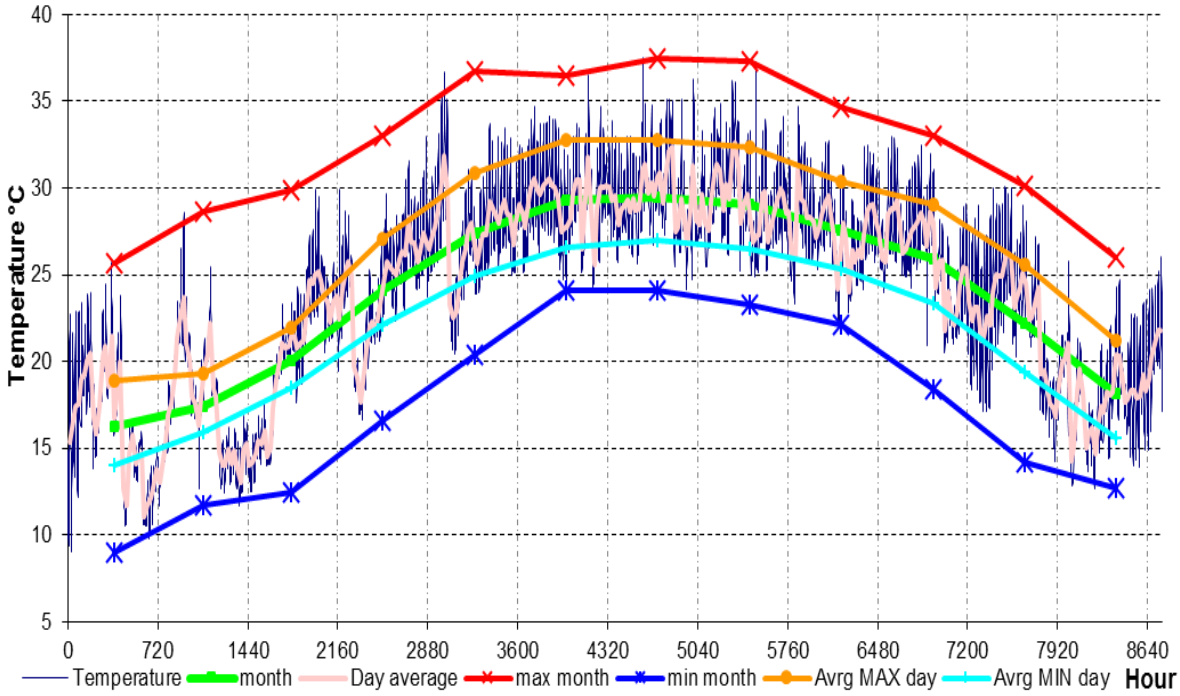

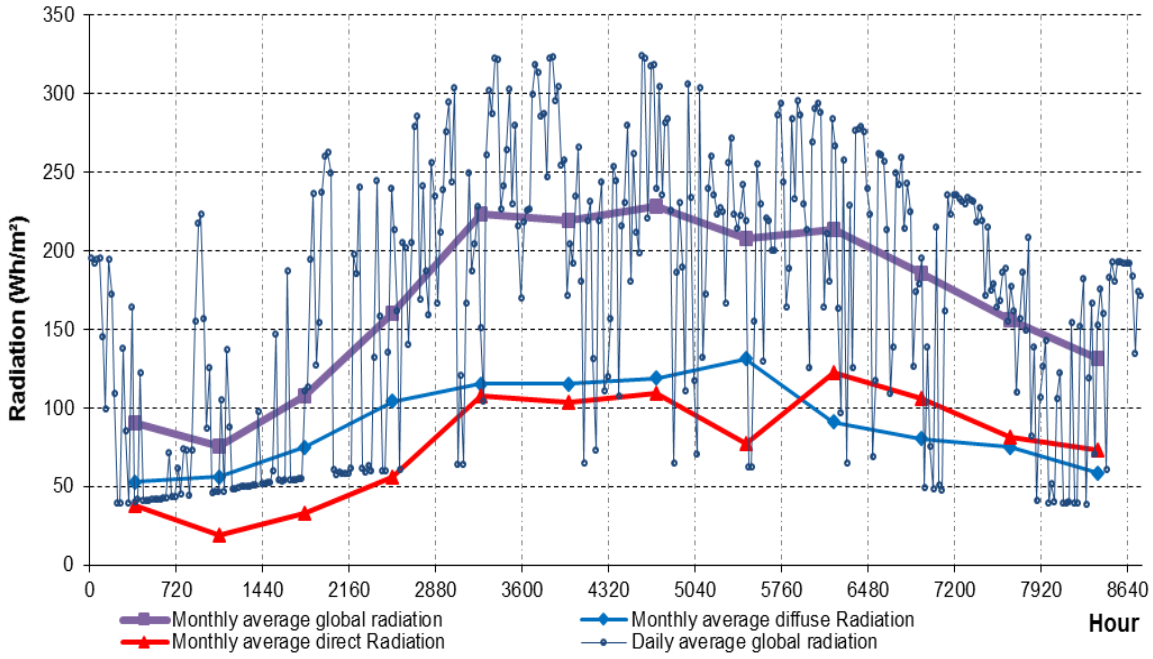

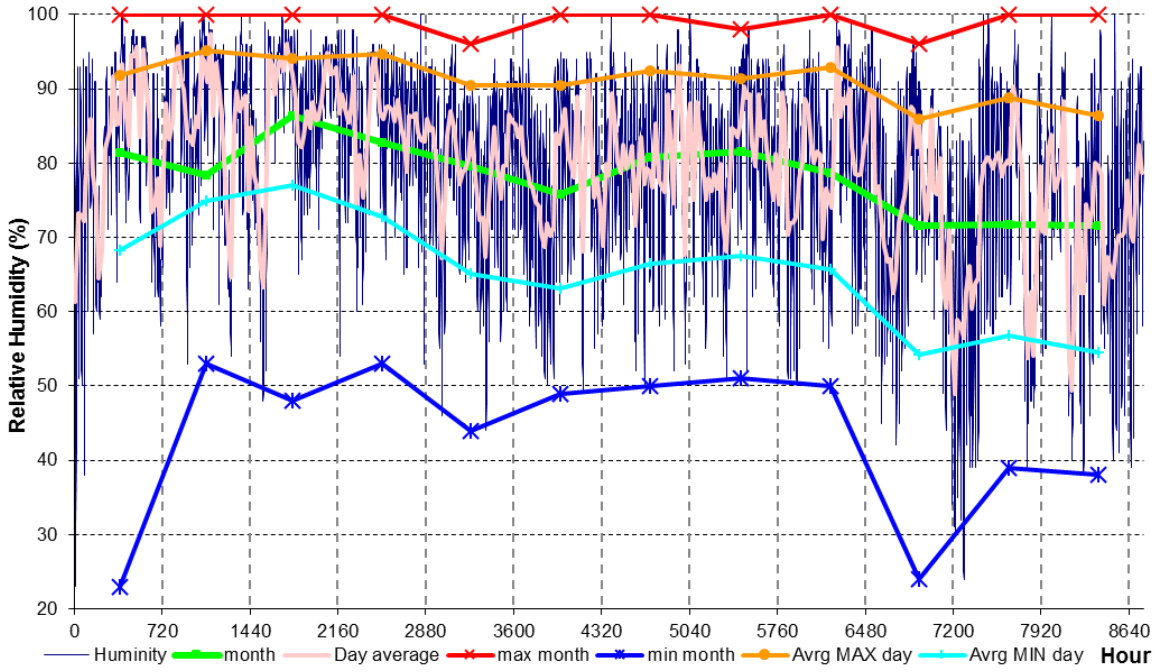

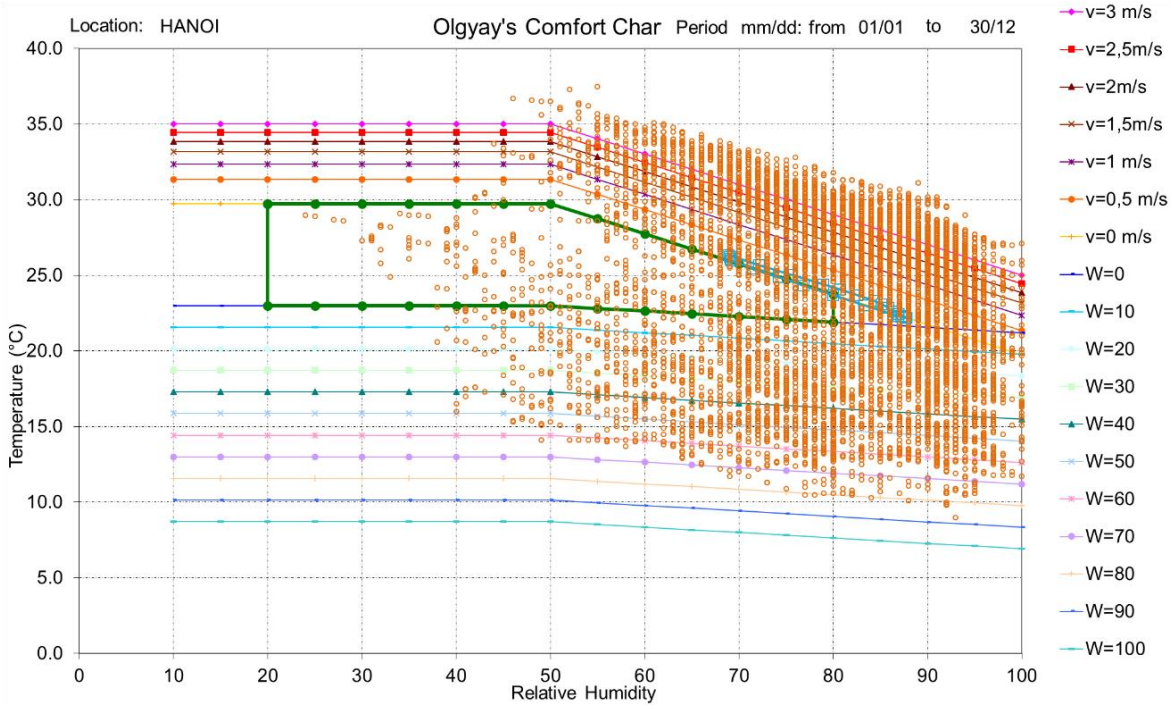

Figure 2-11 Hanoi's temperature hourly, relative humidity, radiation and Olgyay' Comfort chart, TMY.

The average hourly values for twelve months in Cantho have been visualized and can be seen on Olgyay's Comfort Chart, Most of which lie outside the comfort area above, right or below the green area in Figure 2-11. Some passive strategies to improve the thermal

comfort include natural ventilation, forcing air flows by using fans and reducing solar heat gain through the use of overhangs or other shading devices. Natural ventilation is applied when the temperature outside is lower than the temperature inside. The neighbouring buildings can also change the wind's orientation and the wind's velocity in the case of a high density of buildings. The wind flow is considered in the thermal comfort models of chapter 7. The Urban heat island effect is also a significant factor in changes to thermal comfort conditions in urban areas and this impaction will not be analysed in greater detail in this study.

2.3.2.3 Wind

The major wind directions in Cantho city depends on the period of the year (Figure 2-12). Wind speeds for 31% of the time fall between 1.00 –2.00 m/s and for 29% of the time fall between 2.00 – 3.00 m/s. The wind's direction varies and can be subdivided into three periods: a South–East wind prevails from January to April, a South–West wind prevails from May to September and the East and North-East wind prevails from October to December. These orientations should be borne in mind when devising natural ventilation strategies during the early design phase's process of planning and architectural design.

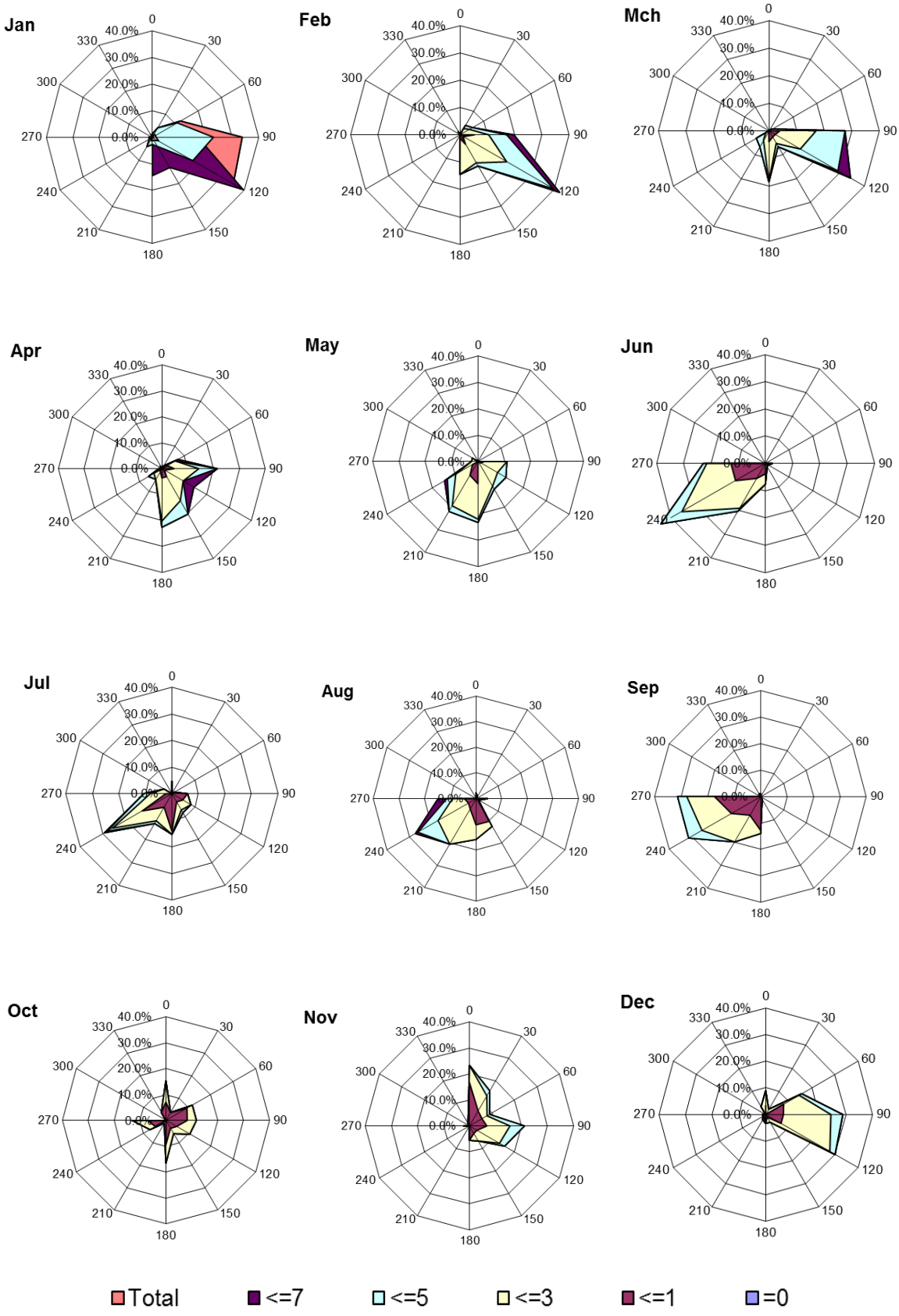

Figure 2-12 Frequency of wind speed and wind direction per month, Cantho, Vietnam.

2.4 Cantho's housing context

2.4.1 Rural types

Detached houses have been built along rivers and rural roads in the rural areas of the Mekong Delta which takes advantage of transportation, by means of waterways and roads. Metal roofs and plastic ceilings are very commonly used. The doors and windows are large enough to allow for natural ventilation while shadings and overhangs also reduce solar gain. Local materials or clay bricks were used for external walls (Figure 2-13 and Figure 2-14). Metal roofs with plastic ceilings are widely used because of their light weight and low cost. Hence, thermal comfort in these buildings is not good, especially during the noon time in summer period. Fans are used to partially improve the thermal comfort but comes at the expense of energy use and at the peril of the occupants' health.

Figure 2-13 Housing types in rural areas in Mekong Delta

Figure 2-14 Detached houses in Mekong Delta, [12]

2.4.2 Small scale individual developments: apartments, terraced, detached

The three main urban housing typologies in urban areas of Vietnam include: detached house, terraced house and apartment [13]. Terraced houses have recently become very popular and have become increasingly narrower and longer (and go by other names such as “Tube house” or “Shop house”). Generally, they do not have back gardens or very small ones. Their widths vary between 4m and 10m and their depths vary between 12m and 30m (Figure 2-15). The amount of daylight they receive and the natural ventilation they experience is limited due to their being long, deep terraced houses. However, this housing type has been opted for new large scale housing projects because their cost for infrastructure and land are lower than they are for detached and semi-detached houses.

Figure 2-15 Terraced houses in new urban areas at South Cantho and Caikhe.

An urban detached house is usually a free-standing building, which has up to three storeys, and is located on a plot surrounded by gardens and has at least 3 facades which open out onto the garden (Figure 2-16). The plot ratio for a detached house can be no more 50%, a figure based on Ministry of Construction, 2009. This housing type incurs large land use and comes at a considerable construction cost.

Figure 2-16 Detached house in urban areas, Khuong Island, Cantho.

An apartment is a housing type that has more than 2 floors, a corridor, a staircase and an infrastructure system which allows for many housing units. A crucial advantage is its low land cost per square meter floor area (Figure 2-17 and Figure 2-18). In Cantho, as well as in many other cities in the Mekong Delta, the memory of old apartments previously used by governmental staff (with their low quality and limited floor area per housing unit) has made it difficult to convince newcomers to choose to live in apartments. Agricultural experience, where people are used to having their own house and land, also becomes a factor in preferences being expressed for terraced houses. However, the apartment type could be a good option for high population density areas and for lower and middle income groups. Moreover, the apartments have been designed with flexible layouts, come with appropriate furniture, are well managed and focus on customer preferences.

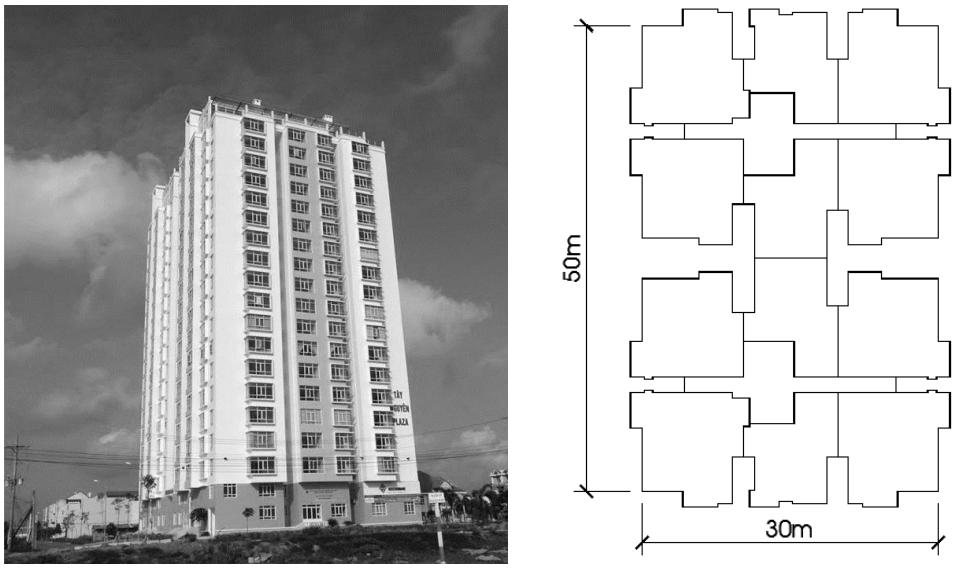

Figure 2-17 Front facade and section of Tay Nguyen Plaza Cantho, 2013.

Figure 2-18 Five floor apartment 91B and public facilities, Ninh Kieu, Cantho.

2.4.3 Large scale housing projects

Large scale housing projects, which combine infrastructure, housing, commercial and public areas, have been developed in almost every single city in Vietnam. This new urban model provides a large number housing units for people at all income levels. A difficult issue concerns the allocation of appropriate percentages of the total area for each function of each project; these percentages depend on the neighbourhood's existing infrastructure and the developers' expectation of profitability, Figure 2-19. The government can build main roads to connect the projects, and can introduce other infrastructure systems such as parks, hospitals and schools. These infrastructural provisions can also lead to an improved land value.

These large scale housing projects have formal subdivisions and each plot is around 100m^2. Streets vary in width, from between 8 and 16 meters, thereby providing excellent access by car. This formal subdivision type is likely to be affordable to middle and high income households.

Figure 2-19 Public space in the large scale housing project, Namlong, Cantho

2.4.4 Urban forms

Figure 2-20 Possible urban density on an 8,000 sqm-site dependent on building typology, [14]

Urban forms can impact on living quality within houses such as the view, their thermal comfort and indoor air quality. The reflection from neighbouring buildings, road surfaces, water and from green areas directly affects the local climate. Hence, the allocation of the three main housing types (terraced, detached and apartment buildings) and of other appropriate infrastructure systems, should be considered during the early design phases. Developers may consider the planning and preferences of users in order to arrive at a reasonable profit for a certain location which has natural landscaping for instance. Different housing typologies have different building densities and public areas can be enlarged in the case of high-rises and medium-sized high-rises (Figure 2-20).

2.4.5 Materials and technologies for buildings

Typical solutions for external walls consist of one or two layers of clay brick and have external and internal plastering. These construction types have a high thermal mass but create a heavy load on the building's foundations. Light blockwork concrete for internal walls to reduce dead load, construction time and labour cost.

Roof constructions are primarily metal and they have a plastic or carton ceiling, clay tiles, reinforced concrete with water resistant and a thermal isolation layer. Roofs which have a plastic ceiling are widely used because of their light weight and because the materials come at a low cost. Hence, thermal comfort in such buildings is not good enough for occupants, especially during the noon time in summer period. Fans are used to partially improve the thermal comfort with limit velocity (0.6m/s) in order to protect the occupants' health.

Windows with two glass layers are widely used in office and residential buildings. They are appropriate for insulation in the case of air-conditioned rooms. The reflecting glazing layer is used to reduce solar gain but results in the windows being expensive and limits the view, due to their dark or blue colour.

2.4.6 Street types, squares and public life

Main roads (which connect all internal roads to the main access roads) are financed by public funding. The internal roads have different widths based on their transportation capacity and transportation means. The width of sidewalks vary from 3m and 6m depending on the road function Figure 2-21). Road surface materials are selected on the basis of their traffic density, their load capacity and the life cycle of their maintenance and include asphalt, reinforced concrete or concrete blocks. In soft soil conditions, the sub-base is black sand

or river sand, which has a thickness of one meter, or sometimes more, based on the organic layer after the natural soil has been removed. The sub-base's thickness depends the natural ground characteristics and safety levels at certain locations.

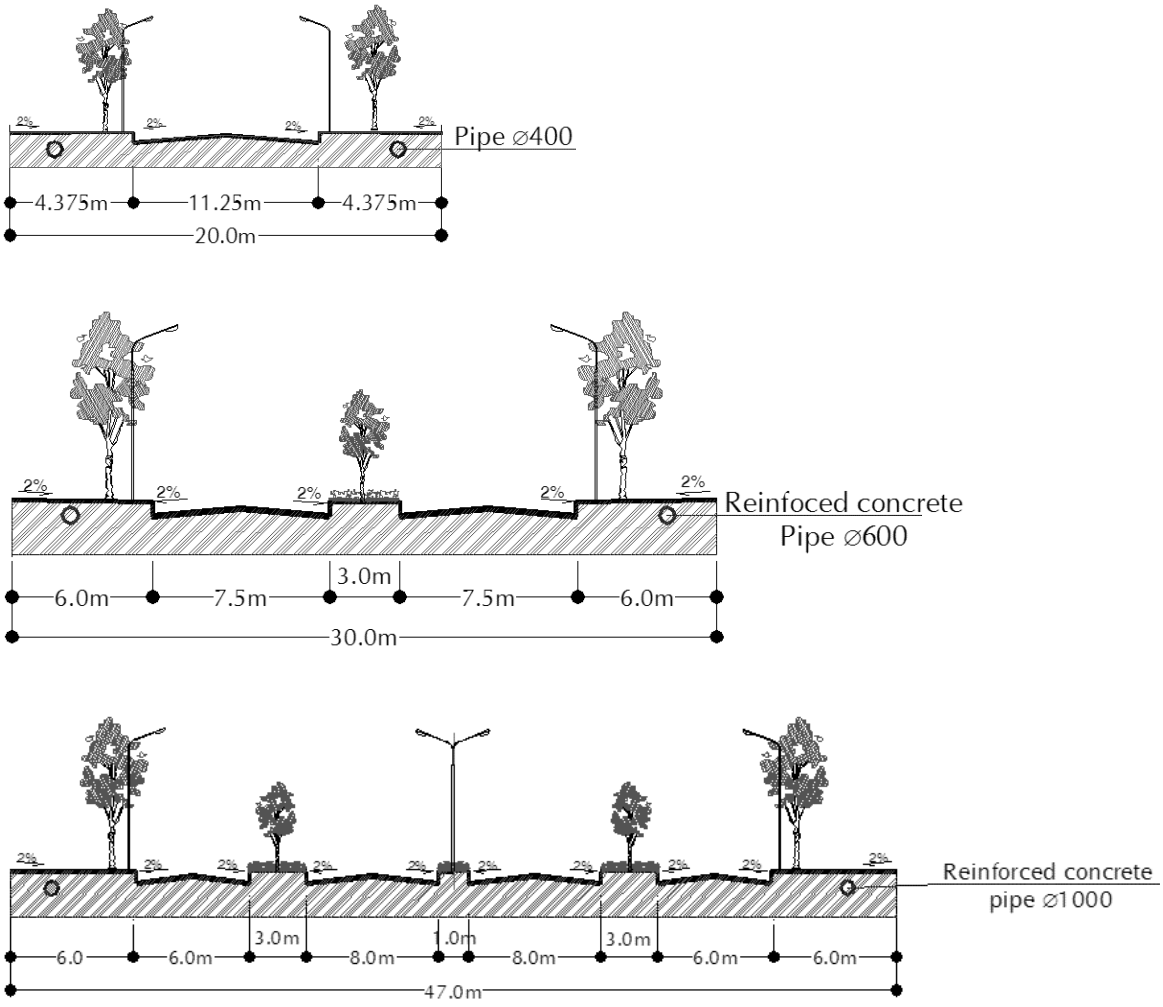

Figure 2-21 Different cross sections of some road types in the large scale housing projects.

2.5 Cut and fill and river sand for sustainable urban development

The "cut-and-fill" principle generates highland, while creating water surfaces of the new urban areas [15] p.248. This approach can conserve existing natural rivers by limiting the filling area or by creating new canals for local soil to fill nearby areas up to the required safety level (2.7m), (Figure 2-22 and Figure 2-23). A large amount of river sand has been used to fill in almost all of the large scale housing projects. The average black sand's

thickness is between 1m and 1.5m depending on the differences in the natural ground levels.

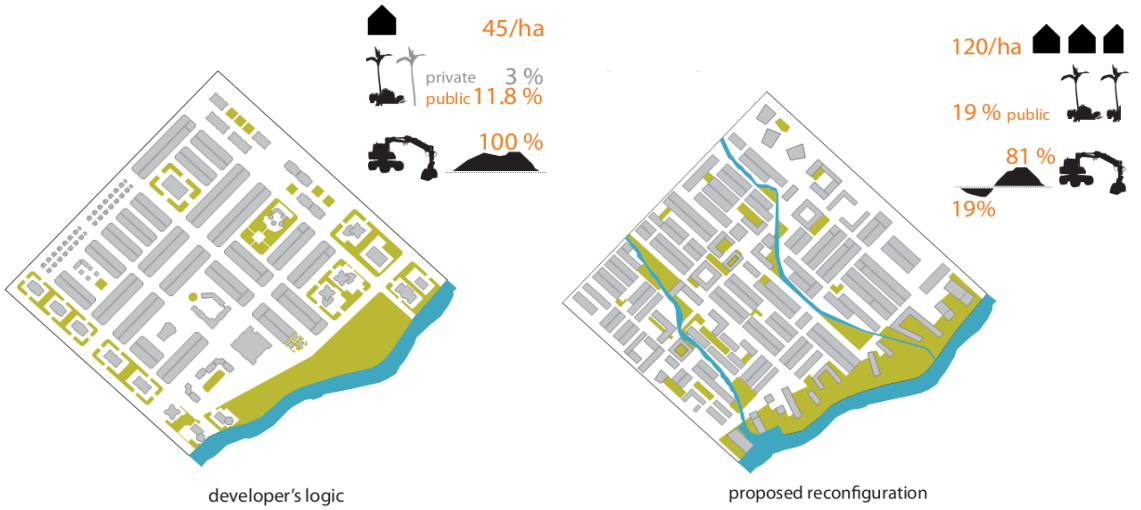

Figure 2-22 A large scale housing project at South Cantho city [16] p.156.

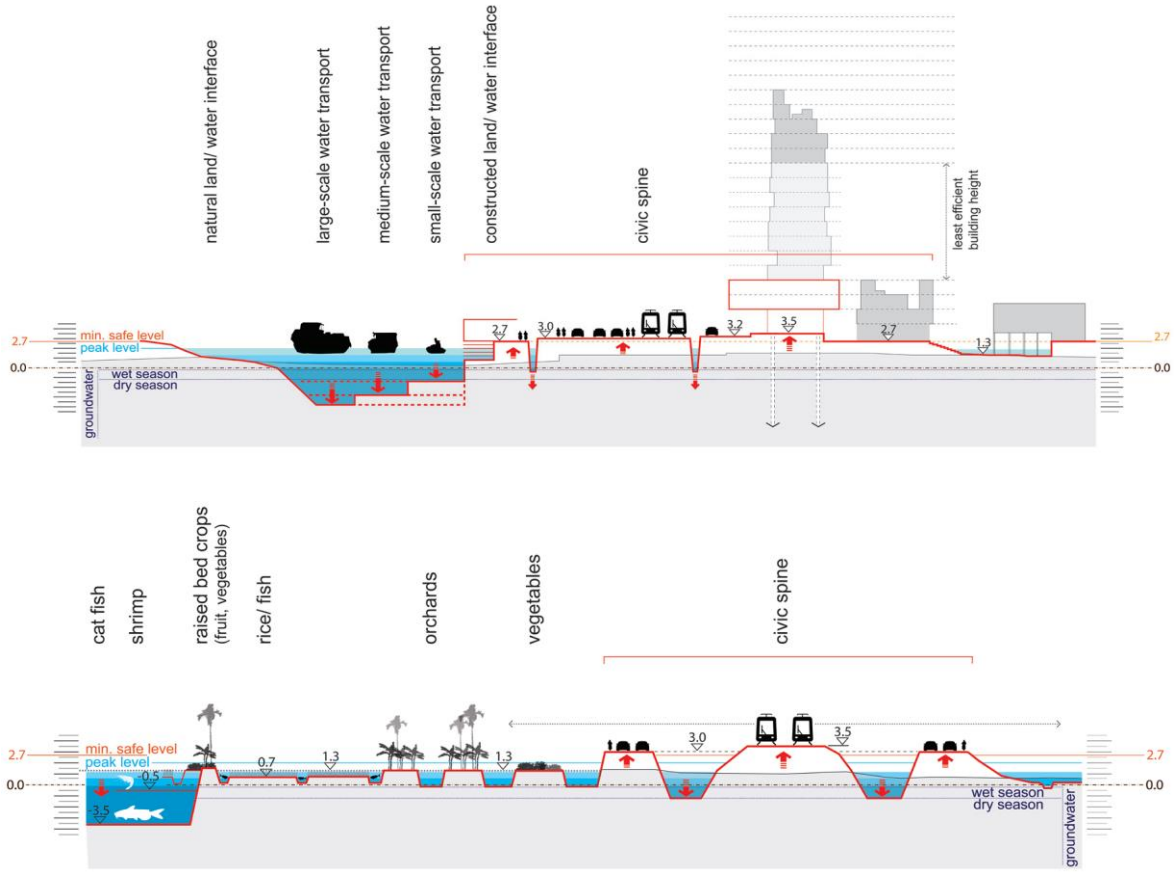

Figure 2-23 The cut and fill strategy, protection of sensitive eco-systems and creation of mineral platforms for urbanization need to work carefully with the existing topography, soil and water conditions [16] p.78.

References

[1] General Statistics Office, Vietnam, Vietnam population and housing census 2009 - Age-Sex Structure and Marital Status of the Population in Vietnam, 2011.

[2] Centre Population and Housing Census Steering Committee, The 2009 Vietnam population and housing census, Major Finding, 2010.

[3] C. Hirschman, V.M. Loi, Family and Household Structure in Vietnam: Some Glimpses From a Recent Survey, Pac. Aff. 69 (1996) 229–249.

[4] Y. Ke, S. Wang, A.P.C. Chan, P.T.I. Lam, Preferred risk allocation in China's public–private partnership (PPP) projects, Int. J. Proj. Manag. 28 (2010) 482–492.

[5] C. Harris, Private Participation in Infrastructure in Developing Countries: Trends, Impacts, and Policy Lessons, THE WORLD BANK Washington, D.C., 2003. http://elibrary.worldbank.org/doi/pdf/10.1596/0-8213-5512-0.

[6] A.D.B. ADB, Public private partnerships handbook, Mandaluyong City, Asian Development Bank, 2008. http://www.adb.org/sites/default/files/pub/2008/Public-Private-Partnership.pdf.

[7] B.-G. Hwang, X. Zhao, M.J.S. Gay, Public private partnership projects in Singapore: Factors, critical risks and preferred risk allocation from the perspective of contractors, Int. J. Proj. Manag. 31 (2013) 424–433.

[8] T.N. Quy, Current Practices of Public Private Partnership In Low-Income Housing Development In Vietnam, Asian Institute of Technology, 2010.

[9] M.C. Peel, B.L. Finlayson, T.A. McMahon, Updated world map of the Köppen-Geiger climate classification, Hydrol Earth Syst Sci. 11 (2007) 1633–1644.

[10] Vietnam Building Code (Volume III), (1992).

[11] Weather Analytics, Weather Anal. (2014). http://www.weatheranalytics.com/wa/.

[12] P.T. Ly, A Critical Regionlist Approach to Housing Design in Vietnam: Socio-Environmental Organisation of Living Spaces in Pre- and Post-Reform Houses, 2012.

[13] P. Ly, J. Birkeland, N. Demirbilek, Towards sustainable housing for Vietnam, in: Auckland, New Zealand, 2010.

[14] M. Waibel, R. Eckert, M. Bose, V. Martin, Housing for Low-income Groups in Ho Chi Minh City between Re-Integration and Fragmentation, in: 2007.

[15] B. De Meulder, K. Shannon, Water Urbanisms East, Park Books, Zurich, Switzerland, 2013.

[16] OSA/WIT/LATTITUDE, Cantho Masterplan Revision 2030, OSA final report (September 2010), (2010).

CHAPTER 3 METHODOLOGY

The aim of this chapter is to explain the global methodology and different sub models in this study.

The element model for cost control is used to integrate life cycle cost simulation at different scale levels (material, elements, building and neighbourhoods) and for all the phases of the design process (from first design stage to detail design).

Some general concepts and methods, used through different chapters, are described:

- Concepts and symbols used for life cycle costing (LCC)
- The problem of multi-objective optimization
- Latin hypercube sampling as a method to reduce computational time when analysing the design space.
- Sensitivity analysis to analyse the importance of different design parameters.

Table of Contents

3.1	**Introduction**	**43**
3.2	**The element method for cost control**	**44**
3.3	**Life cycle costing (LCC)**	**46**
3.3.1	General description of life cycle costing	46
3.3.2	Discount rate	47
3.3.3	Inflation rate	47
3.3.4	Nominal versus real discount rate	48
3.3.5	Growth rate	48
3.4	**Multi-objective optimization model: Pareto front in case of multi-objectives**	**49**
3.5	**Latin Hypercube Sampling method to select design options for sensitivity**	**49**
3.6	**Sensitivity analysis and selecting a sensitivity analysis method**	**50**
3.6.1	Sensitivity analysis	50
3.6.2	Selecting a sensitivity analysis method for this study	52

3.1 Introduction

The global research objective is the development and applying of a ‘general’ and ‘expandable’ approach to the optimisation of design choices. By ‘general’ means the applicability of different situations, while ‘expandable’ means that the approach can be further elaborated in different ways. For this purpose, sub-models have been elaborated to support these objectives.

(1) The element method for cost control was extended to be applicable in the case of large scale housing projects from material level, over construction elements, up to building layouts and urban forms.

(2) A cost model for pile foundation depending on soil properties, building layout (such as height, width and depth) is used to select the pile foundation with the lowest cost per ton capacity.

(3) A market value model considers housing preferences in order to allocate urban area for specific housing types (terraced house, detached house or apartment) and for commercial facilities.

(4) The thermal comfort and energy model takes into account dynamic occupant behaviour, wind pressure and a low energy design approach by estimating the operational cost throughout the whole service’s lifespan.

(5) The optimization method searches for optimal solutions on the multi-dimensional Pareto front.

These models are integrated to create insights into the cost and quality of housing projects. They will be described in detail in the following chapters.

In this study, housing quality refers to and focusses upon, housing preferences, thermal comfort and daylight. Firstly, housing preferences are considered by measuring the willingness to pay for specific characteristics of dwelling units and of infrastructure systems. Secondly, at the technical level, the lowest possible life cycle cost that provides a minimal thermal and day light comfort is searched for.

The housing cost considers the housing elements, the infrastructure system and the land cost. Housing elements are limited to walls, roofs, floors, windows and the building’s foundation. In a soft soil areas, the foundation cost for high rise buildings is based on a

more detailed estimation which takes into account the building's layout, wind and seismic loads. The lowest, pile foundation cost per supported ton for a given soil condition is searched.

3.2 The element method for cost control

The element method for cost control of the building was established in Great Britain and applied in several countries [1] [2]. This method was elaborated making use of the coding system in the BB/SfB-plus that extended from CI/SfB Construction indexing manual [3] [4]. The element method is used for cost estimation and cost control during the different stages of the design process. The cost estimation of the building or the infrastructure on the urban level is constructed based on hierarchical and functional elements, such as foundations, external walls, door, window, roof and roads (Figure 3-1). Each element can use one or various materials and different work sections such as concrete work, brickwork and painting. The elements evolve during the design process from roughly described entities to fully detailed entities. The cost per m² of floor is calculated based on their unit rate and the quantity for one m² of floor area. The impact of the building geometry and the urban layout on the cost of each element is made explicit via the "ratio" (quantity of element per m2 of floor area.

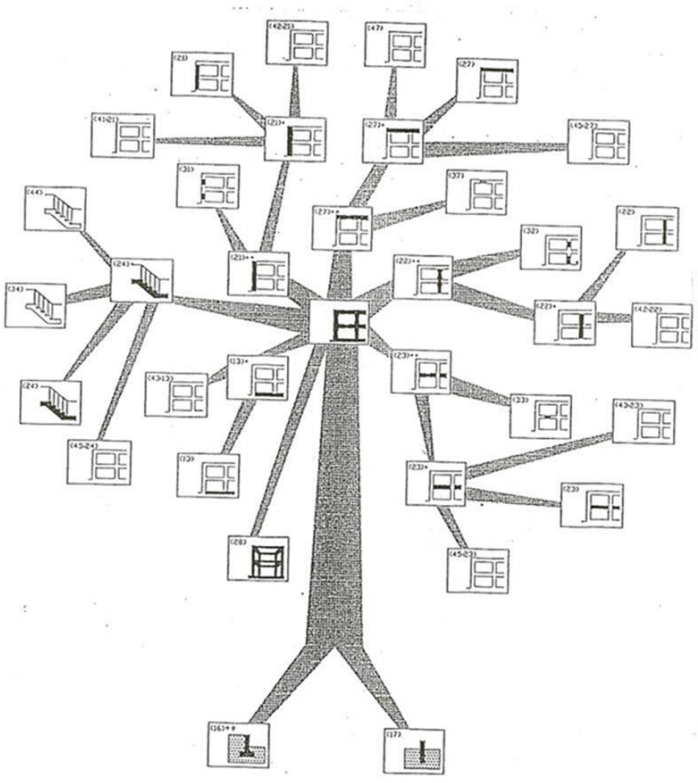

Figure 3-1 Hierarchical structural tree of building elements [3].

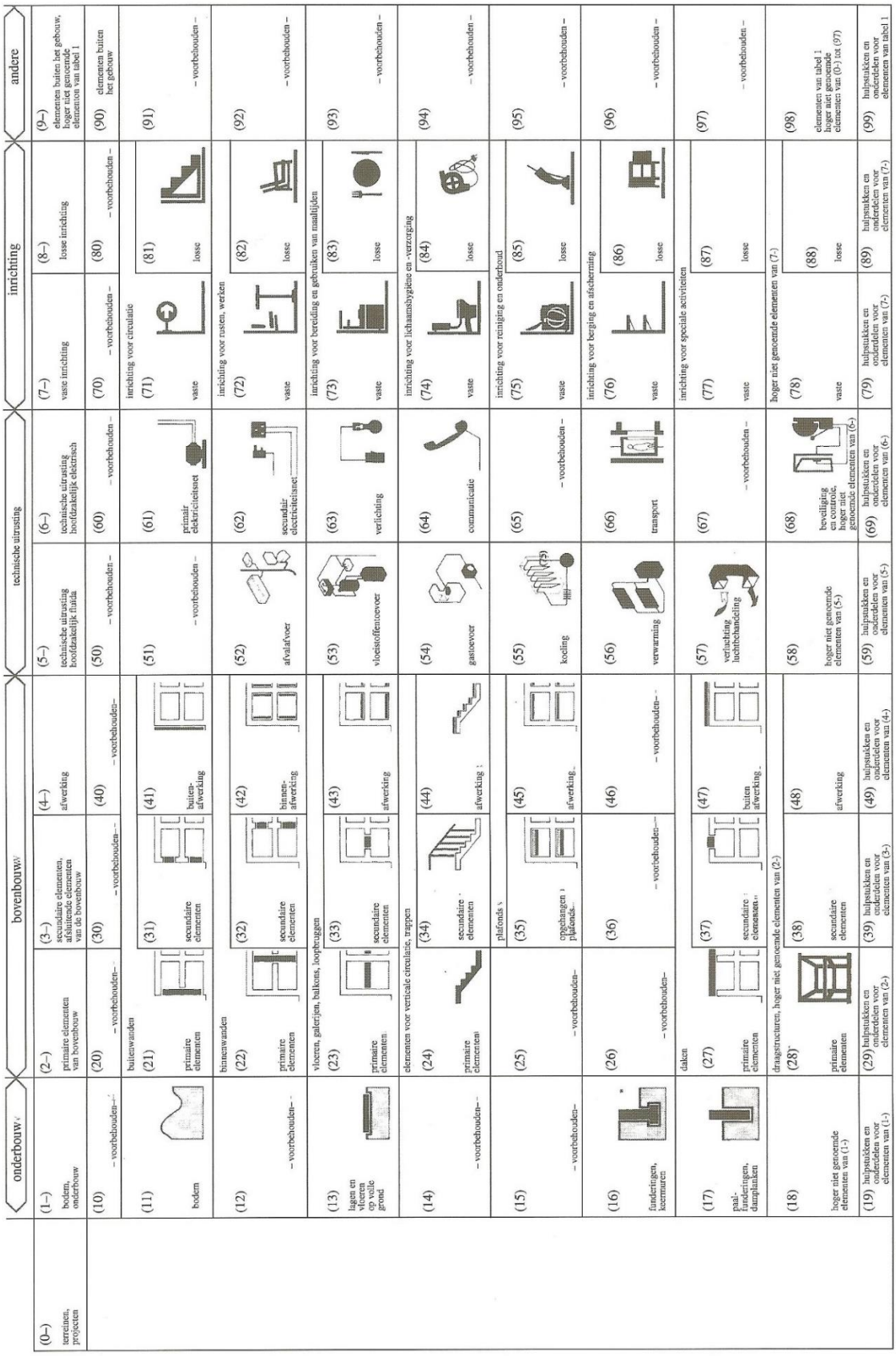

Figure 3-2 The element structure of a building [3]

Compared to existing black box approaches, the element method for cost control was originally developed as a glass box [3]. Changing building parameters can influence ratios and elements' unit rates [5]. This method is able to employ the buildings' basic parameters, such as width, depth and height, to estimate construction costs.

Buildings can be subdivided in various ways; five levels are considered in this approach which include: building materials, processed materials, elements, buildings and neighbourhood (Figure 3-3). These elements are defined as a part of building which fulfil a set of functions. The external wall, for example, separates the inside climate from the outside climate and the roof separates inside and outside at the top of a building. There are two groups of elements: "space-delimiting"- functional elements, such as external walls, internal walls or roofs and "space equipping" – functional elements such as heating, cooling, lighting, water supply and sewerage.

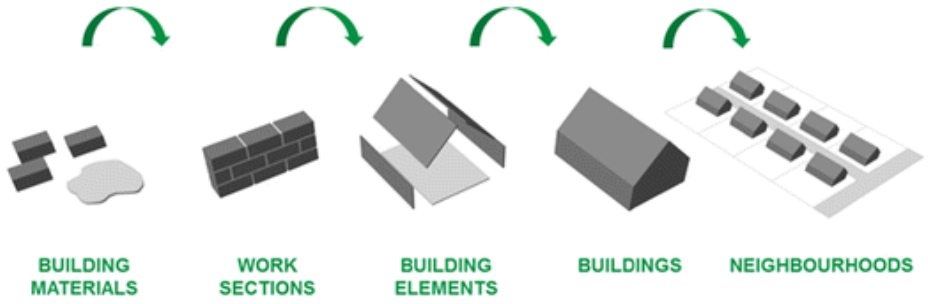

Figure 3-3 Building elements of different levels [6]

3.3 Life cycle costing (LCC)

3.3.1 General description of life cycle costing

The investment cost as well as the operational cost and demolition cost at the end of the building's life cycle are included, leading to the whole life cycle cost. The LCC of buildings is defined in ISO 15686 as: the total cost of a building or its parts throughout its life, including the cost of planning, design, acquisition, operations, maintenance and disposal. Stakeholders of a housing project should care about balancing initial capital cost with whole life cost. Housing developers focus often only on capital costs, excluding running costs, because they suppose users will be responsible for the cleaning, maintenance, energy costs, etc. However, tenants want housing units that are efficient, reliable and easy to adapt. With low running costs they will balance the rental charge or price with the whole life costs before selecting a dwelling. The developers need to think about LCC or whole life appraisal [7].

3.3.2 Discount rate

The discount rate converts future costs and revenue back to the present moment. The higher the discount rate, the lower the impact of future expenditure is.

3.3.3 Inflation rate

Inflation (or deflation) describes the increase (or decrease) of the nominal price of a basket of goods and services. In case of constant inflation (i) the cost in year t (Pt) of a basket costing now (t = 0), (P_0) can be estimated by using the following formula:

$$P_t = P_0 * (1 + i)^t$$

In consequence, the purchasing power (PP) of an amount X_t at moment t is:

$$PP[X_t] = \frac{X_t}{(1 + i)^t}$$

3.3.3.1 Present value and total present value

The present value of future cost is defined as the amount of money, required to be saved today at a (nominal) interest rate r, to have the money available (C_t) at moment t (after t periods)'. For this purpose, it can be calculated by using the following formula.

$$PV[C_t] = \frac{C_t}{(1 + r)^t}$$

The formula above assumes that 'r' is constant over the period considered. It should be interpreted as an average rate over the period considered. The rapid reduction of the present value of future costs, even for relatively low discount rates, is illustrated in Figure 3-4.

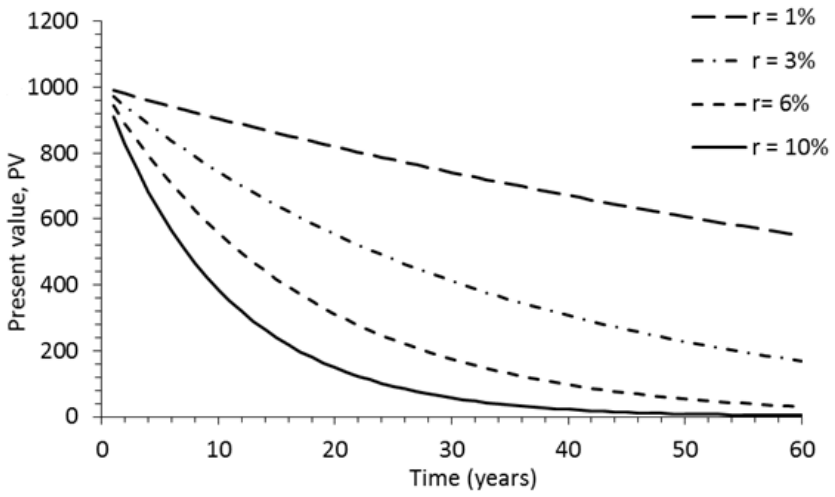

Figure 3-4 Present value of 1,000 money units at moment tfor different discount rates.

3.3.4 Nominal versus real discount rate

The 'real' rate calculates how the purchasing power evolves over time and takes nominal inflation and nominal interest rates into account. The real discount rate (r') can be calculated by using the following formula.

$$r' = \frac{(1+r)}{(1+i)} - 1$$

$$PP[C_t] = \frac{C_t}{(1+i)^t} = \frac{C_0(1+r)^t}{(1+i)^t} = C_0(1+r')^t$$

3.3.5 Growth rate

A growth rate 'g' reflects the growth of a selected basket of goods and/or services like: materials, energy or labour cost.

$$p_t = p_0(1+g)^t$$

The growth rate of prices can fluctuate annually. In the formula above 'g' represents the annual average growth rate over a period, up to year t. If a constant yearly growth rate of 'g' is assumed, then the price evolution is exponential.

3.4 Multi-objective optimization model: Pareto front in case of multi-objectives

Pareto optimum cases are that subset of the considered set of solutions for which no objective can be increased without a decrease in another objective. The principle is illustrated below [8].

The concept is illustrated in Figure 3-5 for a problem which has two objectives namely, reducing c (life cycle cost) and increasing the quality reflected in the price people are willing to pay for the housing unit. Option A is better than option F because c(A) < c(F) and p(A) > p(F), it offers a lower cost for higher quality (expressed as a high price). Option A and option D possess equal quality p(A) = p(D) but the cost of option D is higher than that of option A. Therefore, option A is superior to option D. Option E requires the same cost as option D, however, the willingness to pay for E is higher than option D.

When the same reasoning is followed for all of the options, the combination situated on the dotted line are the subset of the Pareto front. The Pareto front becomes a surface in cases which have three objectives. If the budget allows to pay for option A, then one will never select option B because the quality increase per extra spending, from C to A, is much higher than from C to B.

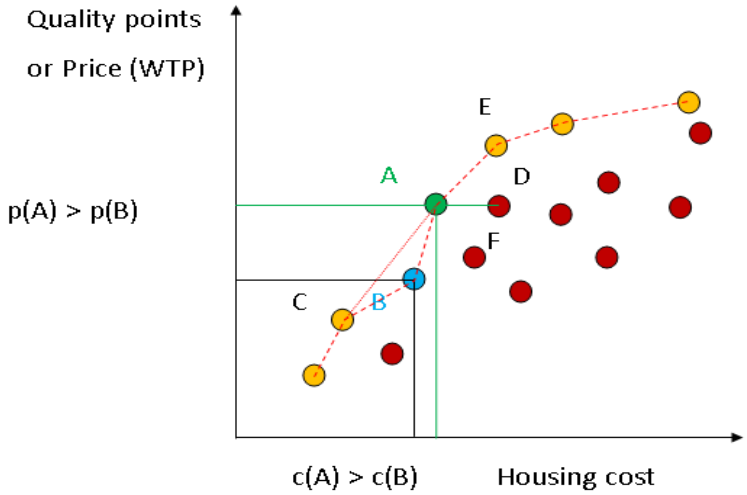

Figure 3-5 Pareto set for maximization quality and minimization of cost.

3.5 Latin Hypercube Sampling method to select design options for sensitivity

Latin hypercube sampling (LHS) method is an improvement on the random sampling methods [9]. The LHS is constructed by subdividing the range of each of M independent variables into an N_{sim} non-overlapping segment of equal probability. Thus, there are $(N_{sim})^M$

cells in the design space. A single value is chosen randomly from each interval; the values are randomly matched to create selected combinations from the design space, with respect to the density of each interval. The LHS is available in most statistical programs such as R [10] and Simlab [11].

Latin hypercube sampling (LHS) is an easy-to-use, popular experimental design technique which provides a good global parameter search. LHS is a statistical method used to produce a distribution of plausible collections of parameter values from a multi-dimensional distribution. The technique was originally described by McKay et al [12].

For the regression-based sensitivity analysis, SimLab recommends the sample size of 1.5 up to 10 times the number of input variables [11]. For the present study, LHS was therefore chosen with 200 simulation runs for 17 independent input parameters for materials over building element to urban layout levels.

3.6 Sensitivity analysis and selecting a sensitivity analysis method

3.6.1 Sensitivity analysis

The concept of sensitivity analysis (SA) has been defined differently, in view of different methods analysed, aims and problems. SA has been defined as an evaluation of the effect of a given input variable on the output [13]. Direct or indirect approaches can be used to measure sensitivity as well as system derivatives such as $S_{x_j} = \frac{\partial Y}{\partial X_j}$, where Y is the output of interest and X_j is the input factor [13].

The concept of SA has been used to understand relationships and the relative importance of design parameters on a building's performance. Some benefits of SA can be classified as follows [14].

- To evaluate impacts of all input variables on a model outcome.
- To explore relationships between the inputs and outputs of the model.
- To simplify the model by removing inputs that have very small effect on outputs.
- To detect unexpected outputs based on the inputs.
- To support an optimization by seeking for zone in the input space to obtain minimum or maximum simulation output.

Some SA approaches can be distinguished by their methods, purposes and sensitive indices. A typical procedure, by which to analyse sensitivity, consists of the following steps [13].

- **Step 1**: Defining the goal the output function.
- **Step 2**: Selecting which input factors should be included in the SA.
- **Step 3**: Evaluating the uncertainty of each input by assigning a range and its probability density function.
- **Step 4**: Selecting a SA method on the basis of the natures of the problem at hand, the number of model evaluations and model execution time, the presence of a correlation structure between inputs factors.
- **Step 5**: Creating an input sample with N input vectors and a sampling method of the method chosen for SA.
- **Step 6**: Running the model on N input vectors to have N corresponding outputs.
- **Step 7**: Analysing the model inputs and outputs in a graphical way.

In practice, these steps may be repeated many times to eliminate unimportant input parameters. The question is: what SA method is most appropriate to this study? [15] provides a review of the SA methods which can be partitioned into three groups: (1) methods to evaluate the output of each variable at a time, while other variables are kept constant (6 methods), (2) methods are based on the generating samples of input vectors and associated outputs (10 methods) (3) and methods to perform a partitioning of the input vector based on the output vectors (4 methods).

Elsewhere, in another review [16], the SA was classified into three groups: local sensitivity, global sensitivity and screening methods.

A local approach to SA involves computations based on the one-parameter-at-a-time (OAT) approach. This is the effect the factor's variation has when all other factors are kept constant at a central (nominal) value. A global method should instead evaluate a factor's effect while all others vary too. Hence, there are a large number of input vectors for the model. The screening method is a variation on the sampling-based method. The purpose is to reduce computing time for high dimensionality models. Morris (1991), for example, employs this screening method. The global sensitivity analysis consists of regression method, Screening-based method, Variance-based method and Meta-model based method [18].

According to Frey etc. all (2003), the SA can be categorized into 3 groups [17]:

- Mathematical approach typically involves obtaining the output for a few values of the input ranges. Some methods are used that are the Nominal Range Sensitivity

Analysis method, the Different Sensitivity Analysis, the method of Morris and most approaches which use the OAT method.

- Statistical approaches need huge numbers of model evaluations, which are created randomly, on an input sample space.
- Graphical methods give representation of sensitivity in the form of graphs or charts. Those methods can be used as a screening method before further analysis of a model and to complement the results of mathematical and statistical methods for better interpretation.

3.6.2 Selecting a sensitivity analysis method for this study

In sensitivity analysis of building performance models, computational cost becomes a significant obstacle for a large sample size. The Regression-based method is the most widely used method for sensitivity analysis in building energy analysis because it only requires moderate computational cost for building performance simulations [19]. The regression-based methods was chosen for SA [20]. The standardized regression coefficient (SRC) is applied for SA of building energy models in this dissertation.

- First step, the slopes of the multiple linear regression of all input parameters are calculated based on the data.
- Second step, sample standard deviations of the input parameters and output results are calculated based on the data.
- The last step, the standardized regression coefficient (SRC) values are calculated by dividing the sample standard deviation of each parameter by the sample standard deviation of the output result (life cycle cost or energy cost) and multiplying the regression slope of each parameter.

Simulation outputs are generally nonlinear, multi-modal, discontinuous, non-monotonic [11] and may contain both continuous and discrete variables, due to the complexity of detailed building simulation models and so global sensitivity analysis should be opted for ahead of the local one.

The uniform distribution of the parameters was used for the sample with a size of 1.5 up to 10 times the number of input variables [11]. For the present study, the sample size was increased with 2000 simulation runs for 17 independent input parameters for materials over building elements to buildings and urban layouts. This method was applied for sensitivity analysis of three housing types: terraced house, detached house and apartment.

References

[1] a.a., Cost control in building design : a programmed text, London Her Majesty's stationery office, 1968.

[2] R. Flanagan, B. Tate, Cost Control in Building Design, Wiley-Blackwell, 1997.

[3] F. De Troyer, BB/SfB-plus Een fuctionele hierarchie voor gebouwelementen, Uitgeverij ACCO, Leuven, 2008.

[4] A. Ray-Jones, D. Clegg, CI/SfB construction indexing manual, 3rd edition, London: RIBA, 1976.

[5] F. De Troyer, Graphical tools for cost-conscious design, in: India, IAHH, 2003.

[6] D. Trigaux, L. Wijnants, F.D. Troyer, K. Allacker, Life cycle assessment and life cycle costing of road infrastructure in residential neighbourhoods, Int. J. Life Cycle Assess. 22 (2017) 938–951.

[7] R. Flanagan, Carol Jewell, George Norman, Whole Life Appraisal for Construction, Bakckwell science, 2011.

[8] R.T. Marler, J.S. Arora, Survey of multi-objective optimization methods for engineering, Struct. Multidiscip. Optim. 26 (2004) 369–395.

[9] A. Saltelli, S. Tarantola, F. Campolongo, Sensitivity Analysis as an Ingredient of Modeling, Stat. Sci. 15 (2000) 377–395.

[10] The R Project for Statistical Computing, (2015). http://www.r-project.org/.

[11] SIMLAB, Simlab 2.2 software for for Sensitivity and Uncertainty Analysis, IPSC, 2011. https://ec.europa.eu/jrc/en/scientific-tool/simlab-software-sensitivity-and-uncertainty-analysis?search.

[12] M.D. McKay, R.J. Beckman, W.J. Conover, Comparison of Three Methods for Selecting Values of Input Variables in the Analysis of Output from a Computer Code, Technometrics. 21 (1979) 239–245.

[13] Andrea Saltelli, Stefano Tarantola, Francesca Campolong, Marco Ratto, Sensitivity analysis in Practice, John Wiley & Sons, 2004.

[14] D.J. Pannell, Sensitivity analysis of normative economic models: theoretical framework and practical strategies, Agric. Econ. 16 (1997) 139–152.

[15] D.M. Hamby, A review of techniques for parameter sensitivity analysis of environmental models, Environ. Monit. Assess. 32 (1994) 135–154.

[16] P. Heiselberg, H. Brohus, A. Hesselholt, H. Rasmussen, E. Seinre, S. Thomas, Application of sensitivity analysis in design of sustainable buildings, Renew. Energy. 34 (2009) 2030–2036.

[17] H. Christopher Frey, Amirhossein Mokhtari, Tanwir Danish, Evaluation of Selected Sensitivity Analysis Methods Based Upon Applications to Two Food Safety Process Risk Models, in: Releigh & North Carolina: North Carolina State University, 2003.

[18] W. Tian, A review of sensitivity analysis methods in building energy analysis, Renew. Sustain. Energy Rev. 20 (2013) 411–419.

[19] Y. Yildiz, K. Korkmaz, T. Göksal Özbalta, Z. Durmus Arsan, An approach for developing sensitive design parameter guidelines to reduce the energy requirements of low-rise apartment buildings, Appl. Energy. 93 (2012) 337–347.

[20] A.-T. Nguyen, S. Reiter, A performance comparison of sensitivity analysis methods for building energy models, Build. Simul. 8 (2015) 651–664.

CHAPTER 4 SIMPLE MODELS FOR PREDESIGN PHASE OF LARGE SCALE HOUSING PROJECTS

In this chapter simple models, which can be used at a “pre-design” phase, are presented in order to arrive at the first cost estimation. In common practice large scale housing projects are subdivided into different zones and only one dwelling type for each zone is designed (detached houses, terraced houses and apartments). Different non-residential zones (public spaces, commercial facilities and social facilities) are provided. The focus of this research lies on the residential facilities composed of only one type of housing units. Costs are based on design parameters within each zone (street width, combination of street types, technical choices for building elements). For ease of use, a similar approach is used for each zone. The combination of different zones and types should be elaborated and redefined in subsequent steps in the design process, but are not considered in this analysis.

Table of Contents

4.1	**Large scale housing projects**	**57**
4.1.1	Hierarchy of design decision processes in large scale housing projects	57
4.1.2	Street pattern and technological solutions	58
4.2	**Typologies abstracted from observed developments**	**60**
4.3	**Illustration of model approach of the different types**	**63**
4.3.1	Terraced house	63
4.3.2	Apartment	67
4.3.3	Detached house	69
4.3.4	Greens, water areas and filling soil	72
4.4	**Typical materials and technologies**	**74**
4.5	**Conclusions**	**74**

4.1 Large scale housing projects

Large scale housing projects combine residential zones, commercial facilities, infrastructure systems, green-water areas and public spaces. In some cases, the housing projects do not have all of these components because they are located close to good public or commercial facilities. The residential zone is subdivided into smaller models in order to analyse cost and quality. The focus, then, is on different residential types (detached, terraced house and apartment), infrastructure systems and commercial and public areas (Figure 4.1).

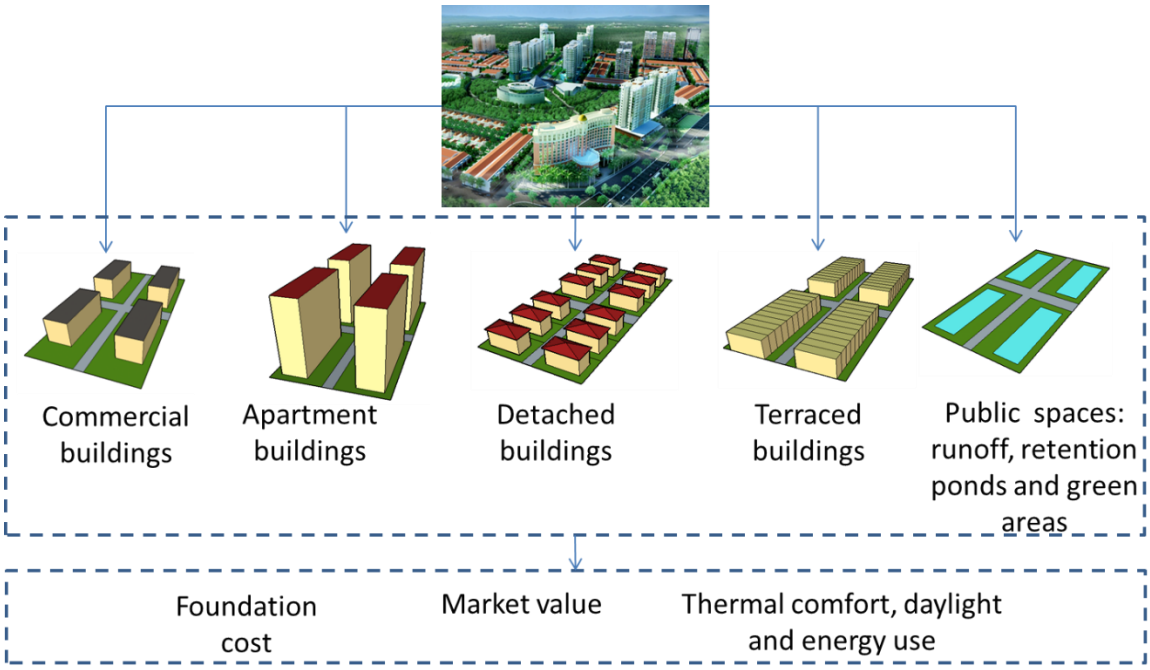

Figure 4.1 Simplified model of the large housing projects.

4.1.1 Hierarchy of design decision processes in large scale housing projects

A common approach to housing projects is location selection, urban planning and architecture elaboration (Figure 4.2). (1) The location influences land cost in the acquisition of agricultural or private land, the cost for provision of infrastructure systems, the cost for sand fill and the cost for the infrastructure to connect to the city centre. (2) The planning and design stages are evaluated on the regulations and norms of housing for new urban areas. (3) Land fill also depends on safety regulations. (4) Developers construct infrastructure systems such as roads,

electricity supply lines, sewage and rainwater evacuation systems as well as water supply systems. The final phase is the actual construction of the facilities.

Step1: Planning and design stage.

Step2: Land fill.

Step 3: Infrastructure provision.

Step 4: Residential and other facilities.

Figure 4.2 Representations depicting the process that large scale housing projects undergo.

4.1.2 Street pattern and technological solutions

The street pattern of each housing project depends upon the natural landscape, its functional requirements and water surface (Figure 4.5). In the schematic models used in the early phase, the street pattern is distributed along three road levels, including a main road which provides access to the area, the road parallel to the building's width (Rw) and the road parallel the building's depth (Rd). The same schematic approach is used for the four building types considered: detached, terraced, apartment and commercial building (Figure 4.3 and Figure 4.4).

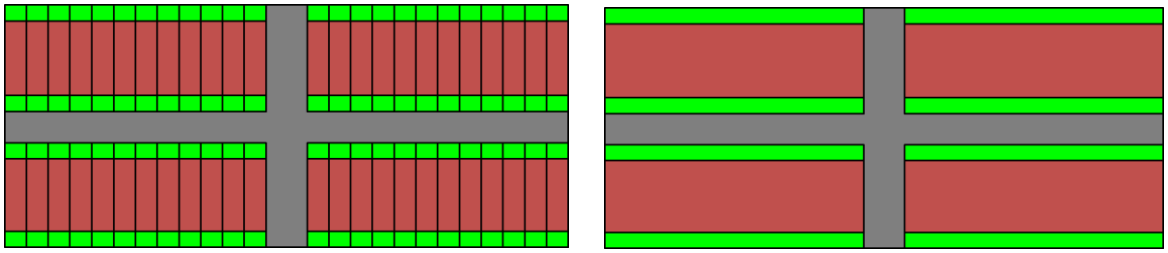

a) Terraced with no shared external walls b) Terraced shared with external walls

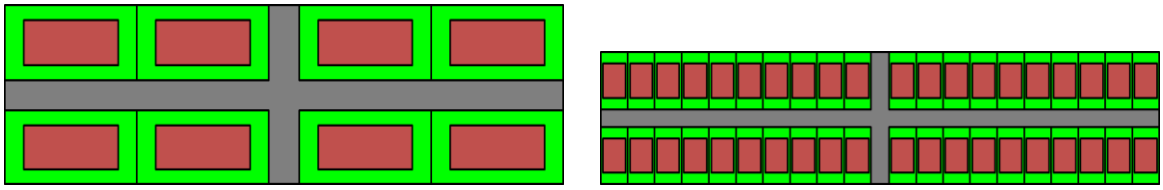

c) Apartment buildings d) Detached houses

Figure 4.3 Schematic graph of dwelling types (detached houses, terraced houses and apartments).

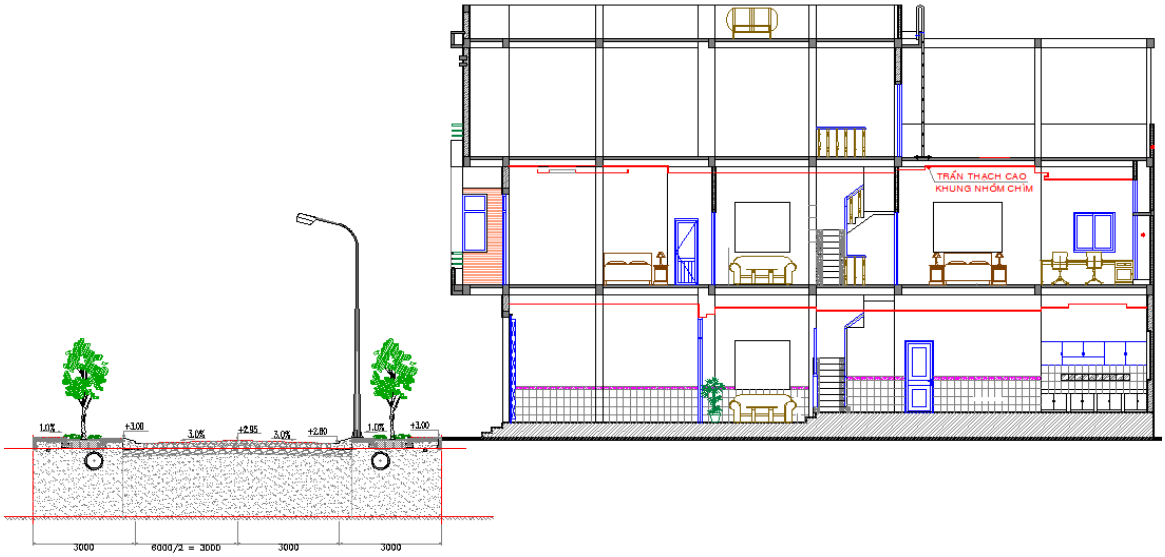

Figure 4.4 Typical example of street typology, setback and cross section of a terraced house

The large scale housing project is simplified into three types of “fragment”: apartment, detached and terraced fragments. The total cost of infrastructure, land acquisition, filled sand areas, water areas and green areas is then calculated.

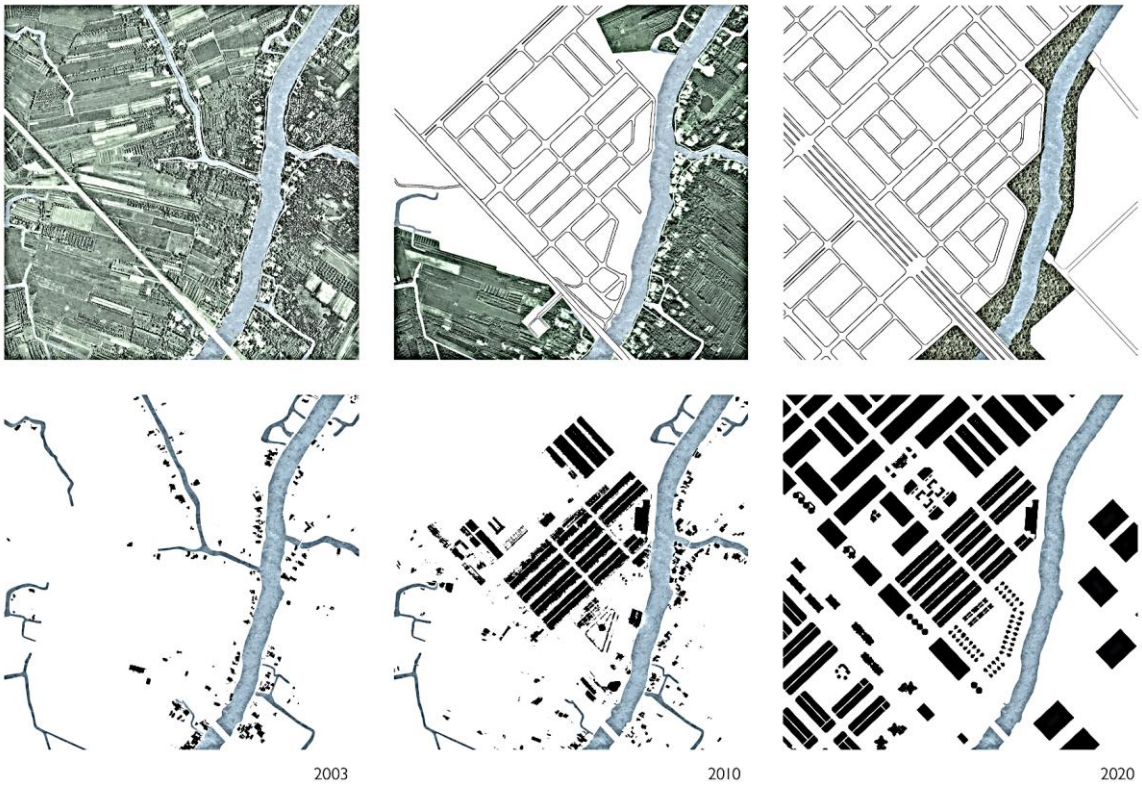

Figure 4.5 Real street pattern and building typology in the large scale housing project, named the 586 project, Cantho city [1]

4.2 Typologies abstracted from observed developments

Three housing types are examined in order to cover the common typologies. Terraced, detached houses and apartments are included in the cost model (Figure 4.6). Detached and terraced housing units, which have three floors, are popular in almost every housing project (Figure 4.7 and Figure 4.8). Apartments with a central corridor, providing only a minimal natural cross ventilation, are also very common (Figure 4.9).

Figure 4.6 Global impression of housing types: terraced, detached houses and apartments collected from different locations.

Figure 4.7 Cross section and view of typical terraced units in Cantho [1]

Figure 4.8 Typical detached unit (Nam Long, D2-26 Street 10, 510m^2)

Figure 4.9 Typical high rise (1,545sqm, 772m^2, 49.9% built-up density, 19 floors, 7.54 ratio between total floor area and residential area, 156 housing units, H=50m, 566 people)

4.3 Illustration of model approach of the different types

Following the input of the global geometry, five aspects of the housing projects can be analysed: population density, circulation density, residential build-up areas, residential-open and the ratio of the following building elements: external walls, internal walls, ground floor and the roof.

4.3.1 Terraced house

The terraced house type can be subdivided into shared external walls, by neighbours and those who have no shared walls with neighbours (Figure 4.10 and Figure 4.11). Double walls is due to the fact that units were built at different times. This type of construction increase the cost of walls and wastes construction material.

Figure 4.10 Terraced houses in the large scale housing project 91B, Cantho.

Figure 4.11 a) Terraced houses do not have shared external walls because they were built at a different time. b) Terraces with external walls are shared by neighbours.

The urban layout of terraced houses is described by using the key parameters, which are as follows: number of floors, width of roads and the width and depth of the building (Figure 4.12 and Figure 4.14). For this simplified urban fragment, the percentages of circulation, residential-open and residential-built-up areas have been calculated by using the element method for cost control [2] and [3].

Table 4.1 Input parameters of terraced house without shared walls

Brief description of project	Value	Unit
Total floor area	225	m^2
Number of floors	3	Floor
Area/floor	75	m^2
Floor height	3	m
Perimeter/floor	40	m
Internal wall/floor	20	m
For building plot	**Value**	**Unit**
Width of plot	5	m
Area of plot	100	m^2
For neighbourhood fragment	**Value**	**Unit**
Number of buildings/row	12	Building
Width of street // W	6	M
Width of street // D	8	m

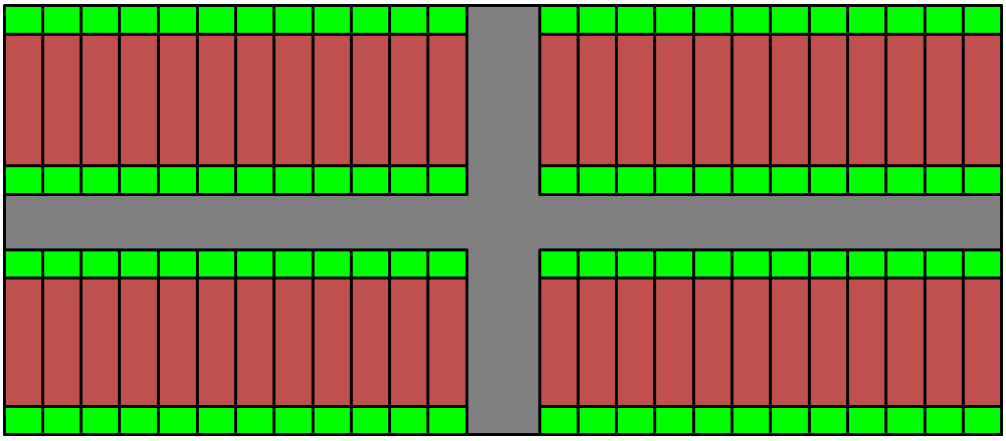

Figure 4.12 Urban form of terraced house, "Tube House" constructed at different times.

Graphical tools are used to visualize the consequences of the design decisions adopted (De Troyer, 2003). The graphical tools can indicate how cost-effective a given project is expected to be. Variants can be tested to reach certain population, circulation density, residentially built up and residential open areas. The area of the external walls in the unshared wall with neighbouring buildings is nearly three times larger than the wall-sharing option (Figure 4.13 and Figure 4.15).

Table 4.2 Input parameters of terraced houses with shared walls.

Brief description of project	Value	Unit
Total floor area	2700	m^2
Number of floors	3	Floor
Area/floor	900	m^2
Floor height	3	m
Perimeter/floor	150	m
Internal wall/floor	405	m
For building plot	Value	Unit
Width of plot	60	m
Area of plot	1200	m^2
For neighbourhood fragment	Value	Unit
Number of buildings/row	1	Building
Width of street // W	6	m
Width of street // D	8	m

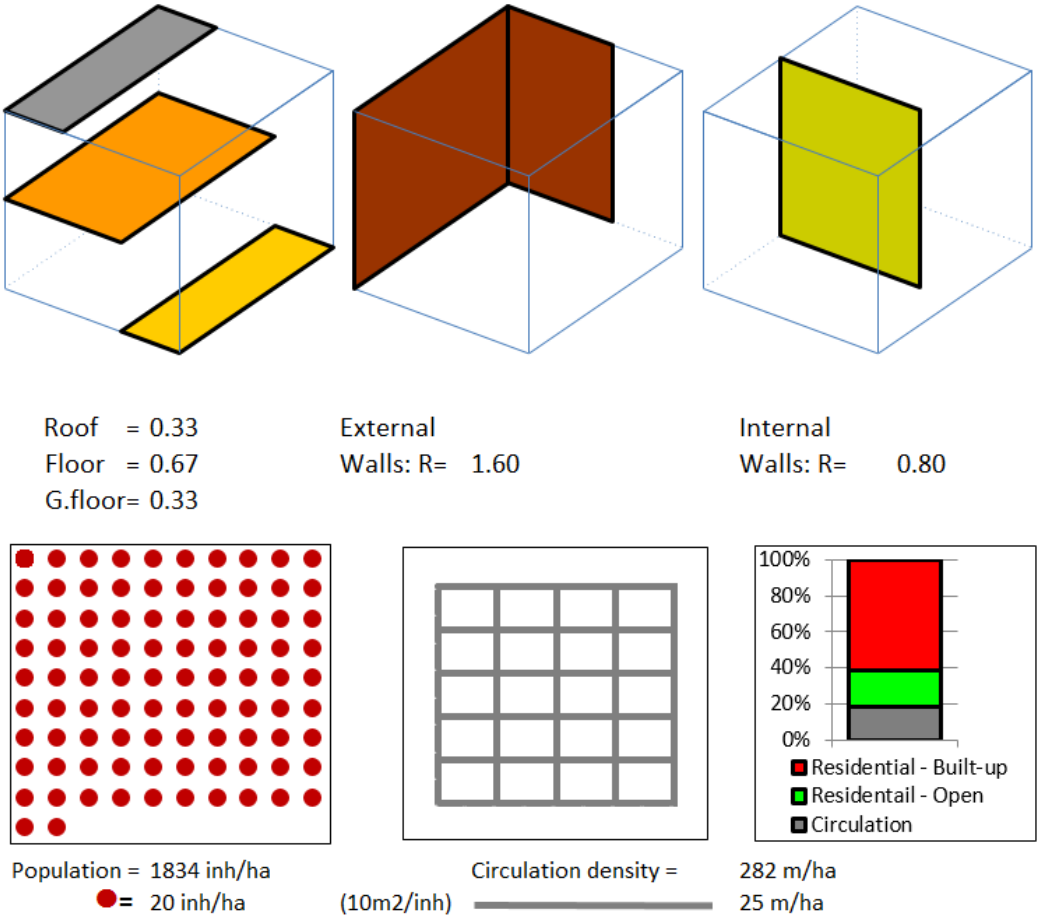

Figure 4.13 Characteristics of urban form of terraced house, "Tube House" constructed at different times.

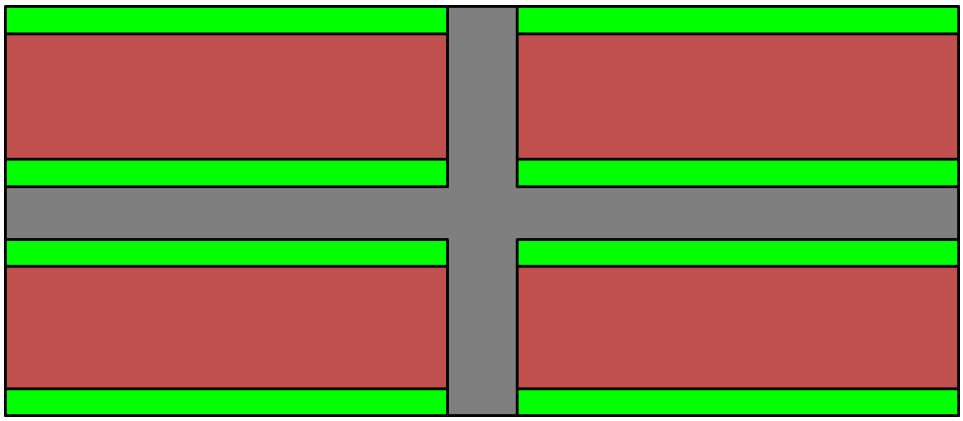

Figure 4.14 Urban form of terraced houses which were constructed at the same time, (L=60m, D=20m, Rl=6m, Rw=8m).

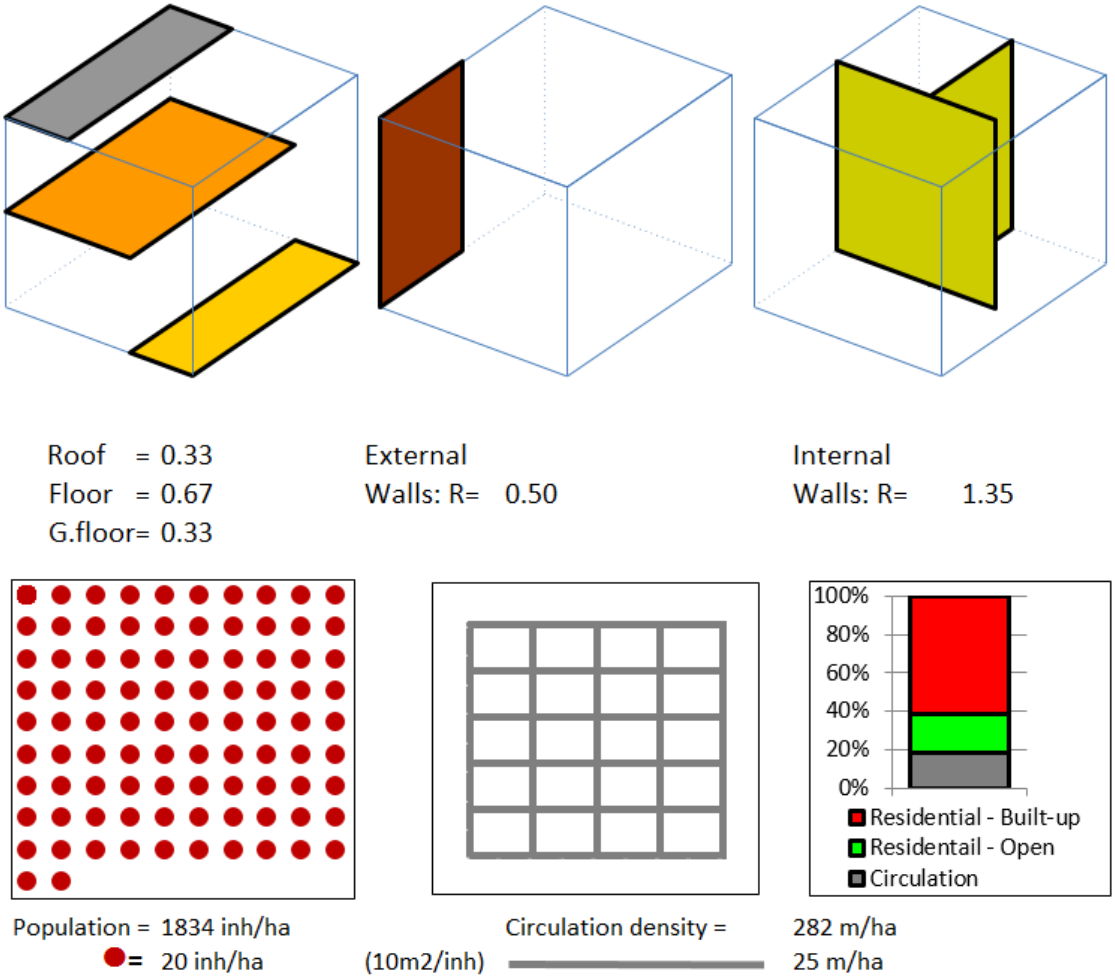

Figure 4.15 Characteristics of urban forms of terraced houses which were constructed at the same time.

4.3.2 Apartment

Investments in apartment has risen in Cantho city, as well as in other cities in the Mekong Delta (Figure 4.16). The variation of apartment typologies is shown in Figure 4.17. Some significant benefits of apartment are their low land cost per square meter floor area and more green area available to the public. Their external wall ratio is the lowest, though, compared to the detached and terraced houses (Figure 4.18). Open spaces or green areas are quite large and can be repurposed for public activities.

Figure 4.16 Five floor apartment in the large scale housing project 91B and Taynguyen Plaza apartment 21 floors at Cantho.

Table 4.3 Input parameters of apartment.

Brief description of project	**Value**	**Unit**
Total floor area	9000	m^2
Number of floors	10	Floor
Area/floor	900	m^2
Floor height	3	M
Perimeter/floor	136	M
Internal wall/floor	364	M
For building plot	**Value**	**Unit**
Width of plot	70	M
Area of plot	2100	m^2
For neighbourhood fragment	**Value**	**Unit**
Number of buildings/row	2	Building
Width of street // W	12	m
Width of street // D	14	m

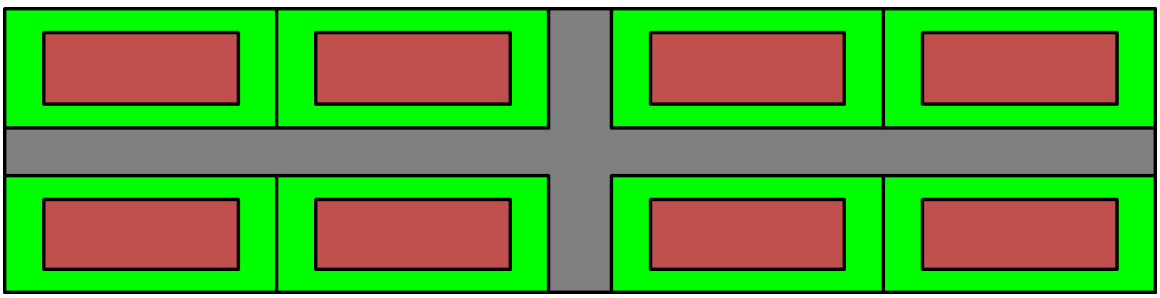

Figure 4.17 Urban form of apartment (5 floors, L=50m, W=18m, Rl = 12, Rw =16m); (Plot: W=30, L=70m)

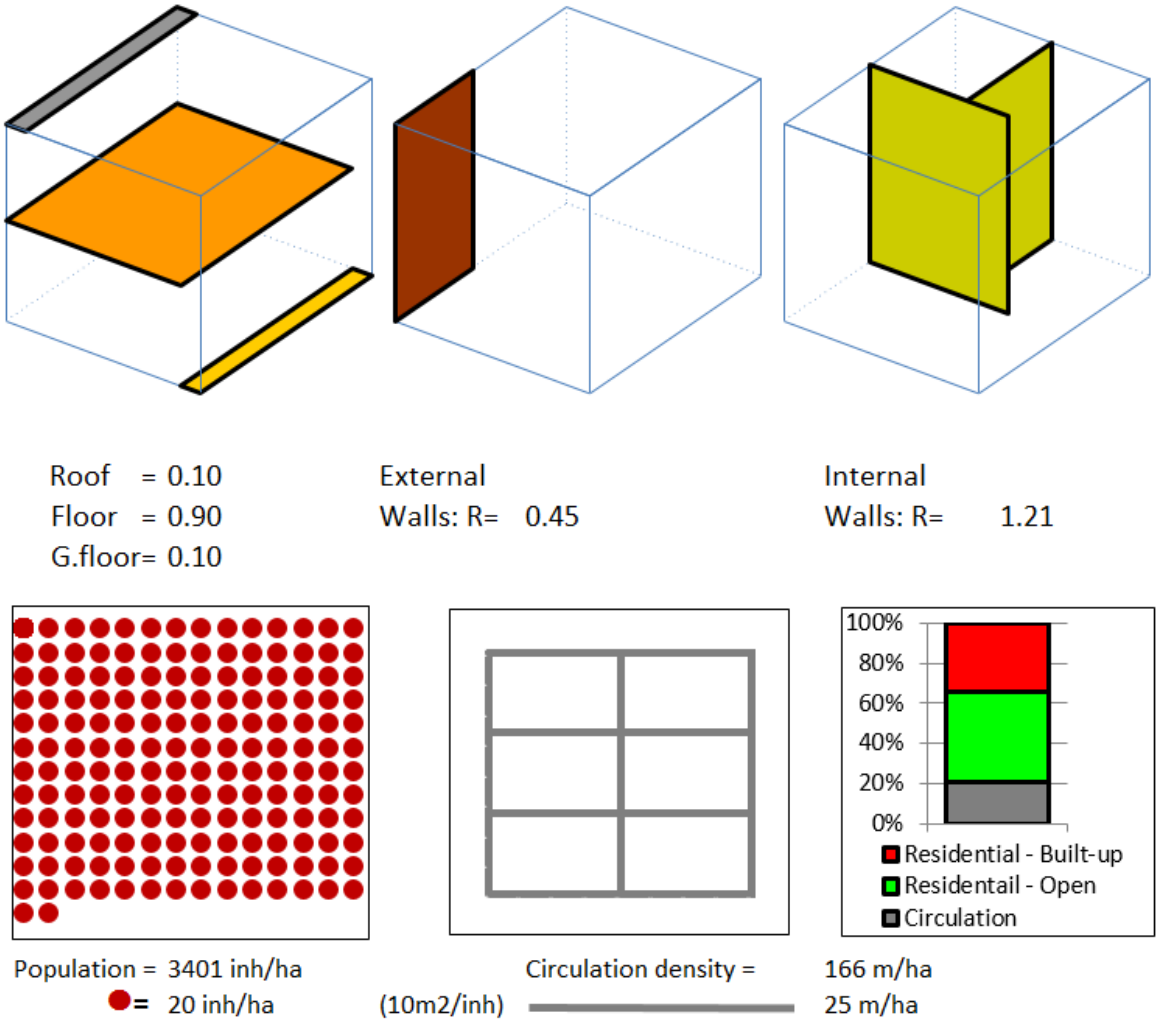

Figure 4.18 Apartment with 5 floors.

4.3.3 Detached house

The urban variation Figure 4.19 of a detached houses are simplified in the schematic models of Figure 4.20. The ratio of external walls is 1.10 and there is a high ratio of green area due to the fact the buildings having more than two facades (Figure 4.21).

Figure 4.19 Detached house in Nam Long project, Cantho

Table 4.4 Input parameters of detached house.

Brief description of project	Value	Unit
Total floor area	360	m^2
Number of floors	3	Floor
Area/floor	120	m^2
Floor height	3	m
Perimeter/floor	44	m
Internal wall/floor	30	m
For building plot		
Width of plot	12	m
Area of plot	240	m^2
For neighbourhood fragment		
Number of buildings/row	10	Building
Width of street // W	6	m
Width of street // D	8	m

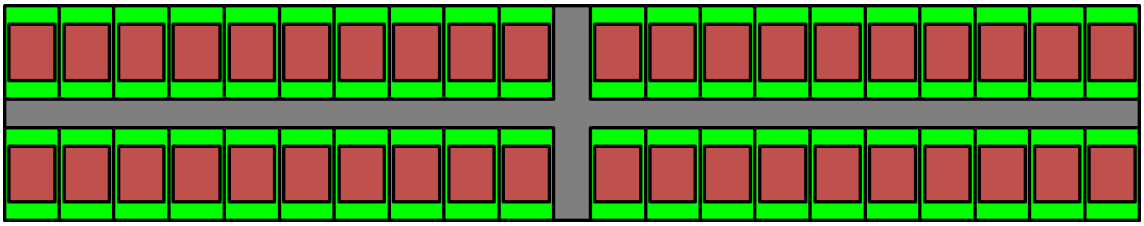

Figure 4.20 Urban form of detached houses.

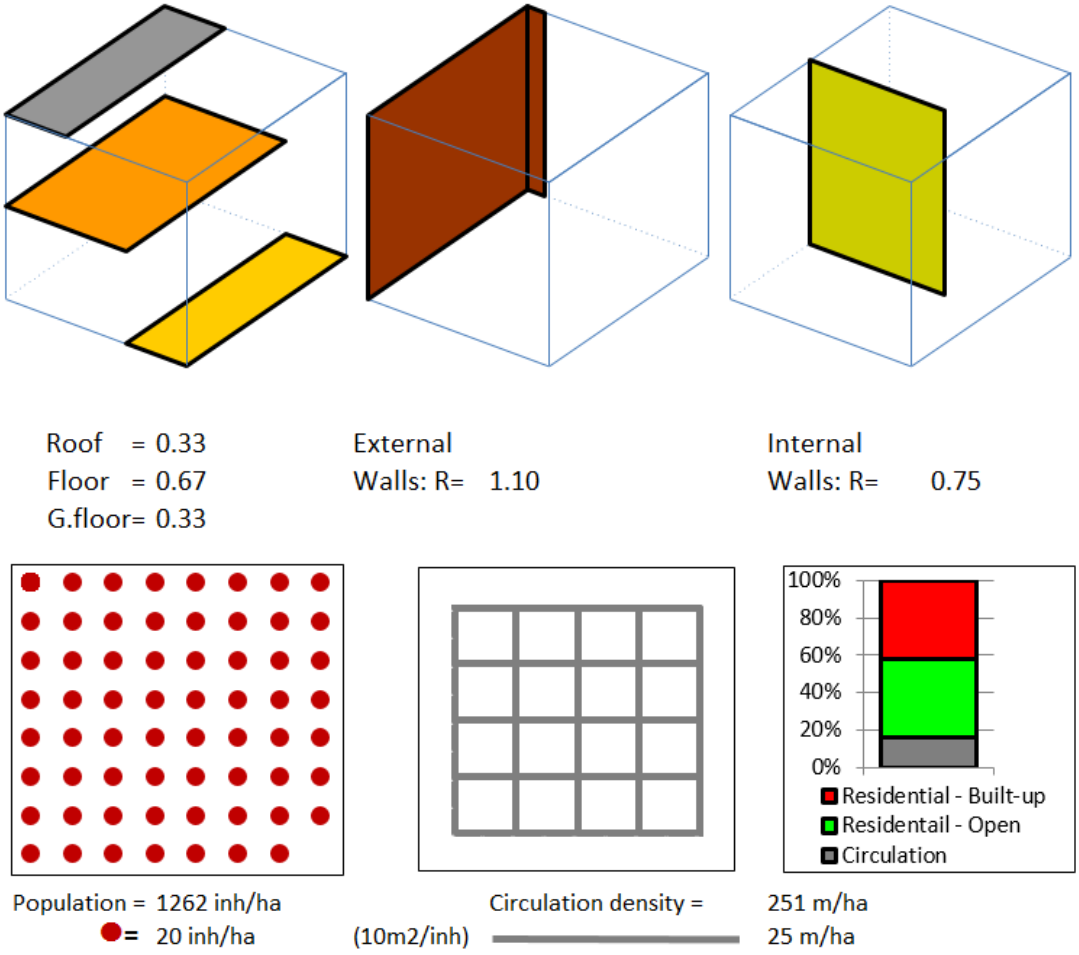

Figure 4.21 A three-floor detached house.

The infrastructure cost of a detached house is, per meter square of floor area, three times higher than an apartment and are represented for the three housing types, Figure 4.22. The cost of the roof and the floor on grade of an apartment is lower than others due to the large number of floors. The cost of internal and external walls (in the case of terraced houses with shared external wall) is similar to the apartment case. This helps to reduce the construction cost of the terraced house.

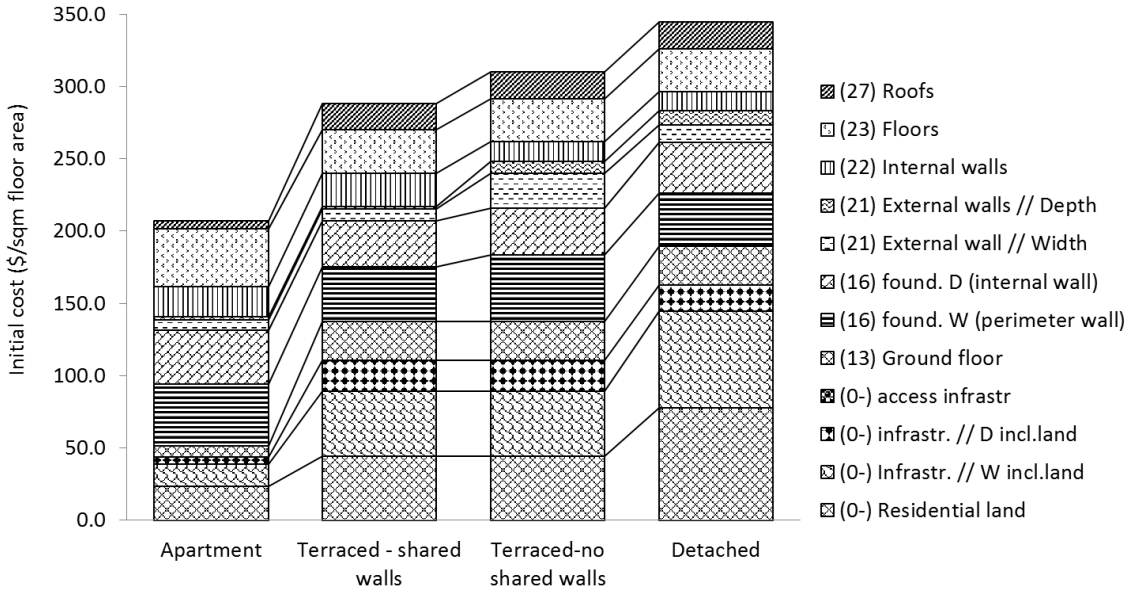

Figure 4.22 Initial cost per m² floor area, including land and infrastructure systems

4.3.4 Greens, water areas and filling soil

Most new housing projects were designed as isolated island connected to already existing roads. More and more it becomes forbidden to fill all existing small rivers and disconnect them from the major rivers. Sand for raising the ground level of the dwelling plots covers either from orchards, small rivers or canals. Asphalted and hardened soils drastically change the soil's permeability, making the existing water management challenges more pronounced (Figure 4.23), [1].

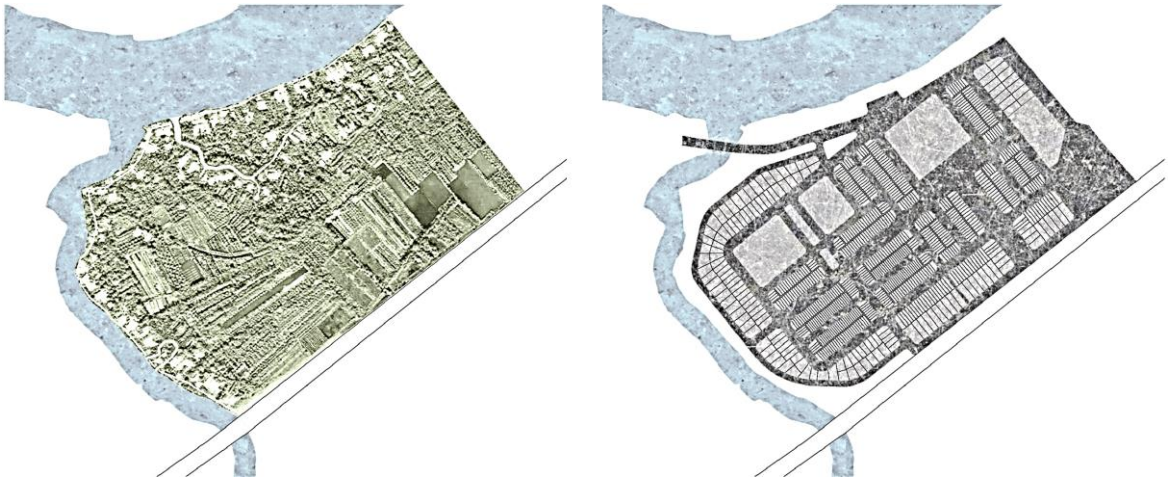

Figure 4.23 The large scale housing project, before and after [1].

For a given case study the research group of Prof. Kelly Shannon described a proposed design alternative as follows: "*that intervention determines the ground relief, water ecology and road infrastructure and proposes a series of public spaces while leaving the rest to be in-filled according to the prevailing and conventional Vietnamese real estate logics*". This approach can conserve existing natural rivers, limit filling areas, create new canals and provide enough local soil to fill the area up to the required safety level (2.7m). The revision to masterplan of Cantho is integrated water management system that has five main principles [4]: as much as possible cut-and-fil balance, space for the rivers, water retention basins, storm water drainage system coupled with road infrastructure and de-centralized water purification systems.

A large amount of river sand has been used to fill in almost all large scale housing projects to date. The average black sand thickness is between 1m and 1.5m, depending on different natural ground levels. The consequence is that this leads to riverbank landslides all along Mekong riverbanks.

Figure 4.24 Filled sand at a housing projects at Cantho [1].

4.4 Typical materials and technologies

Reinforced concrete structures have been used as structural components for almost all of the residential buildings. Clay bricks and concrete blocks are used for masonry work for both external and internal walls. Corrugated iron sheets for roofing (with or without insulation) with some erosion protection layers, clay tiles and lightweight ceiling materials.

4.5 Conclusions

At the early stage designers should have an overview of ranges of elements of a building with its layout. The element method and graphical representation are crucial tool for designers to select a design option. For different housing types, cost of land and infrastructure system is 30% for apartment and 60% for detached building. In this design stage, building layout and urban pattern can be changed easily and avoid a problematic errors that cannot be corrected in the detail design stage. The model can be used like a cost estimate for multiple level from material, element and building up to urban level.

References

[1] P. Eyben, Water Urbanism Cantho: Alternative urban development in Hung Phu, Viet Nam, Master Thesis, KU Leuven, 2011.

[2] F. De Troyer, BB/SfB-plus - Een functionele hiërarchie voor gebouwen, ACCO, Leuven, 2008.

[3] K. Allacker, F. De Troyer, D. Trigaux, T. Geerken, W. Debacker, C. Spirinckx, J.V. Dessel, A. Janssen, L. Delem, K. Putzeys, Sustainability, Financial and Quality evaluation of Dwelling Types - SuFiQuaD - FINAL REPORT, Brussels, 2011.

[4] OSA/WIT/LATTITUDE, Cantho Masterplan Revision 2030, OSA final report (September 2010), (2010).

CHAPTER 5 FOUNDATION COST

High-rise residential buildings has become common practice in many new housing projects as a response to a rapid population growth. In the fertile Mekong Delta, agricultural land is under pressure from residential and other functions. The high-rise buildings reduce land cost per square meter floor area but they require deep pile foundations due to the thick layers of sedimentation.

This chapter describes a cost estimation model for pile foundation as well as for land cost. The model is applicable in the early design stage. As a case study, the soil conditions in Cantho city are examined. The model can support designers, developers and policy makers in the early design stages.

This chapter is based on the publication:

Nguyen Van, T., Nguyen Hieu, T., De Troyer, F. (2016). Managing Pile Foundation and Land Cost for High Rise Buildings in the Early Design Stages. Architectural Engineering and Design Management, 12 (3), 151-169.

Table of Contents

5.1	**Introduction**	**79**
5.2	**Foundation types**	**80**
5.2.1	Shallow and small wood piles	80
5.2.2	Small pile	81
5.2.3	Large pile	81
5.3	**Assumptions and Standards**	**82**
5.3.1	Building height	82
5.3.2	Soil properties	83
5.3.3	Building layout	83
5.3.4	Pile foundation approach	83
5.3.5	Input parameters	84
5.4	**Analysis of methodology**	**84**
5.4.1	Optimal cost per ton capacity of pile foundations	85
5.4.2	Fundamental frequency (building period)	87
5.4.3	Loads upon foundation	89
5.4.4	Correction factor to shear lag effect of the reinforced concrete rigid frame	97
5.5	**Results and Analysis**	**100**
5.5.1	Cost optimal piles for five locations at Cantho	100
5.5.2	Wind load as a function of building height	101
5.5.3	Seismic load as a function of building height	103
5.5.4	Lateral loads transfer to pile foundations	104
5.5.5	Foundation cost integrated with building height and land costs	105
5.6	**Sensitivity analysis**	**107**
5.7	**Parameter study and rules of thumb**	**108**
5.8	**Conclusions**	**109**

5.1 Introduction

In high density areas, a reduction in building foot print can be reached, for the same population density, by erecting higher buildings. In this way more public or green areas can be preserved. In recent years, as an answer to rapid population growth, building high-rise residential buildings has become common practice for many new housing projects. However, the foundation cost per square meter of floor area of high-rise building represents a high percentage of the construction's cost. They can vary, to a significant degree, due to soft soil conditions as well as different loads such as dead, live, earthquakes and wind loads from superstructures. A model to control the unit cost of the element 'foundation' for high-rise buildings, then, is crucial.

Three existing types of cost estimation studies can be distinguished: detailed study, interpolation of statistical data and the simplified glass box models. (1) A detailed cost estimation has been developed for detailed design stage, when crucial decisions have already been made and it is too late to change the project in any significant way. (2) Statistical methods are based on the historical data of constructed buildings [1], [2] and [3]. Models suppose a linear correlation between final cost and design parameters [4], [1], [5], (Lowe et al., 2006), [6], [7], [8] and [9]. The Artificial Neural Networks (ANN) multi-linear and non-linear relationships can be identified between construction costs and parameters [5], [10], [11], [12] and [13]. A study by Tan (1999) describes that the relationship between construction cost and building height has been impacted by technology, building design, demand and institutional factors [2]. A statistical method was used to see the relationship between height and construction cost for the buildings and resulted in a U curve [3], Figure 5-1. These cost models need to be validated and contextualised with historical data, which is expensive to collect and difficult to update. (3) Another approach is the element method for cost control, which was developed as a glass box and which is unlike the black box approach [14]. When building parameters are changed, this can influence ratios and unit rates of elements. Then, the total construction costs are reflected [15] . This method is able to use the building's basic parameters such as width, depth and height to estimate the construction costs. The effects of building height and footprint area on construction costs have also been studied by Chau and his colleagues [16]. The element method can be used to integrate different approaches. Structure and foundation costs calculated can be integrated to the in extended element method for cost control.

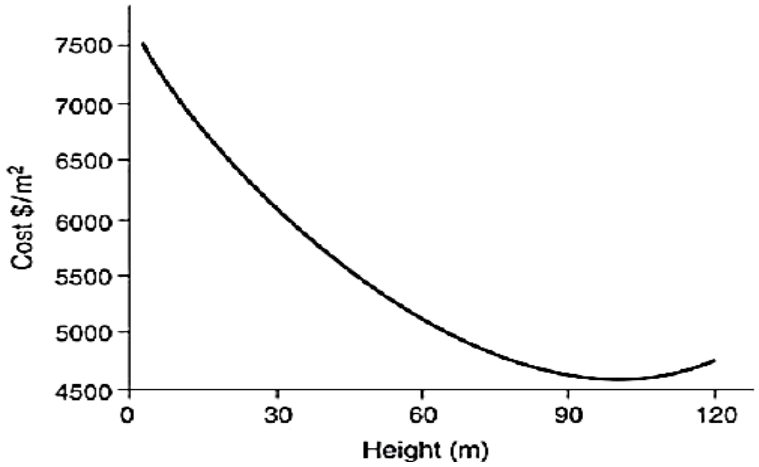

Figure 5-1 Cost $ per square meter of gross floor area vs. height (Hong Kong) [3]

The element method has the capability to consider basic design parameters in the early design stages. However, the integration of the original global layout and the pile foundation for soft soil conditions, into the cost model are non-existent. Hence, the aim of this part is to propose a new method for approximate cost estimation for the pile foundation in a soft soil condition at the early design stage. The cost estimation model is able to integrate various building parameters: height, depth, subsoil properties, wind and seismic loads.

The remainder of this chapter is organized as follows: in section 5.2 the foundation types applied in the region are described. In section 5.3, assumptions and Standards are explained in order to construct the model. In section 5.4 the different steps of the methodology are: the optimal cost per ton capacity of pile foundation, correction factor to shear lag effect of the reinforced concrete rigid frame, loads upon foundation by wind and earthquake and fundamental frequency or building period. In section 5.5 results are reported and discussed in detail. In section 5.6, 5.7 and 5.8, the sensitivity analysis, parameter study and rules of thumb are discussed in order to understand significant parameters and ways by which to use the model and conclusions.

5.2 Foundation types

5.2.1 Shallow and small wood piles

Shallow foundation on soil with a limited stiffness or small wood piles of 7cm to 10cm diameter and 5 meters in length, have been applied for rural, detached buildings with one or two floors, Figure 5-2.

Figure 5-2 Small melaleuca wood piles. Melaleuca grows very fast in The Mekong Delta.

5.2.2 Small pile

Small reinforced concrete piles have sections of between (25 * 25 cm) and (40 * 40 cm). In the urban areas, they are installed by using the compression method. A load of about 50 to 150 tons is used with hydraulic jacks (Figure 5-3). This approach can control for the quality of the piles but the construction cost can remain high as a result.

Figure 5-3 Installing reinforced concrete piles using the compression approach.

5.2.3 Large pile

Large diameter piles are used for heavy structures, such as bridges, high-rise buildings and industrial buildings (Figure 5-4). Their diameters vary from between 0.4m and 2.5m. Soft soil conditions may lead to this foundation option being selected. Due to the section, the installation of steel reinforcement, the pouring of concrete and the control of concrete quality may also be difficult.

Figure 5-4 Large diameter pile foundations for heavy structures.

5.3 Assumptions and Standards

5.3.1 Building height

This study focuses on high-rise buildings with rigid reinforced concrete frames. The number of floors varies from 2 to 25 floors and 3.6 m floor height is initially chosen. The limit to 25 floors is based on the high-rise buildings standard in Vietnam [17]. Moreover, the maximum height of reinforced concrete rigid frames should be about 20 to 25 floors [18], because economical rigid frames for buildings is up to approximately 25 stories, above this height their drift resistance is costly to control [19]. Other structure systems should be used when buildings are in excess of 25 floors (Figure 5-5).

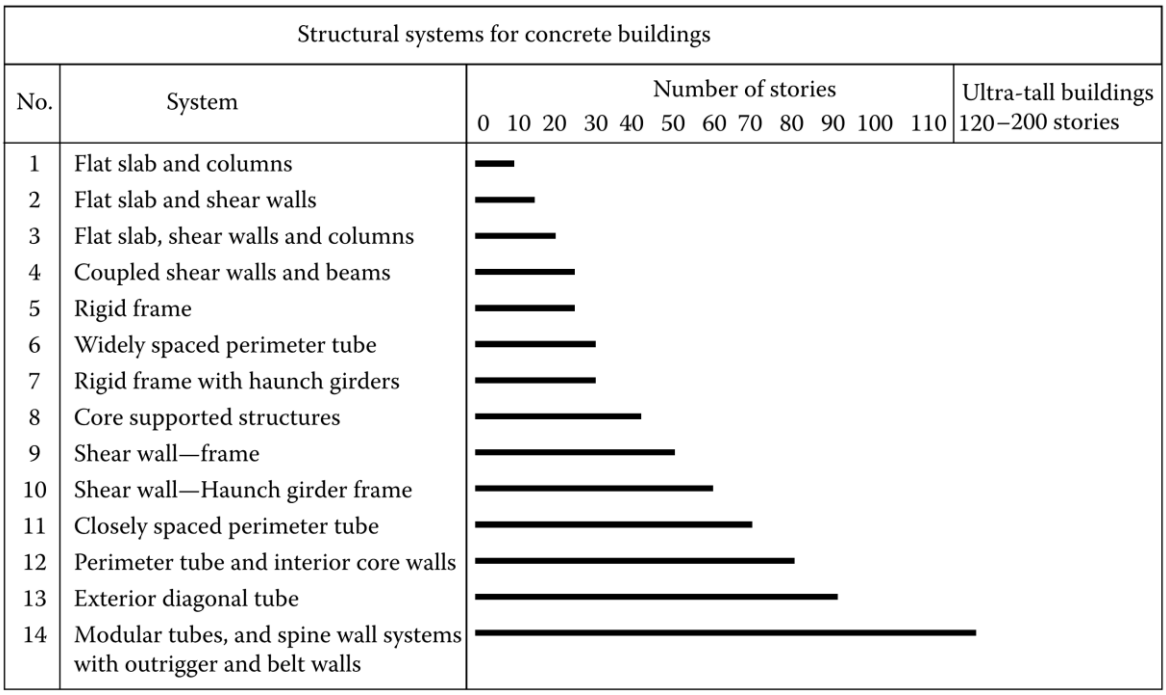

Figure 5-5 Structural systems categories [19].

5.3.2 Soil properties

Traditional methods to obtain soil properties are applied, which include soil samples, standards penetration test (SPT), cone penetration tests (CPT) pile static and dynamic load tests on sites. The CPT for the estimation of static axial pile bearing capacity is the most common situ tests for soil properties. CPT is the most applicable soil tests for analysing pile foundations because of its simplicity, rapid applicability and cost effectiveness [20] and [21].

5.3.3 Building layout

Rectangular floor plans are chosen because plan forms, such as L, I, H, U, Z and □ shapes, can be combined from the simple rectangular building layouts with settlement joins. Firstly, damages due to vertical settlement differences of different blocks can be avoided by settlement joints to separate building blocks with differing loads. Secondly, different soil properties in different positions in built up areas can occur, resulting in different vertical settlements. Thirdly, the natural frequencies of these structures depend on detailed floor plans, specific loads and exact height are very specific case by case.

5.3.4 Pile foundation approach

In Cantho city and in other similar cities in the Mekong delta area, pile foundations for high-rise buildings have been commonly constructed by compressed and bored piles. The bored piles can maximize soil bearing capacity. Nevertheless, more complex technologies

and heavy construction equipment must be used to manage their quality which leads to high construction cost. Bored piles, therefore, should only be used for heavy load foundations, such as bridge foundations. Compressing piles, with a square section of between 25 cm and 40 cm are chosen for analysis in this study, based on the pile foundation design standard [22].

5.3.5 Input parameters

Input parameters are subdivided into four groups. Firstly, structural parameters are the number of bays, width of the bays, columns and beam sizes, floor thickness, number of floors and soil properties. The next group is finishing elements including external and internal walls. The third group is load type and consists of wind, seismic, live and dead loads. The live load is 300 kg/m^2 floor area for all kinds of functional rooms, based on [23]. The density of reinforced concrete is 2,500 kg/m^3. The clay brick wall has a density of 1,500 kg/m^3. The wind pressure in Cantho city is 95 kg per square meter. The average ground acceleration is 0.0669 m/s^2. The final group includes land costs at different locations. Land costs for new urban areas in Cantho city, including infrastructures such as sewerage, electricity and road systems, can be found in official documents and in free market transactions. The construction cost of pile foundations are also based on market rates as of 2011. The average USD exchange rate used is 20,000 VND.

5.4 Analysis of methodology

The cost model is elaborated in six steps (Figure 5-6). (1) The cost of optimal size (section and length) can be obtained and depends on soil characteristics and cost of reinforced concrete piles with different sections. (2) The vertical loads (including live and dead loads) are then calculated. (3) The dynamic horizontal loads from wind and seismic activity loads were transferred to the pile foundations. (4) All load cases are combined to find the worst case scenario. (5) The total cost of both pile foundation cost and land cost, per one square meter floor area, is estimated in order to look for the building's optimal layout. (6) The sensitivity of the model for the parameters estimated is analysed by using the Latin Hypercube Sampling (LHS) method [24] and [25].

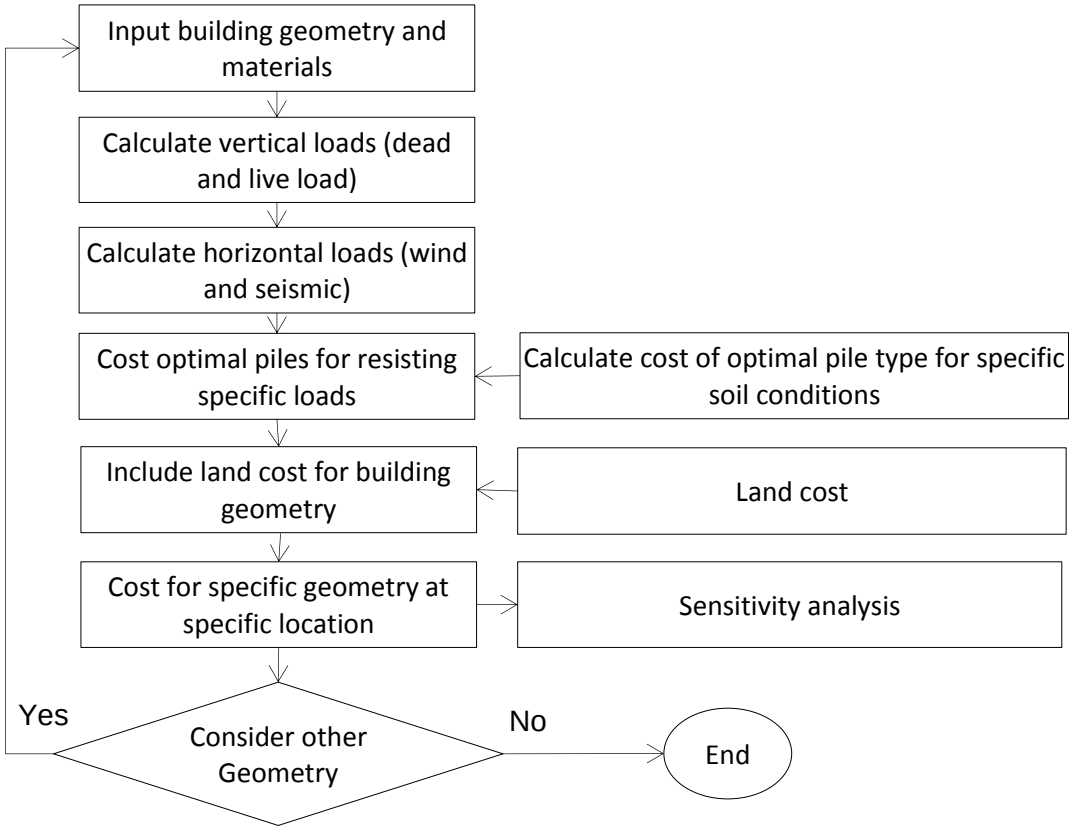

Figure 5-6 Analysis procedure of the pile foundation cost model.

5.4.1 Optimal cost per ton capacity of pile foundations

The general lines of the method can be described as follows: The first point concerns the friction resistance of the soil, as measured through CPT, Figure 5-7, a). Based on this, the total resistance for a specific section over the whole length is calculated (Figure 5-7**,** right, left line: soil capacity curve Ps). This resistance is different for different sections since their surface areas are different and will increase depending on the depth. The compressive strength of the cross section of a pile is calculated for a selected concrete type and reinforcement fraction. An empirical reduction fraction is applied, from certain slenderness points on (pile length over size of square pile), in order to take the slenderness of pile into account (see Table 5-1). The soft soil offers no significant lateral support. This leads to a maximal pile capacity, as represented in Figure 5-7 b): right line, Pp. The bearing capacity reduces with the depth. At the intersection point of both curves (Ps and Pp) the maximum capacity of the pile is obtained in line with the soil's capacity to support this load. The procedure is repeated for each section, since the basic compressive strength is different for each section and the slenderness factor is also different.

Table 5-1 Slenderness ratio of piles, M. Jacobson

λ=L/r	50	70	85	105	120	140
φ	1	0,8	0,59	0,41	0,31	0,23

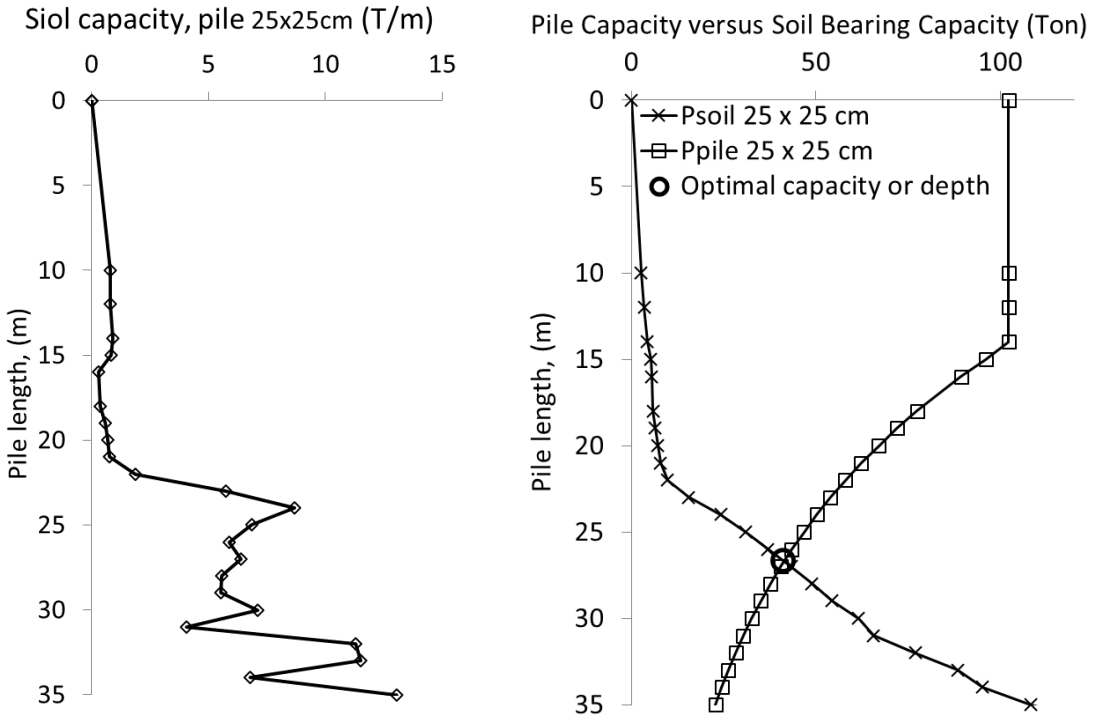

a) *b)*

Figure 5-7 The optimal length pile based on soil capacity; P_{soil} 25 x 25 cm: the pile capacity based on soil properties for pile with section 25 x 25 cm; P_{pile} 25 x 25 cm: the pile capacity based on reinforced concrete piles with section 25 x 25 cm.)

The cost per the running meter pile depends on the following parameters: (1) the quantity of steel and concrete per running meter, (2) on the cost of driving the pile into the soft soil with a hydraulic press. The cost per running meter is proportional to the section of the pile. The total cost is obtained by multiplying the length at maximum capacity and the unit rate per meter. By dividing the cost by the bearing capacity the cost per ton at the maximum load for each of the sections considered is obtained. If from a given depth on no additional soil resistance is measured by CPT (due to the fact that the layer below that point offers no additional support) maximum load is limited to the soil resistance at that depth (below the maximum pile resistance). Since soil characteristics are different at different

locations, the cost per ton for different piles, all used at maximum capacity, should be plotted for every single location (Figure 5-8). The different optimal depths for various pile sections provide data to obtain appropriate pile section based on their unit cost per kN capacity. Once the total load for a given building is obtained, the foundation should be designed with a combination of the most cost-effective piles. If both curves, P_s and P_p, do not intersect then the smallest bearing capacity for both of them is chosen for the optimal cost.

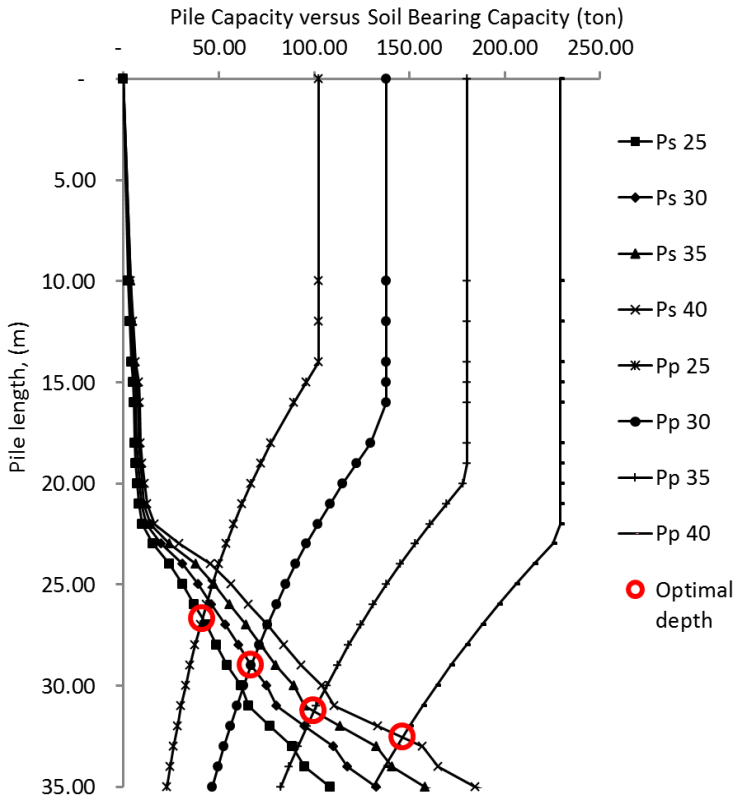

Figure 5-8 Optimal depth or capacity of different pile sections. P_s 25: the pile capacity based on soil properties for pile with section 25 x 25 cm; P_p 25: the pile capacity based on reinforced concrete piles with section 25 x 25 cm.)

5.4.2 Fundamental frequency (building period)

"Natural frequency" or the "period" of building is a critical parameter in the seismic design of buildings because of the strong effect on the seismic load's magnitudes. The natural frequency depends on the stiffness and mass of the high-rise building and affects the values of the lateral loads from both the wind (dynamic load of wind) and the earthquake. Therefore, the stiffness should be designed not only to resist small lateral loads but also to limit the roof displacement to avoid discomfort for the occupants based on the movement. The seismic load dramatically increases during the first stage of the spectrum**.** A

compromise between stiffness and flexibility of structural systems is a significant issue that should be solved in the early design stage.

The natural frequencies can be calculated accurately by the finite element method. This approach requires detailed structural data from buildings and a huge calculation time to simulate large numbers of frame cases because we have to modify input data for each design alternative. However, a simple method to estimate the critical frequency of a wall-frame building was developed with an average absolute error from between 1.6% and 7% for individual frameworks [26]. Statistical methods or empirical formulas are implemented in most building codes. Goel and Chopra proposed the empirical relation for the fundamental period: $T_{G-C} = 0.053*H^{\wedge 0.9}$ [27]. The European earthquake design code [28], proposed the formula of building period is $T=Ct*H^{\wedge 0.75}$. Where Ct is 0.085 for moment resistant space steel frames, 0.075 for moment resistant space concrete frames and 0.50 for eccentrically braced steel frames. H corresponds to the total height of buildings in meters. These approaches are suitable for moment-resisting framed structures. For shear wall buildings, the effect of the wall elements should also be considered. Shear walls are also strongly affected on the fundamental period. Thus, Amant and Hoque propose the following empirical expression for the evaluation of the period:

$$T_{A-H} = \alpha_1 * \alpha_2 * \alpha_3 * C_t * H^{\wedge 0.75}$$

Where C_t is 0.073 for reinforced concrete buildings and α_1, α_2 and α_3 are modification factors along a seismic action direction in relation to the in-fill panel span, number of spans and the amount of infill walls (Figure 5-9) [29]. The relationship between these three methods is shown in Figure 5-10. In future research, the simple empirical formula should be used to obtain the building periods, $T=0.075*H^{\wedge 0.75}$ (Eurocode).

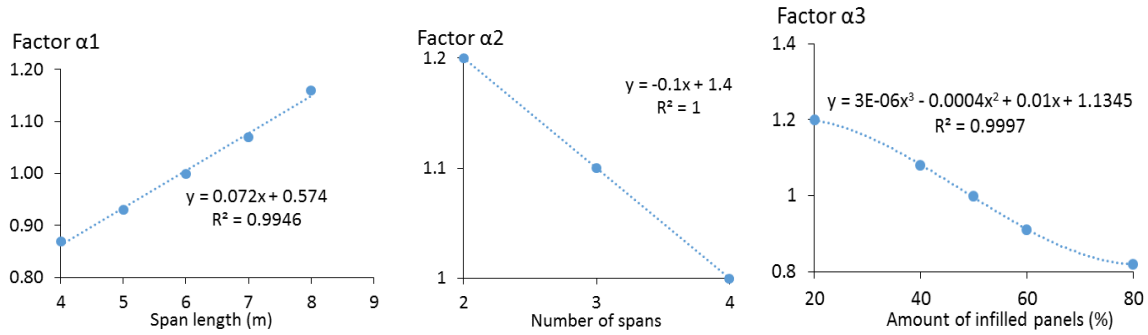

Figure 5-9 Here, α1 is the modification factor for span length, α2 is the modification factor for number of spans and α3 is the modification factor for amount of infill.

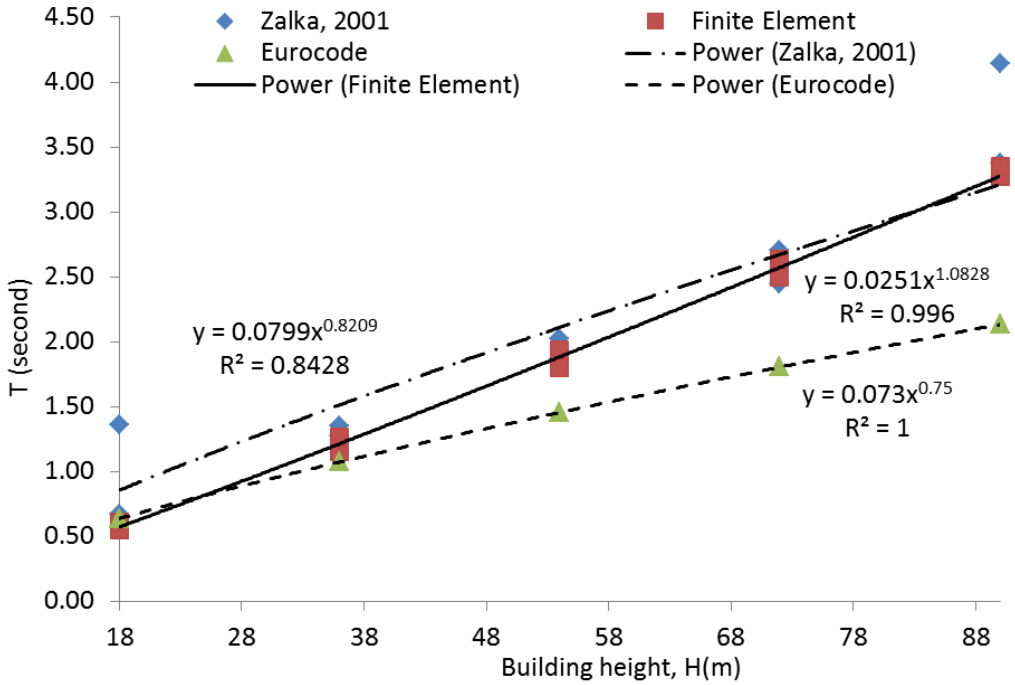

Figure 5-10 Three methods for estimating building periods related to their heights

5.4.3 Loads upon foundation

The aim of the method described in this section is to determine the horizontal and vertical loads on the foundation of high rise buildings, in line with Vietnamese standards which are based on Eurocodes. The parameters describing a building with a rectangular floor plan will be the height, width and depth and the span between columns in both directions (a regular spacing is assumed).

5.4.3.1 Vertical loads: dead loads and live loads

Vertical dead loads are described for common materials (concrete, masonry, tiles) and sections (for walls, floors, beams and columns). The density of reinforced concrete is 2,500 kg/m^3. The clay brick wall has a density of 1,500 kg/m^3. Vertical live loads are predicted by standards [23]. 300kg/m^2. The live load for people and furniture is 300 kg/m^2 floor area for all kinds of functional rooms, based on.

5.4.3.2 Wind load

The wind load, which includes dynamic and static components, was also considered in the calculation process. The procedure to calculate the wind was based on the EN 1991-1-4. The static and dynamic components were obtained by code's second procedure which

provided more reliable results than the first procedure [30]. The formula for wind force was also represented (Eurocodes, 2004).

$$Fw_i = c_s * c_d * c_f * q_p(H_i) * A_i$$

Where:

- $C_s * C_d$ is the structural factor should take into account the effect on wind actions from the non-simultaneous occurrence of peak wind pressures on the surface together with the effect of the vibrations of the structure due to turbulence;
- C_f is the force coefficient for the structure or structural element is related to building layout;
- $q_p(Hi)$ is the peak velocity pressure at reference height Hi, which includes mean and short-term velocity fluctuations, should be determined.
- A_i is the reference area of the structure or structural element.

All components in this formula are defined and their calculated procedures are also explained in (Eurocodes, 2004).

The European wind design code and Vietnamese design standards apply wind speeds as an average over ten minutes registered over a 50 year period. Design wind velocity is 38.8 m/s. The wind pressure in Cantho city is 95 kg per square meter in urban areas.

The wind speed increases, in a parabolic way, with the height and is influenced by the roughness of the terrain (Figure 5-11). For every floor, one must consider total wind force proportional to the facade area (storey height) operating at a specific height. The moment, at the foundation level, is the sum of moments for each floor (Figure 5-12).

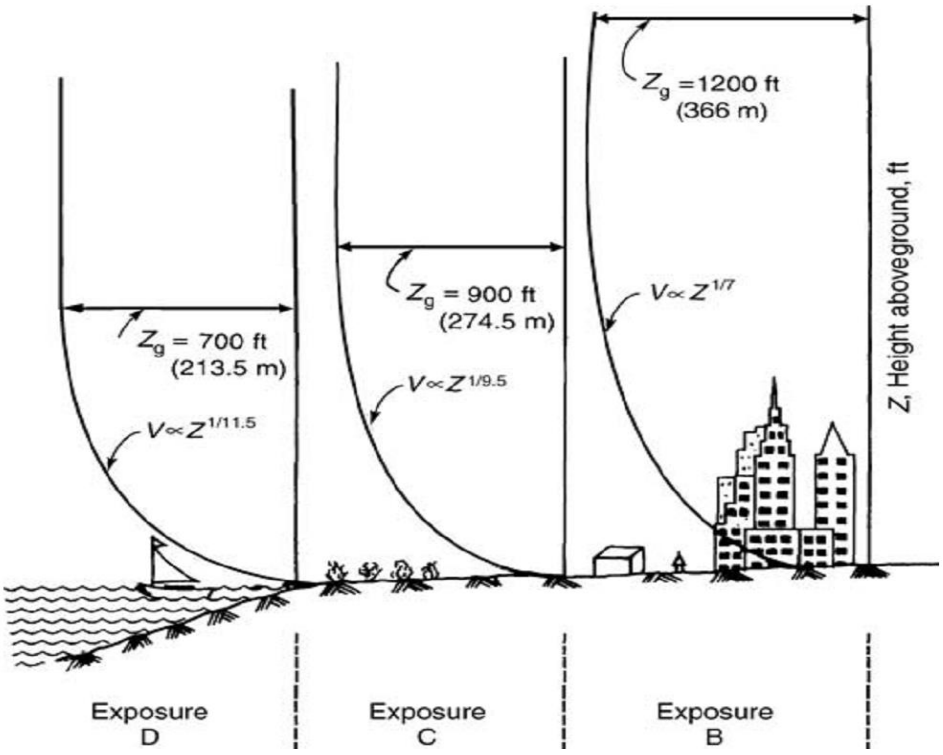

Figure 5-11 Influence of exposure terrain on variation of wind velocity with height. Exposure D: Flat, unobstructed areas and water surfaces outside hurricane-pone regions; Exposure C: open terrain; Exposure B: urban and suburban terrain.

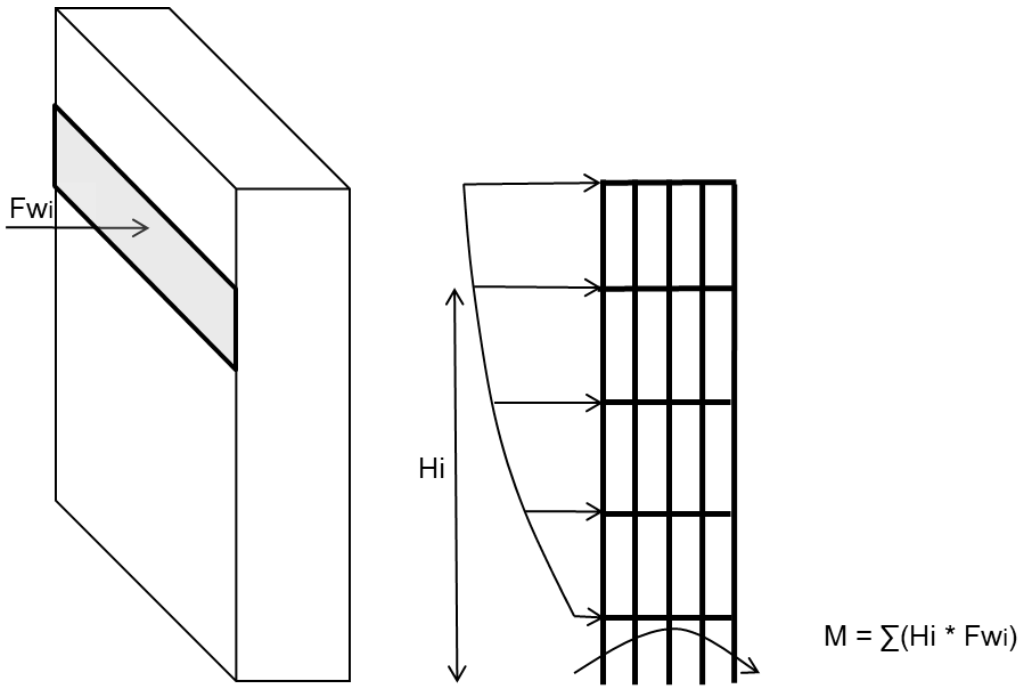

Figure 5-12 The wind load and vertical axial forces of columns at the ground floor with or without the shear lag phenomenon.

5.4.3.3 Response spectrum approach

Response spectrum

The response spectrum was introduced by Biot [31]. He proposed a standard spectral curve based on historical data of the ground accelerations for evaluating a maximum effect on structures [32]. The response spectrum can be understood as an approximate curve of peak responses on top of various recorded ground accelerations. Then this plot can be used to select the responses of linear structures of the buildings when their fundamental frequencies of oscillations are estimated by analysing the structure system during the early design stage.

In the seismic design, an appropriate response spectrum curve has a form as shown in Figure 5-13 [33]. The spectrum must be constructed based on three key points which are the peak ground acceleration S_0, the region of maximum spectral demands (S_m between period T_m and period T_n) and finally a description of the spectral demands larger than period T_n.

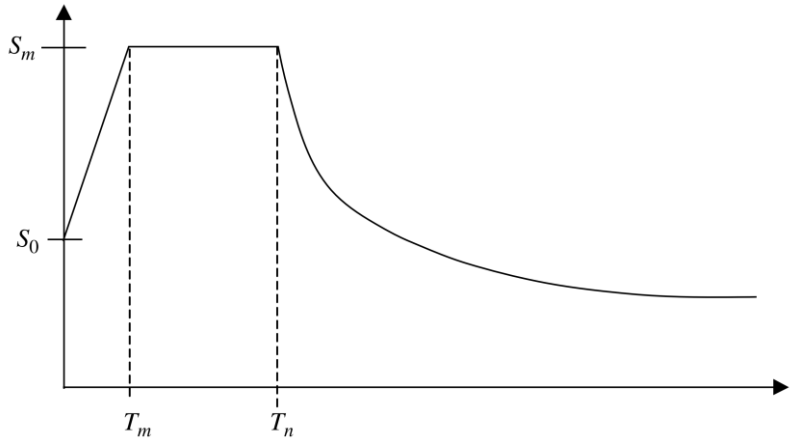

Figure 5-13 Key parameters in design response spectrum [33].

Response spectrum analysis procedure (RSA)

A complex analyses of dynamic responses based on the response spectrum was explained by Hudson [34]. The response spectrum analysis procedure of CEN code is shortly explained in this part. This procedure is to estimate the design spectrum of the peak response of the building for a response spectra of ground by choosing the value from the ground spectrum for the appropriate frequency range. The natural frequency (fundamental frequency) of the building is inside this range. The natural frequency of the building is

calculated by the equation T=0.075*H^0.75, where H is the building height (m). The elastic response spectra of ground for different ground types from type A to type E is visualized in the Figure 5-14 based on the Table 5-2. The building fundamental frequency (T) was calculated for the next step. This frequency value is compared with the constants of spectral acceleration branch T_B, T_C and T_D in order to select a formula to calculate design spectrum $Sd(T_1)$ as those equations that are indicated in the following part. This procedure is followed the Eurocode 8 [28].

$$0 \le T \le T_B: \quad S_d(T) = a_g * S * \left[\frac{2}{3} + \frac{T}{T_B}\left(\frac{2.5}{q} - \frac{2}{3}\right)\right]$$

$$T_B \le T \le T_C: \; S_d(T) = a_g * S * \frac{2.5}{q}$$

$$T_C \le T \le T_D: \; S_d(T) = \begin{cases} = a_g * S * \frac{2.5}{q} * \frac{T_C}{T} \\ \ge \beta * a_g \end{cases}$$

$$T_D \le T: \qquad S_d(T) = \begin{cases} = a_g * S * \frac{2.5}{q} * \frac{T_C * T_D}{T^2} \\ \ge \beta * a_g \end{cases}$$

Where

a_g is the design ground acceleration on type E ground ($a_g = \gamma_I.a_{gR}$);

T_B is the lower limit of the period of the constant spectral acceleration branch;

T is frequency of building;

T_C is the upper limit of the period of the constant spectral acceleration branch;

T_D is the value defining the beginning of the constant displacement response range of the spectrum;

S is the soil factor;

β is the lower bound factor for the horizontal design spectrum, β = 0.2;

q is the behaviour factor taking into account for the non-linear response of the structure, associated with the material, the structural system and the design procedures.

Table 5-2 The values of S, T_B, T_C and T_D of the elastic response spectra

Ground types	S	T_B(s)	T_C(s)	T_D(s)
A	1.00	0.15	0.4	2.0
B	1.20	0.15	0.5	2.0
C	1.15	0.20	0.6	2.0
D	1.35	0.20	0.8	2.0
E	1.40	0.15	0.5	2.0

Note: Ground types may refer to Eurocode 8

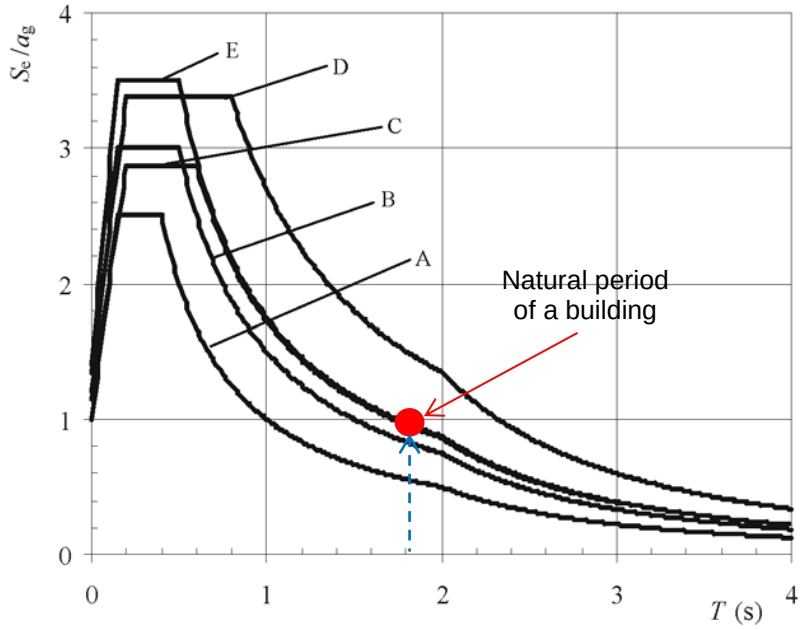

*Figure 5-14 Recommended elastic response spectra for ground types A to E (5% damping), [28]. The circles on curve E are different natural periods of the different building heights, T=0.075 * H^0.75, (Eurocode 8 [28].*

5.4.3.4 Seismic load

In the Mekong Delta area, seismic activities, ground acceleration or ground motions are relatively uncommon. Therefore, buildings have not been considered to require anti-seismic infrastructures by most designers for low seismic activity cities, such as in Vietnam [35]. However, they did not consider of seismic hazards from distant earthquakes. Unforeseen damages of the high-rise buildings may occur where the seismic loads have not been carefully considered. Damage from the seismic effect can reduce the life cycle periods of buildings.

Although estimating earthquake loads is a complex procedure, loads should be estimated in the cost estimation model at the early design stages. This study selected the seismic design procedure of EN 1998-1:2004 [28]; Vietnamese seismic design is also based on the same standard. This standard supports earth acceleration data for Vietnam. Data are available at a district scale throughout the whole country from 2006 forwards [36], (Figure 5-15).

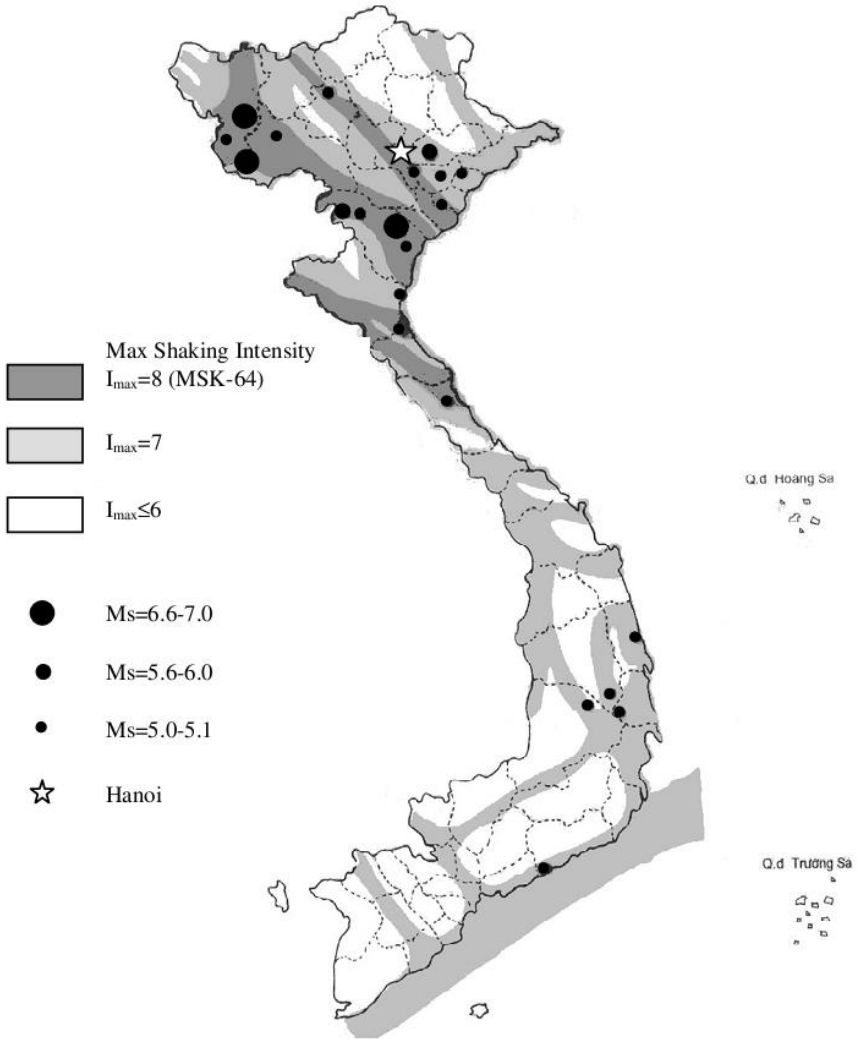

Figure 5-15 Ground acceleration (m/s²) zone map of Vietnam [35]. The study area is located in zone Imax = 7 and Imax ≤ 6.

An earthquake can generate complex dynamic transformation. Detailed simulations have shown that for the size, mass and the structural characteristics, the first transformation of the building structure is the most critical. The building period can be estimated by the traditional method: T (second) = 0.075 * H^ (3/4), [28]. The procedure for the whole building

is as follows: the mass of each floor and the walls going half a floor up and for half a floor below are concentrated in one point. The impact force Fi depends upon the height based on the following formula:

$$Fs_i = F_b \frac{H_i.m_i}{\sum H_i.m_i}$$

Where:

F_i is the horizontal force acting on storey i;

F_b is the seismic base shear;

m_i is the storey masses;

H_i is the heights of the masses m_i above the level of application of the seismic action (foundation or top of a rigid basement).

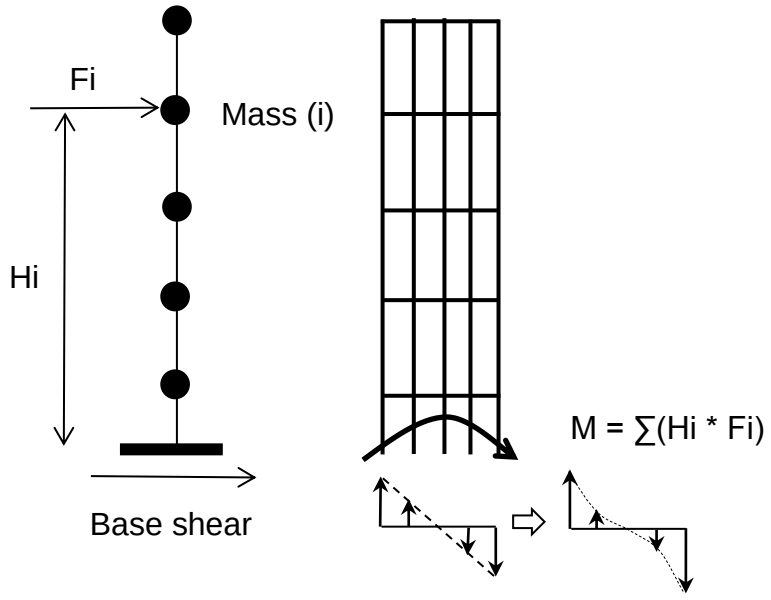

Figure 5-16 The seismic load and vertical axial forces of columns at the ground floor with or without the shear lag phenomenon.

The moment at the foundation is the sum of all of the moments generated by the forces of each of the concentrated masses. Thus the sum of the moments generated by the shear forces of each floor determines the moment at the foundation (Figure 5-16). This procedure to calculate the horizontal force for each floor height is based on ground type E of the CEN standard [28], represented *for soft soil condition at Cantho and calculating*

*seismic load for the elastic response spectrum (*Figure 5-14*). In this case, t*he average ground acceleration at Cantho is 0.0669 m/s^2.

5.4.4 Correction factor to shear lag effect of the reinforced concrete rigid frame

Frame deformations are generated by bending, shearing in beams and by columns and joint rotation. These effects reduce the cantilever stiffness and is called the "shear lag effect". The difference between vertical axial forces, as predicted by ordinary beam theory, is the assumption that plane sections remain plane. The actual distribution due to shear lag is illustrated in Figure 5-17. The axial forces at the front and the rear facades have the largest values. In the first analysis, in the perfect elastic model, the load upon each row of heads of the pile group increases with the distance from the neutral line (Figure 5-18).

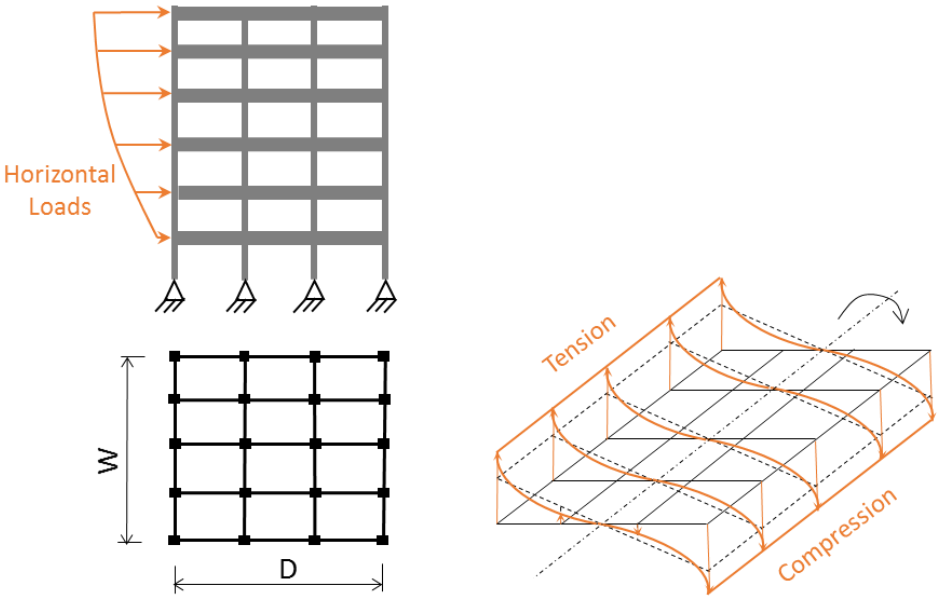

Figure 5-17 In the rigid frame, the axial force distribution under horizontal loads (right) is affected by shear lag phenomenon when the horizontal loads are transferred to vertical axial forces at the foundation level. D is the depth and W is the width of the building.

In this first approach (Figure 5-18 a) vertical loads and horizontal loads are transferred to the foundations through simplified method whereby reaction forces are proportional in a linear way to the external load (linear elastic approach). A finite element method is used for the second step. The structure is simplified to a column and beam structure with stiff internal connections. No transfer of moments, just above the foundation, is supposed (Figure 5-18 b). The output of the finite element method is visualized via "deformed shape" image (Figure 5-18 c) and via a representation of vertical loads upon the foundations (Figure 5-19).

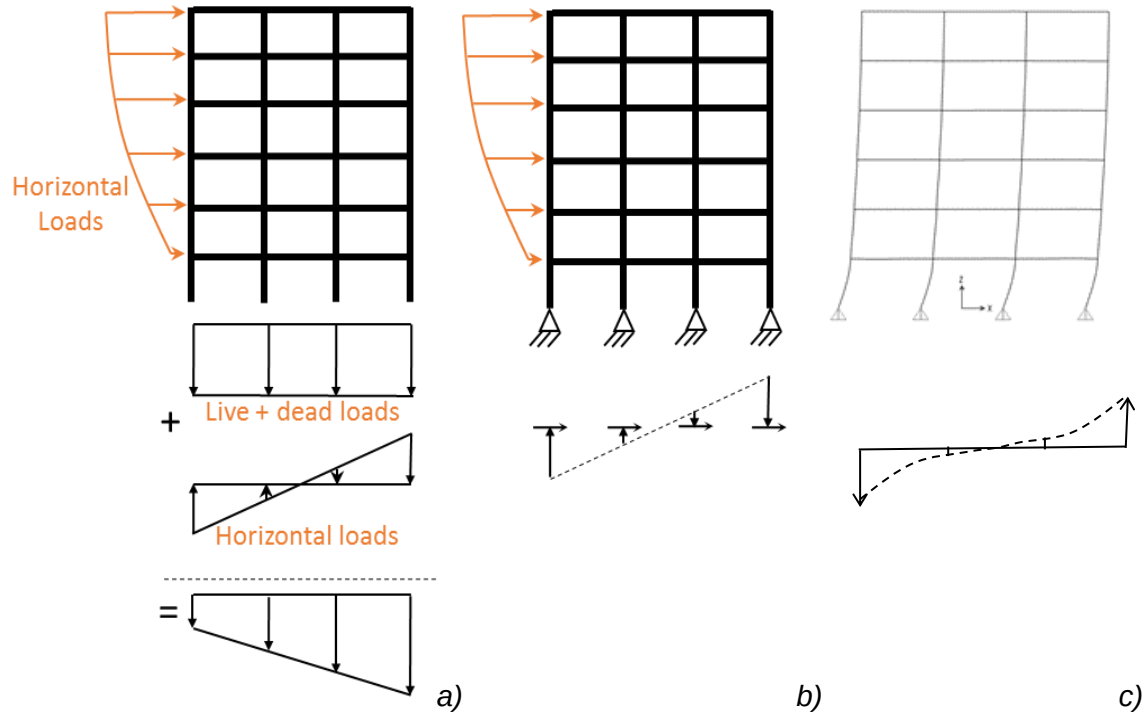

Figure 5-18 Distribution of axial forces from the lateral loads with and without shear lag effect. a) distribution axial forces from dead, live and lateral loads and total axial load; b) axial force of lateral loads without the shear lag effect; c) axial force of lateral loads with the shear lag effect, result from the finite element method.

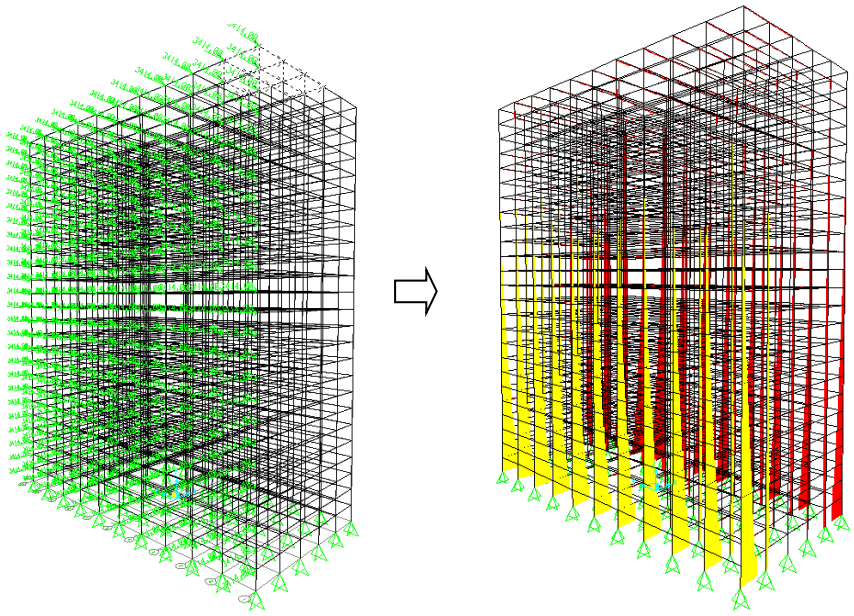

Figure 5-19 The rigid frames are applied the horizontal loads in order to obtain correction factor for shear lag effect. Shear lag effect of 5 rigid bays, 25 floors, 6m bay and 3.6m floor height is analysed by a finite element method.

In the second phase, finite element calculations are used to predict vertical forces in all columns in the rigid frames by varying the frame components. The frame components are the sizes of the columns, beams, number of bays and number of floors. Then, the ratio of the total compression axial forces of both (with and without shear lag effect) is obtained and an approximate formula, to correct the shear lag effect, can be sought out. We define a correction factor $Y= F_{fe}/F_{sim}$. F_{fe} is the total compression forces obtained through the finite element method. F_{sim} is the total compression forces obtained through the simplified elastic mode.

The vertical load, including dead and live loads, is transmitted to the pile's foundations, which is composed of "cost – optimal – piles". The exact grouping of piles around different columns is elaborated in the normal design process at a later phase. In this preliminary cost estimation we can only check how the total number of piles can be derived from the simplified calculation. We compare the average compression forces of the two approaches (Figure 5-18 a) and (Figure 5-18 c). The point loads for the two approaches are compared for the different number of bays and for the different size of the bays combined with different building heights. The building's height, the number of bays and approximate correction factors vary but can still be determined. The correction factor of total axial forces is strongly related to the number of floors by formula Y = 1.39 – 0.0075*X; Where X is the number of floors, which ranges from between 2 and 25 floors (Figure 5-21).

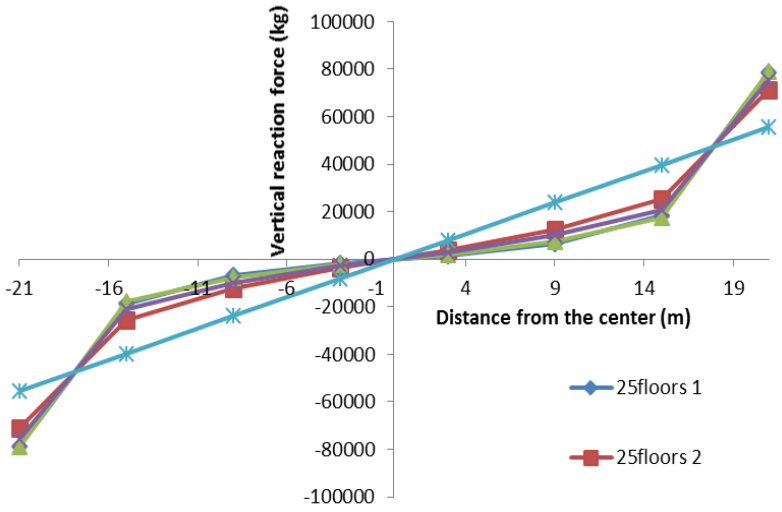

Figure 5-20 Shear lag effect of rigid 7 bays, 25 floors, 6m bay and 3.6m floor height. Axial forces of frame. Total loads with shear lag effect are smaller than total loads with true cantilever.

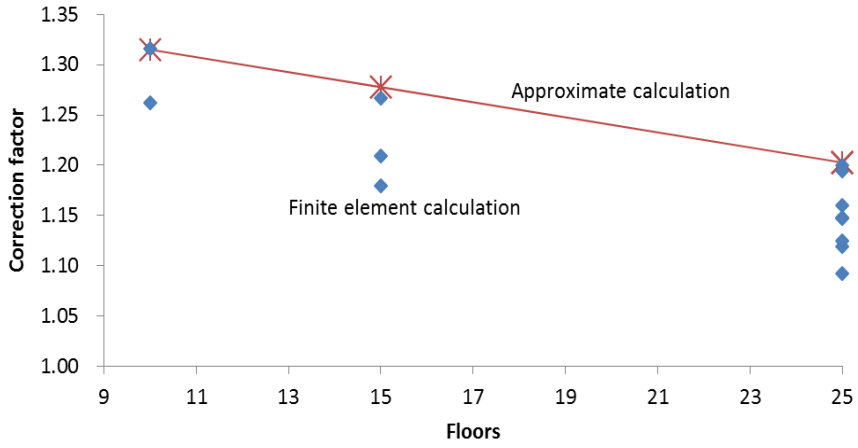

*Figure 5-21 Correction factor for shear lag in the rigid frames: Y = 1.39 - 0.0075*X; X is the number of floors. The approximate calculation is selected on the safe side of the correction factors.*

5.5 Results and Analysis

5.5.1 Cost optimal piles for five locations at Cantho

The optimal capacity of different pile sections, from between 25cm and 40cm with steps of 5 cm each, at five locations in the city are illustrated in Figure 5-22. Then, the cost per ton capacity of optimal piles at different pile sections at five locations in the city are illustrated in Figure 5-23 and Figure 5-24, based on the construction cost of the pile foundation and upon the optimal depths of the piles. At Binh Thuy, which has a thick, soft soil layer (Appendix A) the cost per ton capacity goes up when increasing the section of the pile from (25 x 25 cm) to (40 x 40 cm).

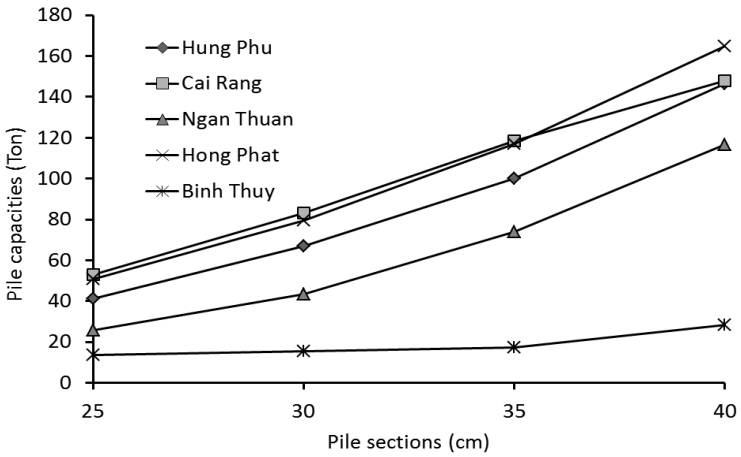

Figure 5-22 The optimal pile capacity based on both the soil and structural properties (Ps: soil bearing capacity of the pile, Pp: capacity of the pile based on reinforced concrete structure).

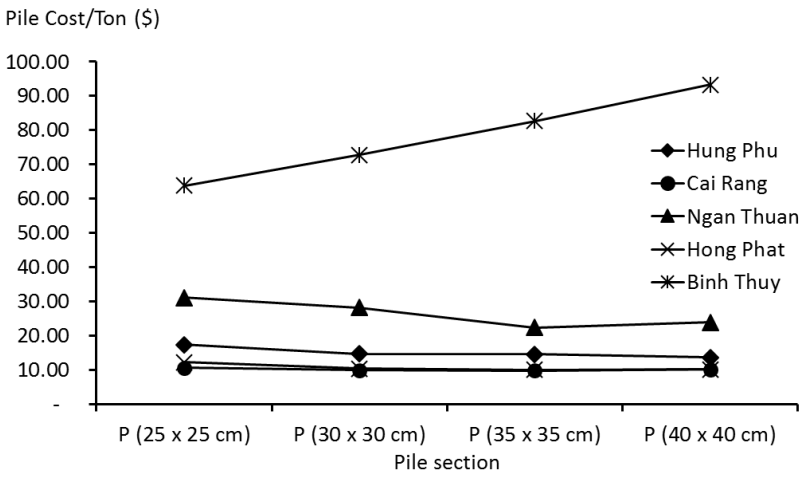

Figure 5-23 Cost of one ton capacity of the optimal pile foundation at Cantho.

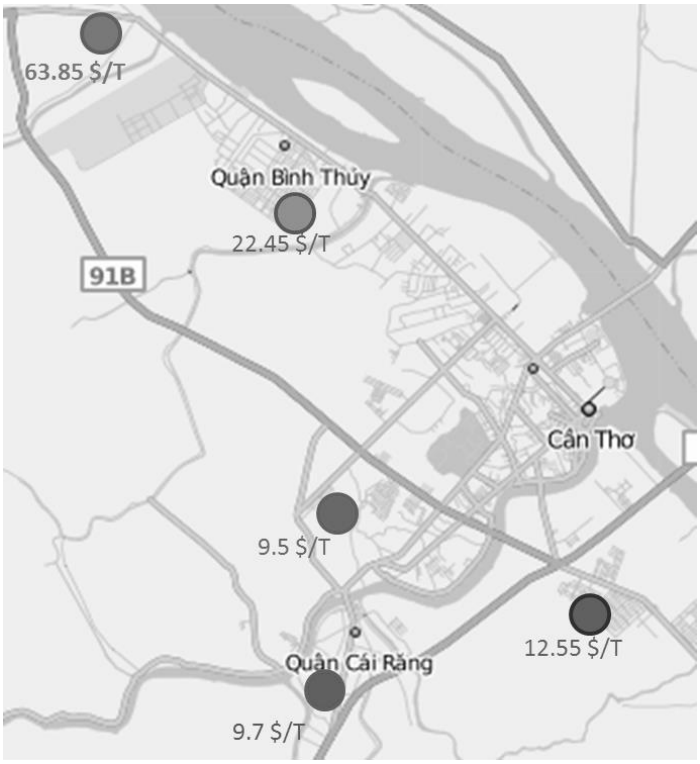

Figure 5-24 Cost of one ton capacity of pile foundation at five places in Cantho.

5.5.2 Wind load as a function of building height

The fundamental frequency of the building is the significant factor of the structure factor. This frequency reduces when increasing the building height. In addition, the wind speed increases in a power law way with the height and is influenced by the roughness of the terrain. For the building from 1 to 25 floors, the ($c_s * c_d$) value varies from 1.03 to 1.26

and the peak velocity pressure $q_p(H_i)$ value consists of static and dynamic components of wind and varies from 116 kg/m² to 287 kg/m². The peak velocity is considered the building height, wind velocity and roughness factor.

All vertical loads of the wind load generate the moment at the foundation level (Figure 5-25 (a)). Then the vertical load of the wind load per square meter floor area is calculated by converted the total moment at the ground floor of the wind loads of all floors. Then the total moment is divided to the total floor areas of the building and multiplied by the correction factor based on the shear lag effect, which is applied to consider the effect of the shear lag for different building heights. The vertical loads on the foundations for different building heights are showed in the Figure 5-25 (b). The vertical load value at each building height is the accumulation of all wind loads on the whole buildings. The results show that the vertical load is reduced when increasing the depth of the building because of the longer moment arm. The building depth, therefore, impacts very strong on the vertical load from the wind on the foundation.

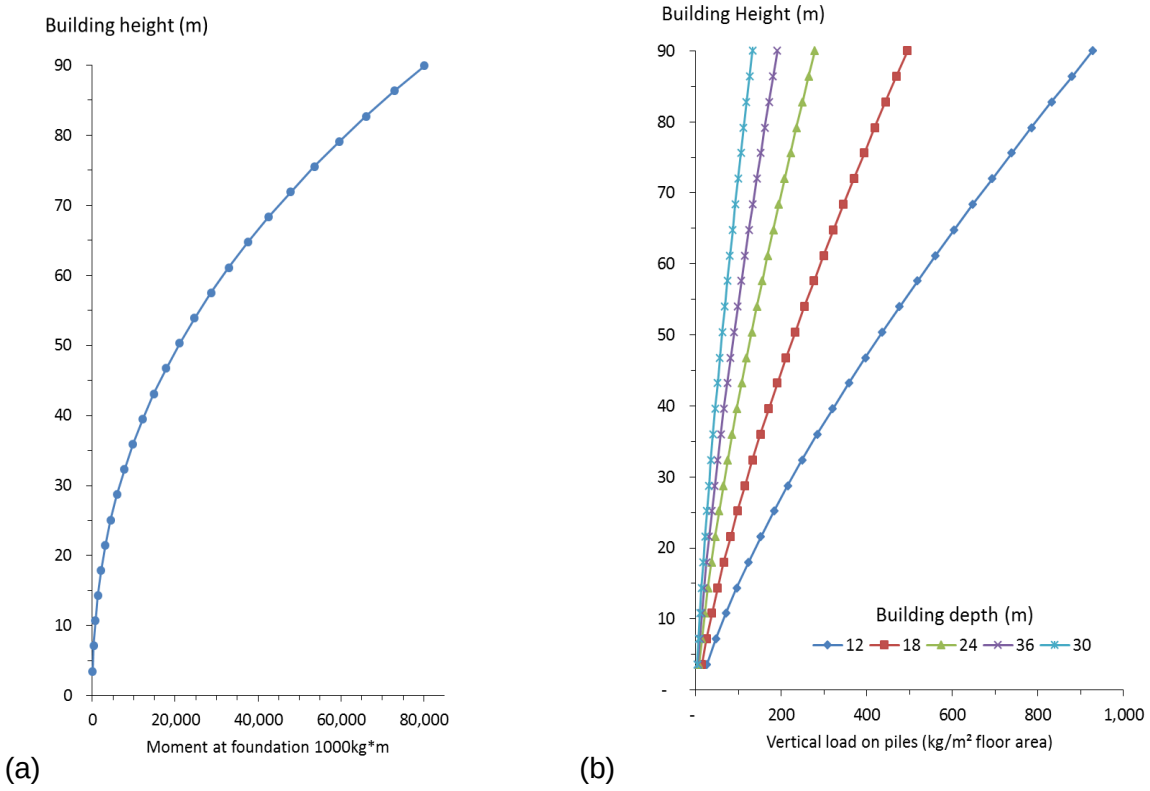

Figure 5-25 The wind load generates the moment at the foundation level and the moment is converted to the vertical loads on piles of the building's width: 42m.

5.5.3 Seismic load as a function of building height

The seismic force at a certain floor of the building is calculated based on the seismic base shear ($Fb = S_d(T_1)*m*\lambda$). Sd(T1) is the elastic response spectrum followed the EN 1998-1:2004 code. The total mass per floor of the building, m, considers the increasing of the column section size related to the building height. The correction factor, the value λ equal 0.85 if $T_1 < 2\ T_C$ and the building is higher than two storeys or λ = 1.0 otherwise. The base shear is distributed into each floor as horizontal loads of the building, these horizontal loads generate moments on the foundation or vertical loads with considered the building width.

The vertical loads on pile foundation per m² floor area that were transferred from the seismic load is showed in the Figure 5-26. The total floor area and the building depths are considered to calculate the vertical loads for the foundation. From the ninth floor the mass factor λ equals 1.0, the load is increased 15% step. Because buildings with at least three storeys and translational degrees of freedom in each horizontal direction, the effective modal mass of the 1st (fundamental) mode is smaller, on average by 15%, than the total building mass EN 1998-1:2004 code.

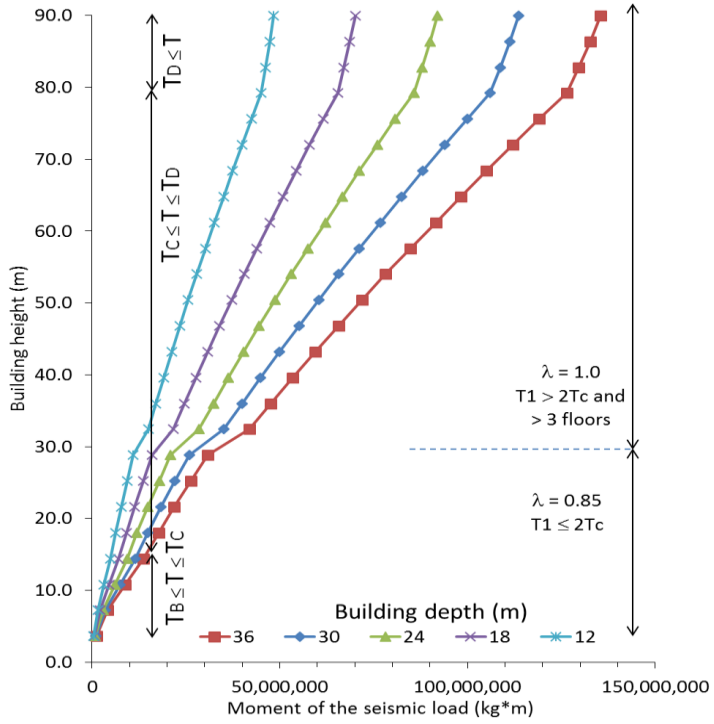

Figure 5-26 Moment of the seismic load at the foundation level. T_B and T_C are the lower and upper limit the period of the constant spectral acceleration branch. T_D value is the definition of the beginning of the constant displacement response range of the spectrum.

5.5.4 Lateral loads transfer to pile foundations

The lateral loads, including wind and seismic loads, are transferred to piles as vertical axial forces based on the true cantilever (Euler theory). In the second step, these are adjusted with correction factors to take the “shear lag effect” into account. A whole range of building depths, from between 12m and 36m, are analysed to address the relationship between load components and their impact on piles. With small building depths, the lateral loads generate large vertical loads on the pile foundations, as shown in Figure 5-27. The vertical loads, generated by lateral loads, vary from between 30% and 130% of the total vertical load from both live and dead loads depending on the building’s depth and height. The lateral loads are significant to design foundations of high-rise buildings in soft soil conditions. For smaller building depths, the vertical loads per square meter floor area of the wind load is larger than the seismic load when the building height is greater than 8 floors. There is a significant increase in the vertical load of the seismic load at floor 9 due to the elastic response spectrum.

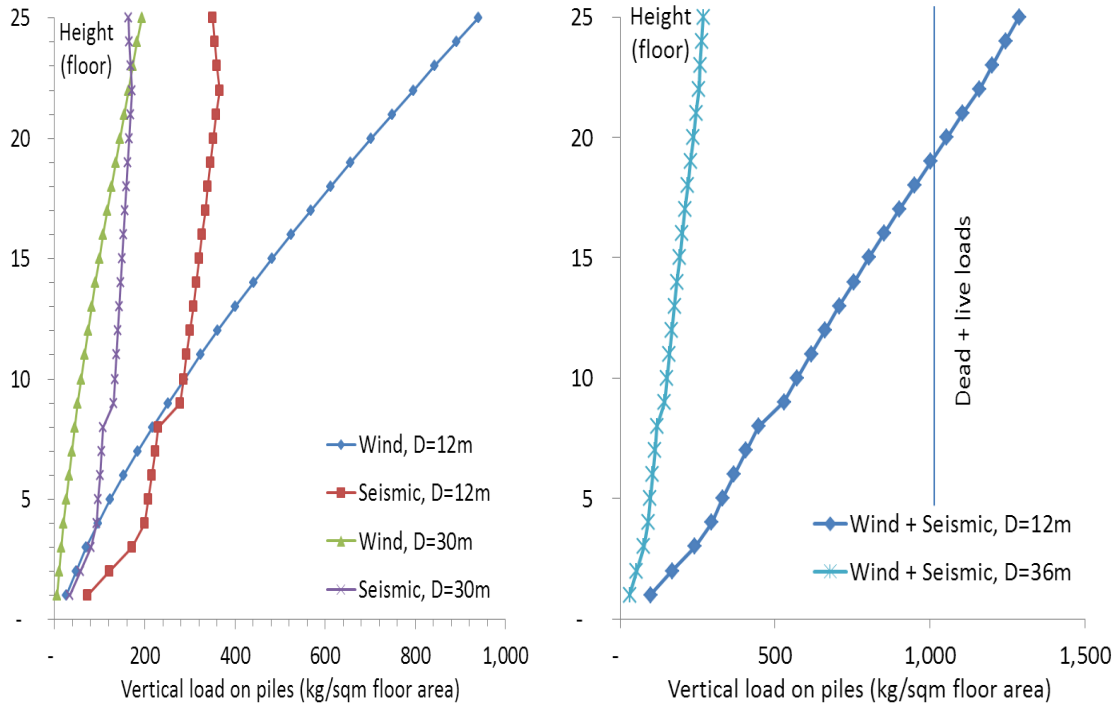

Figure 5-27 Vertical loads on foundation (kg/sq.m floor area).

In order to compare different buildings, the total load is divided by the total floor area. The vertical dead and live loads are constant per m² of floor area. Lateral loads per square

meter of floor area of five building depths and different building heights between 1 to 25 floors (115 design options) are calculated and then a regression formula is elaborated in order to estimate the load on the foundation based on two parameters: building depth and height (see the formula in Figure 5-28). This formula will be used for optimization models in the Chapters 8.

$$VL = a + \frac{b}{D} + c * H + \frac{d * H}{D}$$

a = 956.117; b = -680.684;
c = -2.555; d = 182.497;
VL: vertical load on foundation (kg/m² floor area)
D: building depth (m)
H: building height (m)
(R^2=0.99)

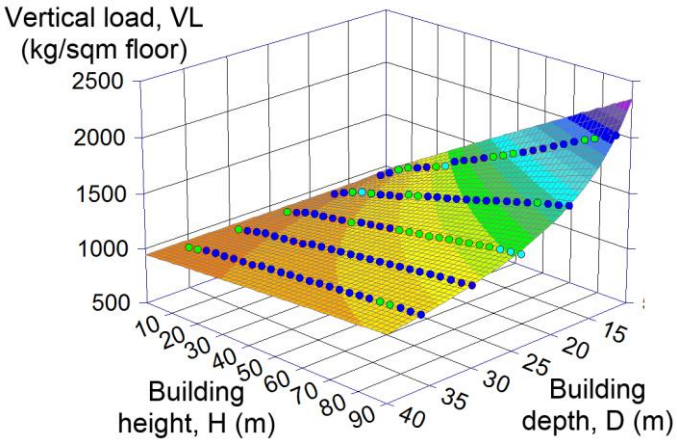

Figure 5-28 Total vertical load per square meter floor area (dead, live, wind and seismic loads) for different building depths and heights are appropriately calculated by the formula.

5.5.5 Foundation cost integrated with building height and land costs

Based on three main parameters (height, depth and land costs), the cost of pile foundations, for different building depths, increases almost linearly with the building's height (Figure 5-29). The interplay of four main parameters (height, depth, costs of foundation and land) will be clarified in this section. In the graphs below, the land cost chosen is 100$/sqm, based on the market price from web sites for land price in 2011 at Cantho; the foundation cost is 70 $ per ton based on the minimum construction cost in the weakest soil properties; the depths are changed from 12m to 36m with a 6m bay. If building depth increases, the minimum costs are almost constant on a low level (Figure 5-30). These results change slightly with several different building depths because seismic loads are related to masses of the structure and the wind pressure has a minor increase when the width decreases. Figure 5-29 shows a jump in foundation cost and also the same effect in vertical loads on piles in Figure 5-27 because of the changing of fundamental frequency related to building height. Since the length of the building has almost no influence on the horizontal loads, the graphs are constructed for an average length of 50m.

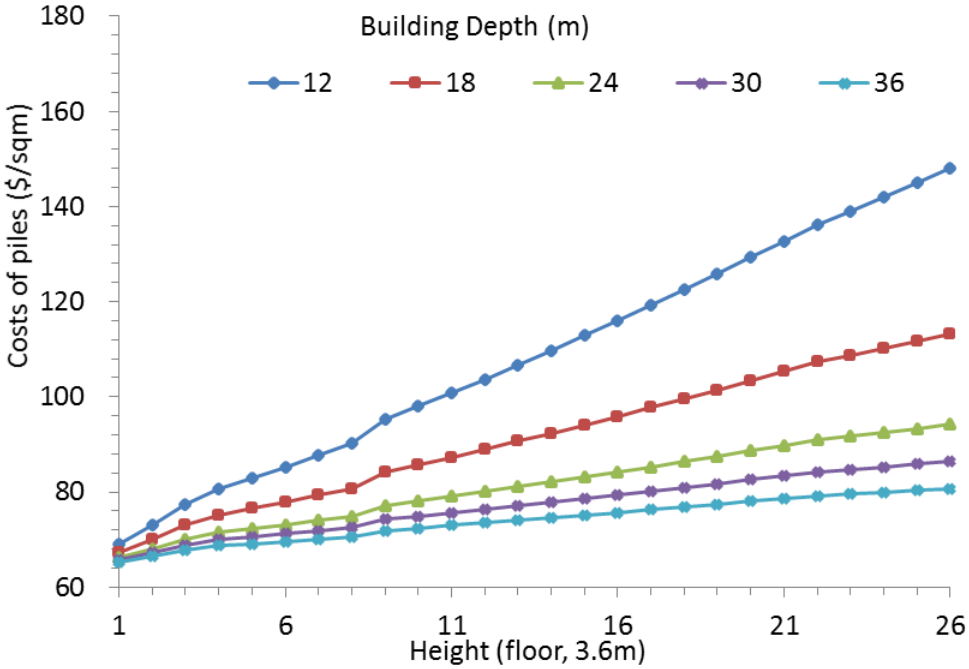

Figure 5-29 The cost of pile foundation per one square meter floor area is evaluated with the pile foundation cost 70$/ton capacity.

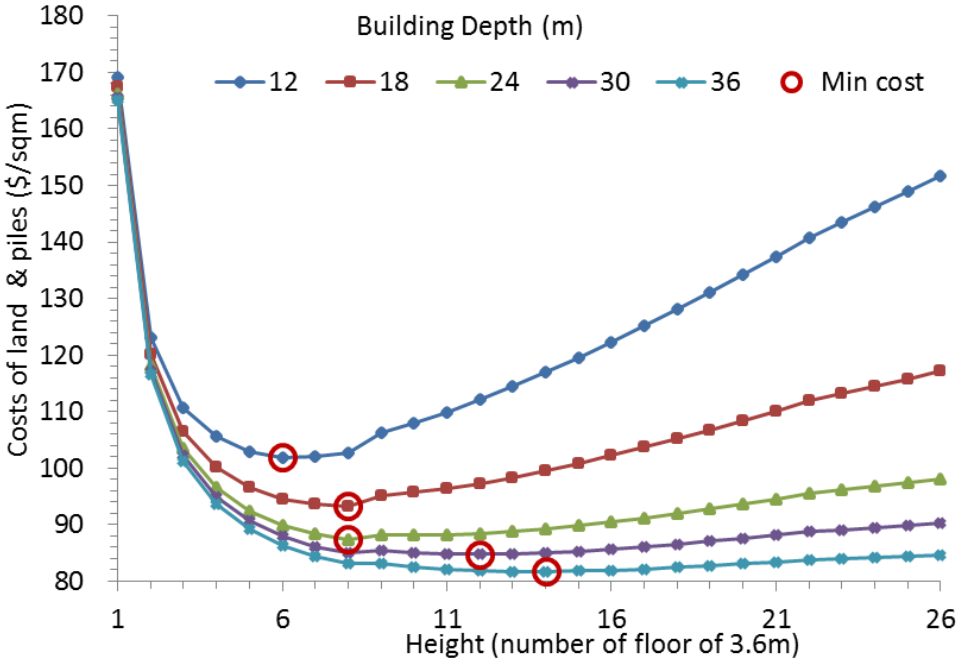

Figure 5-30 The cost of land and pile foundation per one square meter floor area. Land cost = 100$/sqm; Pile cost = 70$/ton.

5.6 Sensitivity analysis

Four parameters (land cost, the pile foundation cost, depth and height) are analysed to determine their effects on the total cost. Clearly, the land cost decreases hyperbolically where the building's height increases. The sensitivity of the model varies, depending on different the building's height, as shown in Figure 5-31.

The standardized regression coefficient (SRC), the global sensitivity analysis approach, which is based on a linear regression of the output on the input vector, is used to analyse this sensitivity. This SA method has been explained in Chapter 3. The most sensitive parameters are the pile foundation cost and the building height, as shown in Figure 5-32.

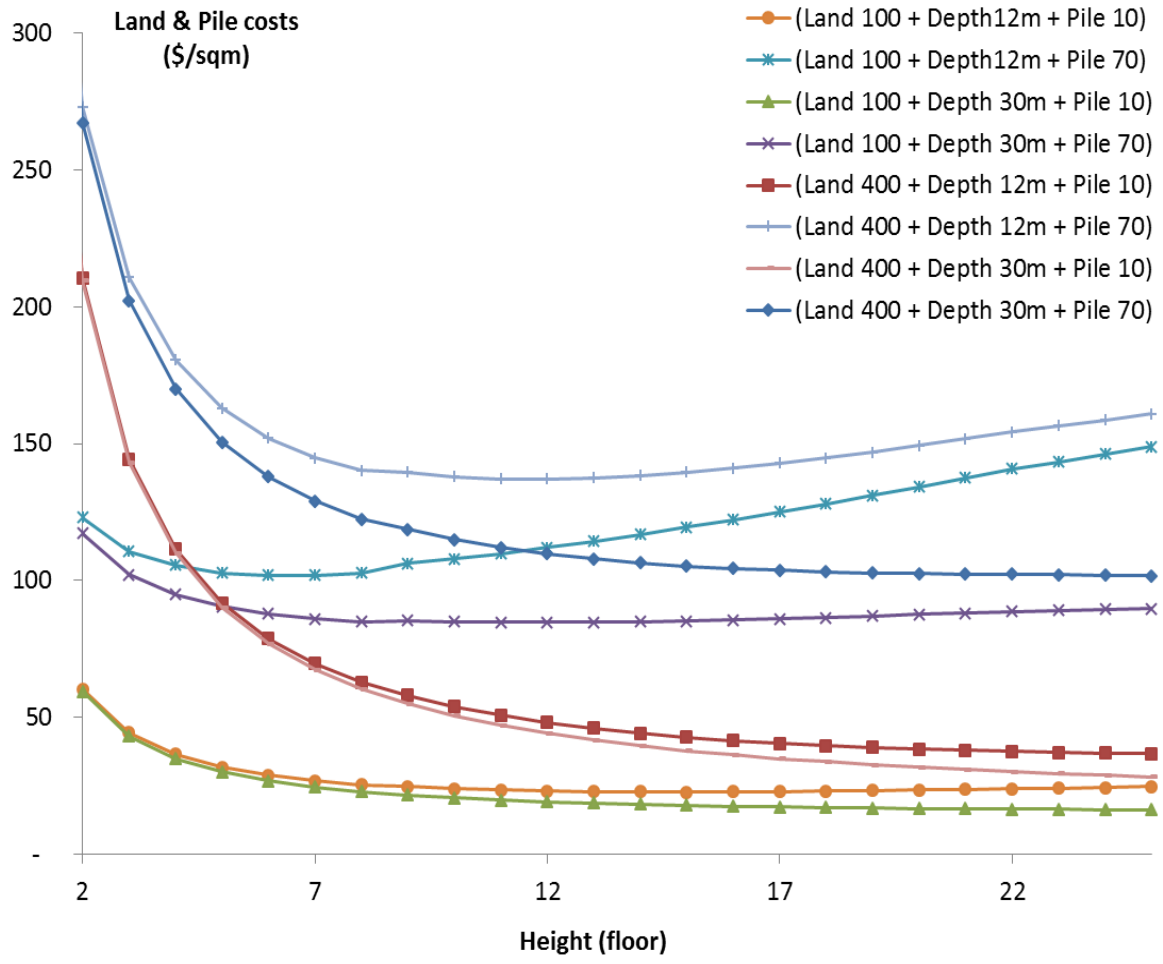

Figure 5-31 Sensitivity analysis of four parameters.

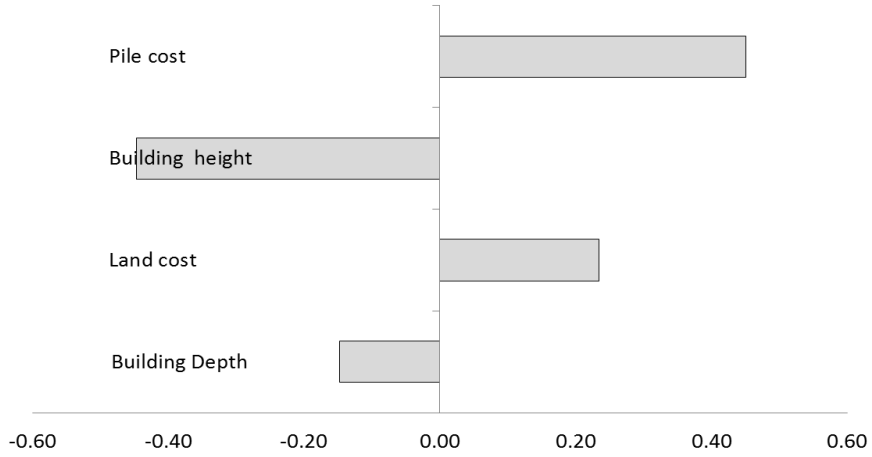

Figure 5-32 Sensitivity of four parameters are ranked by using SimLab or R, the higher absolute value on the horizontal axis indicates the higher impact level of the parameter. A negative sign of the other parameters means that when we increase the parameter, the outputs decreases. Sensitivity values are dimensionless and vary between -1 to 1.

5.7 Parameter study and rules of thumb

Based on Figure 5-29, the effect of the height upon the cost per square meter floor of the foundation can be approximated in a linear way. Three design questions can be considered: the selection of location, the ratio of built-up versus residential areas and building geometry (building height and depth). (1) The location selection determines the land cost and the foundation cost due to soil properties. (2) In order to strive for more open areas, and by keeping the total floor density the same, the building height will be higher. (3) At a certain location and built-up ratio, selecting both the building height and depth will influence the cost of both foundation and land. In conclusion, the interplay of four main parameters (height, depth, costs of foundation and land) are analysed and visualized to support the dissemination of valuable information which is necessary for designers to make decisions in any given situation.

The height parameter seems, in a first approach, to be linearly related to the pile foundation costs (Figure 5-29).Two structural parameters, including building height and pile cost, have critical impact upon the cost. The land cost per square meter floor depends on location, the ratio of built-up areas versus residential area, the soil properties, the height and depth and the interaction of those four parameters. At the early design stage, this information can be used to select the building layout and to minimize the initial cost. The depth and height cannot easily be changed in later design stages.

5.8 Conclusions

There are four significant conclusions as follows: (1) Based on the case study analysis of Cantho city, the Mekong Delta, buildings between 6 and 15 floors lead to the lowest foundation cost per m² of floor, depending on particular soil properties in specific locations. (2) Although it is the critical load for high-rises buildings, the seismic force has not been considered by designers in this city. (3) At the early design phases, when crucial design decisions need to be made, useful information for designers and developers can be found in the cost estimation model and in the graphical representations of the end results. In soft soil conditions, where the cost of a pile foundation is higher, the impact of building layout, height and depth can be derived. (4) The model could also been developed for rigid steel frame buildings. Further research is required to couple this model with finite element programmes in order to calculate fundamental frequency. However, there are some limitations that this current model has not yet covered. Firstly, the model is not appropriate for walled structures because of the distribution of axial forces in the columns for instance. Secondly, the fundamental frequency (building period) of complicated floor plans is not integrated. This can be obtained by using the finite element programmes.

The original contribution of this work consists of the integration of a fast estimation of foundation costs in the element method for cost control. This allows in an early design phase, when different compositions are compared (number of floors, building depth in the two directions), to analyse the cost per m² of floor. The element method for cost control allows for a transparent view on the contribution to the cost of different elements (foundation, external walls, roof and internal walls) including land and infrastructure.

References

[1] S.L. Chan, M. Park, Project cost estimation using principal component regression, Constr. Manag. Econ. 23 (2005) 295–304.

[2] W. Tan, Construction cost and building height, Constr. Manag. Econ. 17 (1999) 129–132.

[3] D.H. Picken, B.D. Ilozor, Height and construction costs of buildings in Hong Kong, Constr. Manag. Econ. 21 (2003) 107–111.

[4] S. Karshenas, Predesign Cost Estimating Method for Multistory Buildings, J. Constr. Eng. Manag. 110 (1984) 79–86.

[5] H. Murat Günaydın, S. Zeynep Doğan, A neural network approach for early cost estimation of structural systems of buildings, Int. J. Proj. Manag. 22 (2004) 595–602.

[6] P.A. Bowen, P.J. Edwards, Cost modelling and price forecasting: practice and theory in perspective, Constr. Manag. Econ. 3 (1985) 199–215.

[7] F. Khosrowshahi, A.P. Kaka, Estimation of project total cost and duration for housing projects in the U.K., Build. Environ. 31 (1996) 375–383.

[8] S. Singh, Cost Model for Reinforced Concrete Beam and Slab Structures in Buildings, J. Constr. Eng. Manag. 116 (1990) 54–67. doi:10.1061/(ASCE)0733-9364(1990)116:1(54).

[9] S. Trost, G. Oberlender, Predicting Accuracy of Early Cost Estimates Using Factor Analysis and Multivariate Regression, J. Constr. Eng. Manag. 129 (2003) 198–204.

[10] W. Yu, M. Skibniewski, Integrating Neurofuzzy System with Conceptual Cost Estimation to Discover Cost-Related Knowledge from Residential Construction Projects, J. Comput. Civ. Eng. 24 (2010) 35–44.

[11] H. Adeli, M. Wu, Regularization Neural Network for Construction Cost Estimation, J. Constr. Eng. Manag. 124 (1998) 18–24.

[12] J. Bode, Neural networks for cost estimation: Simulations and pilot application, Int. J. Prod. Res. 38 (2000) 1231–1254.

[13] M. Arafa, M. Alqedra, Early Stage Cost Estimation of Buildings Construction Projects using Artificial Neural Networks, J. Artif. Intell. 4 (2011) 63–75.

[14] F. De Troyer, BB/SfB-plus - Een functionele hiërarchie voor gebouwen, ACCO, Leuven, 2008.

[15] Frank DeTroyer, Graphical tools for cost-conscious design, in: 2003.

[16] K.-W. Chau, S.K. Wong, Y. Yau, A.K.C. Yeung, Determining Optimal Building Height, Urban Stud. 44 (2007) 591–607.

[17] High Rise Apartment Building- Design Standard, Vietnamese Building Standard, (2004).

[18] M.M. Ali, K.S. Moon, Structural Developments in Tall Buildings: Current Trends and Future Prospects, Archit. Sci. Rev. 50 (2007) 205–223.

[19] B.S. Taranath, Reinforced Concrete Design of Tall Buildings, CRC Press, Taylor & Francis Group, Boca Raton, 2010.

[20] M.H. Baziar, A. Kashkooli, A. Saeedi-Azizkandi, Prediction of pile shaft resistance using cone penetration tests (CPTs), Comput. Geotech. 45 (2012) 74–82.

[21] S. Haldar, G.L.S. Babu, Reliability measures for pile foundations based on cone penetration test data, Can. Geotech. J. 45 (2008) 1699–1714.

[22] TCXD205, Pile Foundation-Design Standard, Vietnamese Building Standard, (1998).

[23] TCVN2737, Design loads, Vietnamese Building Standard, (1995).

[24] M.D. McKay, R.J. Beckman, W.J. Conover, Comparison of Three Methods for Selecting Values of Input Variables in the Analysis of Output from a Computer Code, Technometrics. 21 (1979) 239–245.

[25] J.C. Helton, F.J. Davis, Latin hypercube sampling and the propagation of uncertainty in analyses of complex systems, Reliab. Eng. Syst. Saf. 81 (2003) 23–69.

[26] K.A. Zalka, A simplified method for calculation of the natural frequencies of wall–frame buildings, Eng. Struct. 23 (2001) 1544–1555.

[27] R. Goel, A. Chopra, Period Formulas for Moment-Resisting Frame Buildings, J. Struct. Eng. 123 (1997) 1454–1461.

[28] CEN, Bs en 1998-1:2004, eurocode 8: Design of structures for earthquake resistance, (2004).

[29] K.M. Amanat, E. Hoque, A rationale for determining the natural period of RC building frames having infill, Eng. Struct. 28 (2006) 495–502.

[30] R.D.J.M. Steenbergen, A.C.W.M. Vrouwenvelder, C.P.W. Geurts, The use of Eurocode EN 1991-1-4 procedures 1 and 2 for building dynamics, a comparative study, J. Wind Eng. Ind. Aerodyn. 107–108 (2012) 299–306.

[31] M. Biot, Theory of Vibration of Buildings During Earthquake, ZAMM - J. Appl. Math. Mech. Z. Für Angew. Math. Mech. 14 (1934) 213–223.

[32] M. Biot, A Mechanical Analyzer for the Prediction of Earthquake Stresses, Bull. Seismol. Soc. Am. 31 (1941).

[33] W.-F. Chen, E.M. Lui, Earthquake engineering for structural design, CRC Press Taylor & Francis, 2006.

[34] D.E. Hudson, Response Spectrum Techniques in Engineering Seismology, in: Berkeley, California, 1956.

[35] T.D. Ngo, M.D. Nguyen, D.B. Nguyen, A review of the Current Vietnamese Earthquake Design Code, Electron. J. Struct. Eng. 8 (2008) 32–41.

[36] Seismic design standard, Vietnamese Building Standard, (2006).

CHAPTER 6 MARKET VALUE

Understanding housing preference is crucial information to designers and developers. Many studies have analysed housing preferences. Studies based on questionnaires or historical documents are elaborated with high cost and become outdated by the time they are made available. To understand housing preferences and housing plot preferences, we tested a method to derive them from selected internet websites. Results can be included in a decision model at the early design stage.

This chapter is based on the publication:

Nguyen Van, T., De Troyer, F. (2013). Deriving Housing Preferences from advertising on the web for improving decision making by Economic and Social actors. Deriving Housing Preferences from advertising on the web for improving decision making by Economic and Social actors (ISBN: 9789078862062). RC43 conference 2013, "At home in the housing market". Amsterdam University, 10-12 July 2013 (pp. 104-114)

Table of Contents

6.1	**Introduction**	**115**
6.2	**Literature review**	**115**
6.2.1	The problem of location and land	115
6.2.2	Housing preferences	116
6.3	**Conceptual model**	**116**
6.3.1	Diminishing marginal utility functions of housing preferences	116
6.3.2	Multi-Attribute Utility theory	116
6.3.3	Overview of approach	119
6.4	**Data collection methods (Deriving preferences from the web data and test for small scale plot)**	**119**
6.4.1	Data source selecting	119
6.4.2	Data collection	120
6.5	**Attribute selection**	**121**
6.6	**Developed tool for capturing information**	**121**
6.6.1	Explicitly reported parameters	121
6.6.2	Multiple exponential regression analysis	122
6.7	**Deriving utility functions**	**123**
6.8	**Deriving visual conclusion for stakeholders**	**124**
6.8.1	Visual reference information to make decision for designer	124
6.8.2	Visual reference information to make decision for developers	126
6.8.3	Visual reference information to make decision for customers or users	127
6.8.4	Visual reference information to make decision for policy makers	127
6.9	**Sensitivity analysis**	**128**
6.10	**Conclusions**	**129**

6.1 Introduction

The inadequate condition of urban housing is a global problem and it is the most serious issue in developing countries [1]. One billion people, accounting for thirty percent of the world's urban population, live in poor housing conditions [2]. A high housing demand in urban areas can be predicted based on the already dense population, rapid population growth and high rural-urban migration. With population of 88 million, Vietnam is the third most populated country in South East Asia, is ranked thirteenth in the entire world [3]. More than 30% of total households live in dwellings with less than 36 square meters floor area and 19% of total households live in temporary houses [4].

A stated hedonic price, elaborated by using the questionnaire method, can estimate trade-offs between customer value and the construction cost. In so doing, a priority list of housing attributes can be elaborated [5]. Many researchers try to fill this gap from the preferences in design decisions. The theory of means-end chain is proposed in order to deal with user preferences of housing and to link three aspects: attributes, consequences and values of buildings together [6]. Other researchers use questionnaires to obtain housing preferences and then identify relationships between the willingness to pay and total cost of main housing attributes [7].

To understand housing preferences, we propose a method to derive preferences from selected internet websites and include them in a model for decision making which can be used in the early design stage. This chapter reports a first elaboration whereby only the selling price of developed land can be predicted in 3 steps: (1) select residential land characteristics for large scale housing projects; (2) derive a function by which to predict selling price, based on selected land attributes via regression analysis and (3) link cost and willingness to pay to generate graphs that provide design decision information for designers and developers and which takes users' preferences into account.

6.2 Literature review

6.2.1 The problem of location and land

The main difference between real estate and other products is location value because of the possible links a location provides to other facilities, such as schools, commercial centre, green areas and transportation system. Hence, the method described below is only applicable in cases where the location characteristics of the large scale housing projects are similar but the lot size and characteristics of the project (% green area, % different housing types) are different.

6.2.2 Housing preferences

There are two typical methods by which to generate insights regarding housing preferences: observation of behaviour (hedonic price method) and stated preference method. The hedonic method requires historical data sets and tries to predict prices based on real transactions [9] [10]. Hedonic models have been applied to obtain the relationship between house price, environmental quality [11] and air pollution [12]. While the stated preference method works with questionnaires, whereby people express their willingness to pay for selected attributes

6.3 Conceptual model

6.3.1 Diminishing marginal utility functions of housing preferences

The intuitive behaviour "law" is accepted as a working hypothesis in this study: diminishing marginal utility for each housing characteristic. For example, when the width of a housing plot increases continuously, the price per square meter of land does not increase in a linear way, but follows a curve which slopes less and less (Figure 6.1). Another example is one additional square meter per apartment with 36 m^2 is more appreciated than it is for an apartment with 100m^2. This hypothesis requires a transformation from power function to a linear function in order to apply a linear regression.

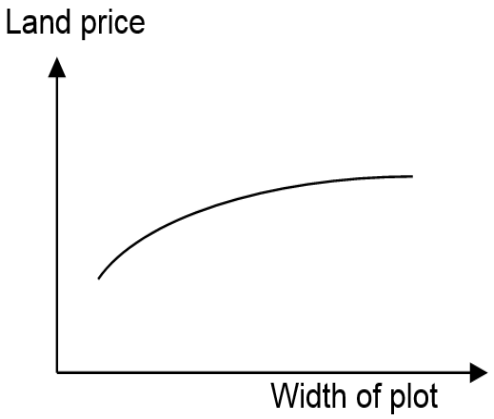

Figure 6.1 Price of land versus width of plot, utility function: $y = \sum a * x^b + e$ and $(0<b<1)$; or $ln(y) = \sum(ln(a) + b * ln(x)) + e$.

6.3.2 Multi-Attribute Utility theory

The approach to a housing characteristic's power function can extend to multiple housing attributes [7]. Two attributes can be presented in three dimensional graphs to search for an optimal alternative within budget constraints or any other constraints. The concept of this approach, also used in the "Multi-Attribute Utility Theory", supports decision-making when a selection is made from a limited number of available alternatives [13].

The method is first illustrated with two parameters in a graphical way and then the elaboration to an approach for a multitude of attributes is explained as a second step. As example, a plot is considered with two basic attributes the width (W) and the depth (D) (Figure 6.2).

The total price is proportional to the total quality that can be expressed as the sum of two power functions, $P = a * W^b + c * D^d$ with ($0 \le b \le 1$; $0 \le d \le 1$). The cost for providing this land is estimated in this example based on the cost per running meter street of a given type (s in VND/m) and cost per meter square of land (p in VND/m^2) $C = W * s + W * D * p$ (Figure 6.2).

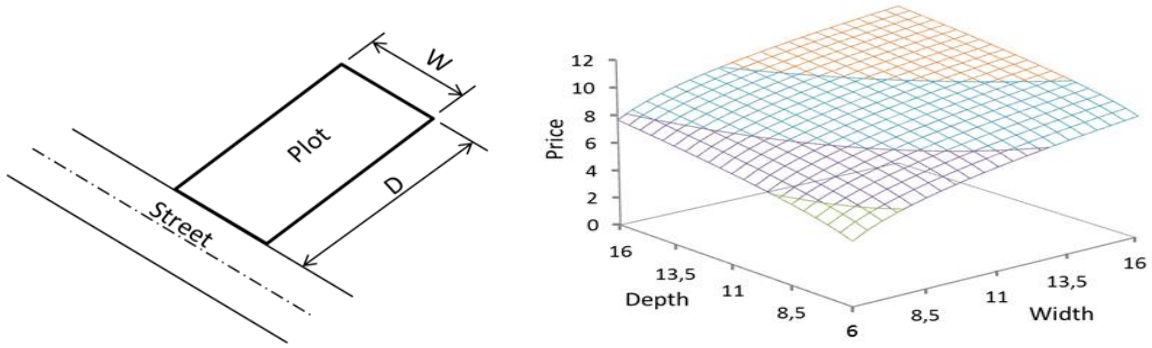

Figure 6.2 Selling price of land is related to width and depth of plot by a power function.

How the margin (with margin is price that is willing to pay minus cost: M = P – C) can be visualized for each of the combination of Width and Depth (Figure 6.3). This three dimensional graph can be transformed into a two dimensional, if the cost of providing the land and infrastructure is represented along the left-right axis and where selling price is on the other axis.

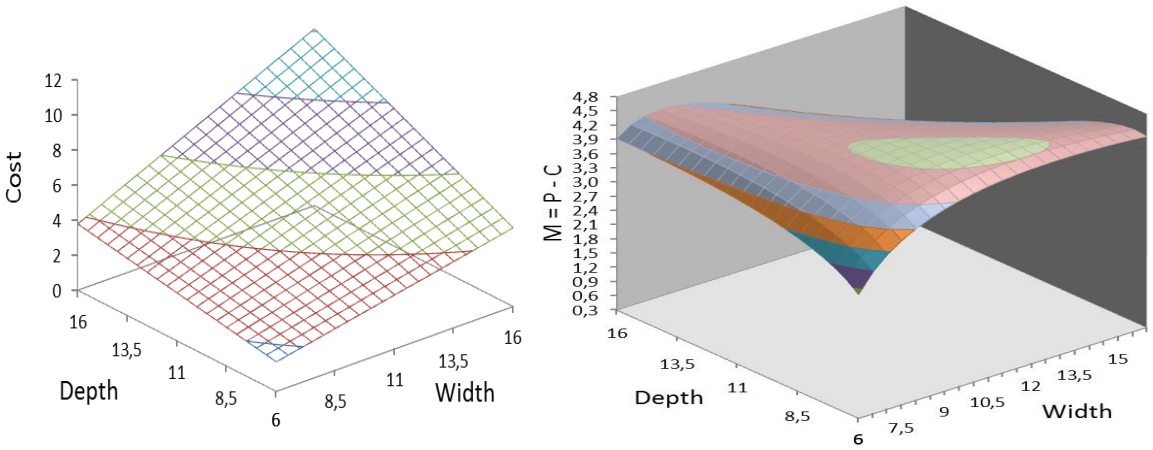

Figure 6.3 Cost and profit of residential plots.

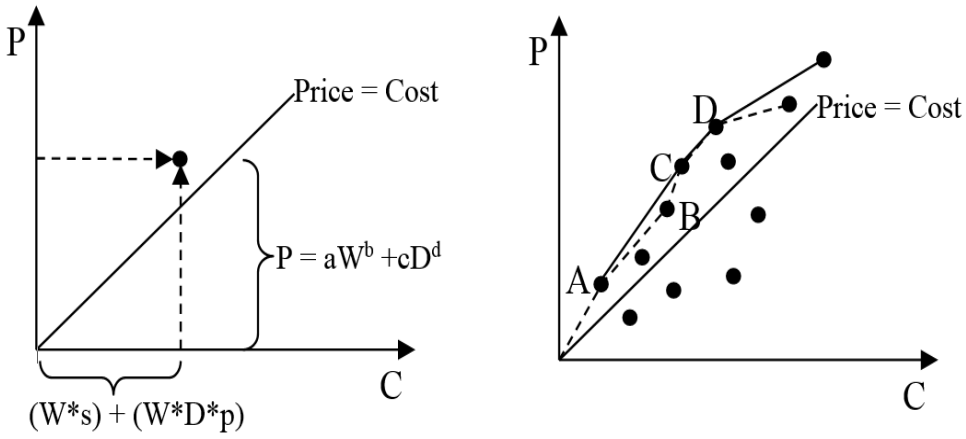

Figure 6.4 Graphical representation of price and cost with two parameters: width and depth of plot.

A point can be calculated for each combination of W and D. If this is done for several combinations we obtain a cloud of points. Under the line “price is equal to cost” the costs are higher than the selling values and, thus, combinations are not interesting for the developers. For every point one can conclude that a point more to the right “or/and” below is not interesting because it generates more costs and/or incurs less profit. Points on the dotted line (Figure 6.4) are interesting based on this elimination step. Starting from the point next to the left point (lowest investment cost), on the dotted border line, one can analyse what is the best additional spending in view of the additional profit earned.

Stepping from A to C will generate a higher additional income per additional cost than from A to B. From the point with lowest investment cost on the next point on the dotted line is selected with the highest slope illustrated with the solid line (Figure 6.4). This reasoning can be repeated from the next selected point on. The new solid line has the slope that is less and less, which reflects the diminishing marginal utilities. The dotted line will be called the Pareto sub optimal points and the continuous line the Pareto optimal points. This approach can be extended to cases in which more than two characteristics are considered. The cost may depend on a complex, inter-related way upon the physical parameters.

6.3.3 Overview of approach

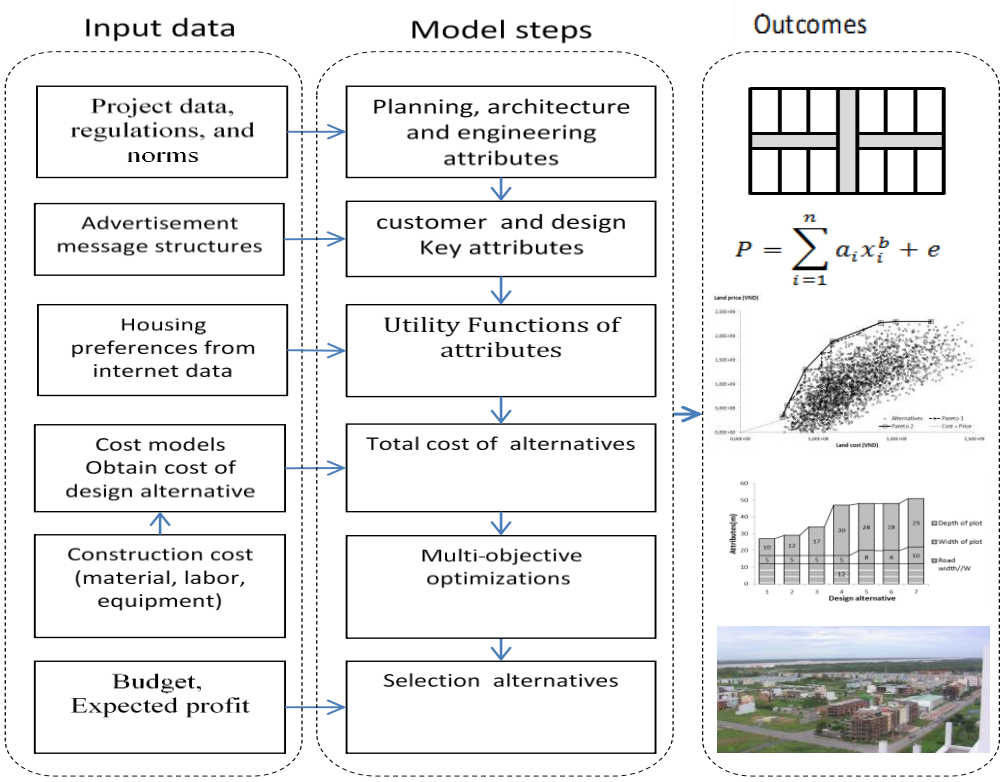

Figure 6.5 Decision based on preferences and designs flowchart

6.4 Data collection methods (Deriving preferences from the web data and test for small scale plot)

6.4.1 Data source selecting

There are two typical methods to develop insights into housing preferences: the "revealed" and "stated" preference method. The revealed method requires historical data sets and tries to predict prices based on real transactions [9] [10]. The stated method works with questionnaires in which prospective residents express their willingness to pay for selected attributes.

In Vietnam, there are four data sources that can be used to analyse the residential land preferences. Firstly, the data of housing transactions can be obtained from government organizations. However, this data cannot explain actual housing preferences because housing prices, according to governmental norms, are lower than for the real estate market [14] [15]. Secondly, transactions in private sector, the data are secret, because of competition, and so cannot be consulted by researchers. Thirdly, by using questionnaires, but this consumes time and funds and was not possible within this research. Fourthly, data on the internet can be collected at low cost, quickly and for a large data set.

The advertising of residential land is primarily posted by real estate agencies and the owners. The advertising messages contain the proposed selling price for residential lands. The advertising messages normally contain three main attributes which include the location, land characteristics. The characteristics of lands are depth, width and road width. The location attributes describe possibilities by which to connect to relevant social and service facilities. This information is available for all potential buyers. However, the information collected from selective websites has some inherent limitations, such as: the information is structured in different ways, characteristics are sometimes omitted, or are downright incorrect, in order to attract the interest of more possible buyers.

This study uses data contained within the internet advertisements on land offered for sale in Cantho making the implicit hypothesis that the final selling price is a fixed fraction of the announced price. The data has been downloaded from three Vietnamese real-estate websites: *batdongsan.com.vn*, *canthoinfo.com*, *mekongland24h.com.vn*. There are, of course, other sites which offer similar information. These three sites are representative, however, due to their high market shares. For instance, "*batdongsan.com.vn*" posts 240 messages for the sale of land and houses every month. While Canthoinfo.com posts 5,750 selling messages for both land and buildings every month.

6.4.2 Data collection

During the data collection stage, some inconsistencies in the data were identified because the data quality could have significant impact on analysis later on. Therefore, some cleaning processes were employed to remove messages that lacked information. Then the selling of dwellings (including land) and residential land only were separated. In this study, only the residential land information of plots within large scale housing projects will be considered.

Data concerning land characteristics and prices was collected through the internet for different large scale projects at various locations in Cantho city. We wrote a program to download data from selected websites automatically and in a way that updating data could be performed automatically and based on huge amounts of data.

There are three criteria that are employed to select the housing price data. Firstly, one full year of data was used to avoid problems with time variations over period longer than one year. Secondly, the data was limited to land within new large scale housing projects in Cantho city. Thirdly, lands which are located along main roads are excluded because these roads connect to the city's road network and focus on commercial facilities. As a result, only 146 lots have been used for analysis in this model. These lots are located in five large scale

housing projects with the same distance to the city centre. Other data should will be collected for housing preferences prediction in the future research.

6.5 Attribute selection

The main purposes of attribute selection are removing irrelevant, unreliable or “noise” generating attributes that do not improve the reliability of predictions. The result is a model that is easier to use. The attribute selection phase tries to identify sufficient critical attributes for a good prediction of the dependent variable: housing price [16] [17]. Previously conducted hedonic price research has normally adopted a statistical selection criteria, based on significance level, as a stepwise selection method [18] [19] [20] [21].

The data was analysed by using the statistical software R which is freely available and open source. With R, the stepwise selection can be implemented with step function both forwards and backwards. This function removes the less significant attributes and calculates “Akaike Information Criterion” (AIC) values [22]. The lowest AIC value indicates the best attribute group which should be selected in order to obtain the hedonic price model. Secondly, the data analysis add-in, in Excel, with its multiple linear regression function can identify significant attributes with a p-value of less than 5%. Expert knowledge is used in parallel therewith to explain the selection or rejection of attributes which are meaningful for prediction of the dependent variable, namely the price. In this study, R’s stepwise selection was used to select residential land attributes.

6.6 Developed tool for capturing information

6.6.1 Explicitly reported parameters

The data is analysed with standard statistical tools to evolve step by step to a smaller numbers of attributes, which still offers a good predictive value [22] [16] [23] [18] [19] [20] [21].

Twelve residential land attributes were chosen as a starting point, based on the literature, expert knowledge and their availability on advertising websites (Table 6.1). In a next step was a reliable subset of attributes was obtained on the basis of established statistical techniques (Table 6.2). Subset 3 has nine attributes and was chosen to identify the value function, because we can predict approximate prices with R-squared (R^2) to be 0.873 for small numbers of attributes.

Table 6.1 Attributes of residential land for detached and terraced housing unites

ID	Attribute name	Unit	Variable Name	Description
0	Price	10^6 VND	pri	Price of residential land
1	Width	m	wid	Width of the residential land.
2	Depth	m	dep	Depth of the residential land.
3	Road width	m	roa	Width of road in front of residential land.
4	Circulation	%	cir	% Circulation or road area of the project
5	Commercial area	%	com	% Land to build commercial facilities.
6	Apartment	%	apa	% Land to build apartments
7	Terraced house	%	ter	% Land to build terraced houses.
8	Detached house	%	det	% Land to build detached houses.
9	Orientation	1 to 8	ori	8 orientations in step of 45^o, from North
10	Social area	%	soc	% Land for hospitals, schools and parks
11	Nearest city centre	1/km	nea	Inverse of distance to city centre
12	Park	%	par	% Green or water area within projects

6.6.2 Multiple exponential regression analysis

Table 6.2 Attribute selection by using multiple linear regression method

Attribute name	Subset 1	Subset 2	**Subset 3**	Subset 4	Subset 5
Intercept	30	-7,762*	**-7,413***	-3115*	-531*
Wid	126*	126*	**126***	127*	124*
Dep	30*	30*	**28***	21*	21*
Roa	9*	9*	**9***	9*	6*
Com	-1,745*	8,097*	**7,928***	3887*	
Apa	-	22,408*	**21,623***	10032*	
Ter	799*	8,887*	**8,649***	4401*	
Det	-1,220*	4,931*	**4,903***	2797*	
Soc	-399	12,272*	**11,832***	3880*	
Cir	-4,131*	3,889*	**3,701***		
Ori	17*	17*			
Nea	2,386*				
Par	-				
R Square	0.877	0.877	**0.873**	0.866	0.713
Akaike information criterion (AIC)	2100	2100	**2102**	2107	2168
Significance F	<0.001				

**p<0.05, linear regression*

Table 6.3 provides an overview of the values and spread of the following characteristics: plot size, road width, distance from the central city and land use. Terraced houses occupied, on average, 26% of land and the circulation covers an average 37% while the area for commercial facilities, social facilities and detached house are very different for the considered projects. In most cases, the living room's main window's opening is oriented to the South, which can capture the maximum amount of cooling air during the summer season.

Table 6.3 Descriptive statistics of the land attributes

Price and land attributes	unit	Mean	Standard Error	Median	Standard Deviation	Min	Max
Price	10^6VND	862	43	660	519	220	2522
Width	m	6.5	0.3	5.0	3.2	4.0	18.0
Depth	m	21.9	0.2	22.6	3.0	15.0	31.5
Road width	m	22.6	0.8	20.0	9.5	8.0	47.0
Commercial area	%	7.7	0.9	1.7	11.3	1.2	37.4
Apartment	%	6.0	0.4	5.6	4.8	1.0	11.6
Terraced house	%	26.1	1.1	17.2	12.9	16.7	61.9
Detached house	%	7.1	0.5	7.2	6.1	1.0	22.2
Social area	%	6.3	0.2	6.4	3.0	1.0	11.1
Circulation	%	37.2	0.4	36.7	4.7	25.6	45.4
Nearest	1/km	0.270	0.009	0.208	0.106	0.192	0.556
Park	%	4.78	0.23	5.89	2.80	0.69	10.21
Orientation	-	5.0	0.2	4.0	2.2	2.0	8.0

6.7 Deriving utility functions

A power function of $y= ax^b + e$ was used to search for utility functions. The nonlinear utility functions are also conceptually interesting even though the linear regression is widely used to build regression equations for preferences with multiple attributes. The approach of minimizing the sum of squared errors is used to search for nonlinear regression functions [24]. An procedure was elaborated by the author based on approaches documented in the literature [25] [26]. The least square method is used to search factors regression function $y= \sum ax^b + e$ with constraint: $0 < b < 1.0$.

$$P_1 = 421{,}4 * wid^{0,6} + 2136{,}5 * dep^{0,2} + 9{,}2 * roa + 9457{,}1 * com + 11679{,}5 * apa^{0,5} + 11065{,}6 * ter + 3901{,}1 * det + 8978{,}8 * soc^{0,2} + 2252{,}4 * cir - 17504 \quad (\textit{Equation 1})$$

$$P_2 = 126 * wid + 28 * dep + 9{,}0 * roa + 7{,}928 * com + 21{,}623 * apa + 8{,}649 * ter + 4{,}903 * det + 11{,}832 * soc + 3{,}701 * cir - 7{,}413 \quad (\textit{Equation 2})$$

In Figure 6.6, the actual price is plotted, versus the two predicted prices, which is based on the two approaches. As can be seen in this case the difference in the predicted prices is not so great and the correlation, visualised in the graph, is not so different. The preferences are only slightly better described by the non-linear utility function than in the linear one (Equation 2).

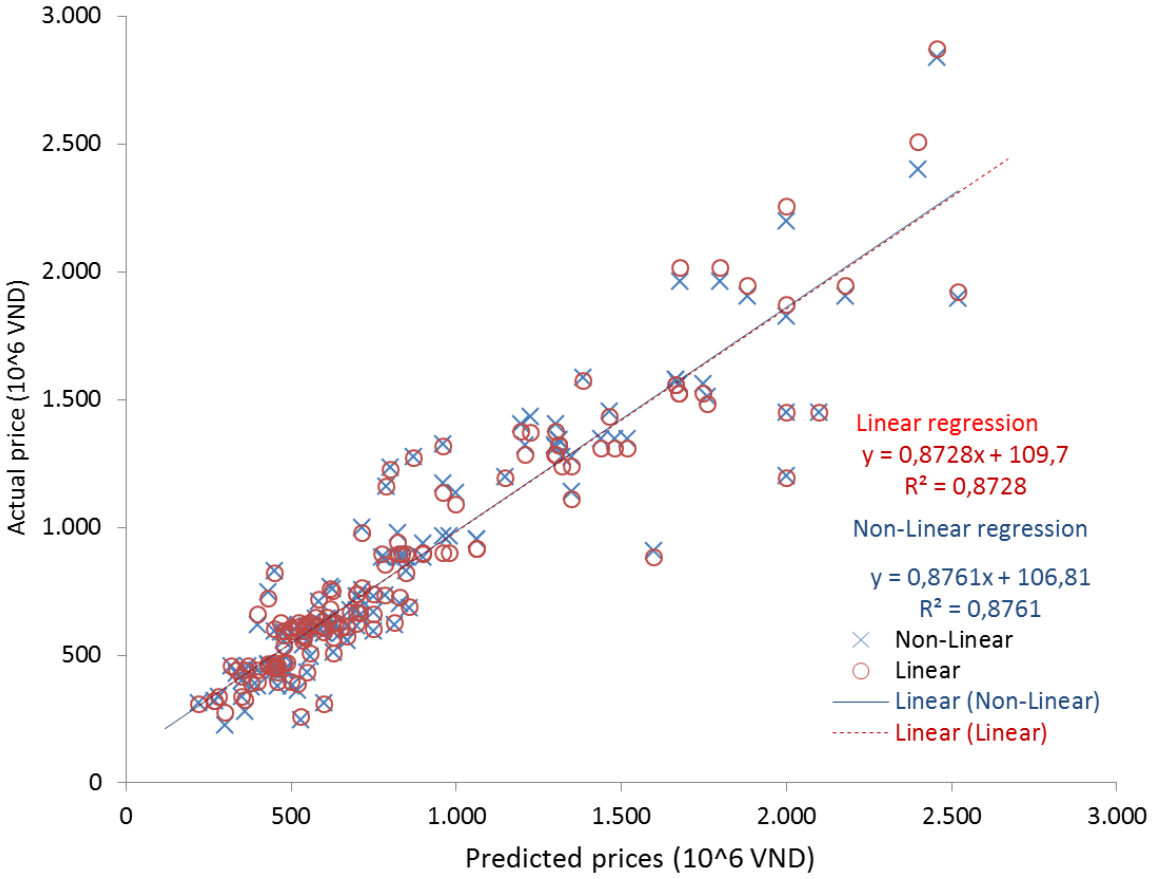

Figure 6.6 Comparison between predicted price and actual prices of two utility functions, (1$ = 20,000 VNĐ). Two regression functions are almost the same R-squared values.

6.8 Deriving visual conclusion for stakeholders

6.8.1 Visual reference information to make decision for designer

As a theoretical exercise, the nine residential attributes were varied within realistic ranges in order to obtain combinations and estimate costs and predict selling prices. A two dimensional graph visualizes all the combinations. The two Pareto fronts are constructed using a software model developed by the author, (Figure 6.7). The Pareto optimal points can support developers who need to optimize profit with limited budget. Each alternative on the Pareto optimal frontier has nine specific values for the parameters: depth, width of plot and road width (Figure 6.8 a) and fraction of the land allocated to different functions (Figure 6.8 b).

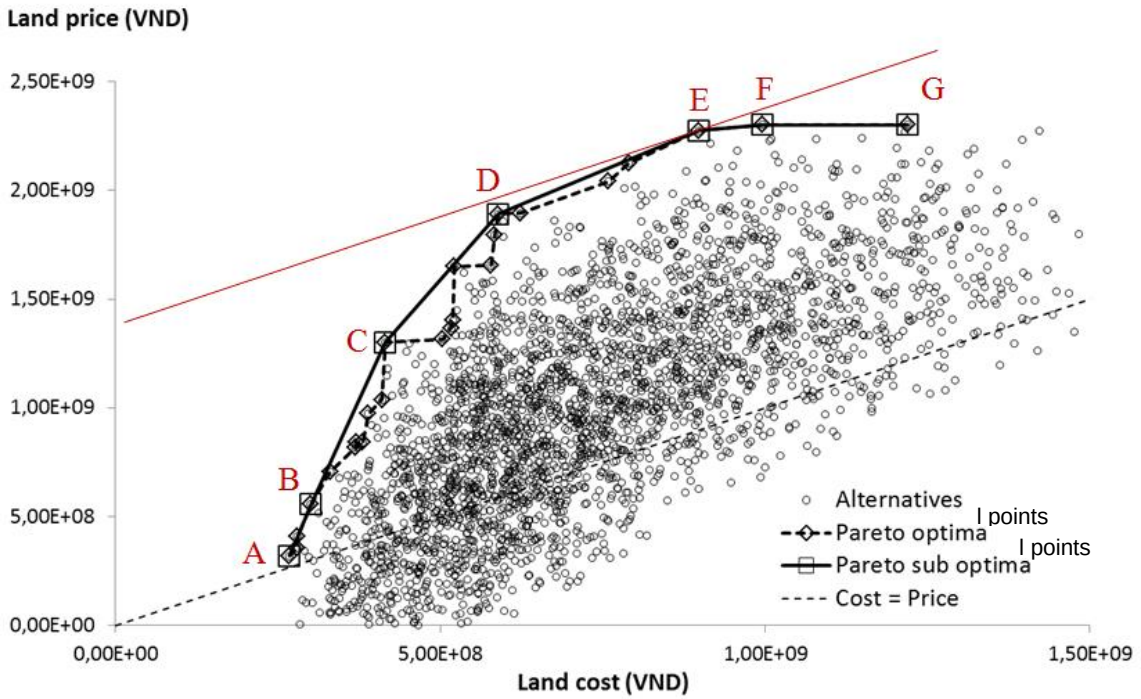

Figure 6.7 Profit maximizations with two Pareto fronts. Alternative E brings the highest profit to the developers, (1$ = 20,000 VNĐ).

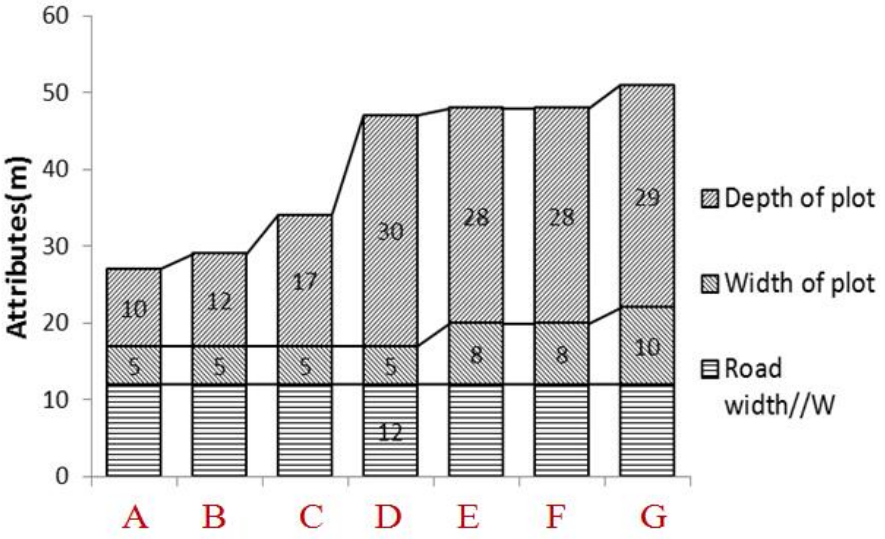

a)

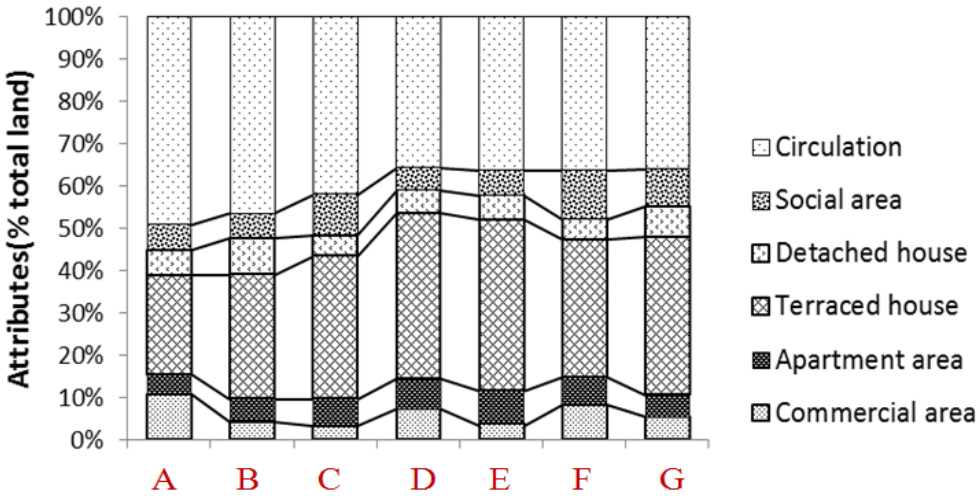

b)

Figure 6.8 Layout properties, Multi-Objective maximizations of the Pareto sub optimal points.

6.8.2 Visual reference information to make decision for developers

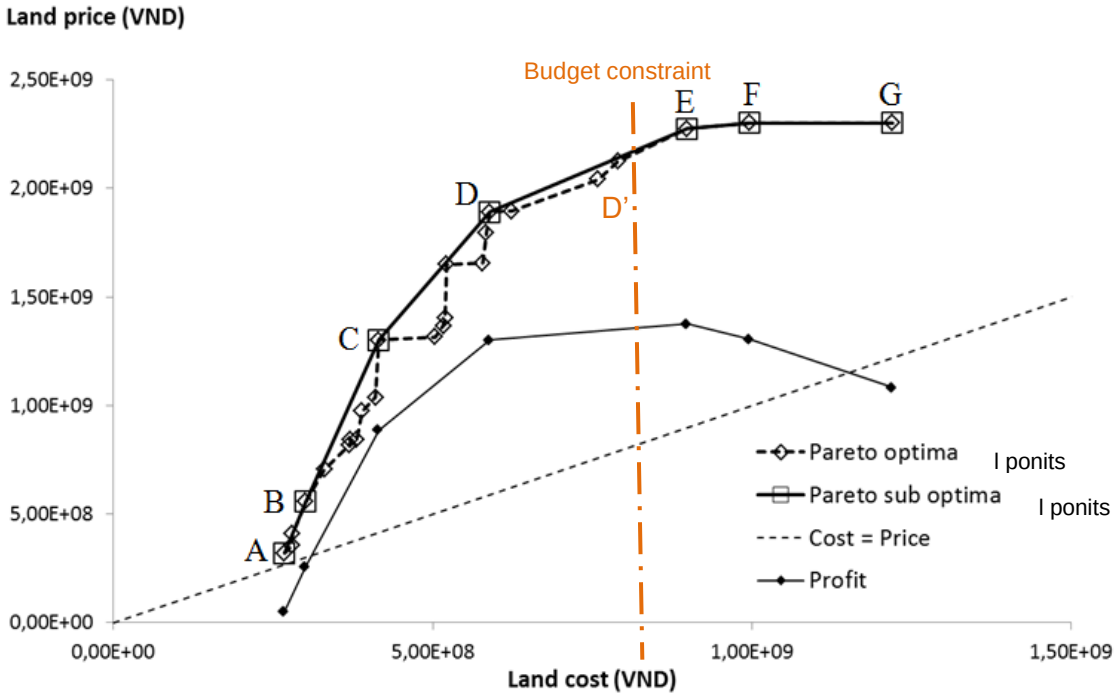

Figure 6.9 Land price and profit of two Pareto fronts, (1$ = 20,000 VNĐ).

The developers can apply three rules in selecting design alternatives. (1) The developers select the alternative with the highest total profit (point E). (2) The developers

select the alternative with the highest total profit within the cost constraint for the initial budget. This may be a point on the dashed line with sub-optimal points. For example, point D' if the budget constraint is represented by the long dashed dot line (Figure 6.9). (3) To move from the cheapest alternative, point A, to the next alternative on the Pareto sub optimal line, such as to B, C and D, as long as the additional income for the additional costs are higher than a particular value. This rule will be applied in cases where the developers have other investment opportunities outside of the possibilities represented by the graph.

6.8.3 Visual reference information to make decision for customers or users

Customers or users are the essential participants in Public-Private-People Partnership model [27]. The options they favour most are those for which they are willing to spend most. For alternatives E, F and G the developers still turn a profit but the maximum profit is only reached for E. Thus F and Gwill not be selected by the developers. Even the step from D to E may not be attractive enough to the developers because the profit per investment is smaller than the profit of the previous step for one capital unit investment.

6.8.4 Visual reference information to make decision for policy makers

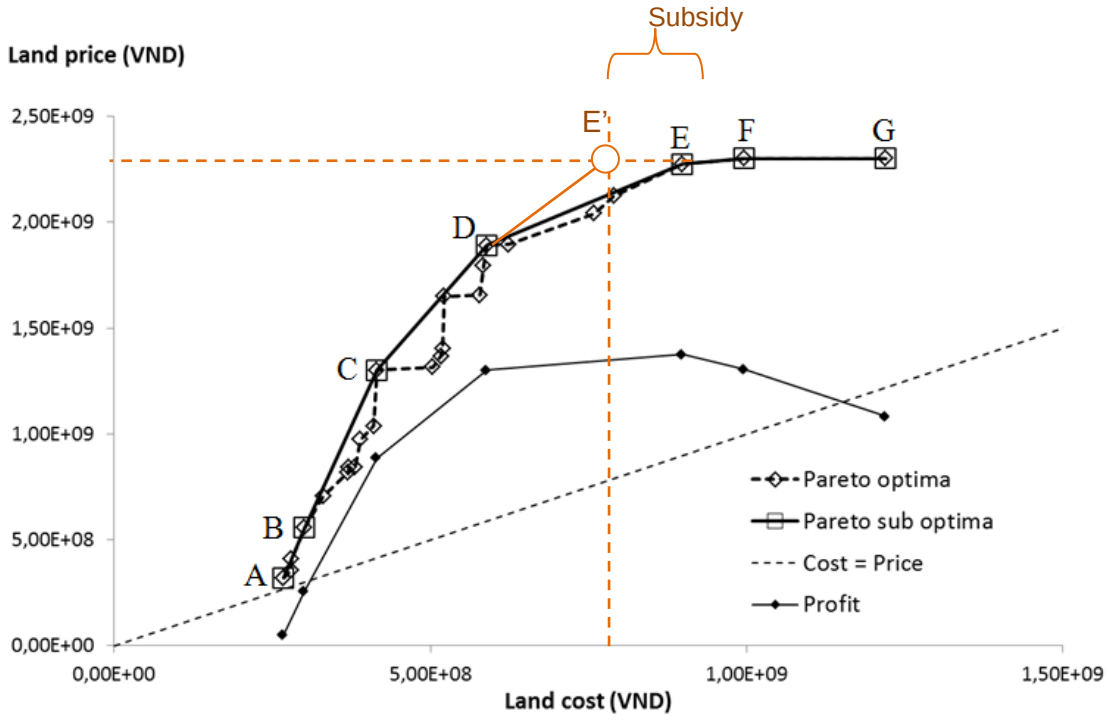

Figure 6.10 Subsidy is a tax reductions, subsidy or provisions of infrastructure to improve profit for the developers, (1$ = 20,000 VNĐ).

Apart from development regulation (e.g.: which percentage of the land has to be provided as a green area) policy makers can use the model to negotiate with the developers in terms of tax reduction, subsidies and/or public budgets for infrastructure provision. In the example above, limited subsidies can make the step from D to E' becomes attractive enough to the developers. The government may allow support for a subsidy value to decrease the cost for developers and to improve the profit of the housing project. In that instance, the alternative E' is more interesting than option E (Figure 6.10).

However, another approach is also possible: since, for solution E, the total income over cost is 2.3, the public authorities may impose this option on developers. They can reach this total profit even if they opt for the less profitable step from D to E. Social goals can be achieved by imposing this step.

The support of governments (e.g.: infrastructure provision) becomes a critical factor so that the developers can reach their expected profit at locations which are far from the city centre and which have insufficient infrastructural provisions. On the other hand, municipalities can desire that developers extend social or green areas, but the profit involved is not interesting enough for the investors. Therefore, the model becomes a glass box for both the developers and for the governmental agencies.

6.9 Sensitivity analysis

There are two types of uncertainty in the model: prediction of preference and of cost. Firstly, preference uncertainty relates to collected data, different times and the analysis method. The land prices may be affected by economic crises and by upgrading infrastructures nearby the large scale housing projects. Increasing sample size and reducing the length of time for data collection can minimize these errors. Urbanization in young cities in the Mekong Delta may also change some value perceptions, regarding owning dwellings, in the urban areas. Secondly, cost models are uncertain when deriving the land costs, unit prices of material and labour costs because they have to be updated very regularly in order to adapt to market prices. The methods for infrastructure systems construction selected and the management efficiency can also reduce costs.

The limits of this model are that it only focuses on the residential land for individual plots in the large scale housing projects and omits effects of existing infrastructures nearby the housing projects. Hence, the model can be improved in two ways; firstly, the model might be improved by taking housing costs into account. In so doing, initial construction cost for the house has to be subtracted from the total cost of land including the house including additional hypothesises. Secondly, besides distance to the city centre, other facilities such

as schools, commercial and social areas also have an impact on the cost and value of housing projects.

6.10 Conclusions

This chapter discusses the procedure to obtain preferences for residential land in the large scale housing projects. Regression functions for residential land are obtained based on web data. The results are analysed and visualised to support stakeholders of the housing projects to make the decisions.

There are two conclusions that can be drawn in this chapter. The first is that housing preferences are (in this case) only slightly better described by an exponential utility function than it is by a linear one. The second is that a visual summary of the model can facilitate in the selection process for different stakeholders (clients, developers and public authorities).

This model can stimulate the housing market by linking the "*willingness to pay of customers*" to "*profit expectations of economic actors*". Firstly, this model can maximize developers' profits by considering housing preferences in real estate market, because it searches the highest revenues with the lowest cost of land developed. Secondly, policy makers have cost estimating tools for housing projects to negotiate with real estate investors via public private partnership and with the participation of users. The model is also useful for policy formulations and social interventions in the market. The model can lead to a win-win-win situation for end users, policy makers and developers. Further research will include other housing characteristics in order to elaborate the model for all kinds of dwelling units.

The model for residential land preferences has some limitations that should be considered for future research and application. First, Cantho is a young city with majority of residents who come from rural areas. Their housing preferences may not be appropriate for urban areas and changing over time. Therefore, housing preference should be confronted with sustainability, life cycle cost and cultural shifts in future. Second, this exploration of deriving preferences from information is at this moment limited by the small number of cases after filtering. This limit may lead to errors in the preferences model. However, there is potential to apply this model in large city and to consider impacts of sub-centres city or satellite cities.

References

[1] X. Bonnefoy, Inadequate housing and health: an overview, Int. J. Environ. Pollut. 30 (2007) 411–429.

[2] UN-Habitat, Housing for All: The Challenges of Aff ordability, Accessibility and Sustainability, Nairobi, 2008.

[3] GSO-VN, General Statistical Office of Vietnam, (2011). http://www.gso.gov.vn/.

[4] MOC-VN, Ministry of Construction of Vietnam, (2011). http://www.moc.gov.vn.

[5] E. Hofman, J.I.M. Halman, R.A. Ion, Variation in Housing Design: Identifying Customer Preferences, Hous. Stud. 21 (2006) 929–943.

[6] B.Z. Zinas, M.B.M. Jusan, Housing Choice and Preference: Theory and Measurement, Procedia - Soc. Behav. Sci. 49 (2012) 282–292.

[7] A. Delgado, F. De Troyer, Modeling Quality And Housing Preferences For Affordable New Housing Developments, Open House Int. (2011) 27–37.

[8] F. De Troyer, BB/SfB-plus Een fuctionele hierarchie voor gebouwelementen, Uitgeverij ACCO, Leuven, 2008.

[9] S. Rosen, Hedonic Prices and Implicit Markets: Product Differentiation in Pure Competition, J. Polit. Econ. 82 (1974) 34–55.

[10] A.C. Goodman, Hedonic prices, price indices and housing markets, J. Urban Econ. 5 (1978) 471–484.

[11] D.M. Brasington, D. Hite, Demand for environmental quality: a spatial hedonic analysis, Reg. Sci. Urban Econ. 35 (2005) 57–82.

[12] K. Beron, J. Murdoch, M. Thayer, The Benefits of Visibility Improvement: New Evidence from the Los Angeles Metropolitan Area, J. Real Estate Finance Econ. 22 (2001) 319–337.

[13] Sylvia J.T. Jansen, Sylvia J.T. Jansen, Roland W. Goetgeluk, The Measurement and Analysis of Housing Preference and Choice, Springer, 2011.

[14] T. Thien Thu, R. Perera, Consequences of the two-price system for land in the land and housing market in Ho Chi Minh City, Vietnam, Habitat Int. 35 (2011) 30–39.

[15] T. Thien Thu, R. Perera, Intermediate levels of property rights and the emerging housing market in Ho Chi Minh City, Vietnam, Land Use Policy. 28 (2011) 124–138.

[16] R. Genuer, J.-M. Poggi, C. Tuleau-Malot, Variable selection using random forests, Pattern Recognit. Lett. 31 (2010) 2225–2236.

[17] U. Grömping, S. Landau, Do not adjust coefficients in Shapley value regression, Appl. Stoch. Models Bus. Ind. 26 (2010) 194–202.

[18] T. M. Conway, R. G. Lathrop Jr., Modeling the Ecological Consequences of Land-Use Policies in an Urbanizing Region, Environ. Manage. 35 (2005) 278–291.

[19] N. Dunse, C. Jones, A hedonic price model of office rents, J. Prop. Valuat. Investmen. 16 (1998) 297–312.

[20] F. Kong, H. Yin, N. Nakagoshi, Using GIS and landscape metrics in the hedonic price modeling of the amenity value of urban green space: A case study in Jinan City, China, Landsc. Urban Plan. 79 (2007) 240–252.

[21] H. Ssegane, E.W. Tollner, Y.M. Mohamoud, T.C. Rasmussen, J.F. Dowd, Advances in variable selection methods I: Causal selection methods versus stepwise regression and principal component analysis on data of known and unknown functional relationships, J. Hydrol. 438–439 (2012) 16–25.

[22] M.R.E. Symonds, A. Moussalli, A brief guide to model selection, multimodel inference and model averaging in behavioural ecology using Akaike's information criterion, Behav. Ecol. Sociobiol. 65 (2011) 13–21.

[23] U. Grömping, Variable Importance Assessment in Regression: Linear Regression versus Random Forest, Am. Stat. 63 (2009) 308–319.

[24] E.J. Billo, Nonlinear Regression Using the Solver, in: Excel Sci. Eng., John Wiley & Sons, Inc., 2007: pp. 313–339.

[25] N. Aliane, J. Fernandez, S. Bemposta, A spreadsheet method for continuous-time model identification, Measurement. 46 (2013) 680–687.

[26] B.D. McCullough, D.A. Heiser, On the accuracy of statistical procedures in Microsoft Excel 2007, Comput. Stat. Data Anal. 52 (2008) 4570–4578.

[27] W. Majamaa, S. Junnila, H. Doloi, E. Niemistö, End-user oriented public-private partnerships in real estate industry, Int. J. Strateg. Prop. Manag. 12 (2008) 1–17.

CHAPTER 7 COMFORT AND COSTS

In this chapter, models are elaborated to predict thermal comfort if minimal light levels are provided. The model considers design decisions at different scale levels: from urban clustering and orientation, through building layout down to material selection. Two key points are addressed:

(1) The development of a surrogate model for predicting wind pressure coefficients (Cp) which is used to predict air flow for cooling via natural ventilation.

(2) An “Energy Management System” (EMS) to simulate, in a dynamic way, occupant behaviour in order to minimize energy use for a pre-set thermal comfort.

General conclusions are formulated.

Some parts of this chapter are based on the publication:

Nguyen Van T., De Troyer F., Trigaux D., Ayu M. (2014). Cost and comfort optimisation for buildings and urban layouts by combining dynamic energy simulations and generic optimisation tools. Cost and comfort optimisation for buildings and urban layouts by combining dynamic energy simulations and generic optimisation tools. Eco-Architecture V (pp. 81-92).

Table of Contents

7.1	**Introduction**	**135**
7.2	**Thermal comfort in built environments**	**135**
7.3	**Predicted Mean Vote (PMV) and Adaptive Thermal Comfort (ATC) approach**	**136**
7.3.1	Predicted Mean Vote (PMV) approach	136
7.3.2	Adaptive Thermal Comfort (ATC)	137
7.4	**Dynamic heat balance of the EnergyPlus simulation tool**	**138**
7.4.1	Heat balance	138
7.4.2	Building energy simulation programs and EnergyPlus	139
7.5	**Multi-zone Airflow Network model**	**140**
7.6	**Surrogate models to obtain the wind pressure coefficient (Cp)**	**140**
7.6.1	Surrogate models	140
7.6.2	Wind pressure coefficient (Cp)	141
7.6.3	Cp meta-model based on Cp Generator TNO for terraced houses	143
7.6.4	Meta-model Cp based on the meta-model Cp of M. Grosso for a detached house and apartment	154
7.6.5	Cp values based on Grosso's model for detached and Semi-detached house	156
7.6.6	Approximation formulas to calculate wind pressure coefficients (detached and Semi-detached house)	157
7.6.7	Approximation formulas to calculate wind pressure coefficients for apartment	159
7.7	**Strategies for comfort (dynamic schedule and user behaviour)**	**162**
7.7.1	Comfort evaluation and strategy based on dynamic schedules for ventilation and cooling	162
7.7.2	Strategy based on dynamic schedules for ventilation and cooling	162
7.8	**Life Cycle Cost: Parameters in EnergyPlus**	**163**
7.9	**Urban forms, geometry and materials of housing types**	**164**
7.9.1	Terraced house geometry	164
7.9.2	Detached house geometry	165
7.9.3	Apartment geometry	166
7.9.4	General options for material	167
7.10	**Results and discussions**	**167**
7.10.1	Case study for terraced house: Varying all selected parameters with fixed building North	167
7.10.2	Energy consumption in case of different orientations for terraced house	169
7.10.3	Case study for detached house: Varying all selected parameters	171
7.10.4	Case study for apartment unit at the middle of the building	174
7.10.5	Case study for apartment unit at bottom, middle and top of building	177
7.11	**Rules of thumb for design**	**179**
7.12	**Conclusions**	**179**

7.1 Introduction

In Asian countries, the average cooling energy in buildings will increase more than hundred percentage by 2050 [1]. Vietnam is one of the fastest-growing economies and high population in Asia. The energy demand in Vietnam for the residential and commercial buildings has become heavy load for the energy supply beside the energy demand of industry sectors. Thermal comfort generates a significant demand on energy in building performance. The sustainable approach, to save energy during the building's life cycle, using passive design strategies include: natural ventilation, reducing solar and internal heat gain, wearing appropriate clothes, using electric fans and, eventually, using cooling systems. The approach includes multiple scales from selecting materials, over building geometries and up to urban forms. Energy saving could be addressed by considering the six driving factors of energy performance (Figure 7-1).

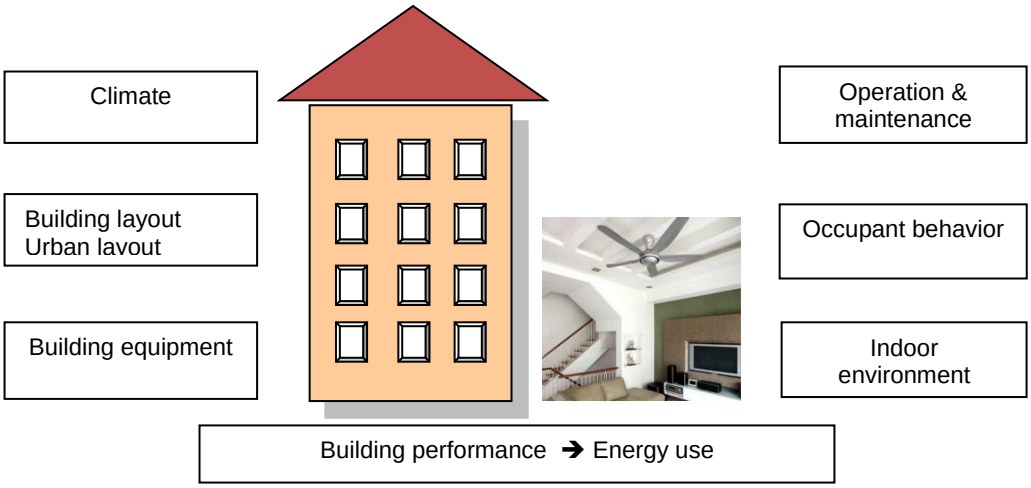

Figure 7-1 Six driving factors of energy performance of buildings (modified from IEA ECBCS Annex 53).

7.2 Thermal comfort in built environments

Thermal comfort in built environments is defined as the "*condition of mind in which satisfaction is expressed with the thermal environment and is assessed by subjective evaluation*" [2]. Thermal comfort is a cognitive process involving many inputs which are influenced by physical, physiological, psychological factors. This comfort is a significant aspect in building science which has a profound influence on the ways through which to design, operate and use energy for heating, cooling and the ventilating of buildings [3]. Designers cannot create a thermal environment that can satisfy every occupant in a living space, due to the physiological and psychological variation of its unique occupants. However, thermal comfort models can generate insights through statistical results based on intensive laboratory

work and in-field experiments. Nevertheless, at present designing a condition by which to satisfy 80% or even 90% of occupants is feasible.

Although thermal comfort is one of the research objectives of human physiology, it has been attended to by building scientists because thermal comfort standards are crucial criteria for an occupants' satisfaction with their indoor environment, health and productivity. In fact, occupants may use a huge amount of energy in order to achieve thermal comfort to counteract inappropriate design alternatives.

7.3 Predicted Mean Vote (PMV) and Adaptive Thermal Comfort (ATC) approach

7.3.1 Predicted Mean Vote (PMV) approach

The thermal comfort level can be estimated by one of two approaches: PMV and ATC. The Predicted Mean Vote (PMV) or Predicted Percentage Dissatisfied (PPD) is widely used metric for thermal comfort performance indicators [4]. Table 7-1 shows that the PMV is obtained based on six input parameters: metabolic rate, clothing insulation, air temperature, mean radiant temperature, air velocity and air humidity. The PMV approach is almost 40 years old and is still used as the best method to evaluate thermal comfort [5].

Table 7-1 Six factors take into consideration when designing for thermal comfort

Determining factors	Explanations
Metabolic rate	The energy generated from the human body
Clothing insulation	The thermal resistance of thermal insulation of wearing clothes
Air temperature	Temperature of the air surrounding the occupant
Radiant temperature	The weighted average of all the temperatures from surfaces surrounding an occupant
Air velocity	Rate of air movement given distance over time
Relative humidity	Percentage of max water vapour in the air for that temperature

The Predicted Mean Vote (PMV) model of Fanger calculates the thermal balance of a person and is the basis of ISO Standard 7730. Depending on the activity empirical data provide the average heat production per square metre body surface. Different equations predict heat losses via the skin (conduction via clothing layer, convection and radiation) and via respiration. The net result is that the body is heated up or cooled down. This heat storage/ release rate is translated into the vote on the 7 points comfort scale, which is an estimate of the expected average vote of a panel of evaluators for a given thermal environment.

In warm climates, an extension of the PMV/PPD model proposes a correction in cases of the natural ventilation (NV) of buildings [6]. The PMV-value is multiplied by the correction factors to obtain the adapted PMV for occupants in naturally ventilated buildings. The

correction factor (called expectancy factor e) reaches a maximum value of 1.0 for air conditioned buildings and a minimum 0.5 for non-air conditioned buildings. Other values of the factor can be selects based on the upper temperature limits in the Table 7-2.

Table 7-2 non-air conditioned buildings in warm climates

Expectancy factor, e	Predicted percentage discomfort (PPD, %)	Predicted mean vote (PMV)	Adjected PMV
1	10	0.5	0.5
	20	0.85	0.85
0.7	10	0.7	0.5
	20	1.2	0.84
0.5	10	1.0	0.5
	20	1.7	0.85

The PMV refers to a thermal scale that runs from Cold (-3) to Hot (+3) as in Table 7-3. The original data was collected by subjecting a large number of people with different conditions within a climate chamber and inviting them to select a position on the scale that describes best their comfort sensation. A mathematical model of the relationship between all the environmental and physiological factors considered was then derived from the data.

Table 7-3 Predicted Mean Vote sensation scale, the recommended acceptable PMV range for thermal comfort from ASHRAE 55 is between -0.5 and +0.5 for an interior space.

Value	Sensation
-3	Cold
-2	Cool
-1	Slightly cool
0	Neutral
+1	Slightly warm
+2	Warm
+3	Hot

7.3.2 Adaptive Thermal Comfort (ATC)

The ATC model is developed based on thermal comfort data in the field [7]. The thermal comfort data are obtained by asking the occupants to give the comfort vote on the scale of ASHRAE [8] (Table 7-3). The ATC considers the indoor operative temperature in relation to the outdoor air temperature as its main performance indicator and is a less complex performance indicator [8] and [9]. The adaptive approach concept is based on the fundamental assumption that "*if a change produces discomfort, people react in ways which tend to restore their comfort*" [3]. The ATC has obtained a privileged place in standards, such as the CEN (2007) and ASHRAE (2004). This approach has been further developed but has been applied

throughout the last 20 years [10]. The ATC is simplified the correlation between the indoor comfort temperature and the outdoor temperature as a linear regression equation in the [11].

$T_{comf} = A * T_{a,\,out} + B$

Where T_{comf} = comfort temperature [°C];

$T_{a,out}$ = monthly mean outdoor air temperature [°C]; A, B = constants.

The application of the ATC approach is clearly simpler than the PMV/PPD approach because that model only considers the air temperature. The ATC allows for a relatively simple comfort assessment for buildings and can be used easily by building designers. In hot and humid climate, the ATC can be used for building with openings leading to same air temperature inside as outside. But this approach is not applicable for our aim, since we need to include dynamic human responses (changing clothes, increasing natural or forced air ventilation and starting cooling). An ATC model for hot and humid South-East Asia was validated with 3430 records in natural ventilation building [12]. The comfort equation for this area is:

$T_{comf} = 0.341*T_{a,out} + 18:83$

Where T_{comf} = comfort temperature [°C]; $T_{a,out}$ = monthly mean outdoor air temperature

7.4 Dynamic heat balance of the EnergyPlus simulation tool

7.4.1 Heat balance

The mechanism of heat balance, between a human body and the environment, can be expressed by an equation (Equation 7.3). This balance is maintained as much as possible by human thermoregulation in the brain. The temperature of the human body varies only in a very small range around 37°C for the average human body.

$M - W = Qsk + Qres + S$ (Equation 7.3)

Where

M	rate of metabolic heat production, W/m^2;
W	rate of mechanical work accomplished, W/m^2;
Qsk	total rate of heat loss from skin, W/m^2;
Qres	total rate of heat loss from respiration, W/m^2;
S	rate of heat storage, W/m^2.

Heat exchange processes between a building and the external environment are illustrated in Figure 7-2.

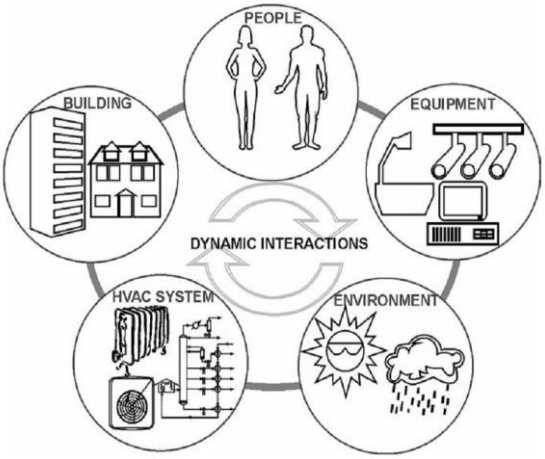

Figure 7-2 Dynamic interactions of (continuously changing) sub-systems in buildings [13]

7.4.2 Building energy simulation programs and EnergyPlus

EnergyPlus has been developed under the supervision of the U.S. Department of Energy and is based on the features and capabilities of BLAST and DOE-2 [14]. The EnergyPlus program combines many program modules that are integrated to estimate the energy use for a building that integrates a variety of systems and energy sources (Figure 7-3). EnergyPlus performs calculations by solving a large series of energy balance equations for the building's systems and surrounding environment. Every detail about the algorithms used within EnergyPlus is carefully described in EnergyPlus's engineering reference [14].

EnergyPlus models can run with different time increments, from one minute to an hour, and consider energy flows for heating, cooling, lighting, ventilation and other sources. A large number of built-in HVAC and lighting control strategies have been integrated through heat balance-based zone simulation, multi-zone Airflow network. In addition, EnergyPlus offers advanced users great flexibility via the Energy Management System (EMS). The EMS provides tools by which to develop custom control actions based on the building's actual status.

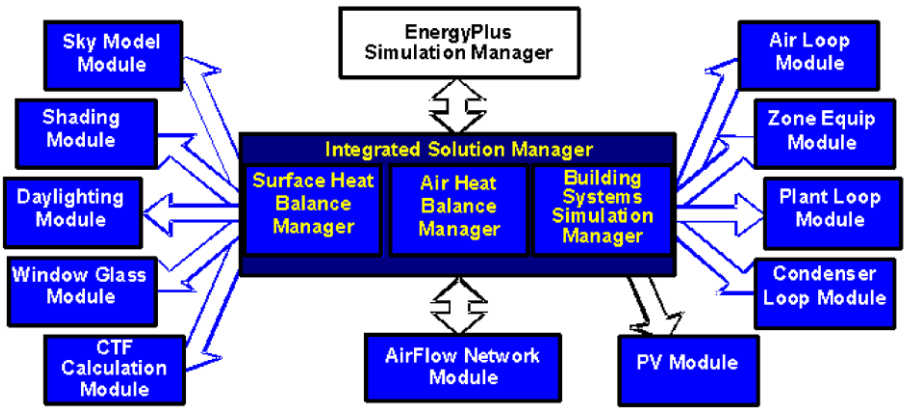

Figure 7-3 EnergyPlus internal elements [15]

Hundreds of building energy simulation tools are available as commercial products. EnergyPlus [15] is selected based on the following advantages: its dynamic simulation with small time steps, extensively tested, modular systems and plant integrated with heat balance-based zone simulation, multi zone air flow, embedded thermal comfort modes as well as allowing for the inclusion of many systems and is freely available.

7.5 Multi-zone Airflow Network model

The airflow network model in EnergyPlus provides the ability to simulate multi-zone wind-driven airflows. The air flow rate is a high sensitive parameter on the outputs [16]. In order to obtain air flow rate, EnergyPlus takes the wind's velocity from the hourly weather data and the wind pressure coefficients (Cp) at different external nodes (Figure 7-4). The Cp values can be calculated with several methods. First, in EnergyPlus, the normalized surface pressure coefficient can be written as (Swami and Chandra 1988). It can calculate wind pressure coefficient values for different wind directions for the rectangular building layout and without obstructions. Second, the Cp values also can be obtained by CFD simulations with complicated building layouts and urban forms. Third, in this study, meta-models for Cp values are developed to reduce calculating time.

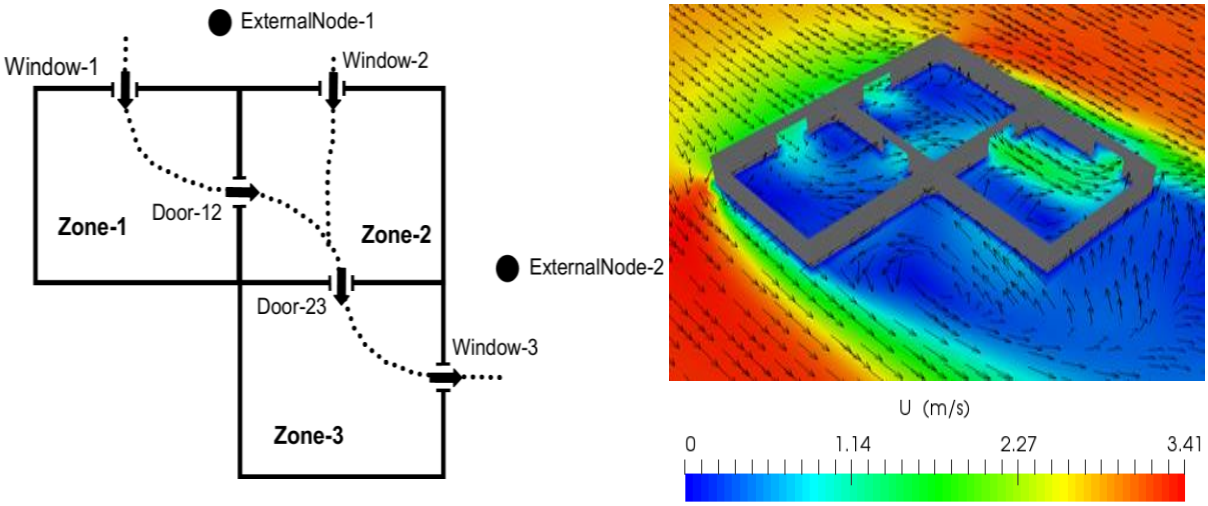

Figure 7-4 Plan view of a simple airflow network showing a possible airflow pattern

7.6 Surrogate models to obtain the wind pressure coefficient (Cp)

7.6.1 Surrogate models

Surrogate models are developed based on different approaches and can be subdivided into three categories: data-fit model, hierarchical model and reduced-order model [17]. A data fit scheme might be justifiable when equations cannot be obtained. The surrogate models are

mathematical models which are built to approximate computationally expensive simulation codes [18]. The models can be created through machine learning or by searching statistical links. A surrogate model can be built using 3 steps (Figure 7-5): (1) Building a detailed simulation model. (2) Running that model for many different cases in order to generate a database of results. In some cases, the data are based on measuring data from full scale models or small scale models. (3) Using those results to train and test the model statistically. More details of surrogate models can be found in [19], [20] and [21].

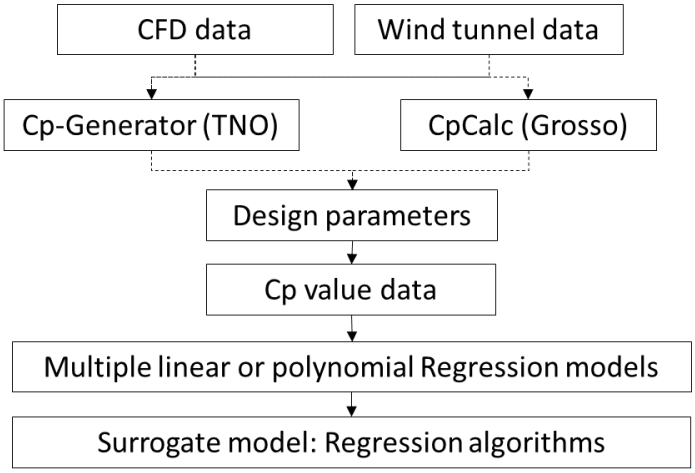

Figure 7-5 The flow chart of Cp value surrogate model

7.6.2 Wind pressure coefficient (Cp)

The wind pressure distribution on the envelope of a building is described by dimensionless pressure coefficients (Cp) which depend on the ratio of the surface dynamic pressure over the dynamic pressure in the undisturbed flow pattern measured at a reference height. Cp values, used to simulate multi-zone airflow network models for natural ventilation, can be obtained from many sources:

- Full-scale measurements when an existing building is being studied. Precise pressures on a particular building in a specific environment can be given. However, they are only applicable to that specific building-layout and to that unique environment. Thus they offer less relevant results for general applicability. Moreover, these real scale measurements require a long measurement period and generate high cost.
- Wind tunnel tests can give more relevant results because changes in building layout and urban layout are made easily. The limitations of wind tunnels includes the requirement of special tools and large wind tunnels for investigating urban models.

- The Computational Fluid Dynamic (CFD) approach has the same advantages as wind tunnel tests. CFD analysis is done on powerful computers, but is still very time consuming.

The aim in this work is to predict the effect of wind flow around the buildings on the infiltration rate. In the case of natural ventilation the infiltration rate depends on the wind pressure on the facades and permeability of the space. In the search for fast prediction models for wind pressure on the facades over the elaboration of the PhD research, first TNO Cp generator and later CpCal model developed by Grosso [22] are used to obtain the Cp surrogate models for the natural ventilation model.

Cp-generator of TNO, a meta-model available via the web, developed in the Netherlands (Toegepast Natuurwetenschappelijk Onderzoek or Organisation for Applied Scientific Research), was used to calculate the Cps on front facade, rear facade and on the roofs of block-shaped buildings situated in an environment with obstructions. This generator is based on finite element calculations and was verified with wind tunnel experiments [23] and by measured data [24]. This approach offers a rather good agreement between measured and meta-model predictions. The TNO Cp-generator approach was also applied in one study in order to obtain the Cps for a large urban fragment [25].

CpCal model was developed by analysing data from wind tunnel tests using a parametrical approach [22]. The model considered climate parameters, environment parameters and building parameters. These independent parameters were varied to generate the data that were used to obtain polynomial functions via regression. Beside the climate parameters, the model allows to vary main parameters such as plan area density, relative building height, building layout and relative position on facades. Many regression functions are used. For each of them the appropriate parameters have to be loaded from data table. This approach makes the model to become complicate to integrate the model into whole building energy simulation programs. In order to simplify this model, a meta-model for Cp is obtained based on the secondary data from CpCal.

Blocken and his group have compared the Cp values estimated through these different methods (Figure 7-6). (1) CPCALC+ is meta-model for Cp values [22]. (2) CpGenerator is also meta-model for Cp values of TNO. (3) Meta_model of Cp in EnergyPlus is the average surface wind pressure coefficient.

Cp Generator offers a specific set of Cp-values that were used in order to generate regression functions. These approaches can save time and cost. They propose correlations between some of the environment's parameters and pressure coefficients. As described in

detail below in this study both Cp Generator TNO and CpCal have been used [22]. CpCal was elaborated to analyse the natural ventilation in the urban areas [27] and empirical formulas, by Swami and Chandra (1988) for the simple building layouts, [28]. CpCal is similar with Cp generator of TNO, but CpCal considers only the same heights for neighbouring buildings.

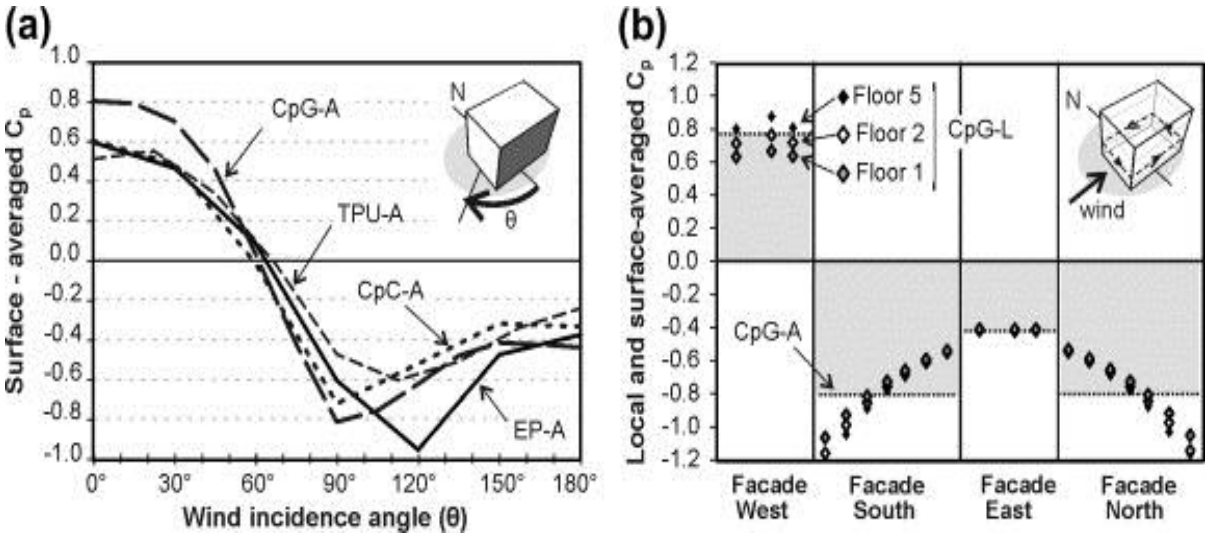

Figure 7-6 (a) Surface-averaged Cp on facade of building versus wind incidence angles (θ) from different Cp sources, i.e. EnergyPlus (EP-A), CpGenerator (CpG-A), CPCALC+ (CpC-A), and wind tunnel tests (TPU-A). (b) Local C_p at window height on the 1st, 2nd and 5th floors obtained with CpGenerator (CpG-L) for the wind direction and comparison with the surface-averaged Cp obtained with the same source (CpG-A), [26].

7.6.3 Cp meta-model based on Cp Generator TNO for terraced houses

7.6.3.1 Terraced house fragment

The simplified urban layout model, as shown in Figure 7-7 and Figure 7-8, represents large scale housing projects which can be found in many suburban areas in Vietnam. Therefore, the terraced house type was selected because this type constitutes the majority of the dwelling units in housing projects. This urban layout is described using the following key parameters: the height of the surrounding buildings, road width, building back garden and the house's width and depth. For this simplified urban fragment, the percentages of circulation, residential-open and residential-built-up have been calculated, using the element method for cost control [29] [30].

Figure 7-7 The large scale housing project Hong Phat, Google earth 7/2015, Cantho.

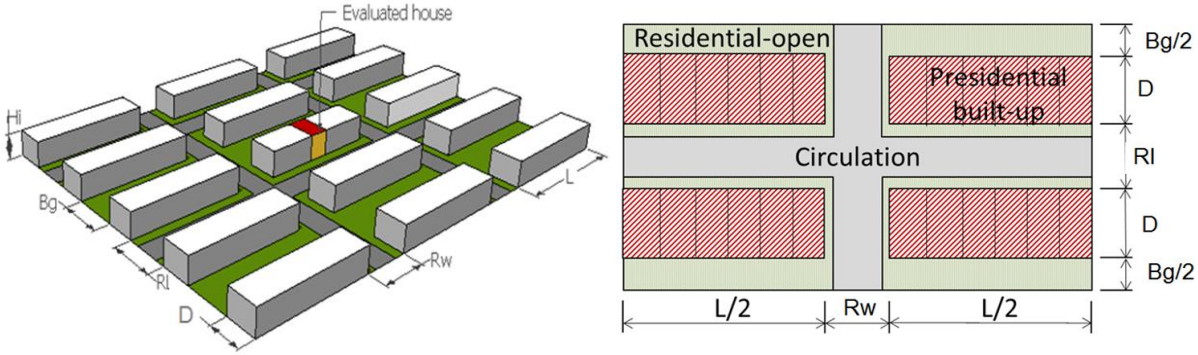

Figure 7-8 Urban form or terraced house type

Table 7-4 Numerical variables and their design options for urban layout (continuous variables).

Design parameters	Abbreviation	Initial value	Range (m)	Step size (m)
Height of surrounding buildings	H1 to H14	9	1 to 36	3
Width of road parallel with terraced row	Rw	12	12 to 24	4
Width of road perpendicular with terraced row	Rl	12	12 to 24	4
Back garden depth	Bg	12	2 to 24	4
Terraced row depth	D	16	10 to 20	2
Terraced row length	L	40	40 to 120	10

7.6.3.2 Wind pressure coefficient (Cp)

Input data, for the Cp Generator, consist of defining the terrain's roughness for the wind's different flow directions and 'obstacles'. An 'obstacle' is referred via a unique name. Following characteristics are associated: locations (x, y) of a corner point, orientation and size (L, W, H) of box Figure 7-9 and. Those data have to be transmitted to the programme as a text file with the correct formatting. A template of the TNO website illustrates the Table 7-5. In a next step the text files are uploaded to the user's account. Results of Cp values are returned and consist of data table and graphical files that can be seen in Figure 7-10 and Figure 7-11.

Table 7-5 Input template text file for Cp Generator TNO

Environment definition	Estimated Building	Obstacles
| wind.Zo | Direction: 0 135 Zo: 3 3 | north arrow compass direction in plan | Direction: 0 | obstacles (position in m(=meter))| Ground level: 0. Roof height : 10	Name : Building x,y : 0. 0. Azimut : 180 L,W,H,#,à,w: 100 14 10 Name: meteo x,y: 1.0E6 -5.0 Azimut: 90.0 L,W,H: 0.1 0.1 10.0	Name: obstacle 1 x,y: -128 68 Azimut: 180 L,W,H: 100 14 9 Name: obstacle 14 x,y: 128 -68 Azimut: 180 L,W,H: 100 14 3 | cp-positions | Building side: facade 1 Pos. x,y : 50 4.5

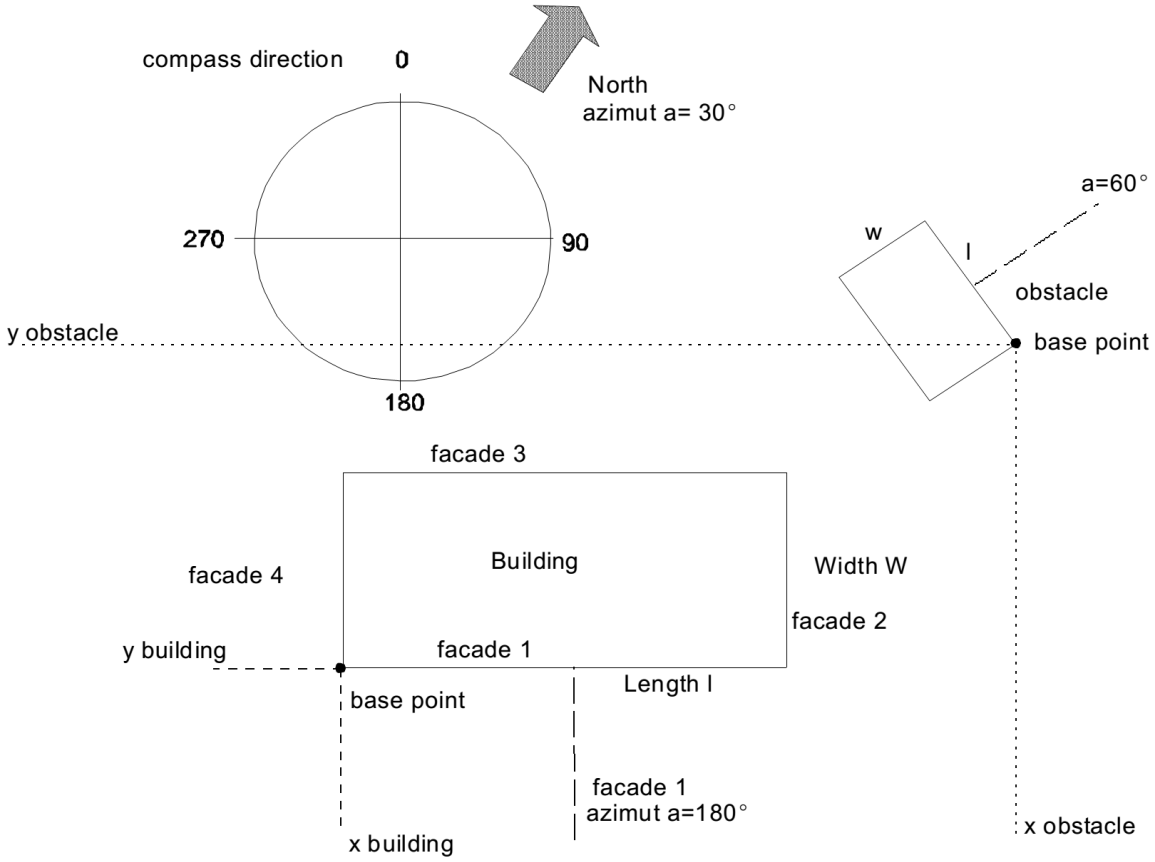

Figure 7-9 Input data of estimated building and obstacles for Cp Generator TNO.

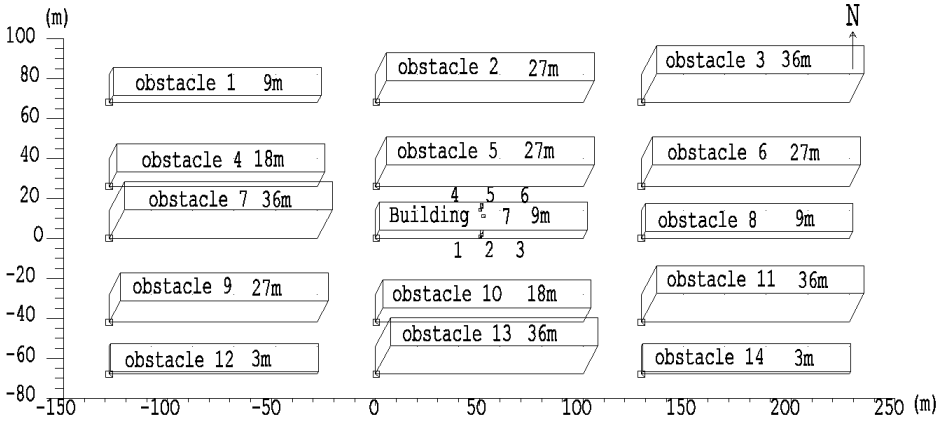

Figure 7-10 The geometry of the building and obstacles to terraced houses from TNO results in order to check the input file data. Points 1, 2 and 3 on the front facade, points 4, 5 and 6 on the rear facade. Point 7 on the roof.

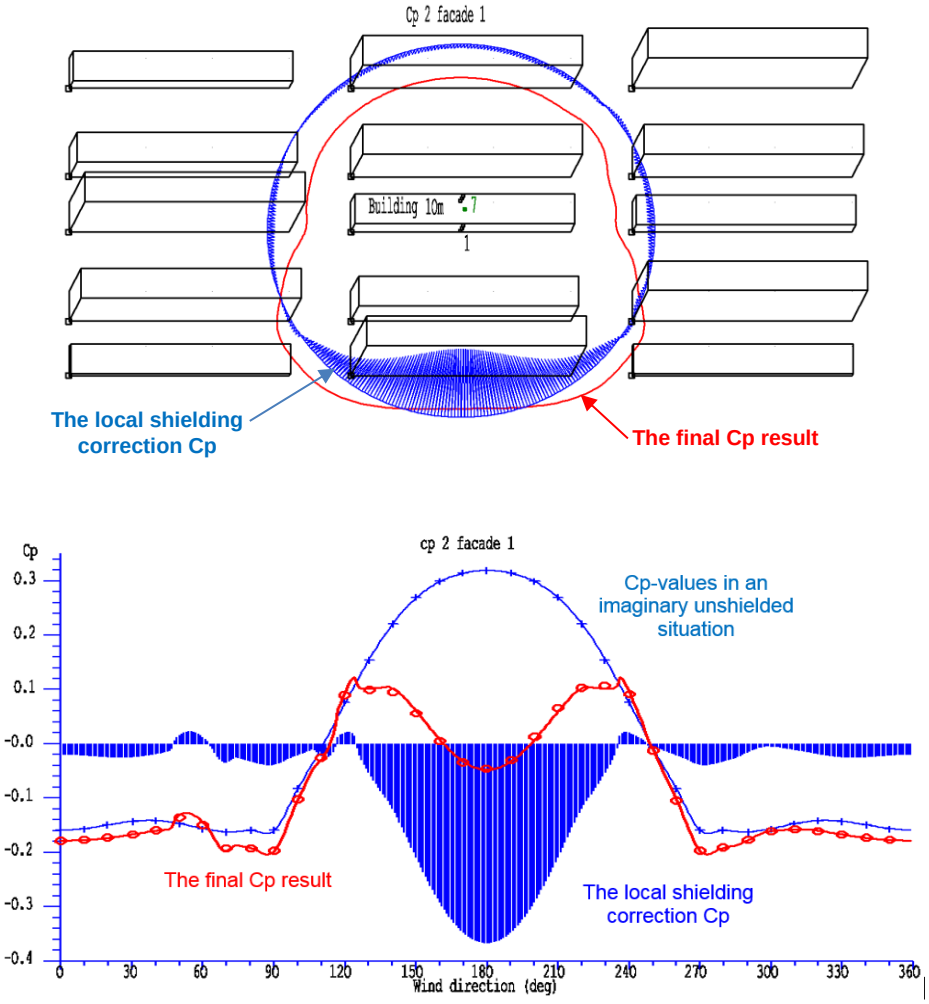

Figure 7-11 Cp values of the middle point in the front facade of the terraced house, two buildings in front of the terraced building deeply influence the wind pressure coefficient of direction 150° to 210°.

7.6.3.3 Multiple linear regressions for wind pressure coefficient (Cp) values

For a specific wind orientation, the Cp value in the middle of the windward facade of the terraced row, situated in the middle of the schematic urban fragment, depends on 19 independent parameters. An overview of those parameters is given in Figure 7-12 and Table 7-6 which include the length of the row of terraced housing units (L), depth of those units (D), width of road parallel to row of units (Rw), width of road perpendicular to the row of units (Rl), building back garden (Bg) and the height of the building and the fourteen surrounding buildings (H) (with i = 1 to14, thus 5+14=19 input parameters). The same dependency is true for the leeward facade and roof. The theoretical combinations that can be derived by varying each parameter are very large. Therefore, as a first step, the "Latin Hypercube Sampling method" is applied to generate 200 combinations of 19 independent parameters. As a second step, the Cp values of those combinations are calculated by using the TNO Cp-generator. As a third step, the coefficients of the equation, predicting the Cp values based on the neighbourhood parameters, are derived via a multiple linear regression method. For example, one regression function for the front facade is Cp of the front facade.

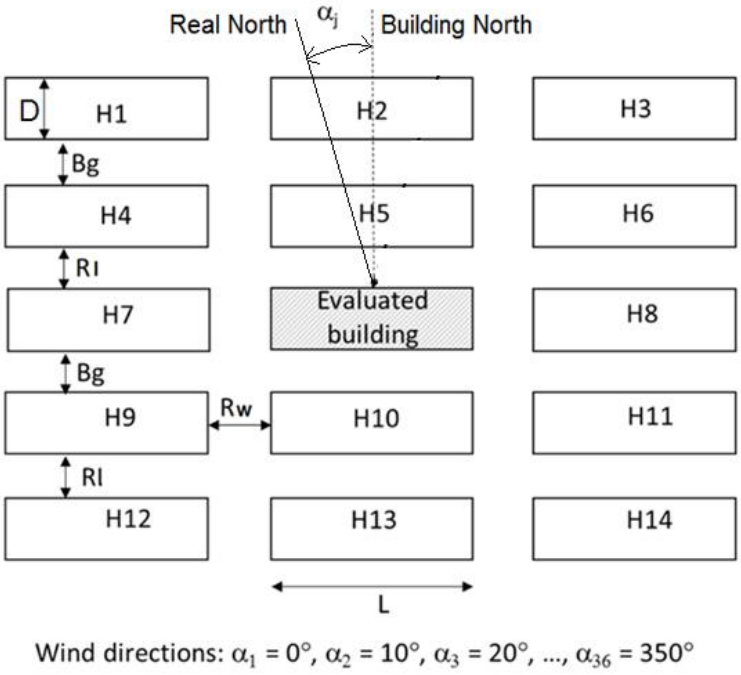

Figure 7-12 The urban parameters H_1 to H_{14}, L, D, Bg, Rl and Rw are varied within their ranges in Table 7-6.

$$Cp_{front} = a_{f1}*H_1 + \ldots. a_{f14}*H_{14} + a_{f15}*L + a_{f16}*W + a_{f17}*Rw + a_{f18}*Rl + a_{f19}*Bg + intercept.$$

The 36 functions of each surface (front facade, rear facade and roof) are

$$Cp_{front} = [f_{\alpha j}(H_i, W, L, RW, RL, Bg)] ;$$

$$Cp_{back} = [f_{\alpha j}(H_i, W, L, RW, RL, Bg)]$$

$$Cp_{roof} = [f_{\alpha j}(H_i, W, L, RW, RL, Bg)]$$

Where Hi (i=1 to 14), W, L, RW, RL, Bg are varied in their ranges in the Table 7-6 and α_j = 0°, 10°up to 350°. The factors of the multiple linear regression are reported in the Appendix B.

Table 7-6 Numerical variables and their design options of urban forms.

Design parameters	Abbreviation	Initial values	Range (m)	Step size (m)
Height of surrounding buildings	H_1 to H_{14}	9	1 to 36	3
Width of roads	Rw, Rl	12	12 to 24	4
Back garden depth	Bg	12	2 to 24	4
Terraced row depth	D	16	10 to 20	2
Terraced row length	L	40	40 to 120	10

Figure 7-15 compares the Cp values obtained from the TNO Cp-generator with those predicted using the multiple linear regression function. The results of one geometric variant are shown in Figure 7-15 for the front and back facade, and the roof and for the 36 wind directions. All coefficients of 108 functions are presented in Appendix B. The regression functions show a high correlation with the case selected via the LHS, the average R^2 = 0.92, R^2 of 200 urban forms are shown in the Figure 7-13 and Figure 7-14. For all other variants a similar good fit could also be found. Linear approximations have been used to derive the driving forces for natural ventilation. The inside air velocity is calculated based on the dwelling's opening characteristics and wind-permeability. This air speed is then used to predict the thermal comfort, based on the Fanger model.

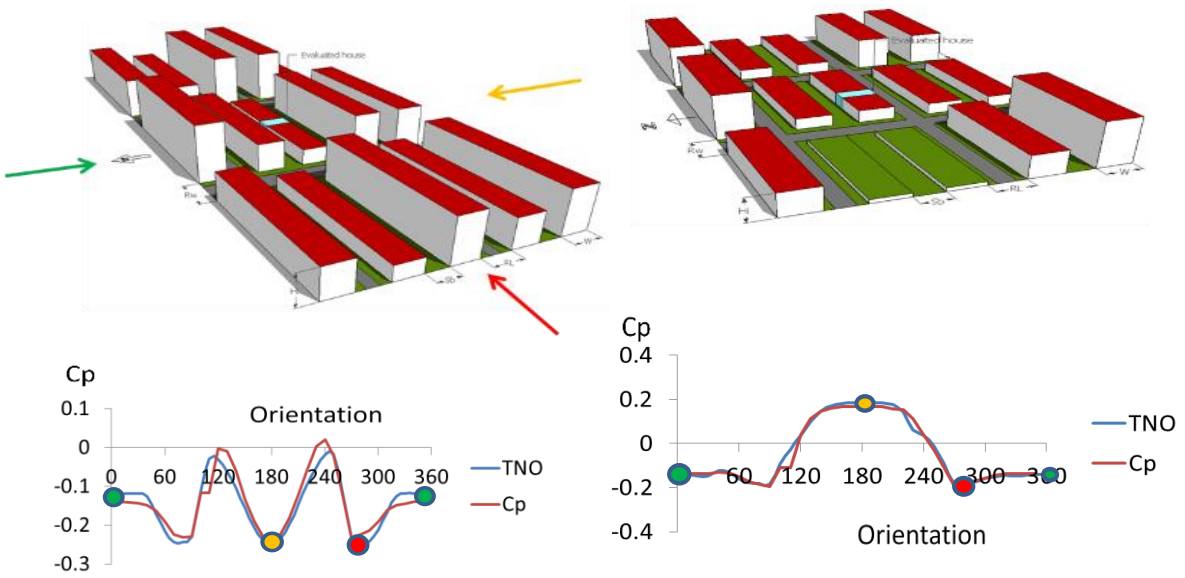

Figure 7-13 Cp value estimation for terraced house patterns by using regression approach based on Cp results of 200 scenarios from TNO Cp-Generator web base.

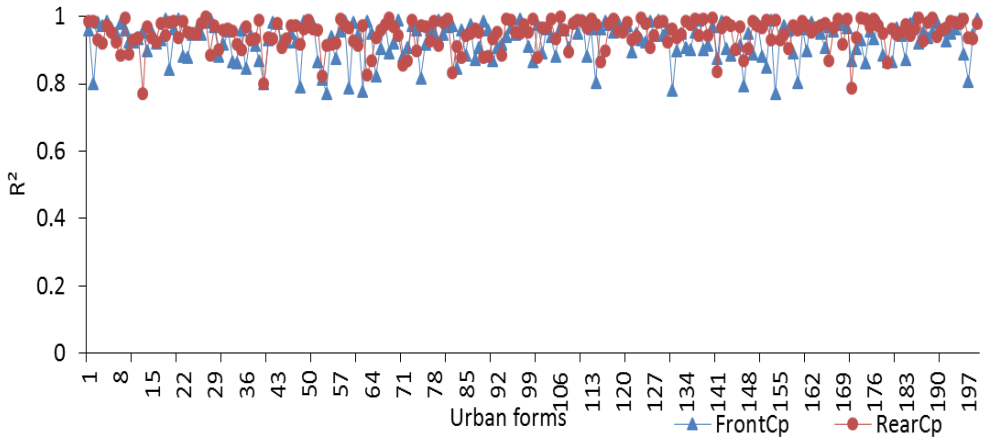

Figure 7-14 R^2 values predicted Cp values and Cp values of TNO CpGenerator of 200 urban patterns, average R^2 of Front facade = 0.93 and average R^2 of Rear facade = 0.95.

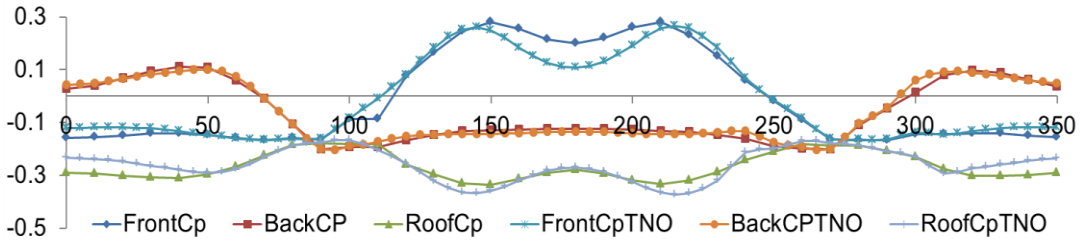

Figure 7-15 Wind pressure coefficient values for multiple linear regression functions (…Cp) and calculation using the by CpGenerator TNO (…CpTNO).

7.6.3.4 CFD results and sensitivity analysis of Cp values for the terraced building urban layout

The aim of this part is not the validation of the wind pressure coefficient (Cp) values, but the CFD results can provide qualitative and quantitative approaches to understand the effect of the different wind directions and the urban layout on Cp values. In theory, Cp is obtained based on the wind direction, the building layout and the urban layout.

In the urban layout in the case of Figure 7-16 that all buildings are 10 m height, 24 m for RI, Rw and Bg. The depth and length of the terraced building are 24 m and 120m. The CFD simulation using OpenFoam calculated the wind pressure and the wind velocity for a computational domain (600 x 600 x 110) m^3 full scale. The basic grids are 5 m and they are smaller near by the buildings in order to increasing quality of the calculation (Figure 7-16). The neighbouring buildings generate an external wind flow on evaluated building. The velocity and pressure of the wind flow from different orientations is related to the urban parameters and different angles of attack. The CFD results visualized in Figure 7-16 show the effect of the urban layout on the wind pressure on the surfaces

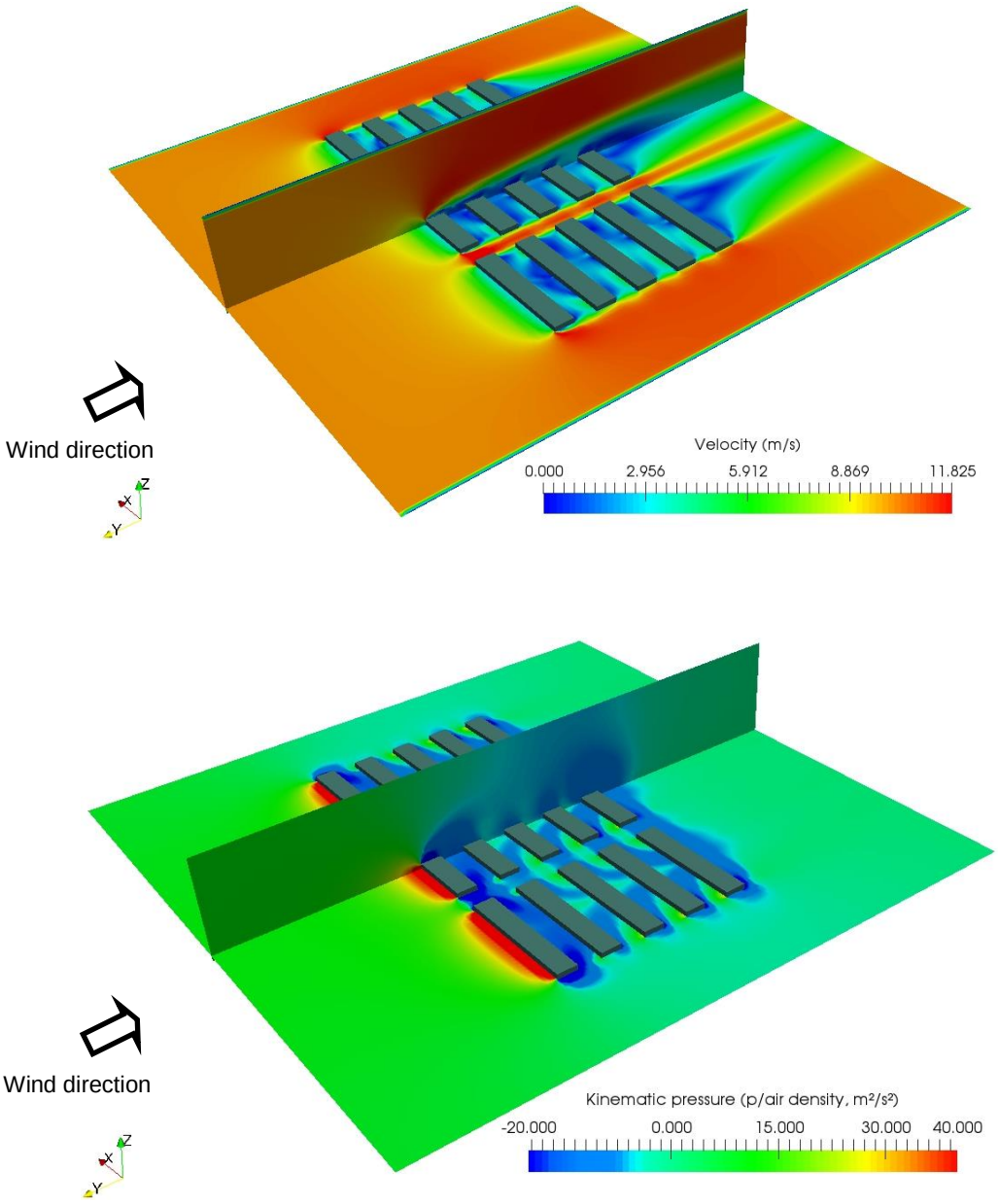

Figure 7-16 The external air velocity and the kinematic pressure of the case with the wind angle is 0° (perpendicular the front facade).

In order to know the impact of different parameters on the Cp values, different parameters of the building and the urban layout are generated by the Latin Hypercube Sampling method and the wind pressure coefficient. The Cp values of the 200 cases were obtained via TNO meta-model (via web base). Then the Cp values of the middle point on the front facade were used to calculate standardized regression coefficient (SRC). The parameters with high absolute value of SRC have an important impact on the Cp values (the left part of the Figure 7-17 to Figure 7-20).

The results shows the wind velocity on the section A-A (Figure 7-17). On the right, the sensitivity analysis of Cp results from TNO model indicate the impact of each parameter on the Cp values for a certain direction.

(1) When the wind angle is 0° (Figure 7-17), the building height of the building H5 in front of the evaluated building has the strongest effect on the Cp values. The width (D), length of the building (L) and the back garden (Bg) also have a strong impact on the Cp. They impact the turbulences of the wind flow. The building H2 and H5 lock the wind flow and generate negative Cp on the front facade of the evaluated building.

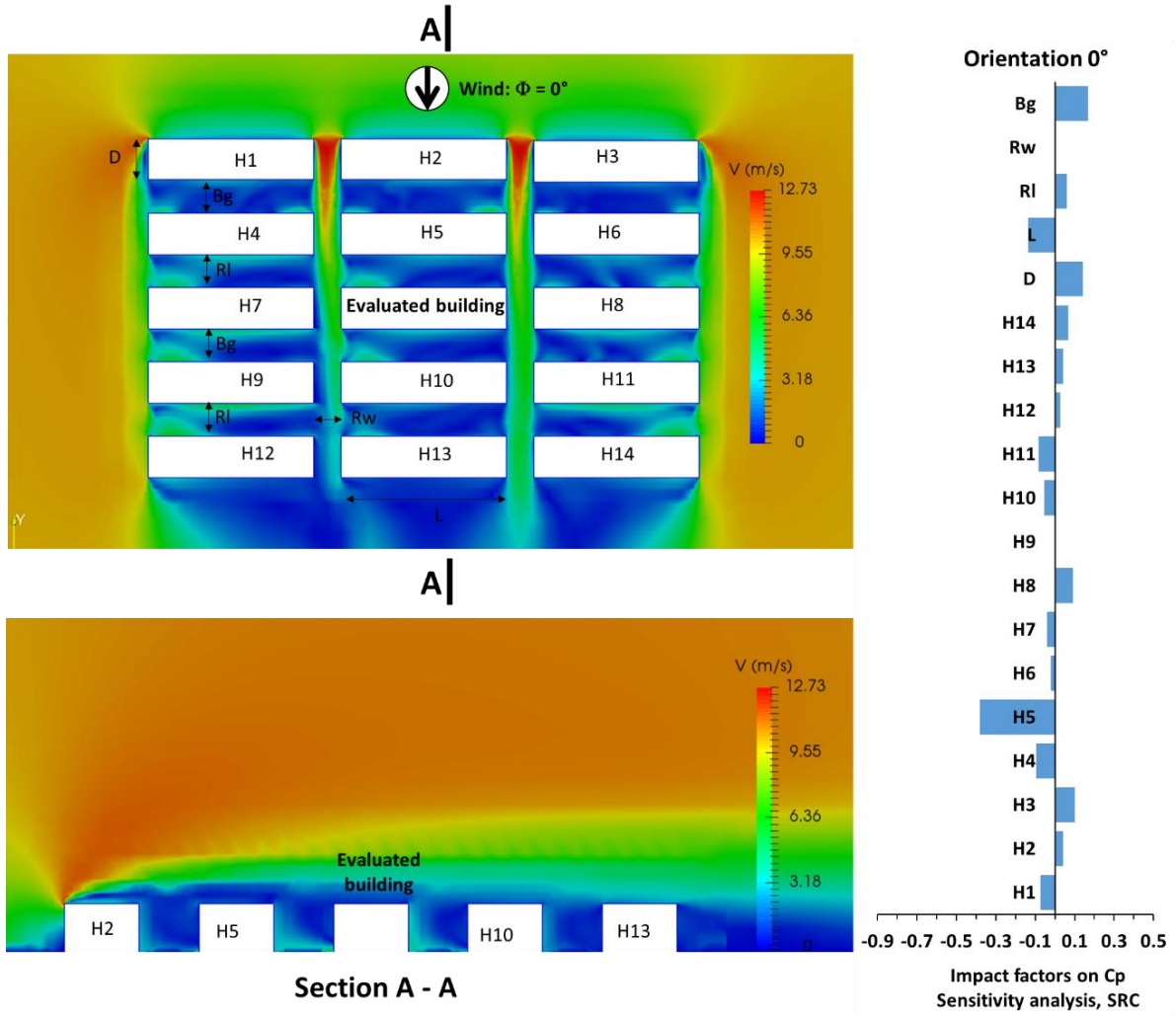

Figure 7-17 The wind speed at 5m above the ground level and section A-A for the orientation 0° is visualized by colours. The results of the sensitivity analysis using SRC method indicate the impactions of the parameters of the building and urban layout.

(2) When the wind angle is 30° (Figure 7-18), the building H5 has also a high impact on the Cp value.

(3) When the wind angle is 60° (Figure 7-19), the building H10 (behind the evaluated building) has a high effect on the Cp value because the back garden varies from small value 2m to 24m. With the back garden 2m, the wind flow is almost locked by the neighbouring buildings.

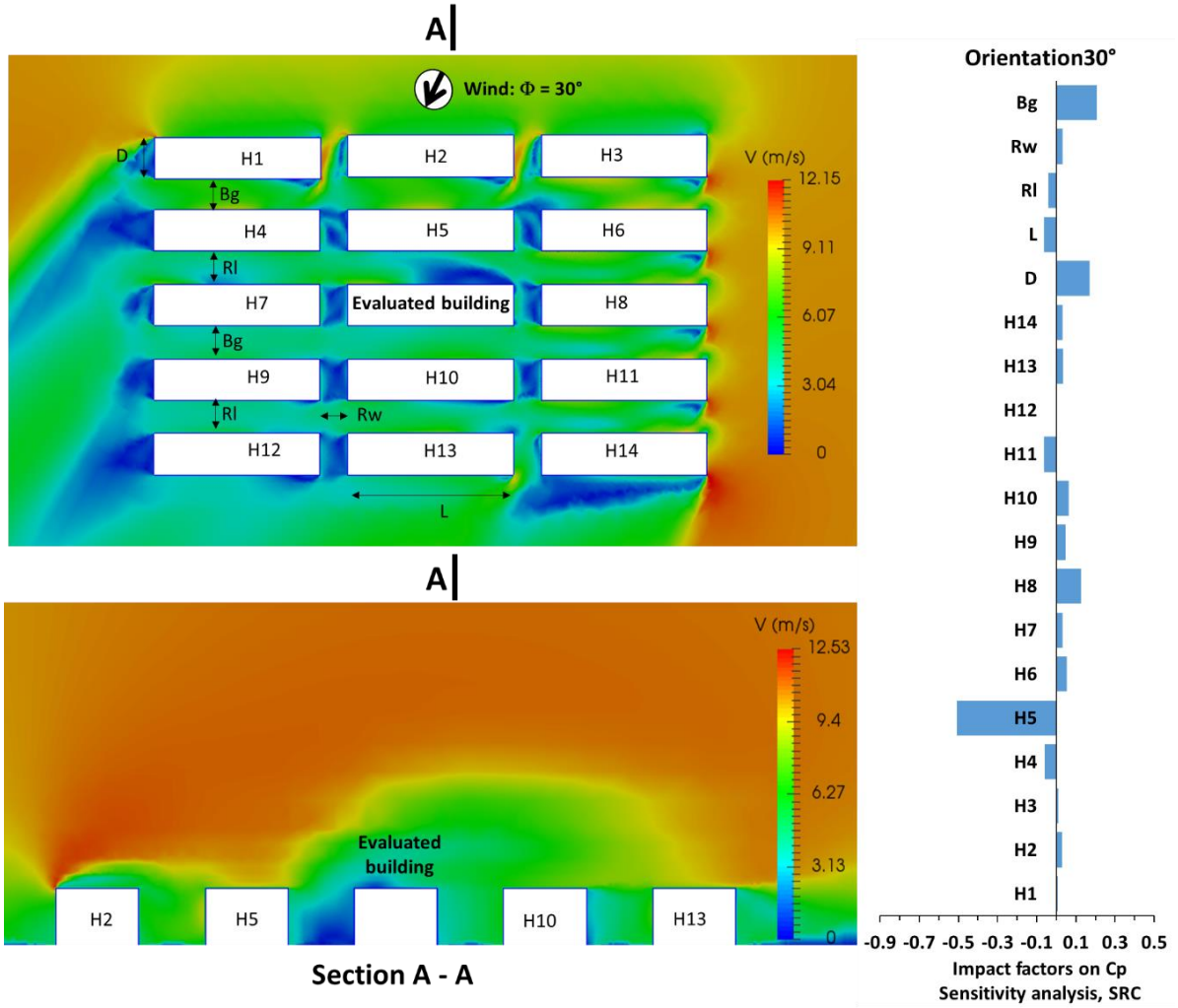

Figure 7-18 The wind speed at 5m above the ground level and section A-A for the orientation 30° is visualized by colours. The results of the sensitivity analysis using SRC method indicate the impactions of the parameters of the building and urban layout.

(4) When the wind flows parallel to facade (Figure 7-20), the building H10 and Width of road parallel the terraced row impact strongly on the Cp value.

The four cases illustrate that the dimensions of the neighbouring buildings and the width of the roads can generate various Cp values. This physical interpretation depends on the interplay of several parameters such as wind direction, building layout, obstructions. Figure 7-17, Figure 7-18, Figure 7-19 and Figure 7-20 support to understand for related wind direction, the wind pressure and the wind speed at different locations in 3D. Those detailed CFD

simulation are too time consuming to integrate them in an optimization via EnergyPlus. Therefore, a surrogate model is used.

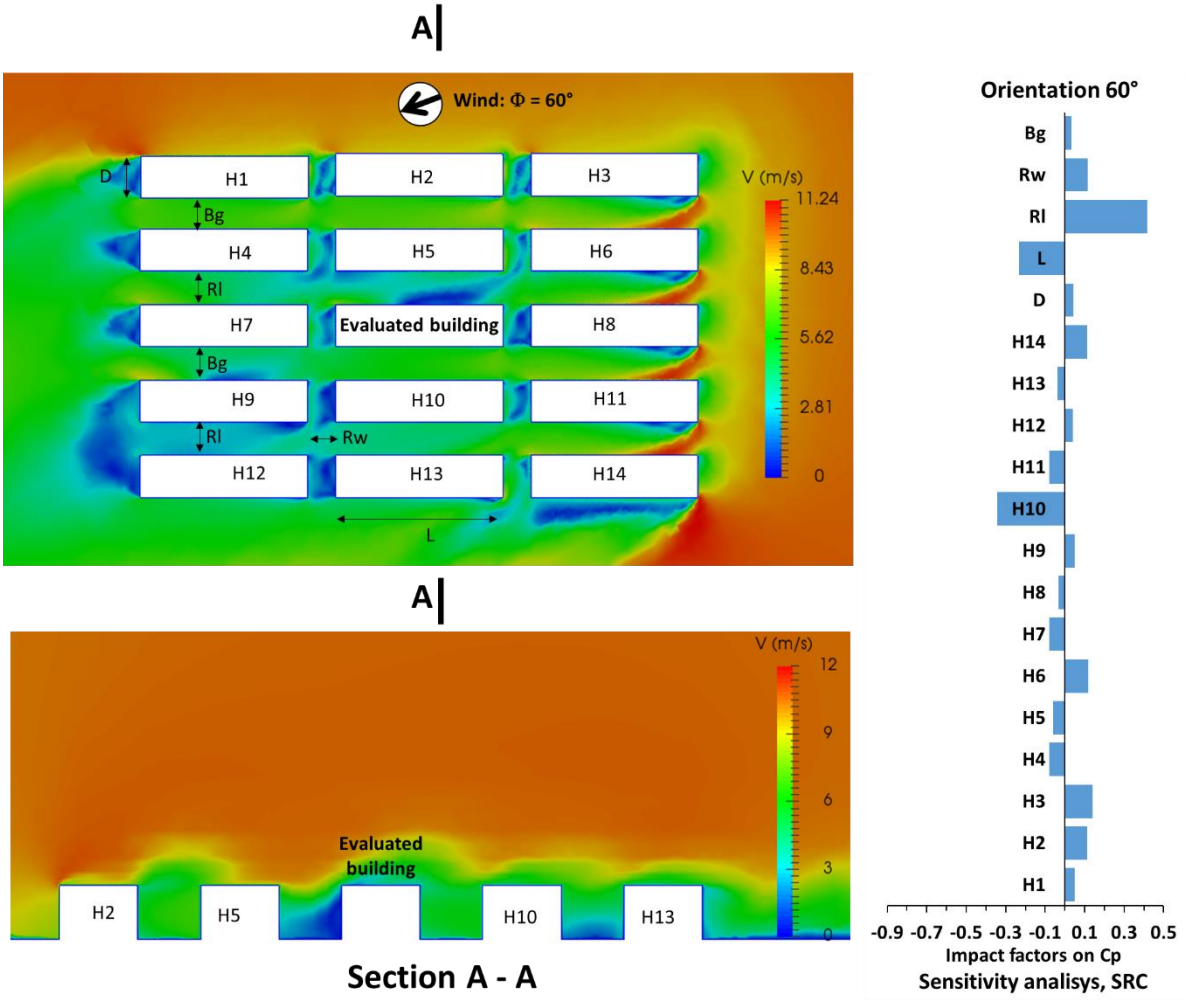

Figure 7-19 The wind speed at 5m above the ground level and section A-A for the orientation 60° is visualized by colours. The results of the sensitivity analysis using SRC method indicate the impactions of the parameters of the building and urban layout. H10 impacts strongly on the Cp because the Bg varies from 2m to 24m.

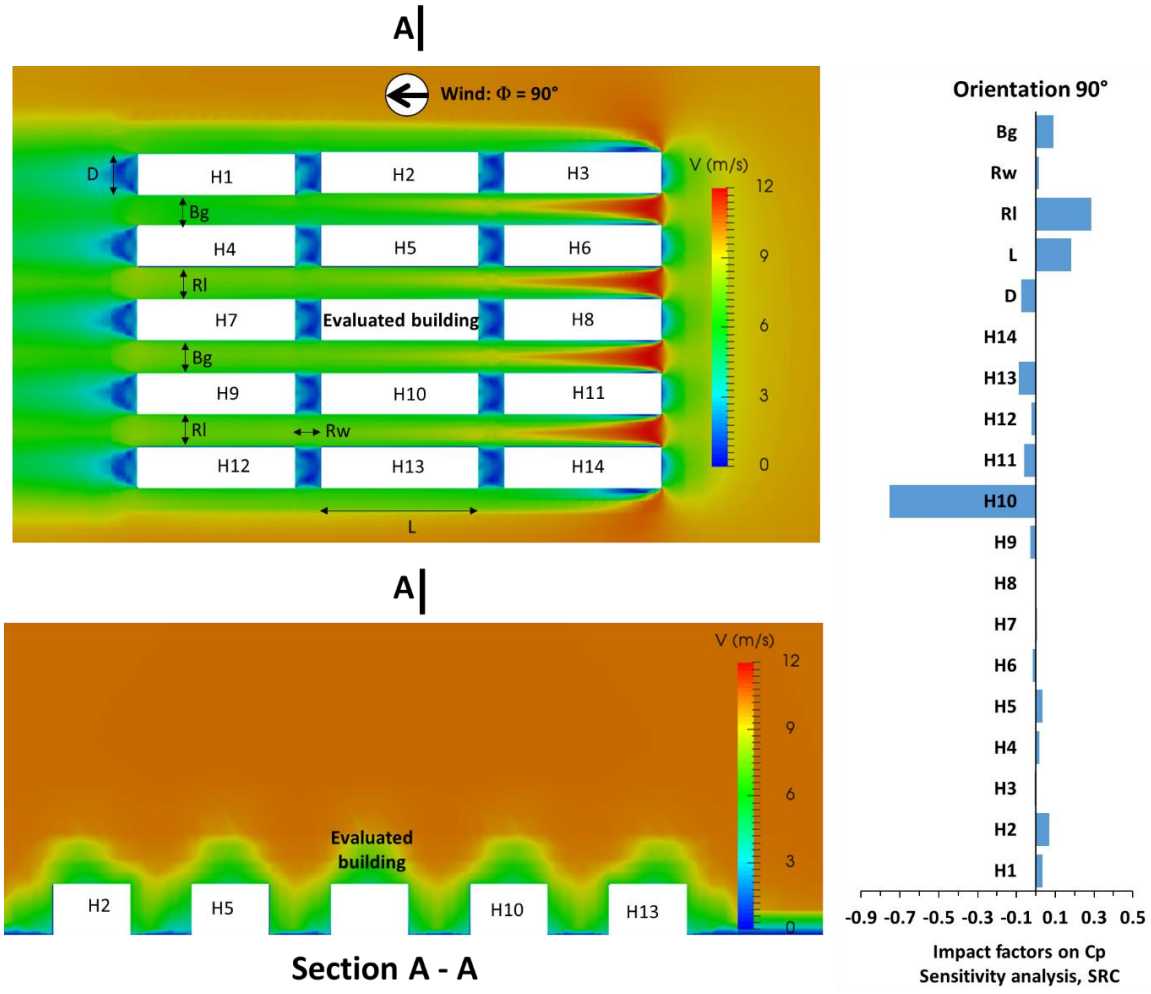

Figure 7-20 The wind speed at 5m above the ground level and section A-A for the orientation 90° is visualized by colours. The results of the sensitivity analysis using SRC method indicate the impactions of the parameters of the building and urban layout.

7.6.4 Meta-model Cp based on the meta-model Cp of M. Grosso for a detached house and apartment

Since the meta-model Cp-Generator TNO was not supported as a web service after 10 years availability, for phase 2 of this study, another way to estimate the wind pressure coefficient had to be found. M. Grosso proposed CpCal [22] also based on a polynomial regression analysis using existing wind tunnel data, also CFD and real measurements. The model calculates local and surface-averaged Cp for block-shaped buildings with flat, shed or gable roofs. The model considers the influence of environmental factors, i.e. incident wind profile and presence of surrounding buildings, described in terms of plan area density and building heights. The model considers three groups of parameters: climatic parameters (wind profile exponent and wind incidence angle); environmental parameters: plan area density (PAD) and relative building height (rbh); geometrical parameters (building proportions

represented by frontal aspect ratio (far = L/H) and side aspect ratio (sar = W /H) (Figure 7-21). Pressure coefficients modelled by M. Grosso's model show a good relation with the one measured by Cermak for a cube in an isolated environment [27],Figure 7-22.

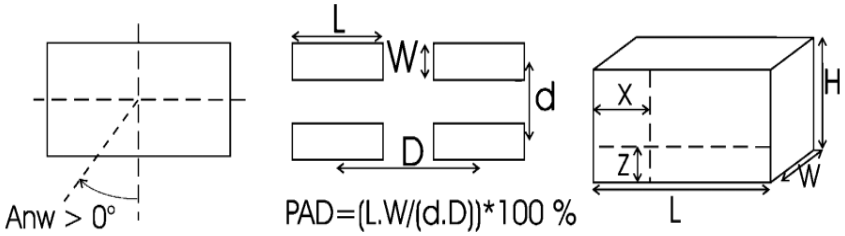

Figure 7-21 Wind incidence (left), definition of plan area density '' pad'' (centre) and building's main dimension's symbols (right) in M. Grosso's model, [27].

$Cp_k = Cp_{rer}(zh) \times CF$

$CF = Cf_{zh}(\alpha) \times Cf_{zh}(pad) \times Cf_{zh.pad}(rbh) \times Cf_{zh.pad}(far) \times Cf_{zh.pad}(sar) \times Cf_{zh,anw}$ (x l)

- $Cf_{zh}(a)$: Coefficients for the equations of the normalized Cp as a function of terrain roughness
- $Cf_{zh}(pad)$: Coefficients for the equations of the normalized Cp as a function of surrounding building density.
- $Cf_{zh.pad}(rbh)$: Coefficients for the equation of the normalized Cp as a function of height of surrounding building.
- $Cf_{zh.pad}(far)$: Coefficients for the equation of the normalized Cp as a function of frontal aspect ratio *far.*
- $Cf_{zh.pad}(sar)$: Coefficients for the equation of the normalized Cp as a function of frontal aspect ratio *sar.*
- $Cf_{zh,anw}$: Coefficients for the equation of the normalized Cp: horizontal distribution versus wind direction

These coefficient values of the regression functions of each orientation are reported in the Table 7-9 for detached house and Table 7-11 for apartment.

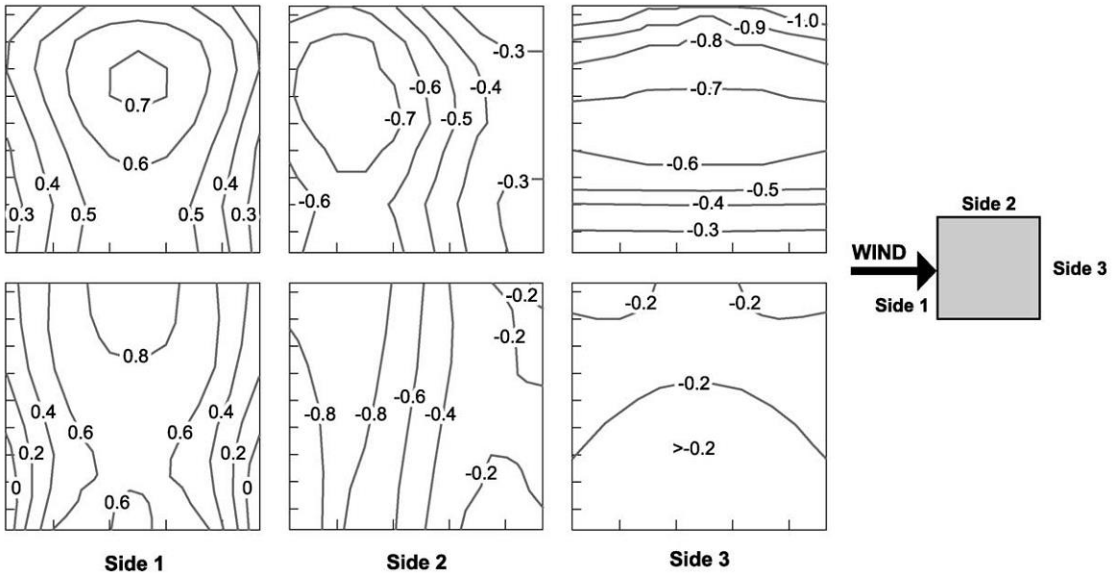

Figure 7-22 Comparison of pressure coefficients modelled by M. Grosso's model (above) and measured by Cermak (below) for a cube in an isolated environment, [27].

7.6.5 Cp values based on Grosso's model for detached and Semi-detached house

The set of 12 regression functions of Cp values, with 30° difference in orientations each in order to reduce number of the functions, were obtained based on the surrogate model approach. (1) A Cp calculation tool using a spread sheet was based on the Cp calculation model of M. Grosso [22] and graphical results drawn up, as seen in (Figure 7-24). (2) This detailed model generated 3,000 combinations based on input parameters: building depth, building width, building height and plan area density (PAD) Figure 7-21. Twelve regression formulas for 12 orientations are formed with these factors. (3) The Cp values that are estimated by these regression formulas are obtained with a high accuracy level with $R^2 > 0.9$.

Table 7-7 Numerical variables and their design options for urban layout (continuous variables).

Design parameters	Abbreviation	Initial value	Range (m)	Step size (m)
Height of surrounding buildings	H	9	9	
Road width parallel with detached row	Rw	12	12 to 24	4
Road width perpendicular with detached row	Rl	12	12 to 24	4
Back garden depth	Bg	12	6 to 24	4
Detached depth	W	6	6 to 12	2
Terraced length	L	6	6 to 12	2
Gap between detached buildings	Ne	6	6 to 12	2

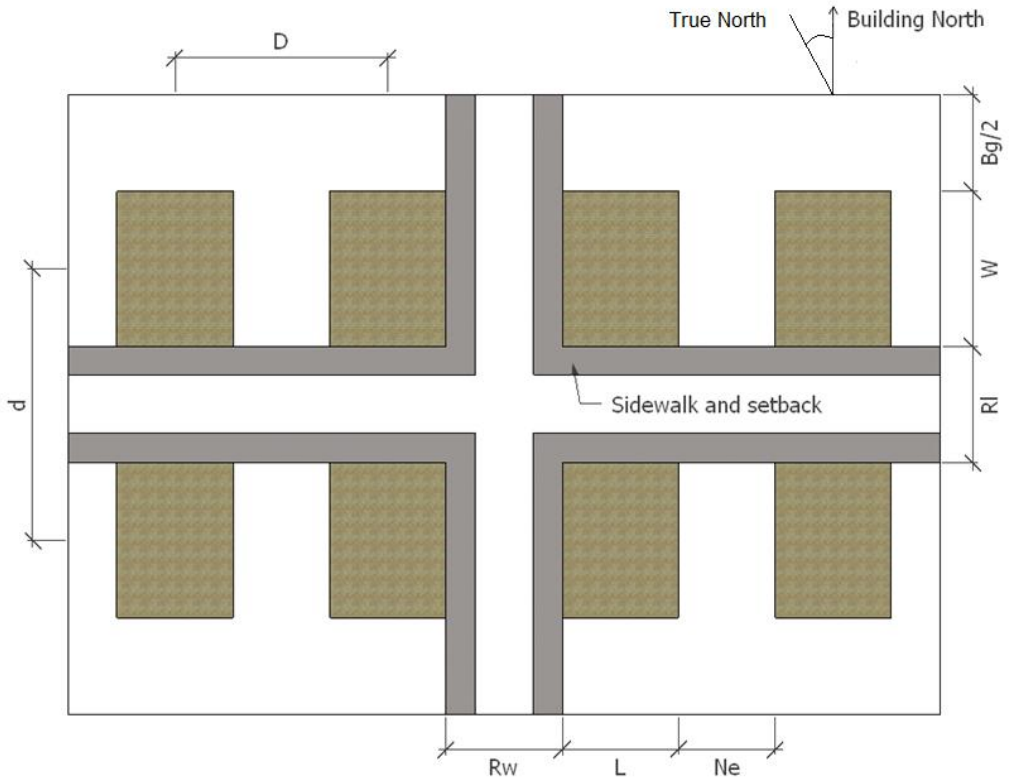

Figure 7-23 The urban form of detached house type

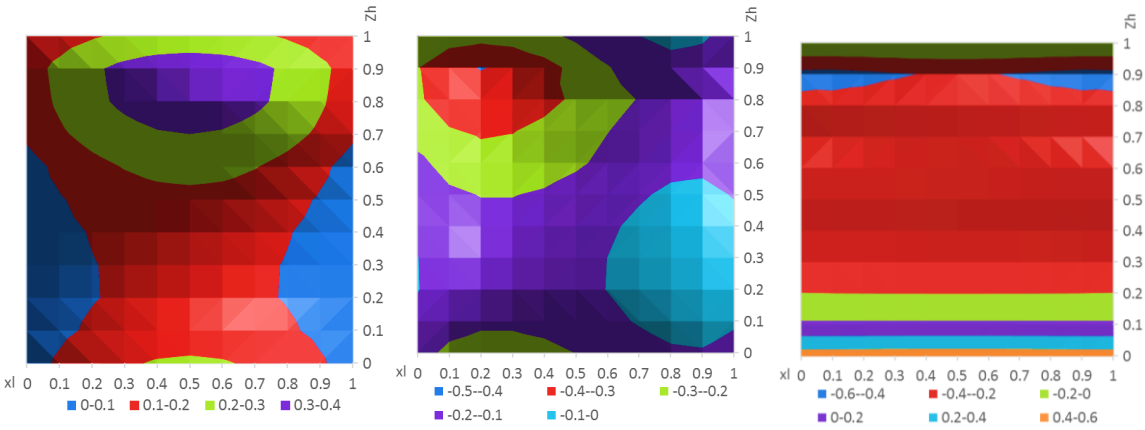

Figure 7-24 Results of a spreadsheet using Grosso's model has been constructed by the author, the xl and zh coordinates of the building width and height with converting scale 0 to 1. From the left to right: side 1, side 2, and side 3.

7.6.6 Approximation formulas to calculate wind pressure coefficients (detached and Semi-detached house)

In detached and semi-detached houses, in this Cp surrogate model, three parameters have been considered including: building width, building length and PAD. Their ranges are defined in Table 7-8. Twelve regression formulas on 12 orientations are formed (factors in the

Table 7-9). The estimated Cp values using these regression formulas correlate well with the model (Figure 7-25).

Table 7-8 Range of input parameters of Cp model.

Parameters	Min value	Max value	Step	Number of steps
With of Building (W)	06m	12 m	2	7
Length of building (L)	06m	12 m	2	7
PAD	3	30	3	10

Table 7-9 Factors of 12 regression formulas of 30° orientations of the detached and semi-detached houses.

Orientation	Intercept	W	W^2	W^3	W^4	W^5
0	-3.255E+01	3.707E+00	-6.343E-01	4.473E-02	-8.701E-04	-1.699E-05
30	-2.384E+01	2.714E+00	-4.645E-01	3.276E-02	-6.372E-04	-1.244E-05
60	-3.131E+00	3.565E-01	-6.100E-02	4.302E-03	-8.367E-05	-1.634E-06
90	3.022E+01	-3.441E+00	5.889E-01	-4.153E-02	8.078E-04	1.577E-05
120	-3.916E+01	8.996E+00	-1.843E+00	1.794E-01	-8.241E-03	1.416E-04
150	-3.003E+01	6.898E+00	-1.413E+00	1.376E-01	-6.319E-03	1.086E-04
180	-2.033E+01	4.671E+00	-9.566E-01	9.315E-02	-4.279E-03	7.353E-05

W: width of detached house

Orientation	L	L^2	L^3	L^4	L^5
0	1.420E+01	-3.069E+00	3.229E-01	-1.653E-02	3.310E-04
30	1.040E+01	-2.247E+00	2.364E-01	-1.211E-02	2.424E-04
60	1.365E+00	-2.951E-01	3.105E-02	-1.590E-03	3.183E-05
90	-1.318E+01	2.849E+00	-2.998E-01	1.535E-02	-3.073E-04
120	1.122E+01	-2.442E+00	2.557E-01	-1.294E-02	2.538E-04
150	8.600E+00	-1.873E+00	1.961E-01	-9.920E-03	1.946E-04
180	5.823E+00	-1.268E+00	1.328E-01	-6.717E-03	1.318E-04

L: Length of detached house

Orientation	PAD	PAD^2	PAD^3	PAD^4	PAD^5	R°
0	3.209E-02	-6.101E-02	1.030E-02	-6.514E-04	1.382E-05	0.92
30	2.350E-02	-4.468E-02	7.541E-03	-4.770E-04	1.012E-05	0.92
60	3.086E-03	-5.868E-03	9.903E-04	-6.265E-05	1.329E-06	0.92
90	-2.979E-02	5.665E-02	-9.560E-03	6.048E-04	-1.283E-05	0.92
120	8.508E-01	-1.332E-01	1.081E-02	-4.438E-04	7.146E-06	0.86
150	6.524E-01	-1.021E-01	8.289E-03	-3.403E-04	5.480E-06	0.85
180	4.417E-01	-6.916E-02	5.612E-03	-2.304E-04	3.710E-06	0.86

PAD: plan area density

$Cp_{orientation(i)}$ = intercept +a_1* W + a_2 * W^2 + … + a_{14} * PAD^4 + a_{15} * PAD^5

Where a_1 to a_{15} are coefficients of the Cp regression formula of detached houses.

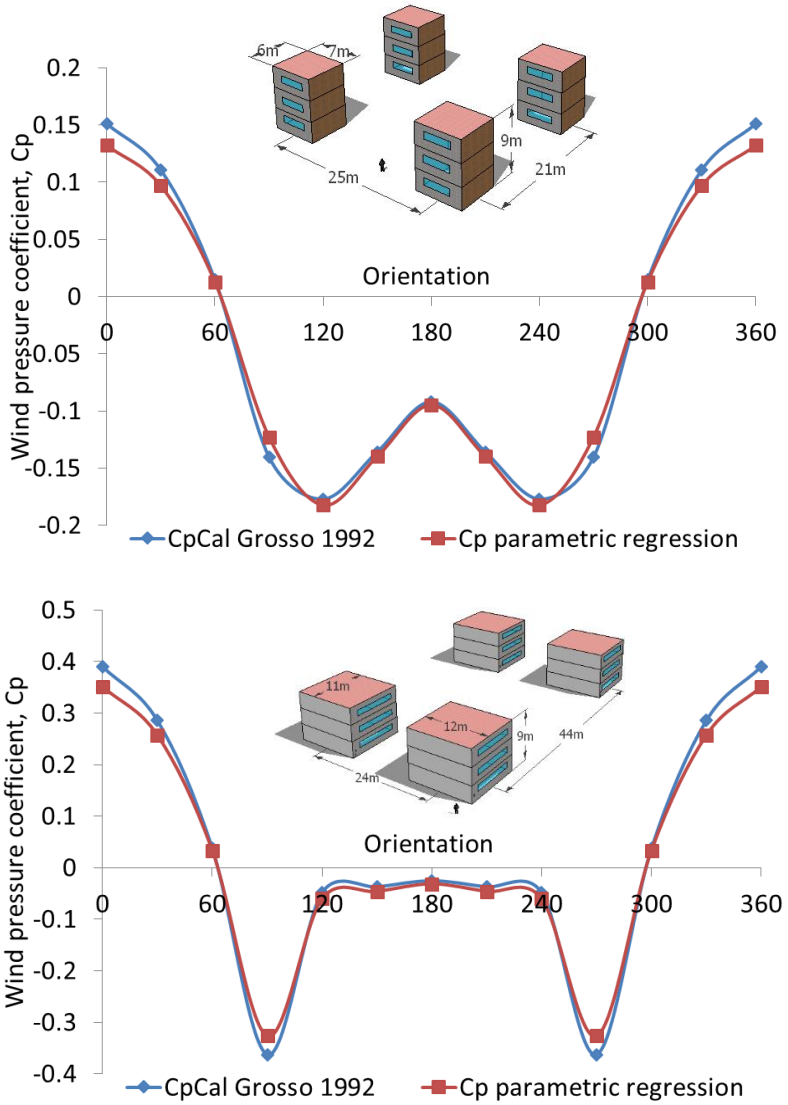

Figure 7-25 Results of the Cp values from CpCal and the surrogate model of 12 orientation of the detached house.

7.6.7 Approximation formulas to calculate wind pressure coefficients for apartment

The same approach was followed for the "detached" apartment blocks, for which there are four parameters: building width (W), building length and average distance between centre points of buildings d and D, defined in Figure 7-21, (defining PAD) are considered in this Cp surrogate model. Their ranges are defined in the Table 7-10 with R^2 = 0.88 and 0.94 for different orientations. Twelve regression formulas for 12 orientations are formed with their coefficients in

Table 7-11. The Cp values that are estimated by these regression formulas are obtained with a high level of accuracy (Table 7-11)

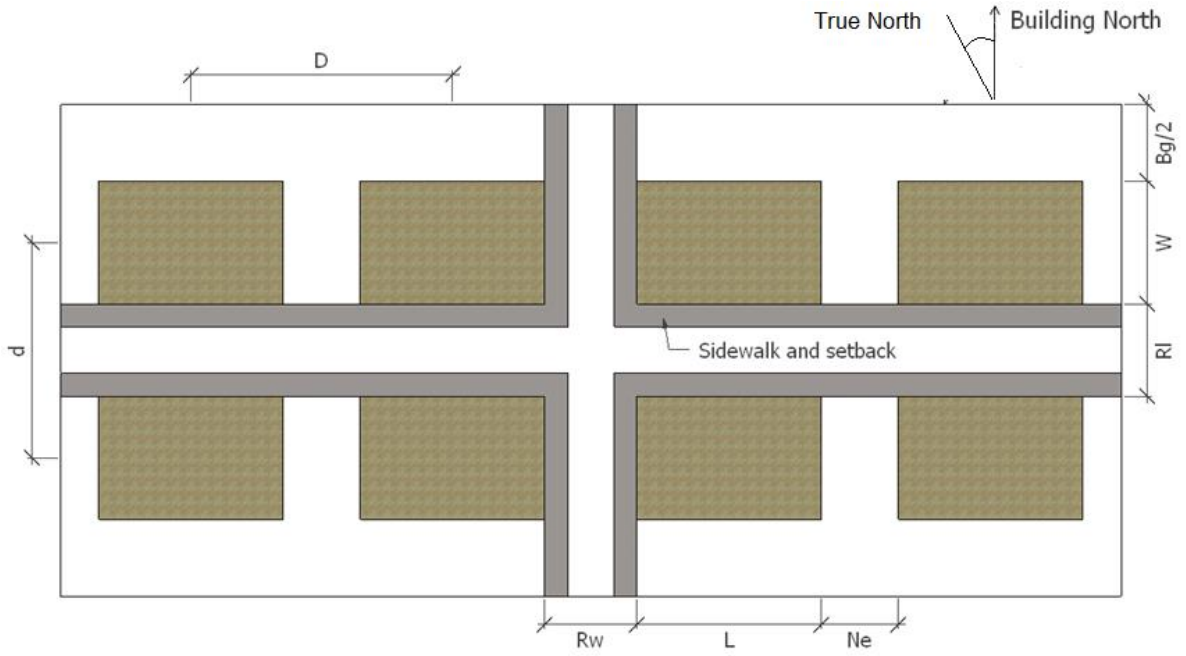

Figure 7-26 The urban form of apartment.

Table 7-10 Range of input parameters of Cp model.

Parameters	Min	Max	Step	Number of Steps
Width of Apartment Building (W)	8	16	2	4
Length of Apartment unit (La)	4	8	2	2
Road parallel the building width (Rw)	18	24	2	3
Road parallel the building length (Rl)	18	24	2	3
Number of floors (Nf)	3	25	2	11
Back garden (Bg)	50	100	5	10
Neighbouring Gap (Ne)	50	100	5	10

Table 7-11 Factors of 12 regression formulas of 30° orientations of apartment buildings.

Orient-ation	Intercept	H	H^2	H^3	W	W^2	W^3
0	5.706E-01	-3.883E-03	4.397E-05	-1.760E-07	9.729E-04	-1.253E-04	3.877E-06
30	4.178E-01	-2.843E-03	3.220E-05	-1.289E-07	7.125E-04	-9.176E-05	2.839E-06
60	5.487E-02	-3.734E-04	4.229E-06	-1.693E-08	9.357E-05	-1.205E-05	3.728E-07
90	-5.297E-01	3.605E-03	-4.082E-05	1.634E-07	-9.033E-04	1.163E-04	-3.599E-06
120	-1.036E+00	1.103E-02	-9.322E-05	3.085E-07	-1.129E-02	8.287E-04	-1.665E-05
150	-7.948E-01	8.458E-03	-7.148E-05	2.366E-07	-8.656E-03	6.355E-04	-1.277E-05
180	-5.381E-01	5.727E-03	-4.840E-05	1.602E-07	-5.861E-03	4.303E-04	-8.644E-06

Orientation	L	L^2	L^3	PAD	PAD^2	PAD^3	R^2
0	1.239E-03	-1.903E-05	9.669E-08	-7.781E-02	5.026E-03	-1.315E-04	0.94
30	9.072E-04	-1.393E-05	7.081E-08	-5.698E-02	3.681E-03	-9.627E-05	0.94
60	1.191E-04	-1.830E-06	9.299E-09	-7.483E-03	4.834E-04	-1.264E-05	0.94
90	-1.150E-03	1.767E-05	-8.977E-08	7.224E-02	-4.666E-03	1.220E-04	0.94
120	-1.700E-02	2.434E-04	-1.430E-06	2.294E-01	-1.730E-02	3.798E-04	0.88
150	-1.304E-02	1.867E-04	-1.096E-06	1.759E-01	-1.327E-02	2.912E-04	0.88
180	-8.829E-03	1.264E-04	-7.423E-07	1.191E-01	-8.984E-03	1.972E-04	0.88

W: width of apartment building

L: Length of apartment building

PAD: plan area density

H: Height of apartment building

$Cp_{orientation(i)}$ = intercept $+a_1 * H + a_2 * H^2 + \ldots + a_{12} * PAD^3$

Where a_1 to a_{15} are coefficients of the Cp regression formula for apartment building.

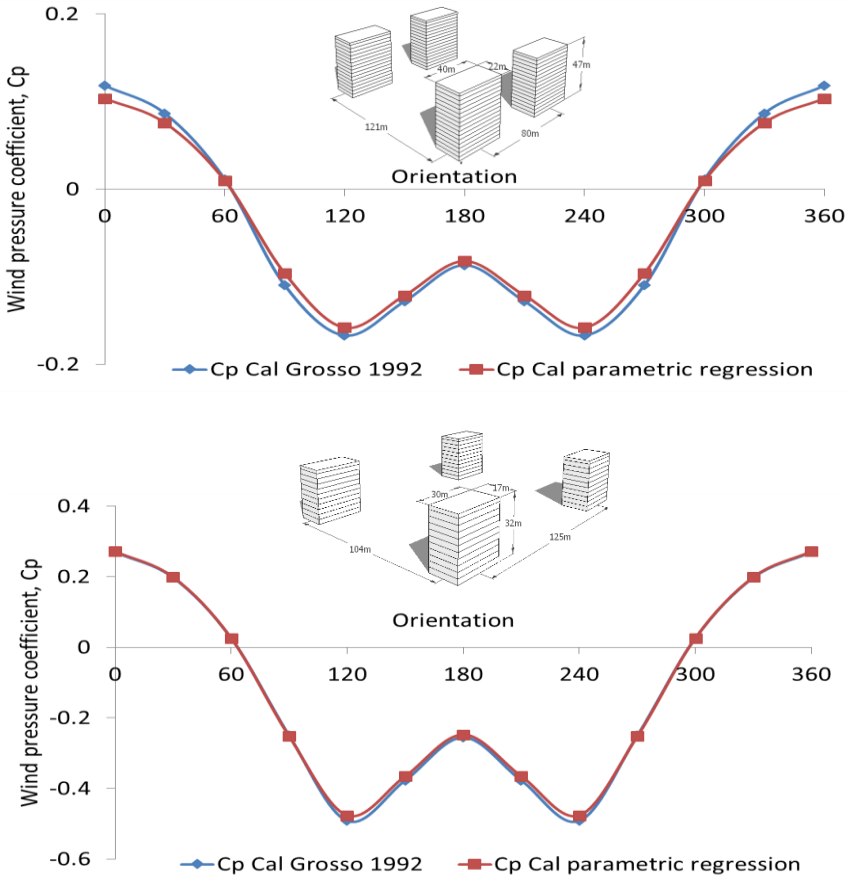

Figure 7-27 Results of the Cp values from CpCal and surrogate model of apartment.

7.7 Strategies for comfort (dynamic schedule and user behaviour)

In this research, the thermal comfort model is based on six input parameters from the PMV approach and an extension model [6]. A dynamic schedule is built via the energy management system (EMS), which is available in EnergyPlus. EMS can simulate different strategies to reach the desired thermal comfort in the naturally-ventilated and air conditioned buildings.

7.7.1 Comfort evaluation and strategy based on dynamic schedules for ventilation and cooling

Fanger (1970) developed a thermal load index, consisting of a "predicted mean vote" (PMV) on a 7 points scale from "cold" (-3) to "neutral" (0) up as high as "hot" (+3), based on the heat balance between the body and the environment. His work was the basis for different thermal comfort standards, such as the ASHRAE Standard 55-92 [2] and ISO 7730 [31]. In this method, thermal comfort is defined as the condition which the PMV is between -0.5 and +0.5 with corresponds to 90% of satisfied users. The PMV can be used to simulate control actions from "passive" to full HVAC [32].

7.7.2 Strategy based on dynamic schedules for ventilation and cooling

In this study, this approach is implemented in the following way: (1) The PMV values for a zero air velocity and minimum clothes-values (0.36), which are representative for the domestic habits in Vietnam, are calculated. The codes to calculate PMV used in EMS are reported in the Appendix D. Using the "Energy management System" in EnergyPlus the following behaviours are implemented. If the PMV value is higher than +0.5 or the indoor air temperature is higher than the outdoor air temperature, the windows are opened, then if comfort levels are still not reached, then fans are switched on first minimal speed and increasing the speed until comfort is reached. In the living areas, fans with three speed levels generate a wind speed of 0.2, 0.4 and 0.6m/s respectively for the living room and the kitchen. In the bedrooms, fans with two speed levels (0.2 and 0.4 m/s) are provided. When the maximal fan velocity is set, and comfort is not yet reached, windows are closed and the cooling system is switched on with a set point of 27°C. This selected set point is based on neutral temperatures of natural ventilation buildings in Thailand [33] and South-East Asia [12]. During the simulations, activity levels of 1.2 met for the living room and 1.0 met for the bedrooms were considered. The living room, kitchen and staircase are assumed to be in use from 5:00 to 9:00 and from 17:00 to 23:00 during working days. At the weekend, the living room is used from 5:00 to 23:00; the bedrooms are used from 23:00 to 5:00.

All lights in the model have been controlled by time schedules and luminance levels, using two light sensors in each zone. The luminance levels for the living room, kitchen,

bedrooms and circulation area are 300 lx, 500 lx, 300 lx and 150 lx respectively. LED lights (69 lm/W) are considered in all zones. An example of input (occupancy schedule) and output (PMV, inside air velocity) is provided in Figure 7-28.

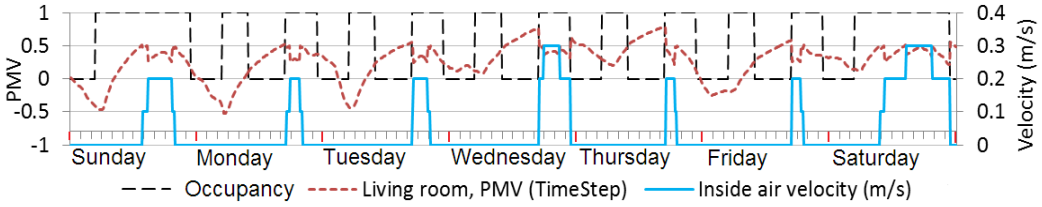

Figure 7-28 Example of a dynamic schedule for one week

7.8 Life Cycle Cost: Parameters in EnergyPlus

In Vietnam the electricity price has increased over the past 8 years, from 7% to 10% per year on average (Figure 7-29). Meanwhile, the average inflation rate is 6.5%, based on data from the World Bank for the years 2000 to 2013. The present value factor for period of 60 years is 4.819 to obtain the energy cost of the life cycle cost.

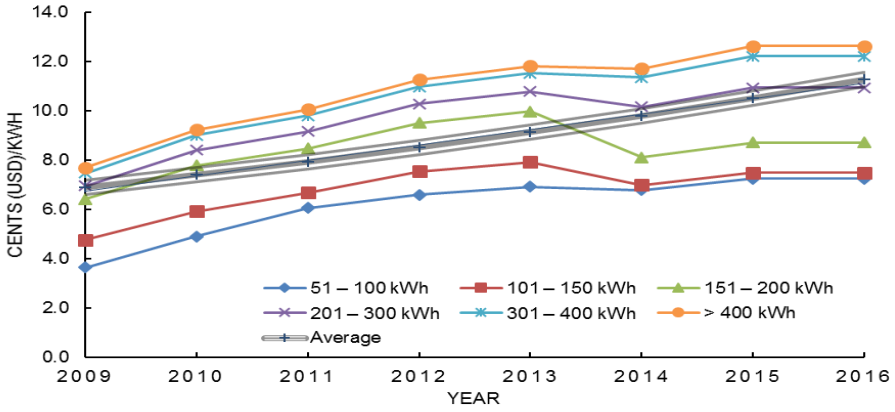

Figure 7-29 Electricity prices from 2009 to 2016 (USD/kWh); the average growth rate is 7.3% annual, based on data of Vietnam Electricity (EVN) group in 2016.

Table 7-12 Other costs and fees

Item name	Value	Frequency
Foundation cost	Auto calculated	Initial cost
Miscellaneous	10 $/m^2	Initial cost
Design and engineering	5%	Initial cost
Contractor	5.5%	Initial cost
Contingency	10%	Initial cost
Building permission, bonding and Insurance	0.3%	Initial cost
VAT	10%	Initial cost
Nominal Discount Rate	8.35%	Yearly
Inflation	6.5%	Yearly
Growth rate of electricity	7.3%	Yearly
Maintenance	370 $	2 years
Replacement	1200 $	10 years
Income from salvage	-60 $	10 years

Note: Interest rates are collected from the World Bank Data; the electricity price is 0.107 USD/kWh based on Vietnam Electricity (EVN) group in 2016.

7.9 Urban forms, geometry and materials of housing types

In this part evaluates the energy use of three housing types in order to identify the impact of the natural ventilation, daylight and solar gain within different urban layouts. The materials are same for these housing types and described in detail in the Table 7-13. The building layout of each housing type is the same for different urban densities. These data are defined in the next subparts.

Table 7-13 Design options and strategies (discrete variables).

Design parameter	Descriptions of design parameter
External walls	Mortar, hollow clay brick, mortar.
Internal Walls	Mortar, brick clay, thermal mass2, mortar
Floor	Floor tile, tile mortar
Ceiling	Concrete slab, ceiling mortar
Roof	Roof asphalt, concrete roof slab, ceiling mortar
Glazing	Single glazed timber frame
Overhang	Tile, concrete slab, ceiling mortar
Internal door	Door aluminium + glazing

7.9.1 Terraced house geometry

As shown in Figure 7-30**,** a simple terraced house model was defined, including seven thermal zones: a stair case, a living room, a kitchen and four bedrooms. The outside doors are modelled as windows. The floor height is three meters and the depth of the circulation zone is four meters. A balcony, functioning as an overhang for shading, is provided along the whole house's width. The geometric parameters of the terraced house, representative for the Vietnamese city of Cantho, are shown in Table 7-14 and Figure 7-30.

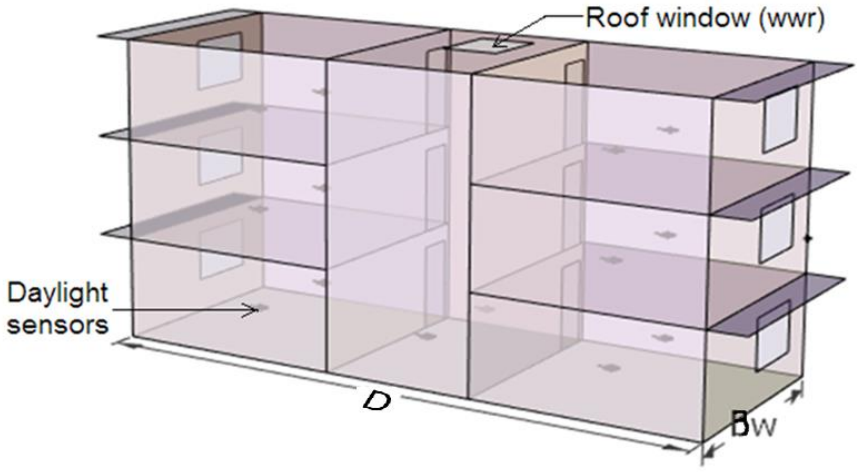

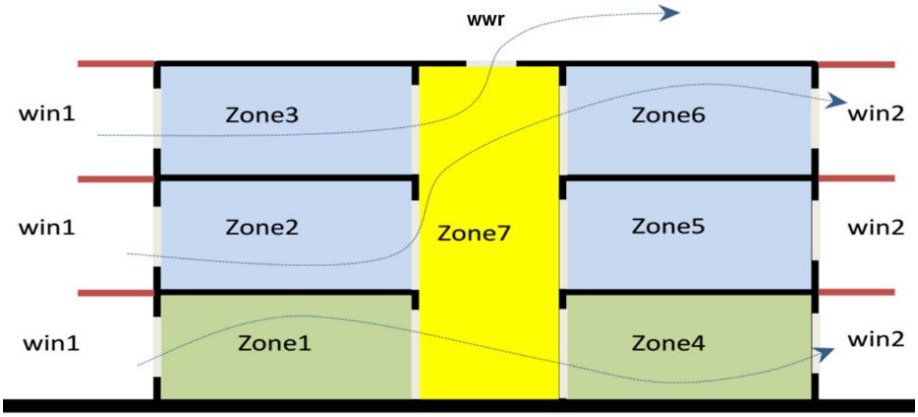

Figure 7-30 Terraced house section, Zone 1 and zone 4 are living room and kitchen. Zone 2, 3, 5 and 6 are bedrooms. Zone 7 includes the stair case and circulation area.

Table 7-14 Numerical variables and their design options (continuous variables).

Design parameters	Abbreviation	Initial value (m)
Terraced house width	Bw	6
Depth of the terraced row	D	16
Depth of front facade overhangs	ov1	1.5
Depth of rear facade overhangs	ov2	1.5
Width of front facade windows	win1	1.5
Width of rear facade window	win2	1.5
Width of roof window	wwr	1.5

7.9.2 Detached house geometry

Detached house geometry is simplified to the following three floors, windows in each facade and overhangs at all sides. Direct and diffuse solar gain are calculated considering overhangs and neighbouring buildings (Figure 7-31 and Table 7-15). The wind pressure coefficient values are obtained using the regression functions with parameters of building and urban scale.

Table 7-15 Parameter values of detached house

Design parameters	Abbreviation	Initial value (m)
Width of detached house	W	6
Depth of detached house	D	10
Depth of front overhangs	ov1	1.5
Depth of rear facade overhang	ov2	1.5
Depth of left facade overhang	ov3	1.5
Depth of right facade overhang	ov4	1.5
Width of front facade windows	win1	1.5
Width of rear facade window	win2	1.5
Width of front facade windows	win3	1.5
Width of rear facade window	win4	1.5
Width of roof window	wwr	1.5

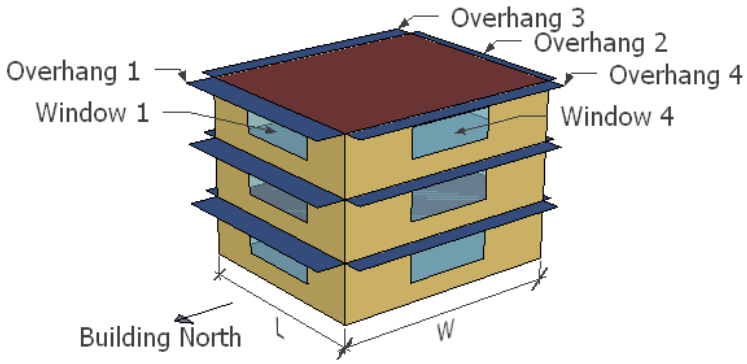

Figure 7-31 Simple detached house geometry within urban patterns. Neighbouring buildings are represented by wall elements that are used to calculate solar gain considering shadow and reflection in EnergyPlus model. Cp values are obtained by using regression functions.

7.9.3 Apartment geometry

In case of apartments, building and urban parameters are simplified similar to detached houses (Figure 7-32). The Cp values for the front and rear facades are calculated by using regression functions for Cp values. First an apartment unit at the half building is analysed. Next, the apartment units at the bottom and top of the building are analysed to derive the impact of the natural ventilation on energy cost.

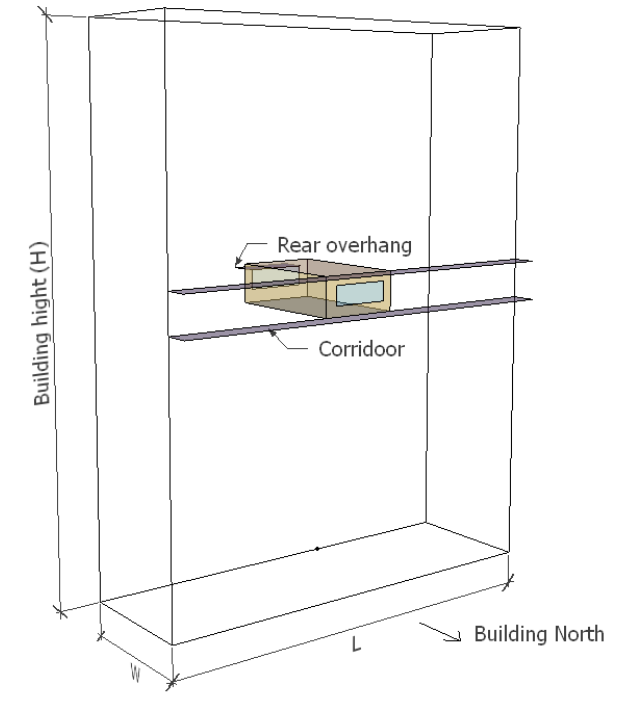

Figure 7-32 The apartment layout with evaluated apartment unit at the middle building.

7.9.4 General options for material

7.10 Results and discussions

7.10.1 Case study for terraced house: Varying all selected parameters with fixed building North

The base case of terraced units have been analysed for the neighbourhood model with North-oriented front facades and six extreme schematic urban forms (Figure 7-33). The resulting life cycle costs (including construction, energy and maintenance) are reported for the base case. Energy costs are minimized by changing the windows and overhangs' sizes.

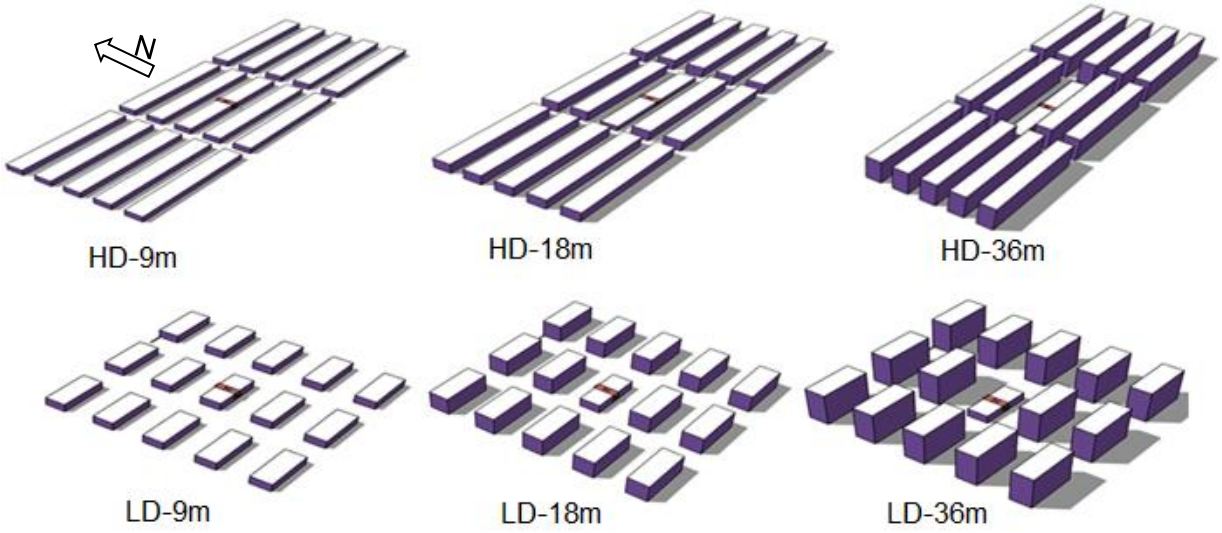

Figure 7-33 Six urban layouts with different built-up ratio and building densities: High density urban (HD): L =120m; D = 16m; Rl = Rw = Bg =12m; Built-up Ratio = 52%. Low density urban (LD): L = 40m; D = 16m; Rl = Rw = Bg =24m; Built-up Ratio =25%.

Figure 7-34 illustrates the working principle of the EMS for one day in April in a bedroom. Additional settings include: sleeping period from 23 pm to 5 am. As a rule, when the indoor air temperature is higher than the outdoor air temperature, the windows are opened for natural ventilation (as shown in Figure 7-34). The PMV values fall between -0.5 and +0.5 during the occupational period (from 0 to 5 am), thanks to the natural ventilation. From 5 am on, nobody is present in the room and fans (and air conditioners) are switched off. From 17:00, the outdoor temperature falls once more below the indoor temperature, so that cooling via ventilation is possible. The windows or doors of the bedroom are opened. From 23:00 on, the bedroom is occupied and additional cooling is required about one hour. A similar regime is simulated via the EMS for every room. The results of EMS controlling for a whole year is presented in Figure 7-35.

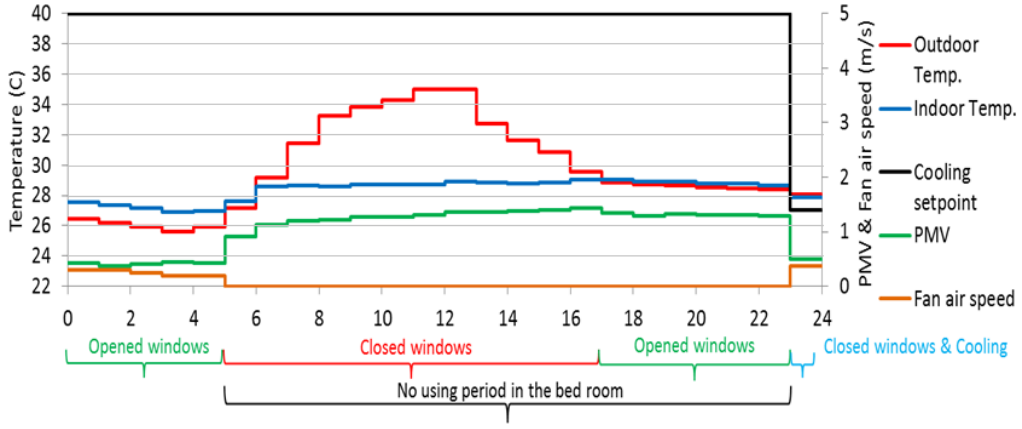

Figure 7-34 Conditions and reactions of one dwelling by using Energy Management System, EMS in EnergyPlus.

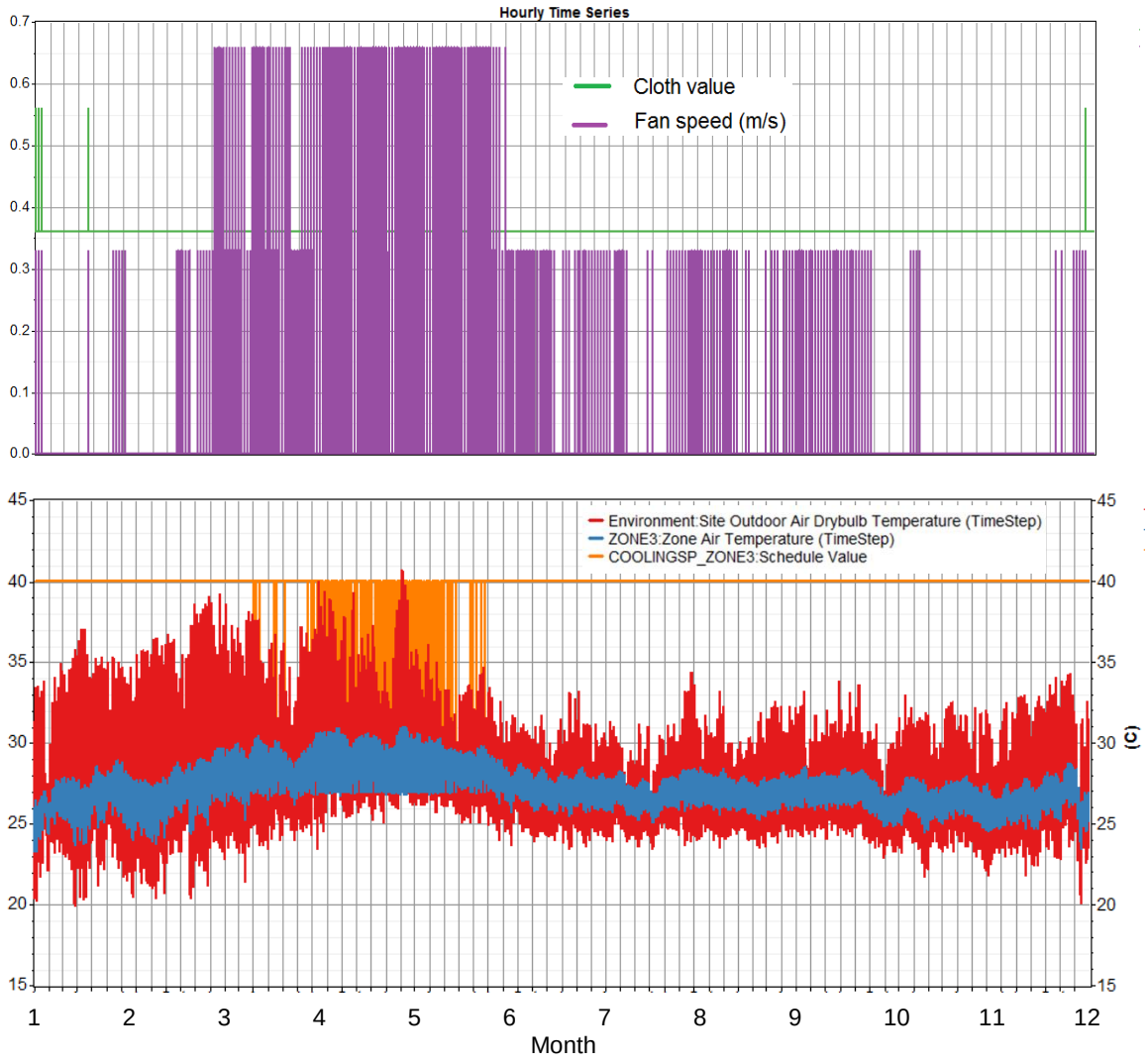

Figure 7-35 The Energy Management System (EMS) tries to keep PMV values between -0.5 and 0.5 for each 10 minutes time step (6 times per hour. Cooling set point is 27°C.

7.10.2 Energy consumption in case of different orientations for terraced house

In this model, natural ventilation occurs during the night when the indoor air temperature is higher than the temperature outside. During the day there is no ventilation in the living room or kitchen because the outside temperature is normally higher than the indoor air temperature. The results show that the building's orientation in the case of low-density urban layouts has a major impact. The orientation has a lower impact on high-density cases (HD-18m, HD-36m and LD-36m) as shown in Figure 7-36 and in Figure 7-37 because the terraced unit is in the shadow of neighbouring buildings and natural ventilation is limited. The energy use is not symmetrical for orientations 90° and 270° due to without cooling system in the kitchen on the ground floor. Moreover, the results show that increasing obstruction heights can reduce the energy use for cooling and fans because solar radiation is blocked.

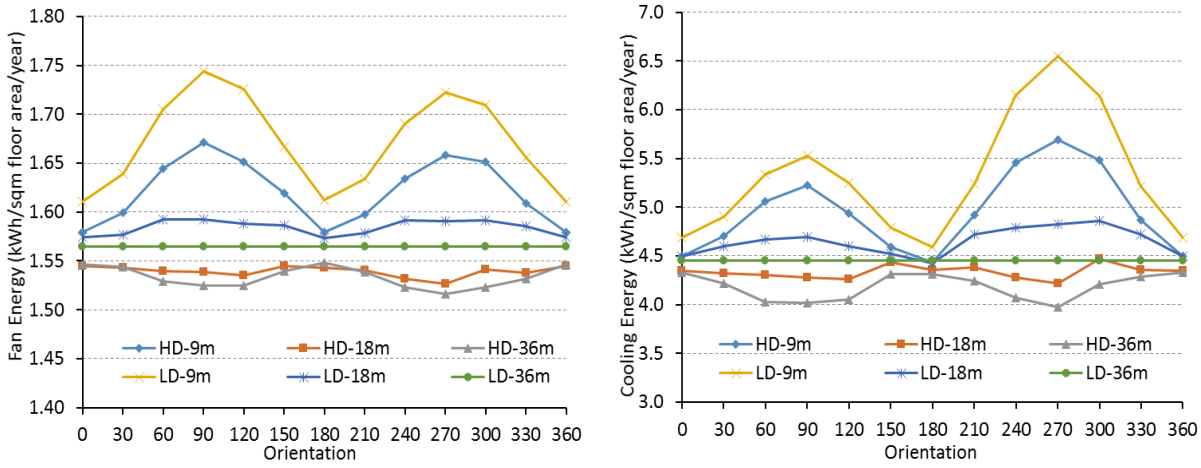

Figure 7-36 Fan and cooling energy of different orientations in six cases.

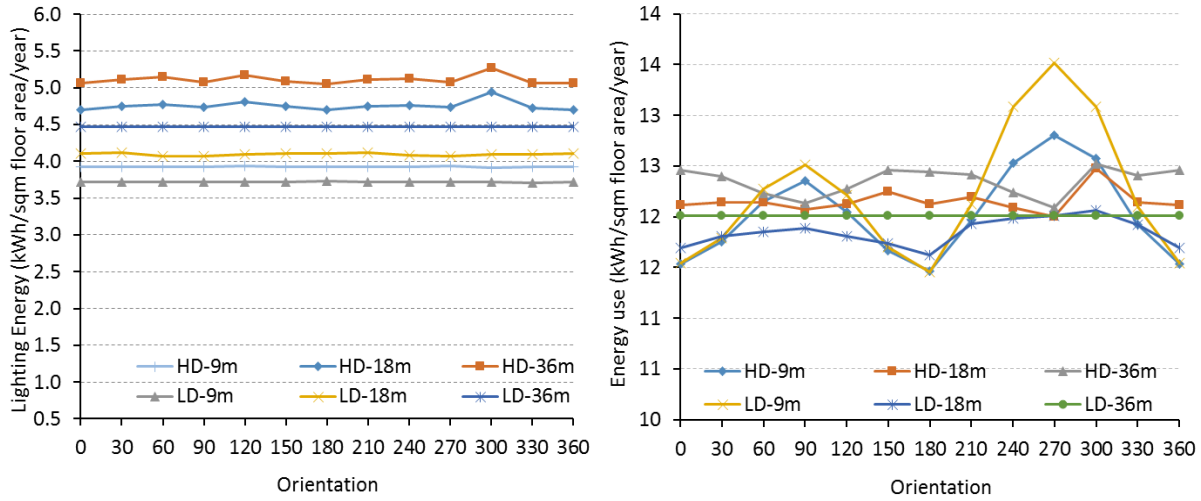

Figure 7-37 Energy use of light and total energy of six cases versus orientations for terraced house type. The yearly cooking energy is 1.52 kWh/m² floor area for all cases.

The orientation, building layout and materials are not changed in order to evaluate the effect of the natural ventilation and solar gain. Beside the wind pressure coefficients, the occupant behaviour is significant to control the natural ventilation by opening the windows when the indoor air temperature is higher than the outdoor air temperature. In Figure 7-38 shows that the energy use per one square meter floor area of the terraced house is related to the urban layouts due to the natural ventilation and solar gain. In Figure 7-38 a) shows that the high density building and the high obstructions limit the natural ventilation.

In Figure 7-38 b) shows that reducing air exchange increases the energy use for thermal comfort (with PMV smaller than 0.5) via fan and cooling due to less solar gain. This consequence proves that the solar gain impacts stronger than the cooling air form the outdoor.

In the Figure 7-38 b) shows that the lighting energy increases when the daylight is locked by the neighbouring buildings. The lights are switched off later in the morning and switched on earlier than in the afternoon. The daylight is considered both direct and indirect solar beam via reflection coefficient factor of different surfaces. The light energy of the case LD-9m is lower than the no obstruction case due to no reflection light from the neighbouring obstructions.

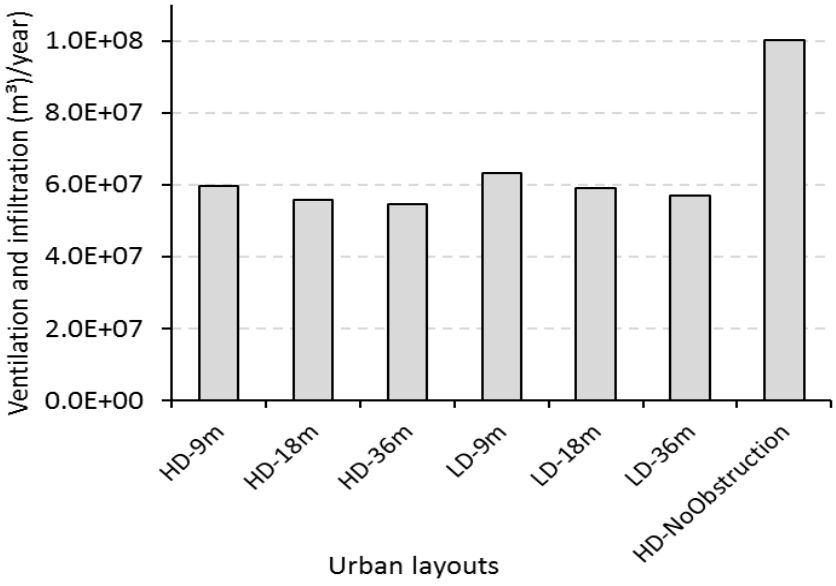

a)

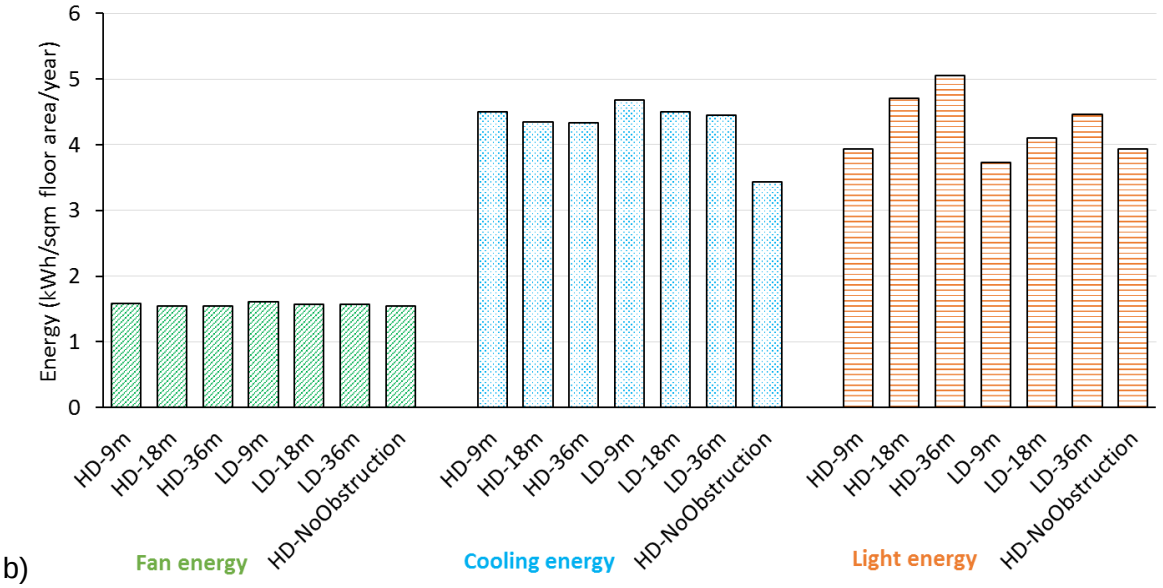

b)

Figure 7-38 The energy use related to the urban layouts due to the annual ventilation and infiltration volume of the terraced house.

7.10.3 Case study for detached house: Varying all selected parameters

The energy use of detached houses is analysed by considering the urban density of three cases (Figure 7-39). The wind pressure coefficients were estimated from the urban layout and building geometry. This means that there are three different Cp value sets with 12 orientations for each urban pattern. The results show that the orientation of the detached building does not strongly impact the energy use for lights, fans and cooling systems (Figure 7-40 and Figure 7-41) because with windows on four sides are able to get natural wind from every orientation. Urban density also has a minor impact on the energy use for different urban layouts.

High density urban (HD)

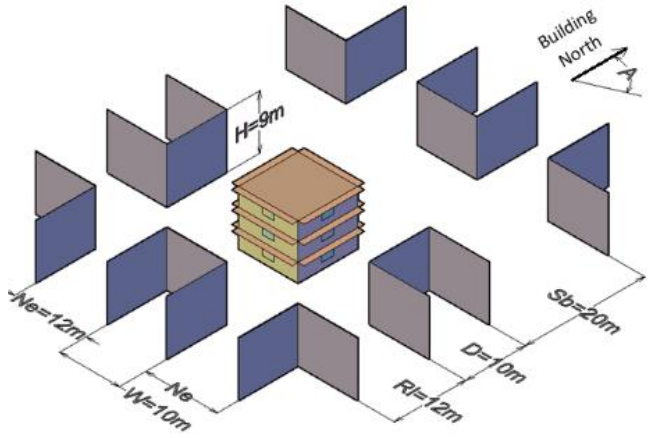

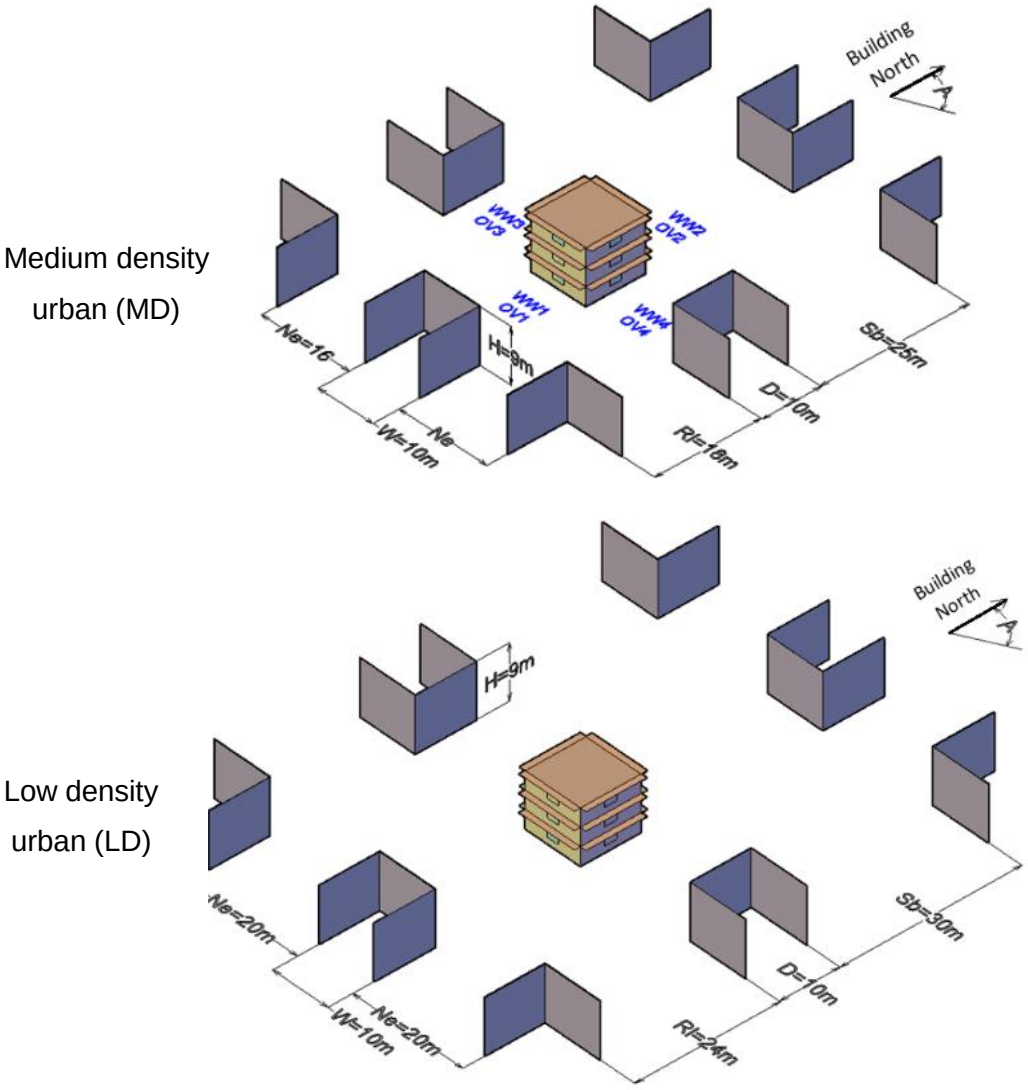

Figure 7-39 Three different cases of detached houses (building size identical, distance different).

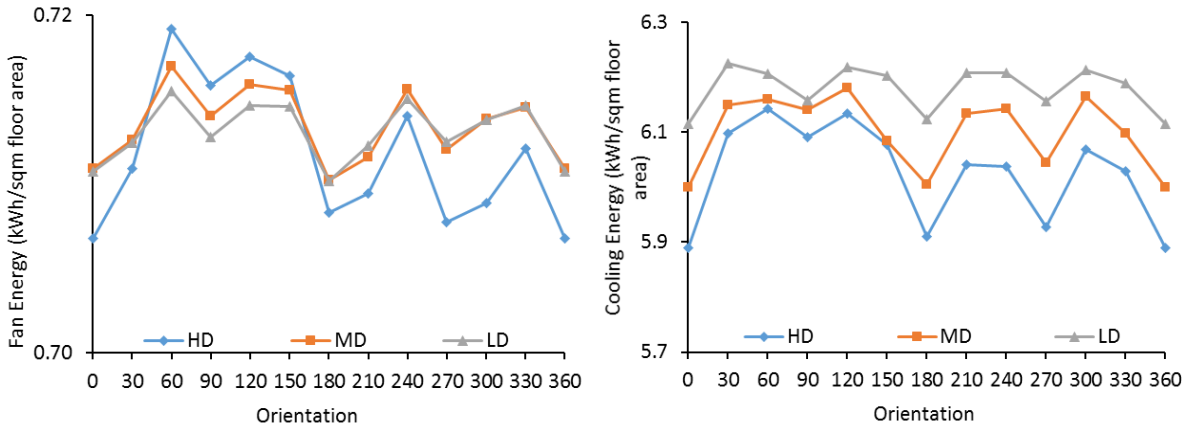

Figure 7-40 Fan and cooling energy of detached houses.

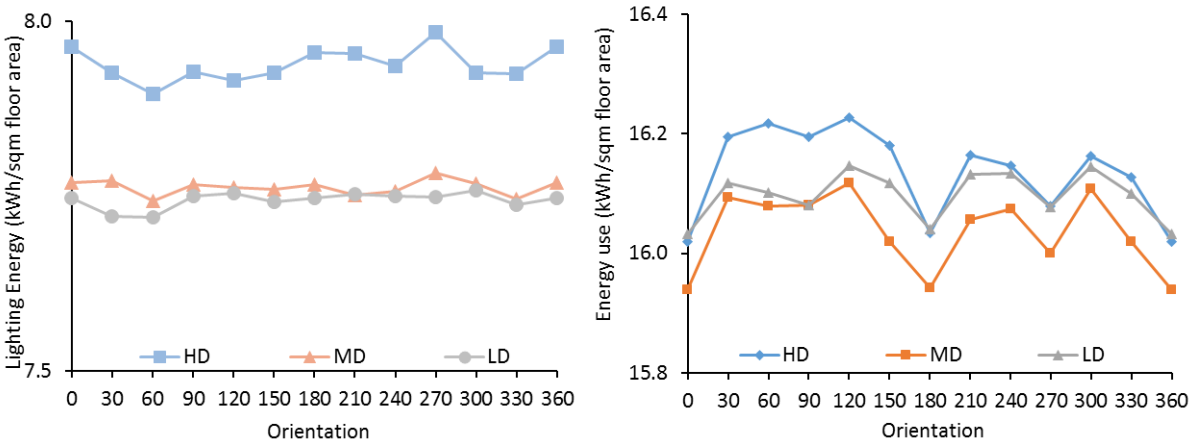

Figure 7-41 Lighting energy and total Energy use of different orientations in three cases of detached house. Energy of cooking equipment is included in the total energy.

Figure 7-42 shows that the energy use per one square meter floor area of the apartment unit is related to the urban layouts due to the natural ventilation and solar gain. In Figure 7-42 a) shows that the obstructions reduce a large volume of ventilation and infiltration of the detached house. In Figure 7-42 b) shows that the obstructions impact lightly on the energy use of fan and cooling. The high window and wall ratio can cool down the building right away after opening windows. In the Figure 7-42 d) shows that the lighting energy is not so different between the cases because of very low building density. Without obstructions the building need a bit more energy for light.

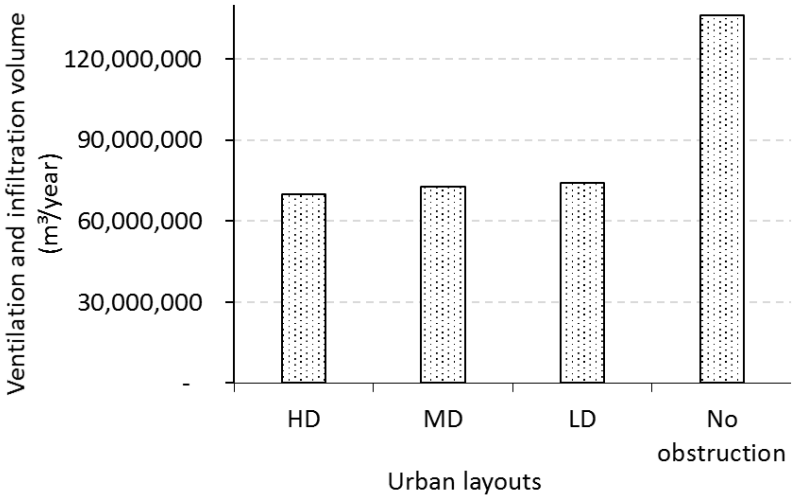

a)

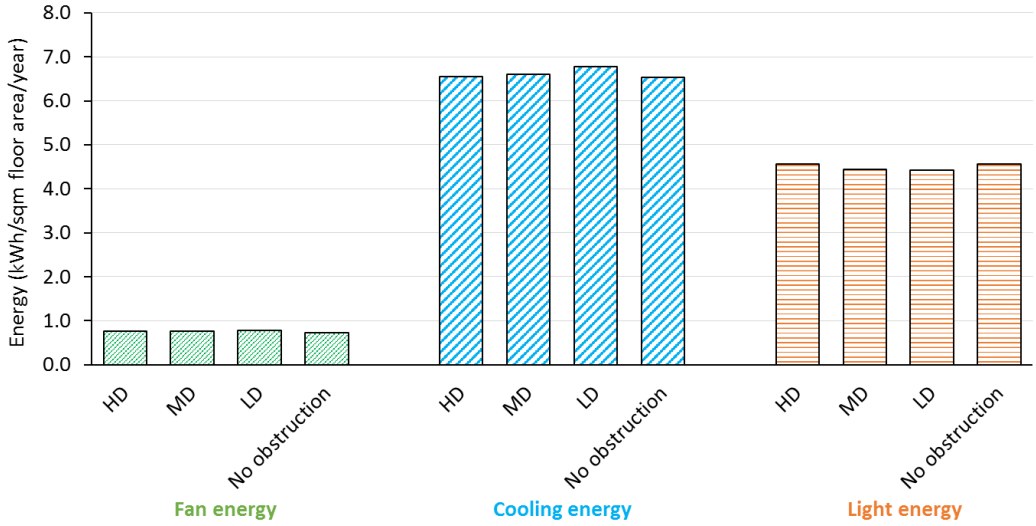

b)

Figure 7-42 The energy use related to the urban layouts due to the annual ventilation and infiltration volume of the detached house.

7.10.4 Case study for apartment unit at the middle of the building

The energy use of the apartment housing type is analysed by changing the urban density and the building heights in six cases (Figure 7-43). The wind pressure coefficients are estimated by the meta-model considering the urban density and building layout. This means that there are six different Cp value sets with 12 orientations for each urban pattern.

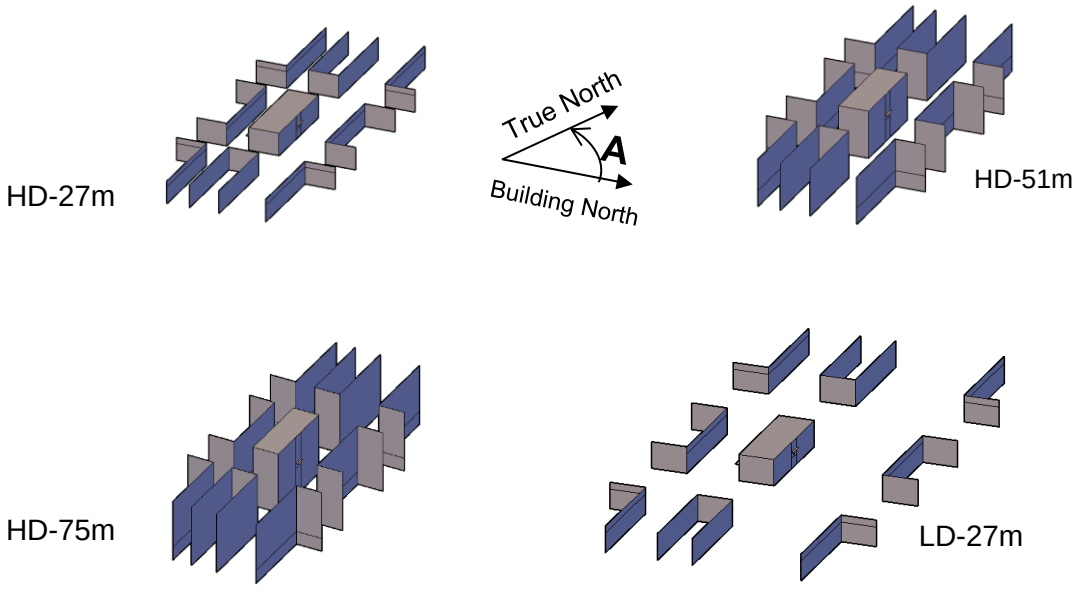

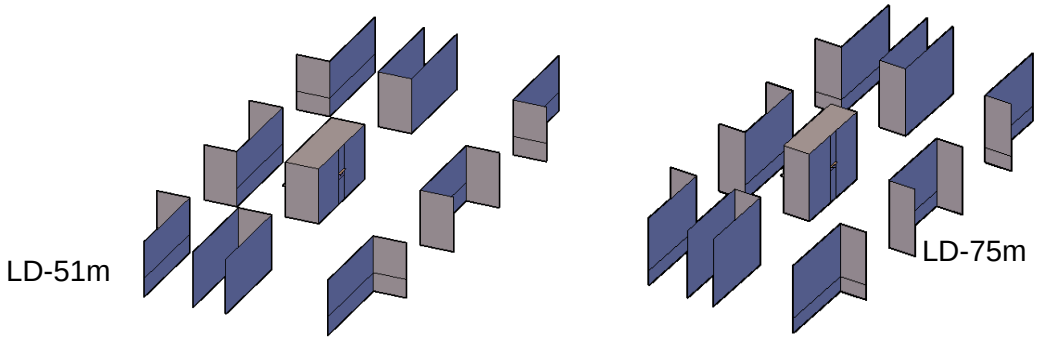

Figure 7-43 Six cases of different building densities of the apartment buildings.

The results show that the apartment building's orientation impacts strongly upon energy use for lights, fans and cooling systems (Figure 7-44 and Figure 7-45). The urban density also impacts upon the energy use for different urban layouts. The orientation has a lower impact in the high-density cases (HD-51m and HD-75m). Moreover, the results show that increasing obstruction heights can reduce the energy use for cooling and fans.

The energy use is not symmetric such as 90° and 270° because the urban and building layouts are not symmetric and the corridor is 1.5m and the overhang is 1m.

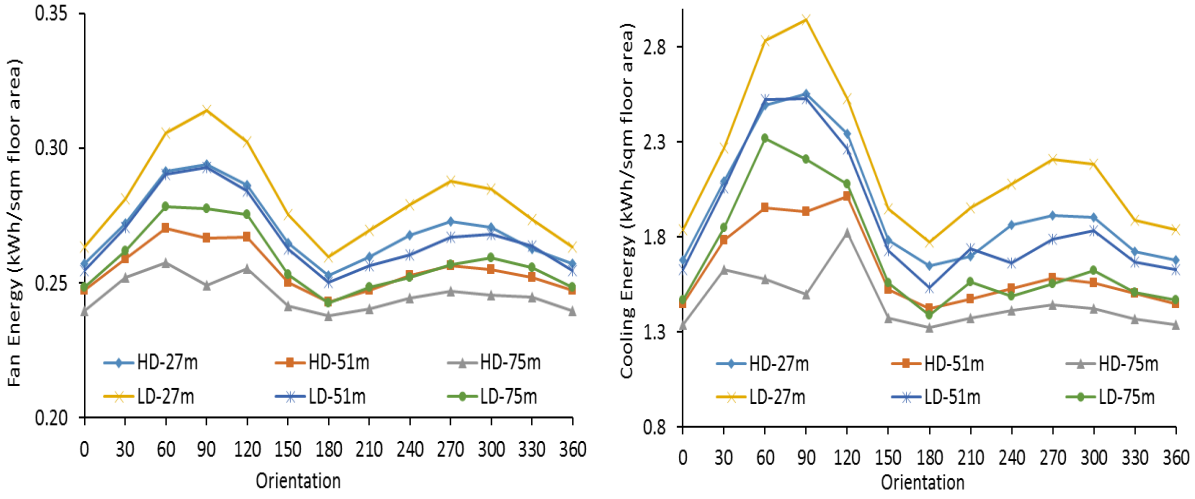

Figure 7-44 Fan and cooling energy of different orientations in six cases of apartments.

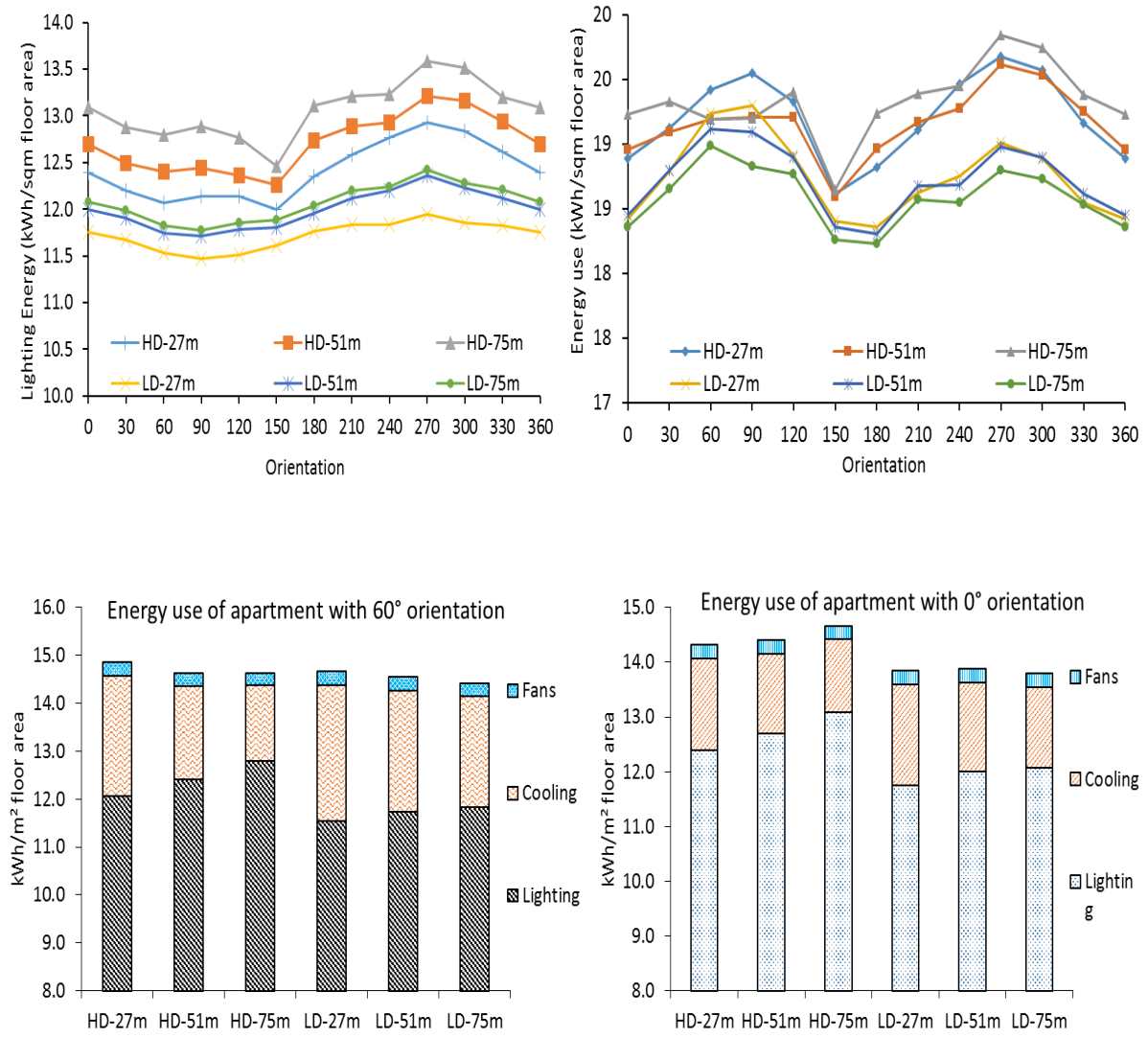

Figure 7-45 Lighting energy and total energy use of different orientations in six cases of apartment.

In Figure 7-46 a shows that the obstructions reduce a large exchange volume via ventilation and infiltration. In Figure 7-46 b shows that the energy use for fan and cooling is reduced due to the shading of the obstructions and the ventilation. This consequence proves that the solar gain impacts stronger than the cooling air form the outdoor. In the Figure 7-46 d) shows that the lighting energy increases when the daylight is locked by the neighbouring buildings. The lights are switched off later in the morning and switched on earlier than in the afternoon. These results also prove that the dynamic schedule can represent the user behaviour.

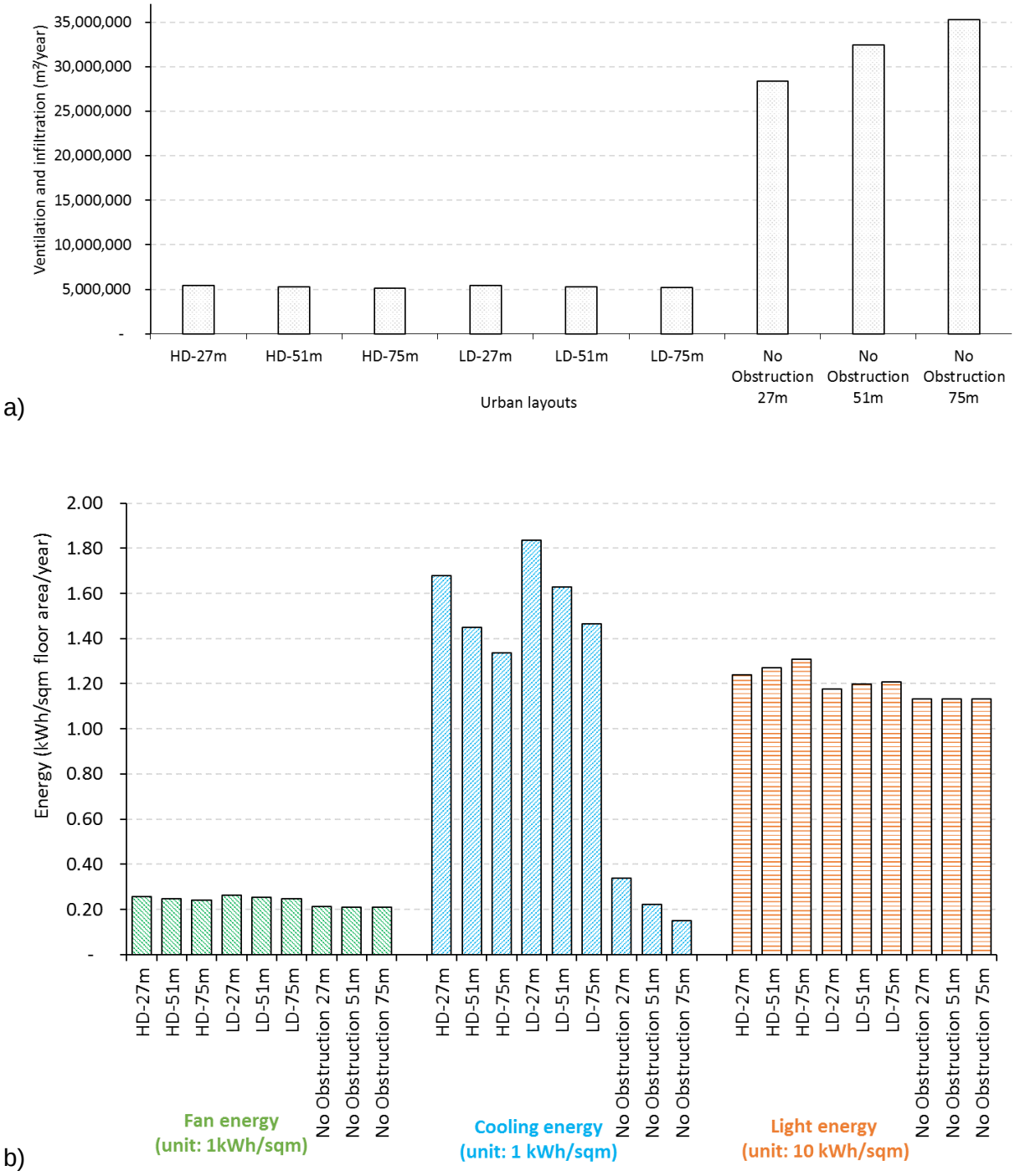

Figure 7-46 The energy use related to the urban layouts due to the annual ventilation and infiltration volume of the apartment.

7.10.5 Case study for apartment unit at bottom, middle and top of building

The aim of this analysis is to understand the combined effect of wind velocity and solar radiation at different heights (including reflection from the ground and from the neighbouring obstructions). Apartment units at the second, twelfth and twentieth floors which face the South

orientation have been analysed, including energy from light, fans and cooling systems. Their results show that apartment units which are higher up are exposed to higher natural ventilation rates because the wind velocity increases with the height of the building (Figure 7-47).

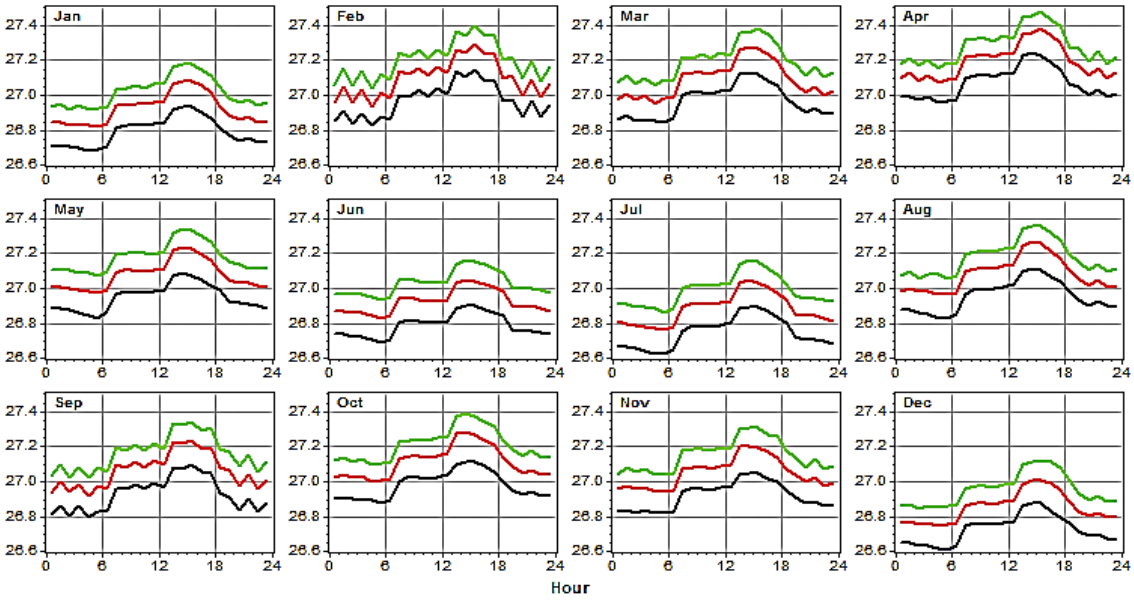

Figure 7-47 A zone's air temperature per hour for an average day of each month of the bottom (green), middle (red) and top (black) cases and their orientation are faced to the North. The higher the floor is, the faster the wind speed is and the lower the energy use per square meter floor area.

The energy use for lights, fans and cooling systems is reduced by the height of the building. When the facades face to the East or West orientations, the energy use reaches high peaks (Figure 7-48 and Figure 7-49). The shading devices can overcome the disadvantages of the orientations to avoid overheating and still getting enough indirect solar radiation for the daylight.

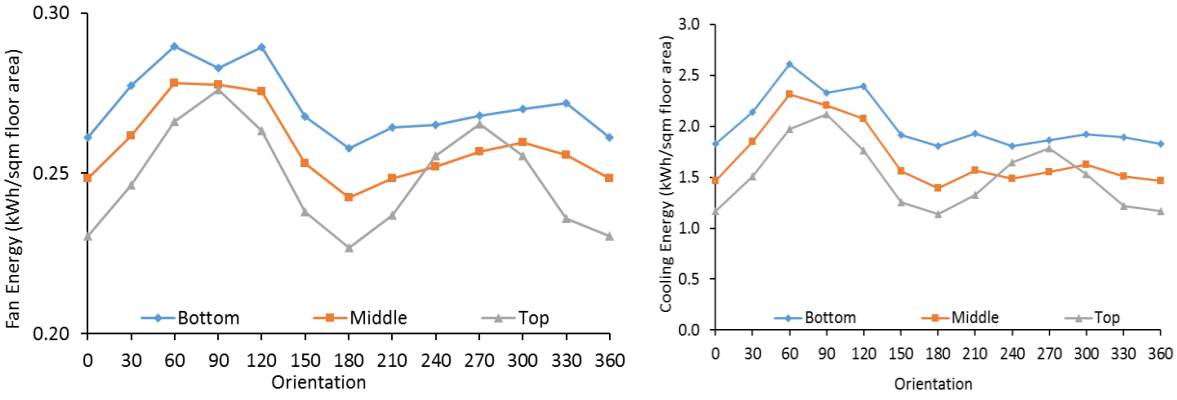

Figure 7-48 Fan and cooling energy use of different orientations in three cases of apartments.

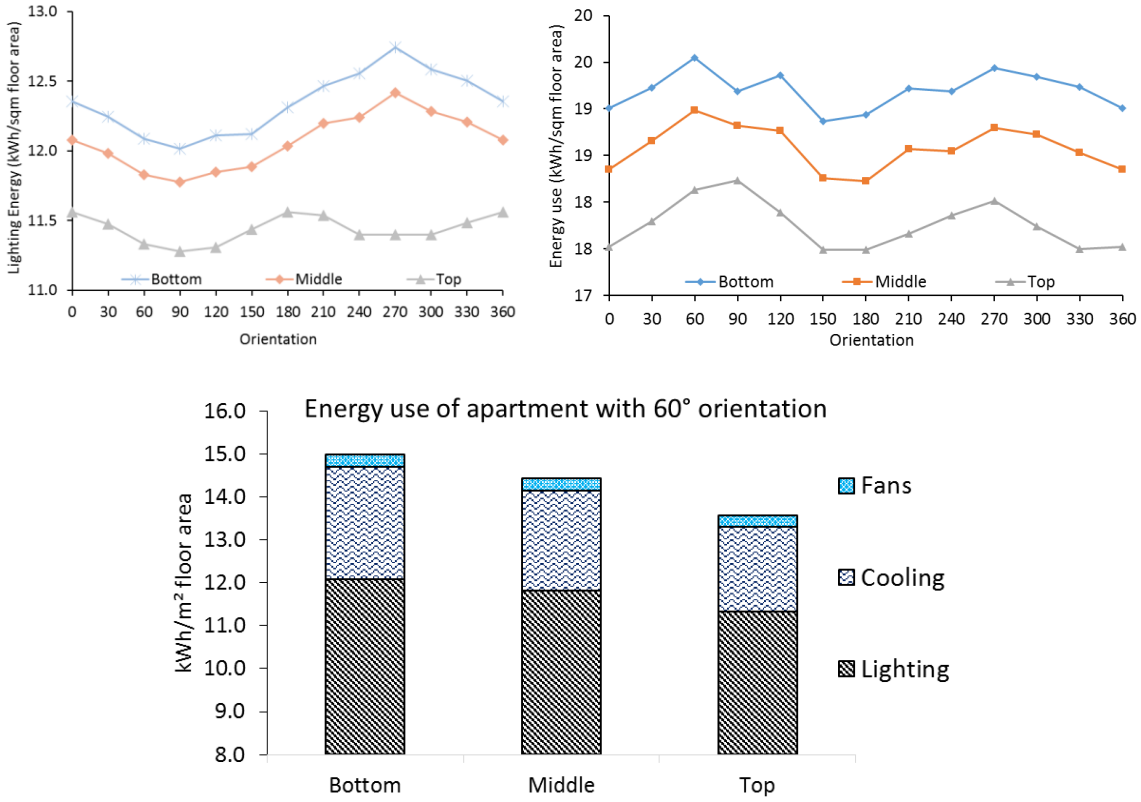

Figure 7-49 Lighting energy and total energy use of different orientations in three cases

7.11 Rules of thumb for design

This chapter has focused on the development of life cycle cost including energy use with respect to thermal comfort and daylight constraints. Different orientations, building heights and distance between buildings have been considered. The quantity of energy used is affected by orientation related to the housing types. Only the front and rear facade of apartments can get wind and solar radiation. Only the front, rear facade and roof of terraced house can get wind and solar radiation.

In the case of detached units all facades with windows can get the wind and the solar radiation from all directions. Therefore, the planning or regulations of a detached house fragment should allow to select orientation freely. The shading devices on the East and the West orientations are significant to avoid overheat. The plants located in the two orientations can work as well as the overhangs.

7.12 Conclusions

There are three main points to conclude upon regarding: Energy Management System (EMS) to control thermal comfort, surrogate models to estimate the wind pressure coefficients and the natural ventilation to impact on the energy use considering different urban layouts.

The EnergyPlus engine's EMS was implemented to simulate "optimal" behaviour from manual (by extended family) to fully automated control. In the dynamic user behaviour, the acceptable level of discomfort is a parameter. This strategy suggests advising strict, sustainable behaviour to occupants or automatic control systems that follows the dynamic schedule defined in the study.

A computationally intensive step to calculating Cp values of various urban patterns and building geometries was solved by developing surrogate models. Those regression models are based on other surrogate models that were developed based on measurement in situ, wind tunnel measurement and CFD simulations. Energyplus only considers average surface pressure for single box building using the normalized surface pressure coefficient [28]. Therefore, the meta-model of wind pressure coefficients allows considering neighbouring obstructions. The regression functions of these meta-model show a high correlation with other surrogate models. These meta-models are used to obtain wind pressures on different surfaces of the building during EnergyPlus simulation and to predict the air flow.

As we know that the sun and wind are significant to design for daylight and thermal comfort in the tropical climate. The results above prove that the neighbouring buildings in the urban scale can provide shadow to reduce solar gain but they also limit the natural ventilation. The natural ventilation is represented by the annual ventilation and infiltration volume. The annual ventilation and infiltration volume are reduced with more than 50% in the cases of terraced house and detached house to compare with the free standing building. This reduction is six times in the case of the apartment building. However, the buildings do not require all possibility ventilation and infiltration volume to cooling the indoor air. The window size and the dynamic occupant behaviour can cool down the buildings in effective and efficient ways. The interactions of the solar gain, the wind, dynamic schedule, materials, building layout, urban layout and orientation are analysed in the optimization process in the chapter 8.

References

[1] M. Santamouris, Cooling the buildings – past, present and future, Energy Build. 128 (2016) 617–638.

[2] ASHRAE, ASHRAE - Std 55-2004 Thermal Environmental Conditions for Human Occupancy, (2004).

[3] R. de Dear, G.S. Brager, Developing an adaptive model of thermal comfort and preference, ASHRAE Trans. 104 (1998) 145–167.

[4] P.O. Fanger, Thermal comfort: analysis and applications in environmental engineering, Danish Technical Press Copenhagen, 1970.

[5] J. van Hoof, Forty years of Fanger's model of thermal comfort: comfort for all?, Indoor Air. 18 (2008) 182–201.

[6] P. Ole Fanger, J. Toftum, Extension of the PMV model to non-air-conditioned buildings in warm climates, Energy Build. 34 (2002) 533–536.

[7] I. Requena-Ruiz, Thermal comfort in twentieth-century architectural heritage: Two houses of Le Corbusier and André Wogenscky, Front. Archit. Res. 5 (2016) 157–170.

[8] J.F. Nicol, M.A. Humphreys, Adaptive thermal comfort and sustainable thermal standards for buildings, Energy Build. 34 (2002) 563–572.

[9] G. Brager, Mixed-mode cooling., Cent. Built Environ. (2006). http://escholarship.org/uc/item/3bb8x7b8 (accessed January 6, 2015).

[10] R.J. de Dear, T. Akimoto, E.A. Arens, G. Brager, C. Candido, K.W.D. Cheong, B. Li, N. Nishihara, S.C. Sekhar, S. Tanabe, J. Toftum, H. Zhang, Y. Zhu, Progress in thermal comfort research over the last twenty years, Indoor Air. 23 (2013) 442–461.

[11] ASHRAE, ANSI/ASHRAE Standard 55-2013: Thermal Environmental Conditions for Human Occupancy, (2013).

[12] A.T. Nguyen, M.K. Singh, S. Reiter, An adaptive thermal comfort model for hot humid South-East Asia, Build. Environ. 56 (2012) 291–300.

[13] Jan L.M. Hensen, Roberto Lamberts, Building Performance Simulation for Design and Operation, Taylor & Francis, 2011.

[14] U.S. DOE, EnergyPlus Energy Simulation Software. U.S. Department of Energy | USA.gov, (2015). http://apps1.eere.energy.gov/buildings/energyplus/ (accessed December 8, 2015).

[15] EnergyPlus, EnergyPlus Energy Simul. Softw. (2015). http://apps1.eere.energy.gov/buildings/energyplus/.

[16] C.J. Hopfe, J.L.M. Hensen, Uncertainty analysis in building performance simulation for design support, Energy Build. 43 (2011) 2798–2805.

[17] M. S. Eldred, D. M. Dunlavy, Formulations for surrogate-based optimization with data fit, multifidelity, and reduced-order models, in: Portsmouth, VA, USA, 2006.

[18] Y.S. Ong, P.B. Nair, A.J. Keane, Evolutionary Optimization of Computationally Expensive Problems via Surrogate Modeling, AIAA J. 41 (2003) 687–696.

[19] S. Koziel, L. Leifsson, Surrogate-Based Modeling and Optimization, Springer, 2013.

[20] V. Machairas, A. Tsangrassoulis, K. Axarli, Algorithms for optimization of building design: A review, Renew. Sustain. Energy Rev. 31 (2014) 101–112.

[21] A.I.J. Forrester, A. Sóbester, A.J. Keane, Engineering Design via Surrogate Modelling, John Wiley & Sons Ltd. Reg, 2008.

[22] M. Grosso, Wind pressure distribution around buildings: a parametrical model, Energy Build. 18 (1992) 101–131. doi:10.1016/0378-7788(92)90041-E.

[23] Nicolas Heijmans, Peter Wouters, Impact of the uncertainties on wind pressures on the prediction of thermal comfort performances, 2003.

[24] B. Knoll, J.C. Phaff, W.F. de Gids, Pressure Simulation Program, in: Palm Springs, USA, 1995.

[25] Y. Sun, Y. Heo, M. Tan, H. Xie, C.F. Jeff Wu, G. Augenbroe, Uncertainty quantification of microclimate variables in building energy models, J. Build. Perform. Simul. 7 (2014) 17–32.

[26] R. Ramponi, A. Angelotti, B. Blocken, Energy saving potential of night ventilation: Sensitivity to pressure coefficients for different European climates, Appl. Energy. 123 (2014) 185–195.

[27] G. van Moeseke, E. Gratia, S. Reiter, A. De Herde, Wind pressure distribution influence on natural ventilation for different incidences and environment densities, Energy Build. 37 (2005) 878–889.

[28] M.V. Swami, S. Chandra, Correlations for Pressure Distributions on Buildings and Calculation of Natural-Ventilation Airflow, 1988.

[29] F. De Troyer, BB/SfB-plus - Een functionele hiërarchie voor gebouwen, ACCO, Leuven, 2008.

[30] K. Allacker, F. De Troyer, D. Trigaux, T. Geerken, W. Debacker, C. Spirinckx, J.V. Dessel, A. Janssen, L. Delem, K. Putzeys, Sustainability, Financial and Quality evaluation of Dwelling Types - SuFiQuaD - FINAL REPORT, Brussels, 2011.

[31] ISO 7730, ISO 7730, Ergonomics of the thermal environment — Analytical determination and interpretation of thermal comfort using calculation of the PMV and PPD indices and local thermal comfort criteria, Thrid edition, Switzerland, 2005.

[32] M. Fadzli Haniff, H. Selamat, R. Yusof, S. Buyamin, F. Sham Ismail, Review of HVAC scheduling techniques for buildings towards energy-efficient and cost-effective operations, Renew. Sustain. Energy Rev. 27 (2013) 94–103.

[33] J.F. Busch, A tale of two populations: thermal comfort in air-conditioned and naturally ventilated offices in Thailand, Energy Build. 18 (1992) 235–249.

CHAPTER 8 OPTIMISATION OF PASSIVE DESIGN FOR THERMAL COMFORT IN A HOT AND HUMID CLIMATE

In this chapter the different models elaborated in the previous chapters are integrated and an optimization method to search for a minimal life cycle cost, for a set of comfort levels, is elaborated.

The three common typologies described in chapter 4 (detached houses, terraced houses and apartments) are considered. For the apartment units the model for selecting the most cost-efficient foundation (chapter 5) in integrated. The model searching for the highest return based on a prediction of the market value (chapter 6) is not included due to the unreliable results based on web data at this moment. The thermal comfort model (chapter 7) is required to predict the life cycle cost for a given comfort level and occupant behaviour.

In this chapter first an optimization method is selected (8.1), the integration of the sub models is described (8.2) and a way to create a graphical overview of the results (parallel coordinates) is presented (8.3).

Then the results for the three typologies are discussed (8.4). The three types are compared (8.5) and global conclusion are formulated (8.6). In a final point (8.7) conclusions regarding the methodologies are summarised.

Some parts of this chapter are based on the publication

Nguyen Van, T., Trigaux, D., Allacker, K., De Troyer, F. (2014). Optimization for Passive Design of Large Scale Housing Projects for Energy and Thermal Comfort in a Hot and Humid Climate. In Rawal, R. (Ed.), Manu, S. (Ed.), Khadpekar, N. (Ed.), Sustainable habitat for developing societies: Vol. 1 (1). 30th International PLEA Conference. Ahmedabad, 16-18 December 2014 (pp. 21-21). Ahmedabad, India: CEPT UNIVERSITY PRESS.

Table of Contents

8.1	**Selection of optimization method**	**186**
8.1.1	Exponential growth of optimization methods	186
8.1.2	Optimization programs selected for energy use and life cycle cost of buildings	186
8.1.3	Concepts behind optimization algorithms	187
8.2	**The integration of the sub models**	**195**
8.2.1	Links between models	195
8.2.2	Optimization algorithm setting	197
8.2.3	Optimization process	198
8.3	**A graphical post processing of the simulation results**	**199**
8.3.1	Pareto front in case of life cycle cost and initial cost	199
8.3.2	Parallel Coordinates	199
8.4	**Results of optimisation**	**200**
8.4.1	Terraced houses: Parameters, Results and Discussions	200
8.4.2	Detached house: Parameters, results and discussions	212
8.4.3	Apartment: Parameters, Results and discussions	223
8.5	**Comparison of the three housing types**	**232**
8.5.1	Comparison including land and infrastructure	232
8.5.2	Comparison without land and infrastructure	232
8.5.3	Comparison of energy use of three housing types	233
8.5.4	Energy use for fans and cooling depending on acceptable PMV levels	234
8.5.5	Overhang, urban layout and orientations	235
8.6	**Findings throughout three housing types**	**236**
8.7	**Conclusions regarding the methodology**	**237**

8.1 Selection of optimization method

8.1.1 Exponential growth of optimization methods

The number of building performance simulation tools developed between 1997 and 2010 increased exponentially from 100 to 389 tools [1] . On the other hand, the number of optimization studies from building science published in scientific papers increased even faster in the period 2007 to 2012 from 30 to 120 studies (Figure 8-1). The selection of an appropriate tool for energy simulation and optimization is therefore a crucial aspect.

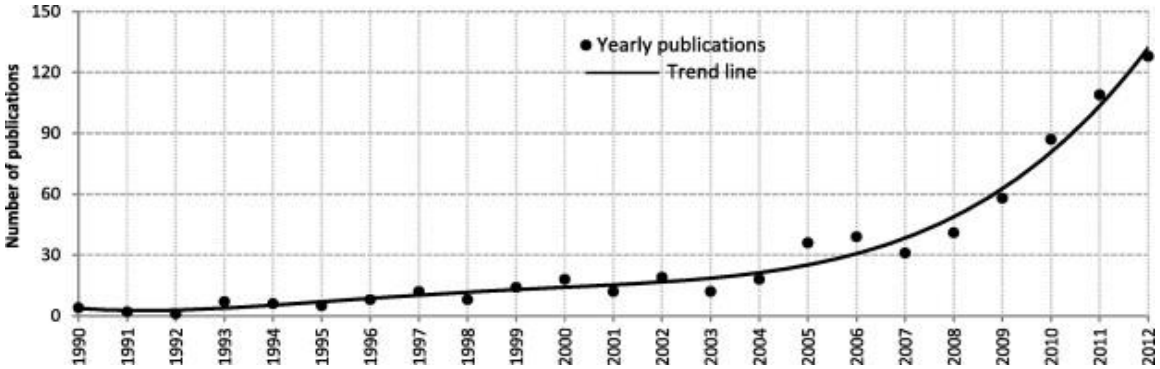

Figure 8-1 The increased trend of the number of optimization studies in building science [2].

8.1.2 Optimization programs selected for energy use and life cycle cost of buildings

Based on interviews [3] of a large number of building optimization experts, almost all selected GenOpt and MatLab as tools for optimization of energy use and life cycle cost. GenOpt is an academic generic optimization tool designed for optimization with a single objective function, thus it is suitable for many purposes in building performance simulation with an acceptable complexity. MatLab environment has been designed for many simulation purposes, so it requires skills to adapt it to a specific use. Table 8-1 gives an overview of the most frequently used optimization programs with key capacities based on [3]. For this study, GenOpt is selected and is coupled with the EnergyPlus engine.

Table 8-1 Optimization programs are applied to building performance optimization based on [3].

Name	Open source	Multi-objective algorithm	Surrogate models available
BEopt	Yes	Yes	No
Dakota	Yes	Yes	Yes
GenOpt	Yes	No	No
jEPlus + EA	Yes	Yes	No
MatLab toolbox	No	Yes	Yes
MLE+ Toolbox	Yes	Yes	Yes

8.1.3 Concepts behind optimization algorithms

8.1.3.1 Optimization algorithms for discontinue problems and selections

The demand for an efficient and effective search method has led to the development of many optimization algorithms. For engineering optimization problems, objective functions are generally non-linear, multi-modal, discontinuous and non-differentiable [9]. The selection of an optimization algorithm for a certain problem is crucial to reaching a global optimal value. The stochastic population-based algorithms (Genetic algorithm, particle swarm optimization and hybrid algorithms) are frequently used in building performance simulations (Figure 8-2). In all cases, they cannot guarantee reaching the real global optimal point, but they can obtain good solutions in a reasonable computational time.

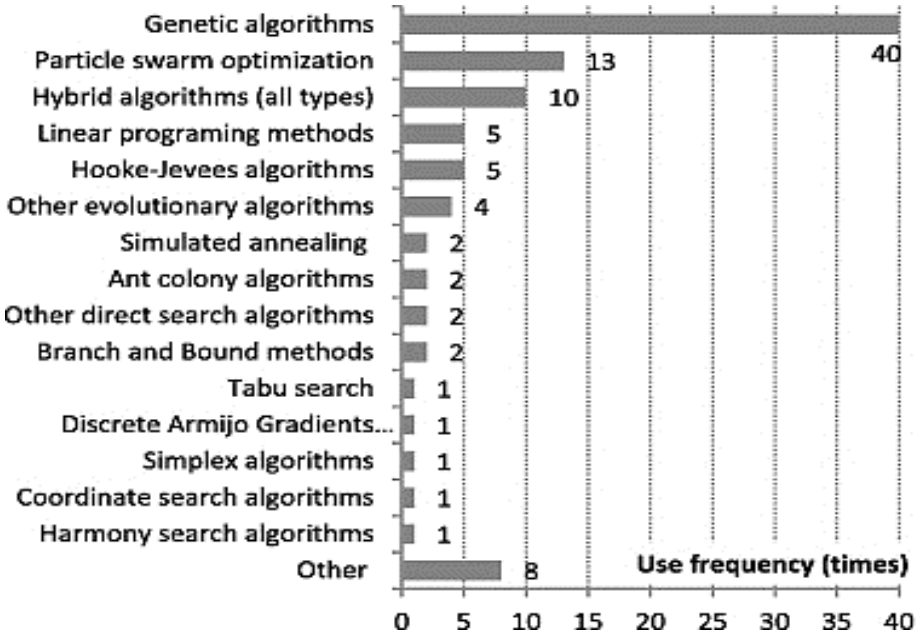

Figure 8-2 Use frequency of different optimization algorithms, the result was derived from more than 200 building optimization studies [2].

8.1.3.2 Particle swarm optimization

The optimization of human comfort in building is always a discrete (not described by continuous objective functions) due to the complex interplay of geometries, materials, natural phenomena (radiation, wind flow, heat accumulation, etc.) and human interactions. Various algorithms for discrete optimization are described in the literature. The most popular algorithms that can handle discrete variables are evolutionary algorithms [2], such as Genetic Algorithm [4], multi-objective genetic algorithm [5] and particle swarm optimization [6]. These methods explore the design space using information from previous analyses to

move toward a better design option. Evolutionary algorithms are easy to understand and to implement for discrete parameters and complex constraints. However, evolutionary algorithms need high computational time, require careful tuning of algorithmic parameters and do not guarantee the global optimality [7]. Therefore, hybrid algorithms (e.g. PSO-GPS [8], GA-GPS [9]) show a good capability in solving problems in cases of discontinuities in building simulations. The hybrid algorithms have been implemented in several computer programs (e.g. GenOpt, Matlab optimization toolbox, etc.).

Kennedy and Eberhart introduced particle swarm optimization (PSO) based on the social behaviour of particles in a swarm [6]. PSO searches use a population of particles moving in parallel in several runs. Each particle represents a candidate solution of the problem. Particles change their positions or states with time and move around in a multidimensional search space [10]. Each particle moves toward the optimum point, based on its previous experience and the experience of its neighbours.

The PSO algorithm can be explained more in detail based on [11], as follows: each candidate for design option is called a "particle" and represents a point in a D-dimensional design space, if *D* is the number of parameters to be optimized. Accordingly, the position of the i^{th} particle is described by the vector $x_i = [x_{i1}, x_{i2}, x_{i3}, \ldots, x_{iD}]$ and the population of *N* particles constitutes the swarm $X= \{x_1, x_2, \ldots, x_N\}$. The particles evolve via trajectories in the parameter space based on the equation of motion: $x_i(t + 1) = x_i(t) + v_i(t + 1)$. Where t and t + 1 indicate two iterations of the algorithm and $v_i = [v_{i1}, v_{i2}, \ldots, v_{iD}]$ is the vector collecting the velocity (changing of parameters per time step) of parameters of the i^{th} particle of the D dimensions.

The velocity vectors govern the way particles move in the design space and are made of the contribution of three components (Figure 8-3). The 'inertia' w of the particle keeps track of the previous flow direction. A 'cognitive component' returns to their own previously found best positions. A 'social component' identifies the propensity of a particle to move towards the best position of the whole swarm. Based on these considerations, the velocity of the i^{th} particle is defined as:

$$v_i(t+1) = wv_i(t) + c_1r_1(p_i - x_i(t)) + c_2r_2(g - x_i(t))$$

Where p_i is the so called "personal best" of the particle. The vector p_i contains the coordinates of the best solution obtained so far by a specific individual. The vector g is the "global best". This is the overall best solution obtained by the swarm. The acceleration constants c_1 and c_2, which are real values and usually in the range from 0 to 4, are called "cognitive coefficient" and "social coefficient". The two coefficients impact on the directions

of particle via 'personal best' and 'global best', respectively. In addition, r_1 and r_2 are two random numbers generated from a uniform distribution in [0, 1], so that both the social and the cognitive components have a stochastic influence on the updated velocities.

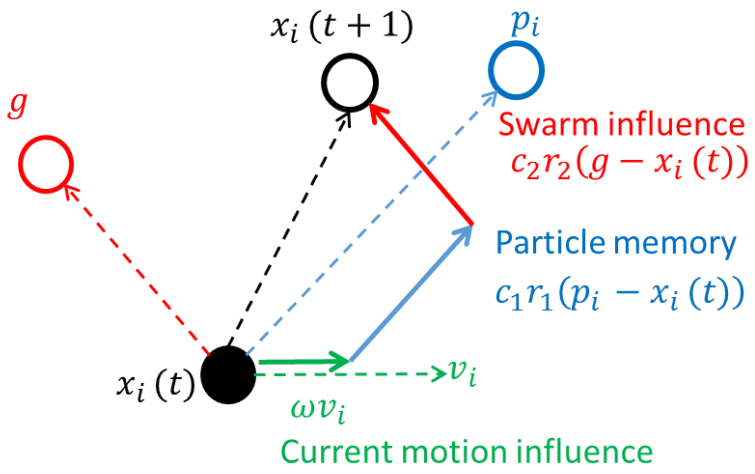

Figure 8-3 Depiction of the velocity and position updates in PSO modified from[12].

A schematic description of the basic PSO algorithm to search for a minimum is reported in the following steps (Figure 8-4). First, the PSO algorithm generates N particles. The particle i^{th} at time t is the position x_i^t that consists of all parameters of the model. All parameters of each particle i^{th} are used to calculate the fitness in order to obtain the particle's best position p_i. In the first generation (t = 0) the global best g is the personal best at this time. Second, the algorithm updates the particles' velocity according to equation of velocity and updates the particle position according to equation of position. Third, a next population at time t^{th} is generated to obtain the personal best position $p_i(t)$. If the fitness $f(x_i(t+1)$ of the particle $x_i(t+1)$ is small or equal $f(p_i)$, the personal best is updated, $p_i = x_i(t+1)$. If the fitness $f(x_i(t+1)$ of the particle $x_i(t+1)$ is small or equal f(g), the global best is updated $g = p_i(t+1)$. Such steps are repeated until reaching a stopping criterion. The criteria are number of generations or no new global best after a certain number of generations. At the end of the iterative process, the best solution is represented by vector g.

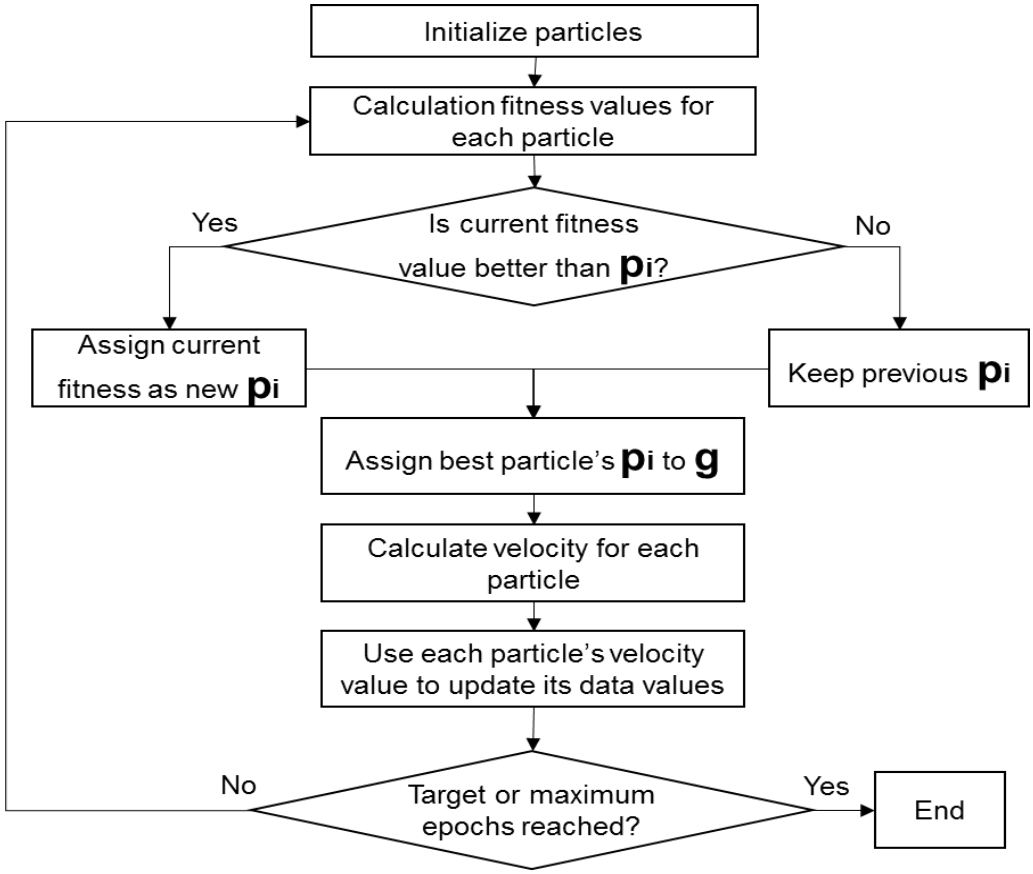

Figure 8-4 Flow diagram illustrating the particle swarm optimization algorithm

The following choice of parameters for particle swarm optimization was proposed by [14] [15] [16] for c1 = 2.8 and c2 = 1.3; for swarm size of 50 in case of high dimensional problems and swarm size between 20 to 50 for low dimensional problems and a general good choice of swarm size of 30 [14]. The number of iterations should be selected based on first trials with a high number of runs and observing the number of runs needed for convergence. The appropriate number of iterations in the cases considered in this research is 200 generations, these iterations were successful for complex building performance simulations [15] [16].

8.1.3.3 Improvement to particle swarm optimization

Improvement algorithm "Direct search" or "pattern search" was developed by Hooke and Jeeves [17] as an addition the PSO approach. The results of PSO become the initial input parameters of the pattern search method. The addition consists of a second step after the previously described phase. The pattern move is used to search the optimal point [18]. The pattern search generates a set of search directions for the set of parameters. For a two dimensional search space, the additional steps are described in a graphical way in Figure

8-5. From the initial optimization point from the PSO, the values of the objective function are calculated in the 4 points at a new step of 50 % from the step used in the PSO phase Figure 8-5. The new provisional optimum is where the objective function reaches a minimum. From the new optimal point, with the same grid size of 50% of the original, the value of the objective function is calculated in the 4 neighbouring points as before. When the objective function is not reduced, 50% smaller steps (grid search) are used to repeat the algorithm. As this leads in the Figure 8-5 the grid size is reduced to 25% of the original one and the previous steps are repeated until reaching to the minimum or maximum parameter ranges.

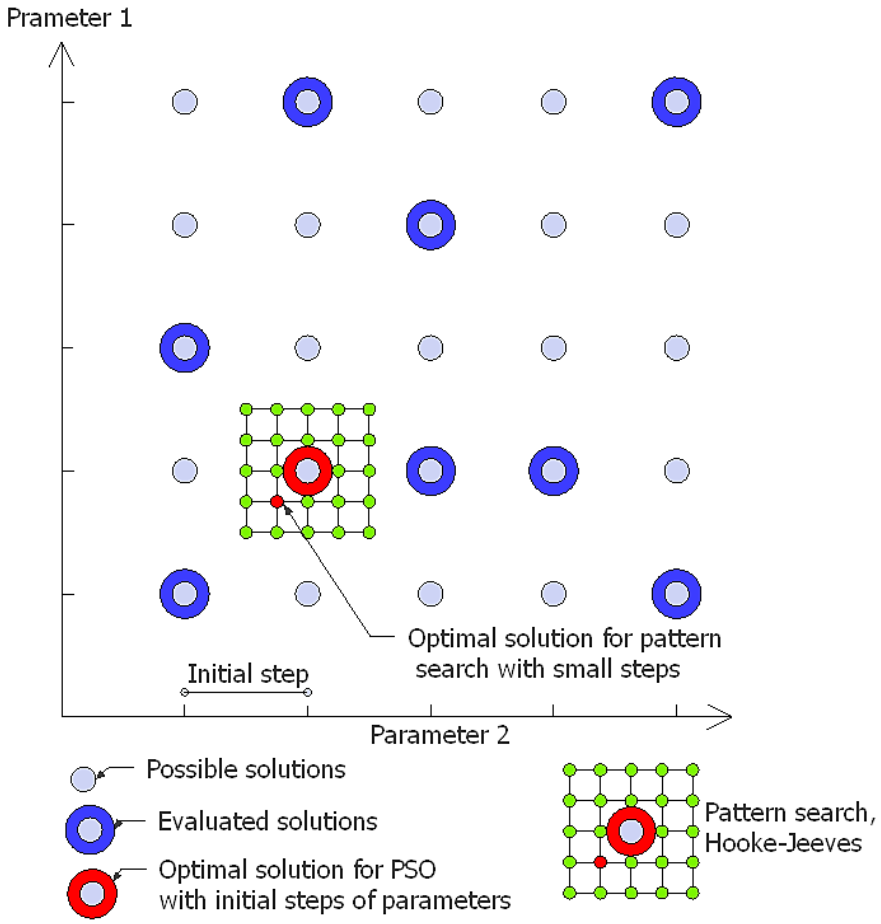

Figure 8-5 The pattern search (Hooke-Jeeves) looks for local optimal solution after PSO algorithm within smaller steps after identifying the global best with the initial parameter steps.

8.1.3.4 Selected optimisation algorithm for the present search

Hybrid algorithm is capable of working efficiently since it performs a global search by way of the particle swarm optimization (PSO) and the Hooke–Jeeves algorithm then search

for a local optimization (Figure 8-6). A combination of the particle swarm optimization (Eberhart and Kennedy 1995) and the Hooke–Jeeves algorithm (Hooke and Jeeves 1961) [9] was selected. A typical result is illustrated in Figure 8-6. By the second phase (Hooke and Jeeves) can achieve an additional cost reductions but required more simulation time than a standard genetic algorithm. This Hybrid algorithm were applied on the optimization process of the terraced house.

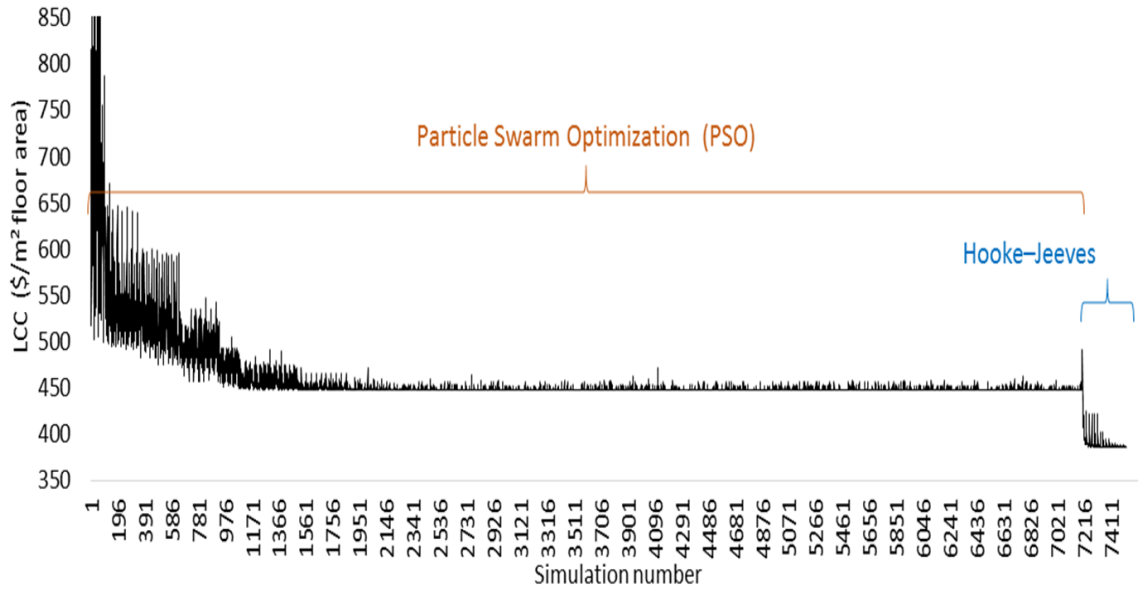

Figure 8-6 The hybrid algorithm is capable of working efficiently since it performs a global search by the particle swarm optimization and the Hooke–Jeeves algorithm then searches for a local optimization.

The efficiency and effectiveness of the optimization algorithms were evaluated by comparing the values of the objective function between the optimization method and 7000 random combinations within the design space of three housing types. In three graphs Figure 8-7, Figure 8-8 and Figure 8-9, the light blue combinations represent the random results, the red combinations represent the PSO results and the green combinations represent the Hooke-Jeeves results. After several generations of swarms The PSO algorithm identifies correctly the direction and focuses their searches on the design space that contain the lowest objective function values. The second phase of the optimal process, the green squares, reaches to the lowest value. The optimization method using PSO and Hooke-Jeeves (GPS) algorithms can be selected for complicated model at the early design stage.

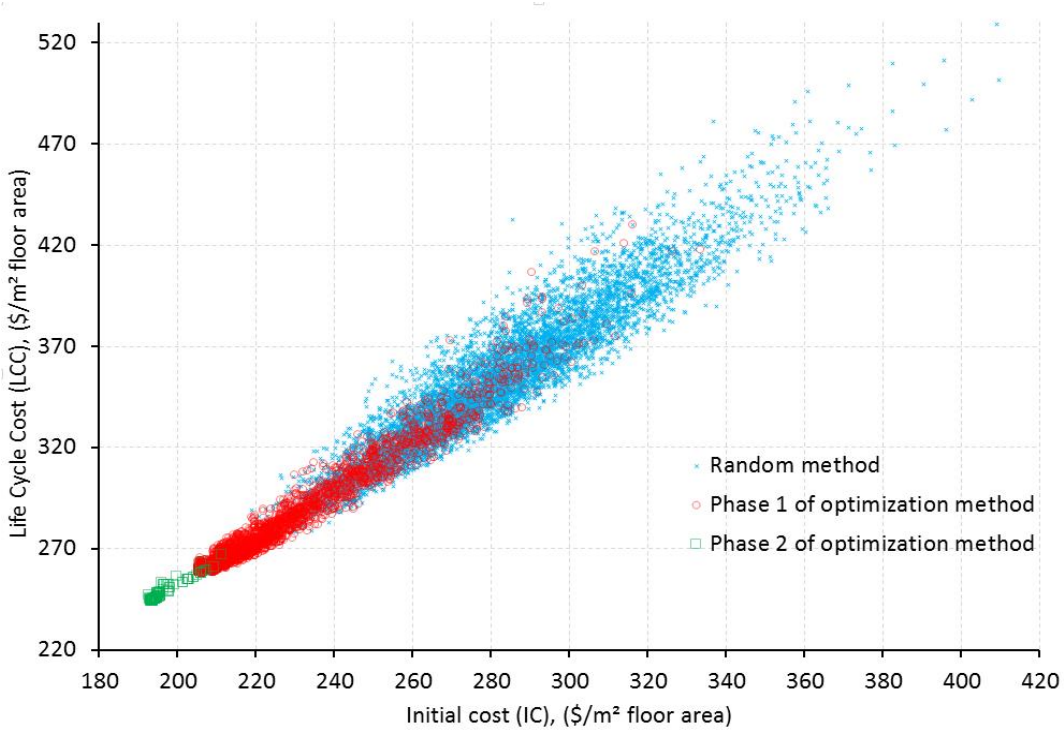

Figure 8-7 The optimization results of the terraced house with the thermal comfort limit PMV = 0.5.

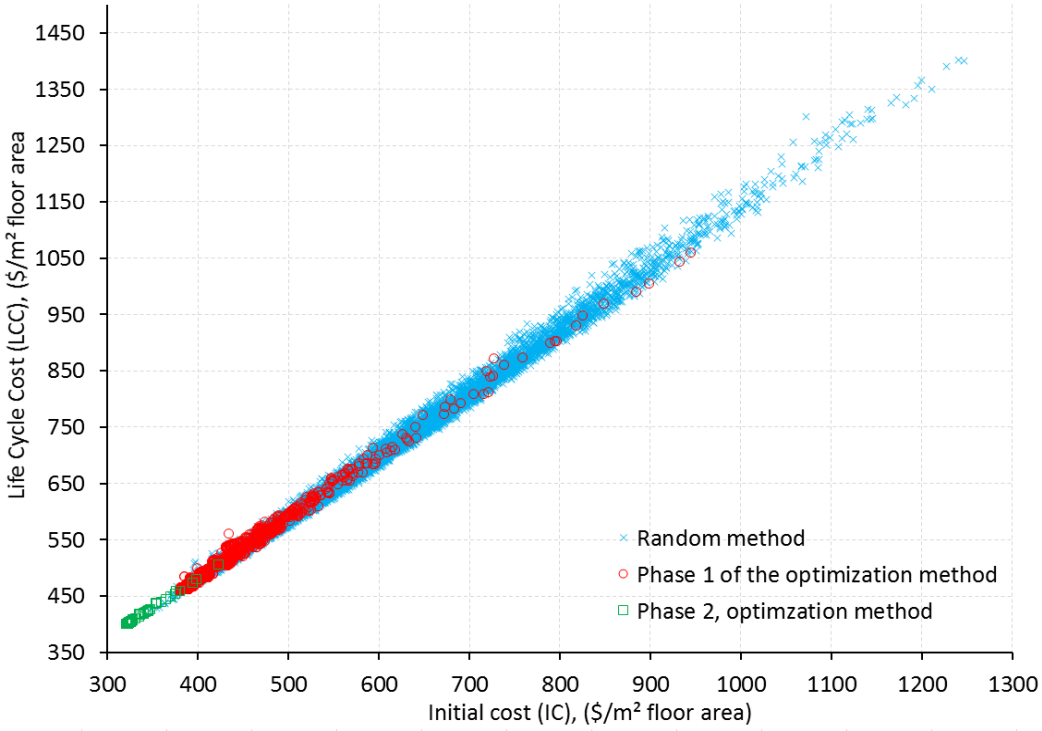

Figure 8-8 The optimization results of the detached house with the thermal comfort limit PMV = 0.5.

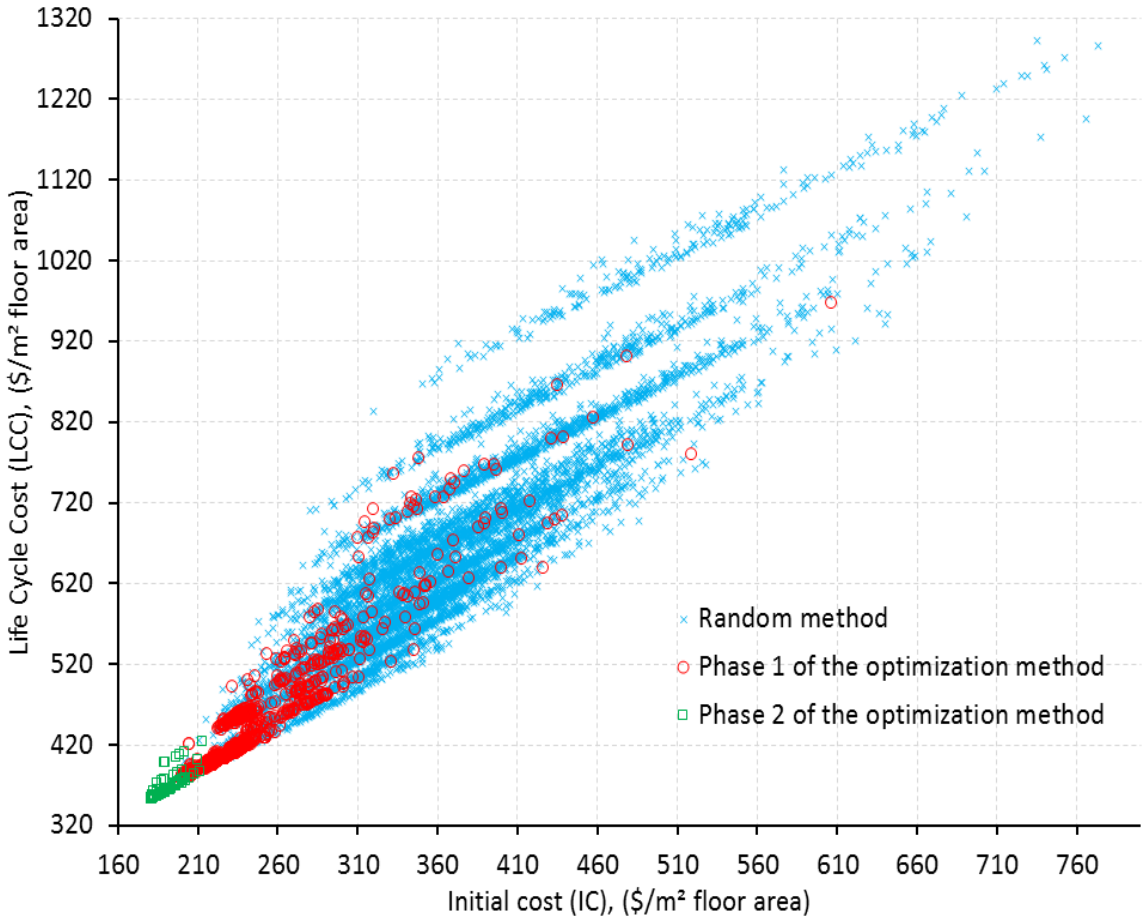

Figure 8-9 The optimization results of the apartment building with the thermal comfort limit PMV = 0.5.

Two significant settings of PSO are number of particles per generation and number of generations in order to reach the minimum value of an objective function. The number of combinations are the product of the number generations and swarm size. Seven trials were applied using terraced house model, which is more complicated than the apartment or the detached house models. The results in the Figure 8-10 show that after 5000 combinations the particles swarm optimization (PSO) algorithm is able to identify the design space which contains the lowest value of the objective function. By doing this test we can identify the appropriate swarm size and the number of generations. In the second phase is Hooke-Jeeves (GPS) by subdividing the steps of the input parameters into small step with 50% and 25% of the initial defined steps for PSO phase. There are different lowest values of the objective function for different settings of the PSO, these differences are eliminated by Hooke-Jeeves phase. Hence, number of particles and number of generations should not be selected too large in order to reduce the computational time.

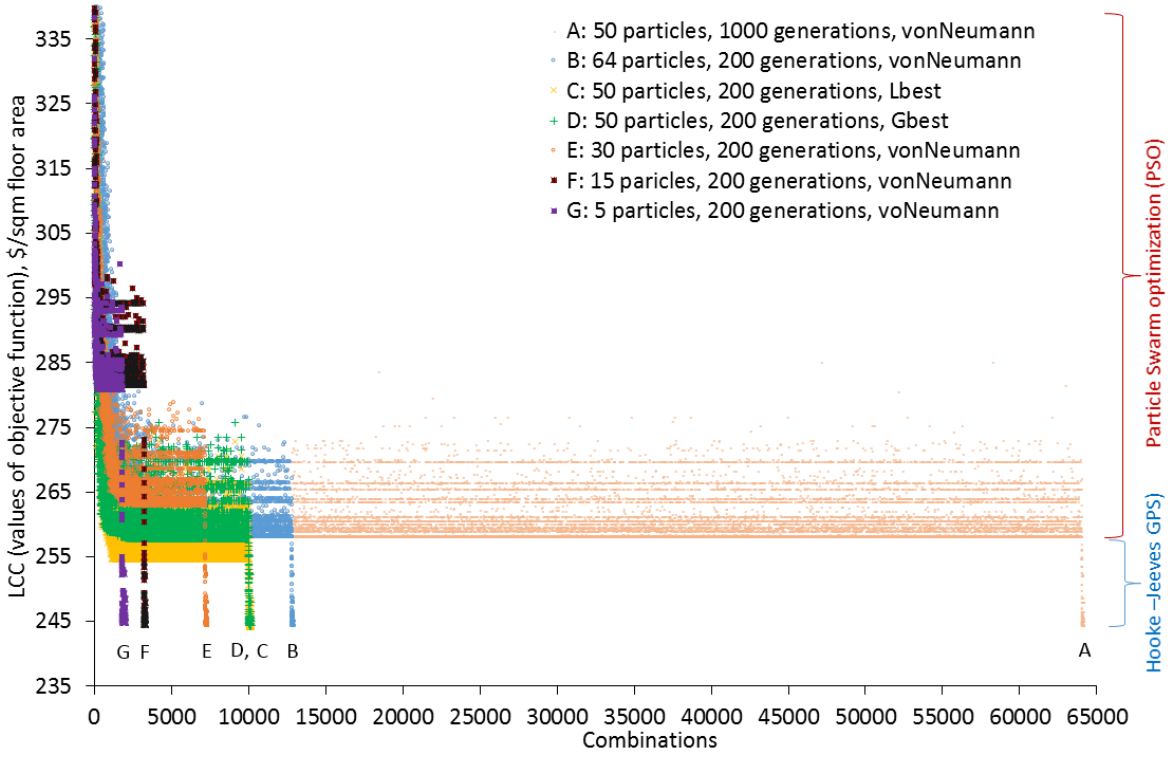

Figure 8-10 Seven trails of the optimization processes using the terraced house model.

8.2 The integration of the sub models

8.2.1 Links between models

The integrated model links many sub models in order to obtain the initial cost and operational cost of each housing type. The network to link the sub models is showed in the Figure 8-11. (1) The initial cost (IC) is calculated by the extended element method for cost control with the different material types, building and urban geometry. (2) The urban and building geometry are the Input data to obtain the wind pressure coefficient values of different orientations for each facade. (3) The dynamic occupant behaviour model simulates the sustainable user behaviour in the tropical climate. This model can adapt clothing, manage natural ventilation, switch on forced air circulation, then close windows and start the cooling system. In this step, the Fanger model for thermal comfort evaluation is applied to calculate PMV values at the time step (10 minutes) for the user behaviour model. The EnergyPlus engine is used to calculate the initial cost and operational cost including the energy cost of light, cooking, fans, cooling system and maintenance cost of the cooling system. (4) The LCC becomes the objective function of the optimisation process. For this optimization tool GenOpt searches solutions in the design space to identify the lowest LCC for a given thermal comfort level. (5) The output results of the optimisation process are visualized by Pareto front with multiple possible design alternatives based on initial cost IC

and LCC. (6) The parallel coordinate graph visualizes the pattern of all parameters in their ranges together the IC and LCC.

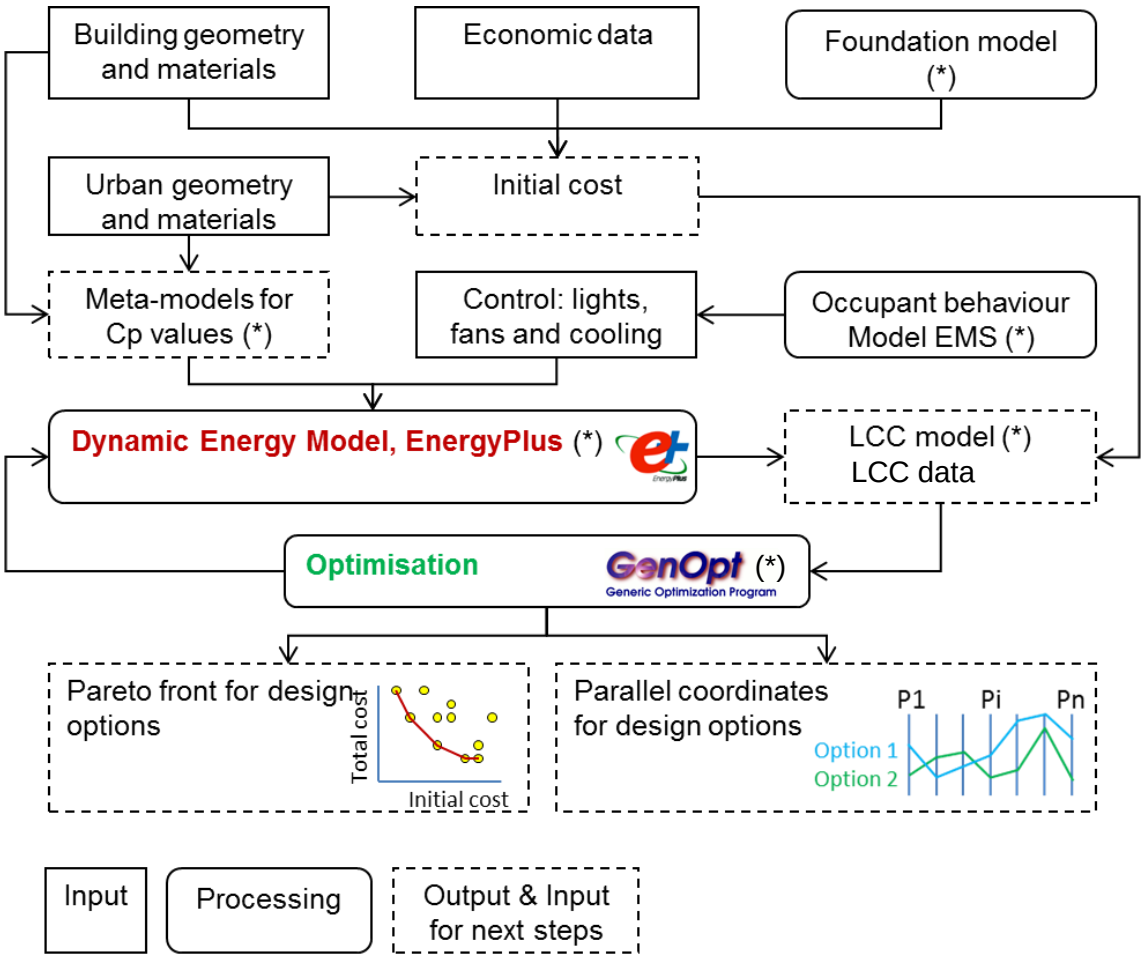

Figure 8-11 Link between different sub-models, models with "(*)" have been developed or extended by the author.

Choices have to be made for:

- A model to predict the inhabitants' thermal comfort.
- A simulation program to predict the indoor climate and the energy use for fans and cooling (if cooling is installed) (EnergyPlus) [19].
- A model describing the behaviour regarding thermal comfort. In cases of overheating, a stepwise strategy has been implemented: (1) adapt clothing, (2) control natural ventilation, (3) switch on forced air circulation and (4) close the windows and start the cooling system.

- A model by which to predict wind loads on the facades of an urban environment.
- A cost function for the investment and life cycle costs for both buildings and for infrastructure system in the urban fragment. This step includes the foundation cost model as developed in Chapter 5.
- An optimisation method by which to search for optimal solutions in the design space. GenOpt [20] was selected and coupled with EnergyPlus for the optimization process.
- A graphical post processing of the simulation results so that they can support to the designers and allow them to combine the quantitative results with aspects that are less easy to be quantified.

8.2.2 Optimization algorithm setting

Details of PSO algorithm are explained more detail in the GenOpt manual. The settings proposed by [14] [15] [16] were tested through trials. The settings of the algorithm was almost by default. A population size of 30 is large enough to allow the search to process from the first generation, which results in acceptable optimization time, 6 to 18 hours with Del Precision T7500 computer: 8 cores 32 GB internal memory and Windows 7. These settings provide good optimization results with both standard benchmark functions and real-world applications using EnergyPlus, as tested by Kampf, Wetter and Robinson [21]. The number of generations was fixed at 200 for all optimizations Table 8-2. Our visualisation of optimization results indicated that most optimization runs reached convergence after around 170 –190 generations.

Table 8-2 Setting in the Command File of the GenOpt

Setting parameters	*Setting values*
OptimizationSettings	
MaxIte	*5000*
MaxEqualResults	*200*
WriteStepNumber	*false*
Algorithm	
Main	*GPSPSOCCHJ;*
NeighborhoodTopology	*vonNeumann*
NeighborhoodSize	*5*
NumberOfParticle	*30*
NumberOfGeneration	*200*
Seed	*1*
CognitiveAcceleration	*2.8*
SocialAcceleration	*1.3*
MaxVelocityGainContinuous	*0.5*
MaxVelocityDiscrete	*4*

ConstrictionGain	*0.5*
MeshSizeDivider	*2*
InitialMeshSizeExponent	*0*
MeshSizeExponentIncrement	*1*
NumberOfStepReduction	*4*

8.2.3 Optimization process

The optimization process can be designed in various ways, through methods, input parameters, constraints and objective functions. For example, Evins et al. conducted their optimization in four steps [22]. (1) The number of parameters are reduced to a more manageable number by eliminating those with little impact on the objectives based on sensitivity analysis. (2) An initial optimisation was performed using all significant variables. (3) A detailed optimisation was performed for the remaining variables. (4) Results were also examined graphically via graphical output.

This study divides the optimization process into three stages, including a pre-processing stage, an optimization stage and a post processing stage. In the pre-processing stage, the optimization problem is formulated by using knowledge of mathematical optimization. The next stage, ranges of design variables and objective functions are then selected for models. For the models and equilibrium should be searched, between models which are too simple or too complicated, in order to prevent the risk to long computational time and inaccurate modelling of building phenomena [23].

The TNO Cp-Generator, CpCal are used to create a set of regression formulas for the wind pressure coefficient based on crucial parameters of building and urban form levels. These formulas of the wind pressure coefficient were explained in Chapter 7. The regression formula of the foundation cost was explained in Chapter 5. All the selected input parameters were defined by their ranges. This process is done in the "***Command file***" of GenOpt. Then the input file is constructed and used to run the simulations in EnergyPlus engine.

In the preliminary testing stage of the optimization, errors during the optimization may occur due to errors in EnergyPlus's simulation and GenOpt. These errors can be detected by monitoring the optimization stage. If the Command file is too long, it should be subdivided into smaller files for testing before combining them into a final file.

In the post processing stage, the optimization results are visualized via the parallel coordinate representation to identify values of design parameters that can be further selected on the Pareto front. The scatter plot is combined with the parallel coordinate plot to understand the sensitivity of some parameters, as illustrated further in the text.

8.3 A graphical post processing of the simulation results

8.3.1 Pareto front in case of life cycle cost and initial cost

The Pareto front concept was illustrated in Chapter 6, for the optimization of a problem which has two objectives: IC (initial cost) and LCC (life cycle cost). Each solution considered is represented by a dot on the graph Figure 8-12. Each possible solution, right and or above another solution, is not interesting since initial and/or life cycle cost are higher, e.g. Option A is better than option F because IC (A) < IC (F) and LCC (A) < LCC (F). Option A and option D possess equal LCC (LCC (A) = LCC (D)), but the initial cost of option D is higher than that of option A. Therefore, option A is superior to option D.

When the same reasoning is followed for all of the options, the combinations situated on the dotted line are the subset of the Pareto front. The Pareto front becomes a surface in cases which have three objectives. If the budget allows to pay for option A, then one will never select option B because the LCC decrease per extra investment, from C to A, is much higher than from C to B.

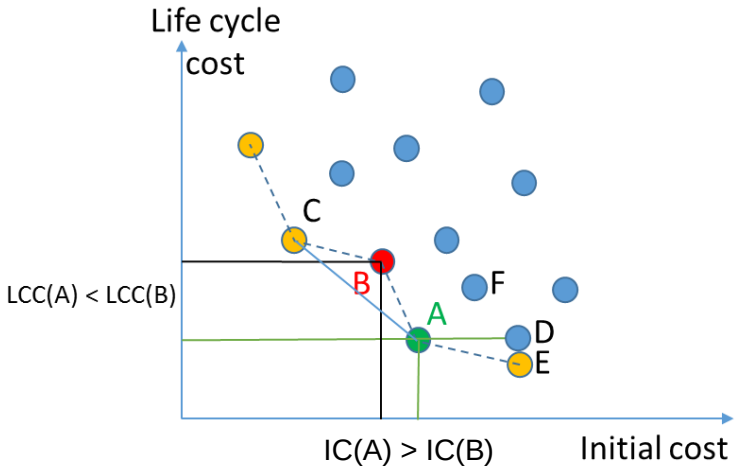

Figure 8-12 Pareto set for the maximization of quality and for the minimization of costs.

8.3.2 Parallel Coordinates

This graphical representation is helpful to communicating the results to designers in order to integrate the quantitative results with hardly quantifiable aspects. Inselberg and Dimsdale [24] introduced Parallel Coordinates, during the 1980's and early 90's, as a representation of multi-dimensional information or data. In a parallel coordinate graph, each parameter is visualized on one axis from a minimum to maximum values of the range considered (Figure 8-13). “Xdat version 2.2” is used for this study [25]. The interactive

parallel coordinate plot shows the links among multiple parameters and significant outputs such as life cycle cost and initial cost. The axes can be easily reordered, coloured and rescaled. Users can use filters to the data sets in order to visualize the effects of changing design parameters.

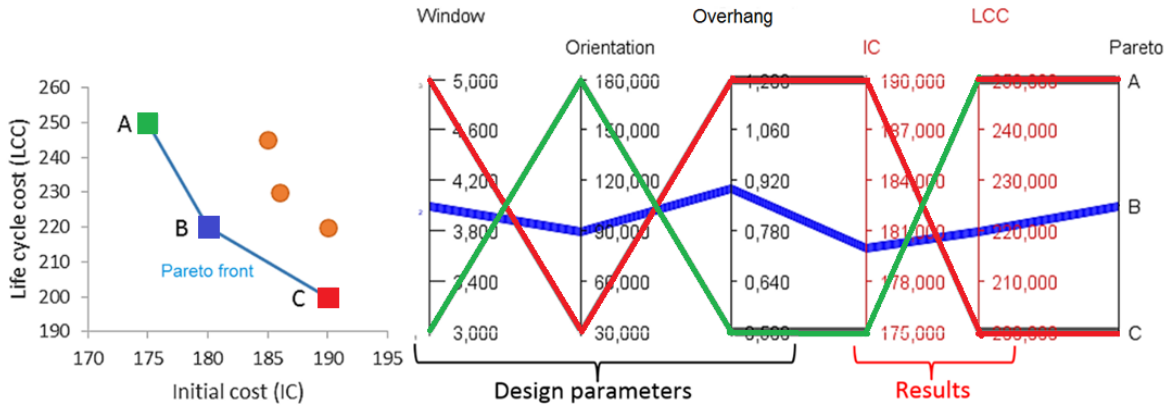

Figure 8-13 Pareto front visualization for solution and parallel coordinates.

Designers can visually read the effect on output results of changing parameters from the parallel coordinate graph. Hence, the combination of both Pareto front and parallel coordinate visualization can facilitate decision making and communication between designers, developers and clients.

8.4 Results of optimisation

8.4.1 Terraced houses: Parameters, Results and Discussions

8.4.1.1 Geometry of abstract urban and building model

Parameters with minimal and maximal values and with considered number of steps are listed in Table 8-3. Figure 8-14 visualises symbols used in the model. This design space contains $8.7*10^{11}$ design options and an EnergyPlus simulation takes about 4 to 5 minutes on each design option for this complicated model. Hence, a huge amount of time was used to calculate every option of the design space. Our model requires 18 hours to complete the 7000 simulations with Del Precision T7500 computer: 8 cores, 32 GB internal memory and Windows 7.

Table 8-1 describes material types and construction elements which are used in the optimization simulation for detached house, terraced house and apartment in the coming parts.

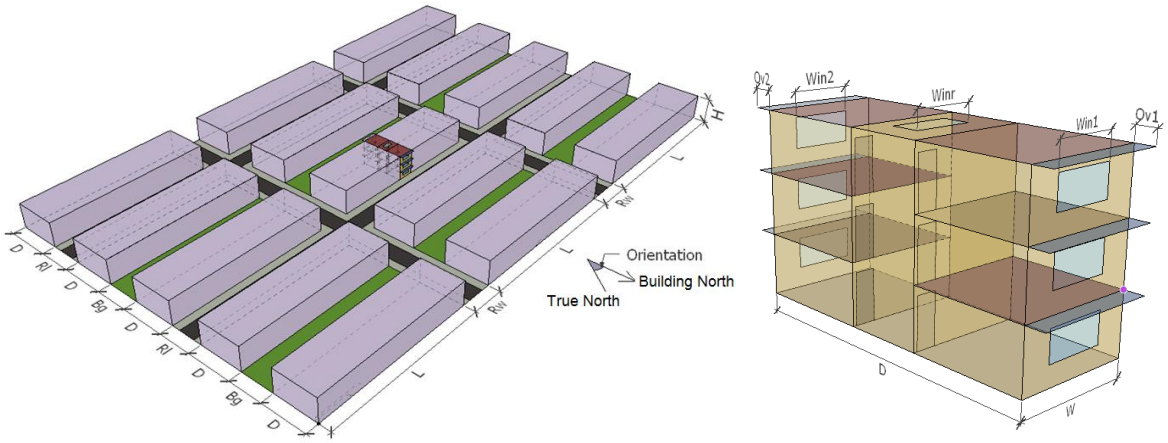

Figure 8-14 Urban form or terraced house type

Table 8. 1 Categorical design options and strategies (discrete variables).

Design parameter	Descriptions of design parameter	Name in EnergyPlus	Item cost (USD/m2)
External walls (5 types)	Mortar, hollow clay brick, mortar.	ExWall1	20
	Mortar, hollow clay brick, hollow clay brick, Mortar.	ExWall2	28
	Mortar, hollow clay brick, air gap, hollow clay brick, mortar.	ExWall3	29
	Mortar, hollow clay brick, 3 cm rock wool EW , hollow clay brick, Mortar.	ExWall4	30
	Outer brick skin, air cavity_3cm, 3 cm rock wool EW, concrete hollow blocks, gypsum plaster.	ExWall5	32.5
Internal Walls (3 types)	Mortar, brick clay, thermal mass2, mortar	InWall1	17
	Mortar, brick clay, thermal mass3, mortar	InWall2	18
	Mortar, brick clay, thermal mass4, mortar	InWall3	19
Floor	Floor tile, tile mortar	Floor	15
Ceiling	Concrete slab, ceiling mortar	Ceiling	40
Roof (4 types)	Roof asphalt, concrete roof slab, ceiling mortar	Roof1	55
	Roof asphalt, roof insulation, concrete roof slab, ceiling mortar	Roof2	64
	EPDM, PUR_FR, aluminium, sloping layer, concrete slab, gypsum plaster	Roof3	70
	Clay roof tiles, PUR_PR, wood fibre board, aluminium, air cavity 2cm, gypsum board	Roof4	72
Glazing (8 types)	Single glazed timber frame	Glazing1	43
	Clear glass 6mm	Glazing2	45
	PYR B clear glass 6mm	Glazing3	48
	Clear glass 6mm, air 6mm, clear glass 6mm	Glazing4	55
	Clear glass 4mm, air 15mm, clear glass 4mm	Glazing5	66
	REF A clear mid 6mm, argon 13mm, clear glass 6mm	Glazing6	94

	Clear glass 4mm, argon 15mm, LoE clear glass 4mm	Glazing7	115
	LoE clear glass, argon 15mm, clear glass, argon 15mm, LoE clear glass 4mm	Glazing8	135
Overhang	Tile, concrete slab, ceiling mortar	Overhang	50
Door	Door aluminium + glazing	Door	40

Table 8-3 The neighbourhood and building geometry of the terraced house.

Variable name	Parameter	Unit	Min	Max	Step
Urban patern parameters					
Rw	Road width parallel building width	m	12	24	2
Rl	Road width parallel building length	m	12	24	2
Bg	Back garden	m	2	24	2
H	Neighbour building height	m	9	36	3
Orientation	Orientation of building	degree	0°	360°	30°
Building geometry parameters					
L	Length of building	m	40	120	10
D	Depth of terraced building (row)	m	12	20	2
W	Width of terraced unit	m	5	10	1
Win1	Window1 width by 1.5 meter height	m	1	5	1
Win2	Window2 width by 1.5 meter height	m	1	5	1
Winr	Roof window width by 1.5 meter length	m	1	5	1
Ov1	Overhang depth of the front facade	m	0.5	2	0.5
Ov2	Overhang depth of the rear facade	m	0.5	2	0.5

8.4.1.2 Optimization results

Figure 8-15 shows that the results of the optimization processes and the Pareto front is generated depending upon the accepted maximal discomfort (PMV maximum 0.5, 1.0 or 1.5). Compared to the worst case generated, the optimal design presents a reduction of 43% of the LCC. This reduction mainly comes from initial land and infrastructure cost due to expensive land and the infrastructure system. On the Pareto front, the urban layout does not vary, the range of the LCC is only related to different combinations of material and building layout parameters. The aim of the optimization process is to inform designers the characteristics of design solutions that perform well.

The second phase of the optimization process using Hooke-Jeeves algorithm divides the initial steps of parameters into small steps. This approach reduces about 5% LCC and LCC of solutions on the Pareto fronts varies very small. This variation may be smaller uncertainty of the unit cost of the construction elements. It means that designers can select solutions on the Pareto fronts freely based on their experience.

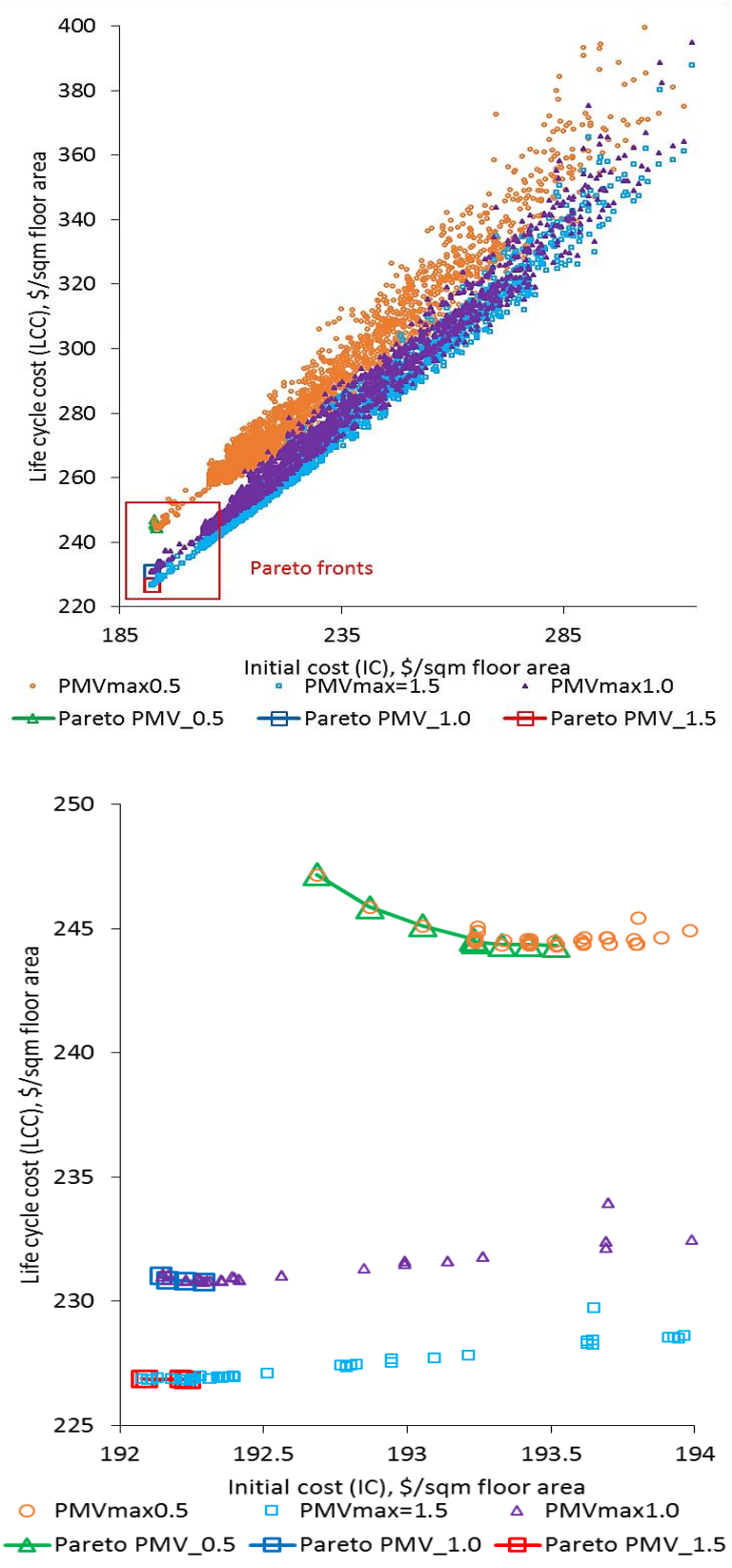

Figure 8-15 Optimization effectiveness using the particle swarm optimization and Hooke-Jeeves algorithms and Pareto front based on optimization results.

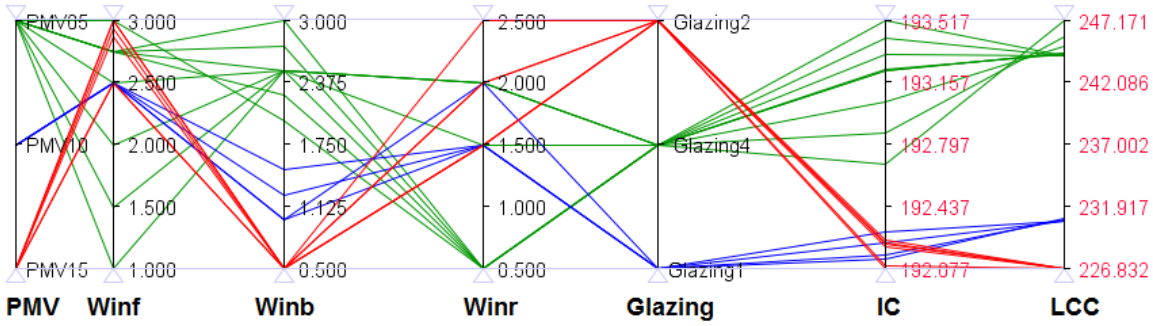

Figure 8-16 Deferent design alternatives of three thermal comfort levels (Maximum PMV = (0.5, 1.0 and 1.5)

Three clusters of points, depending on maximal acceptable discomfort, prove that more comfort requires more energy use. The different settings for maximal allowed thermal discomfort can reduce the energy use from 32% to 43% (Figure 8-17). The initial construction and infrastructure costs for three PMV values do not differ significantly, because the reductions are due to energy use for fans and cooling systems. Therefore, occupant behaviour is a crucial factor in energy saving in the hybrid HVAC and passive design approaches in the tropical climate.

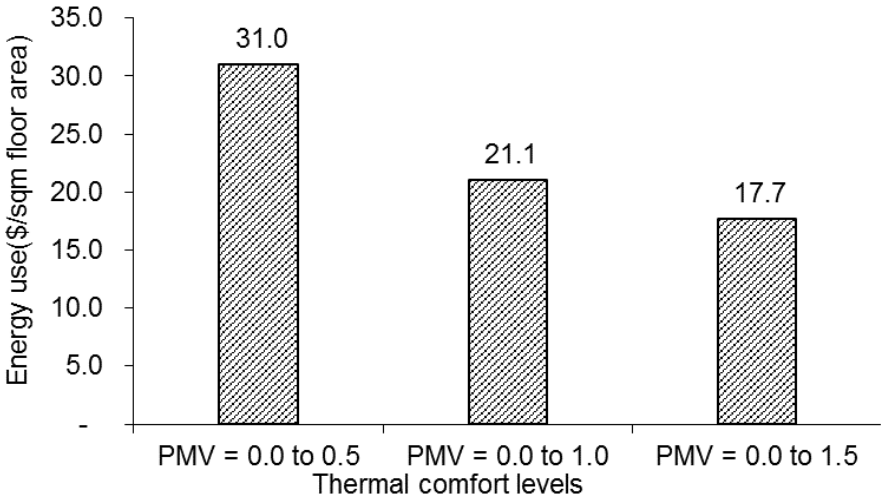

Figure 8-17 Energy use for thermal comfort requirements in case of the terraced house.

8.4.1.3 Parallel coordinates solutions on Pareto front

A Pareto front is represented graphically (top) in Figure 8-18 together with the values of the design parameters that lead to those solutions (bottom). In Figure 8-18, all the parameters are all visualized with the results on IC and on LCC, in the case of thermal

discomfort at PMV maximum 0.5. Blue polylines represent the design options on the Pareto front. For solutions on the Pareto front, several parameters fall on extreme values of the "design space": minimal road widths (Rl and Rw) and maximal values of terraced building length (L), minimal terraced unit width (W) and maximal terraced building depth (D). If design space could include the possibility of longer rows, of narrower streets or of wider units then they would have been selected. Reflecting on the definition of the limits of the parameters is an important task for designers, governments and for users.

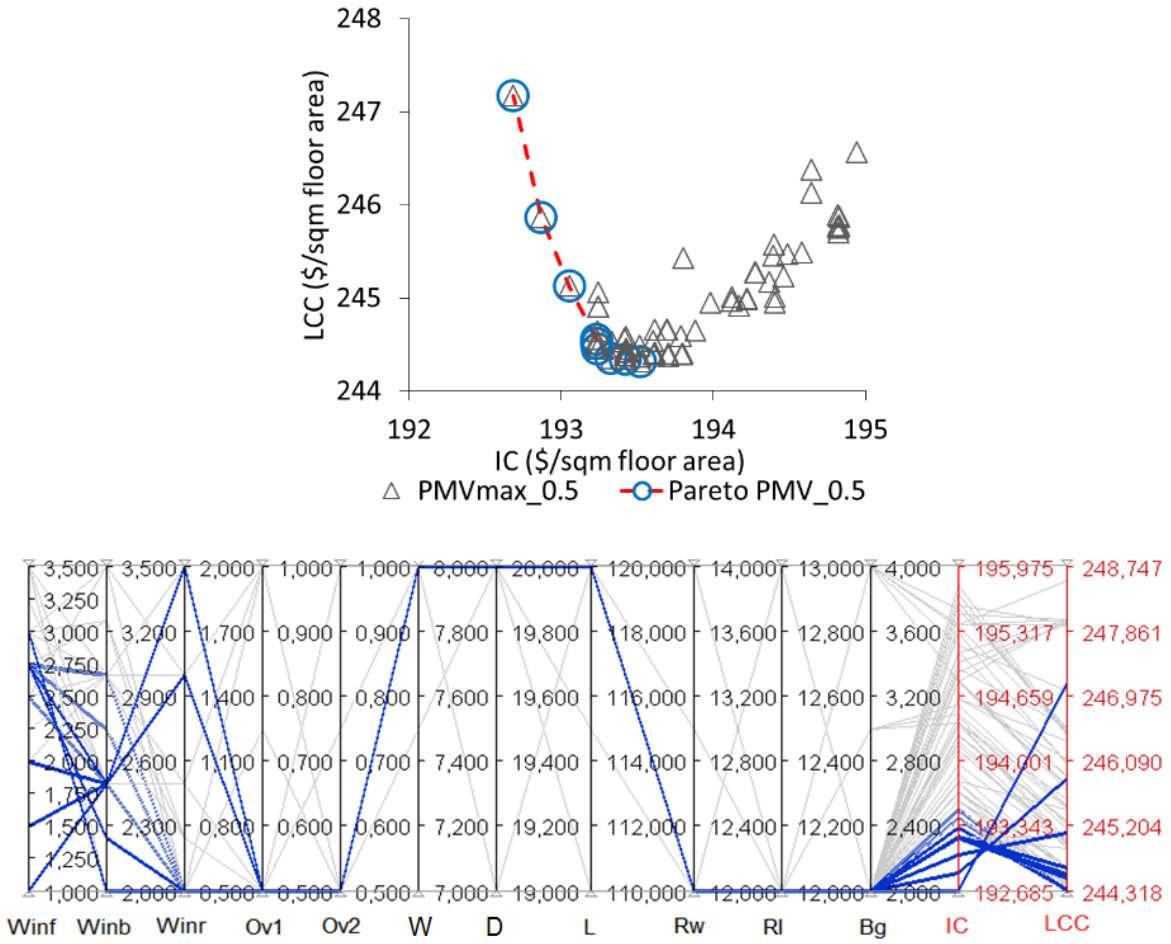

Figure 8-18 Parallel coordinates of the optimization results (with PMV maximum 0.5) balancing IC (Initial construction Cost) and LCC (Life Cycle Cost).

On the Pareto front, the results of several parameters of some solutions are too small for real solutions. In this case designers should consider other criteria such as quality of view, local culture and special requirement for daylight to adjust the size of those parameters. In Vietnam and other Asia countries which effected feng shui concept in architecture, size of doors or windows may be selected by trade-off between simulation results and the fen shui roles.

8.4.1.4 Patterns of the dynamic occupant behaviour of the terraced house

In the dynamic occupant behaviour model, the windows are defined to open when the indoor air temperature is higher than the outdoor air temperature. The windows are controlled individually for each room. By applying this setting, the occupants do not open windows to get hot air from outdoor for most of the day time Figure 8-19. In the living room, the ventilation is on for almost of the time. Occupants in the bed rooms, the natural ventilation is applied some hours for the night time. The results show that the windows or doors should be closed during the noon time and allow a minimum ventilation to keep enough fresh air for users. By doing that way, the heat gain is minimized via the hot air from the outside.

According to the energy use for the bedroom, the average of the cooling and fan energy indicates that the occupants switch on the fan and then the cooling system for some hours from 17:30 to 22:00 in the living room and from 23:00 to 6:00, Figure 8-20. The hot period from March to June is requirement the cooling. The rest time of year, the fans are used high frequently because the fans are enough to reach the thermal comfort condition. Therefore, the occupant behaviour varies during the year in order to minimize the energy use for thermal comfort.

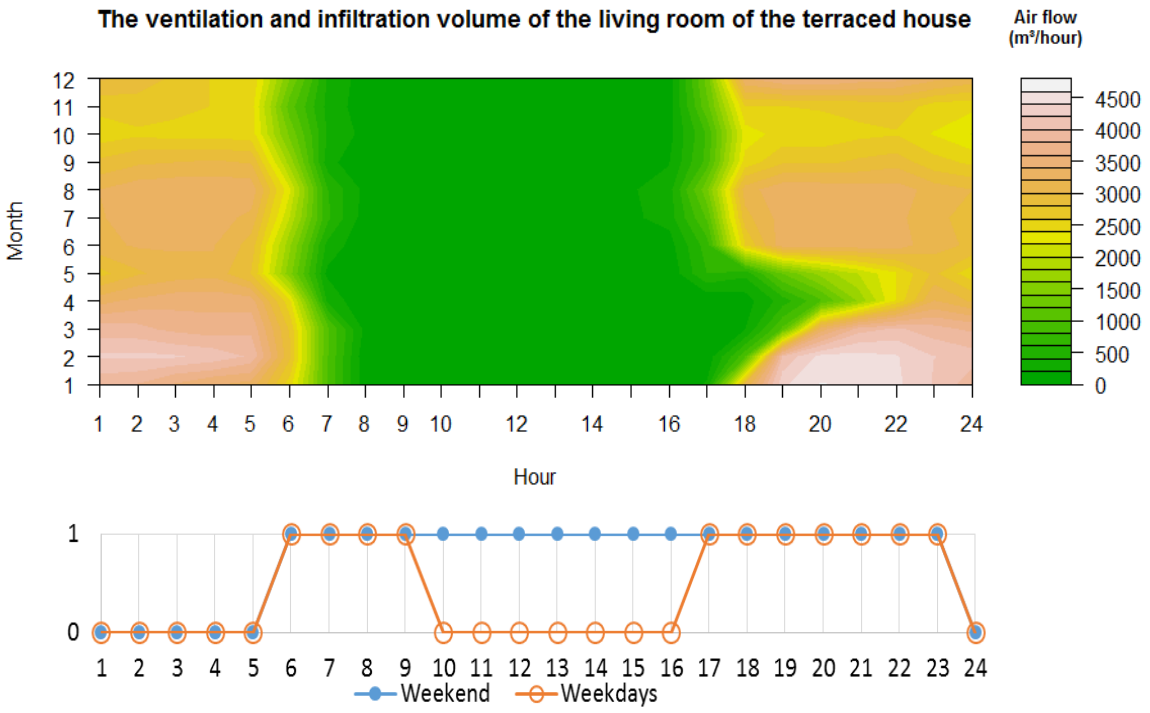

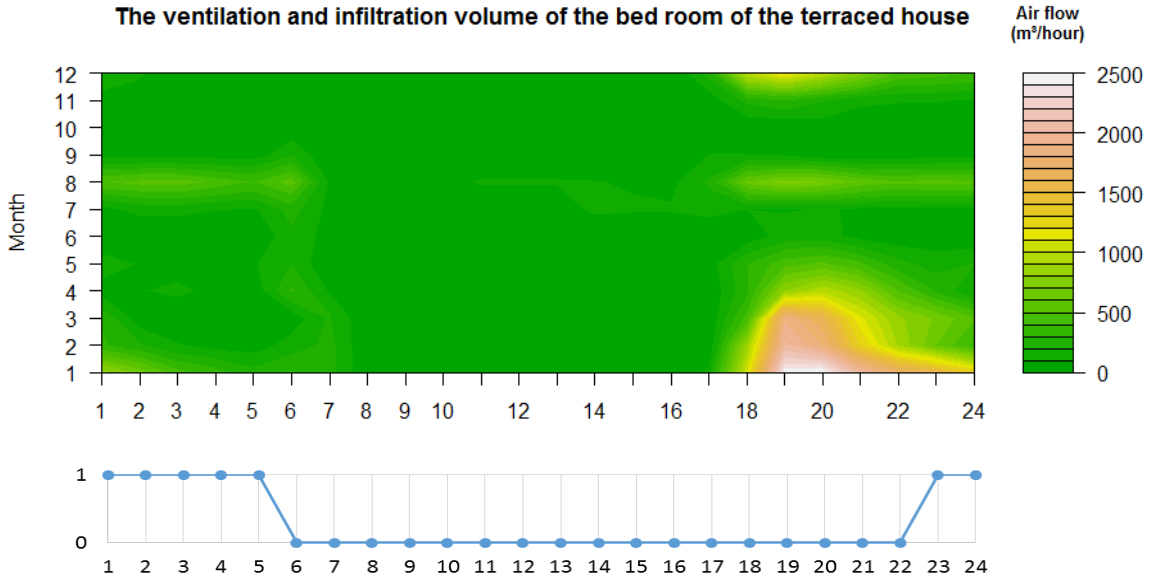

Figure 8-19 The ventilation and infiltration volume of the living room and the bed room of the terraced house.

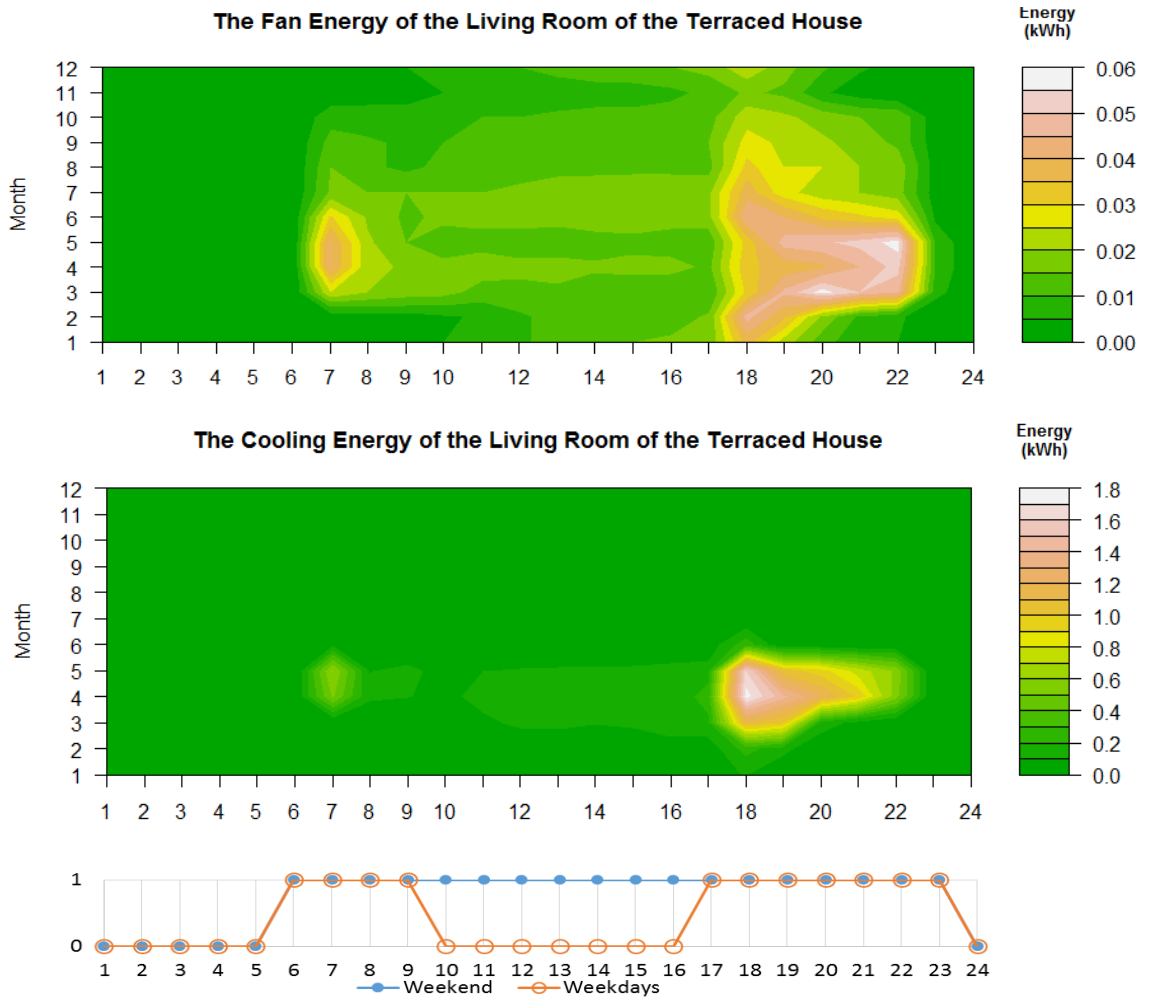

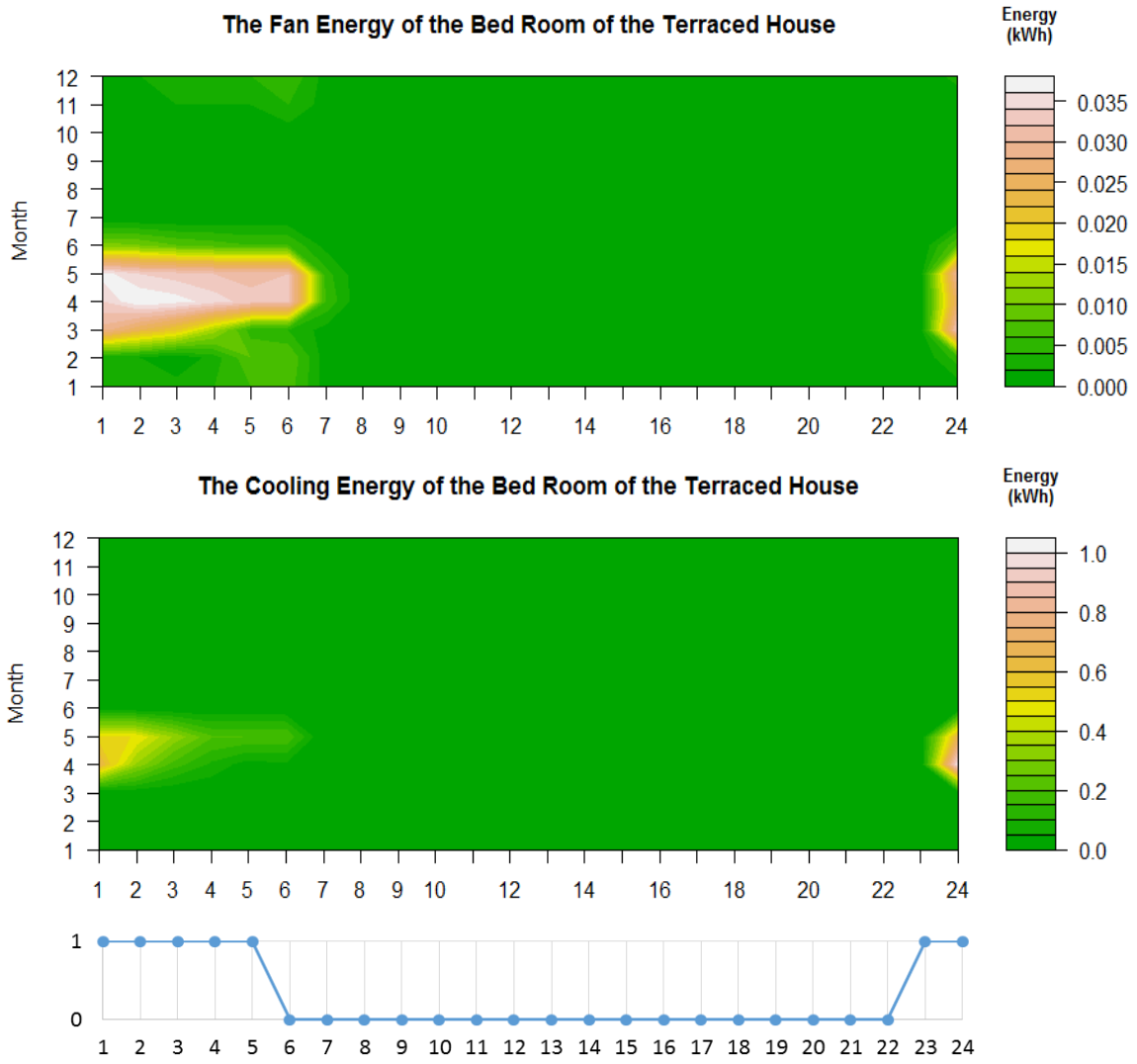

Figure 8-20 The energy use related to occupant behaviour during the year of the terraced house. User behaviour schedules as tool to be included in the optimization

Users strive to avoid discomfort. Their interventions are described by 'dynamic schedules' which the windows, fans and cooling system are controlled based on the thermal comfort constraints. The effect that they have upon the indoor air temperature, compared to the outdoor temperature, is visualized in Figure 8-20. The reduction of indoor air temperature in the living room is achieved because the windows and doors are closed when the inside temperature is lower than the temperature outside. This strategy reduces peak cooling load during the hottest period of the day and allows the cooling air from outside for the rest of the day. This dynamic natural ventilation is more efficient than full-day ventilation or night-only ventilation, analysed in other studies that strive to maximize the benefit of natural ventilation [32] [1].

8.4.1.5 Discussions

On material parameters: specific technical solutions for materials are defined in Table 8-1 in detail. The cheapest roof and external wall are selected for the design options on the Pareto front. Glazing4 has been selected for all design options on the Pareto front in case of PMV, maximum 0.5, because the double glazing reduces the heat loss during the cooling period. In the cases of a PMV maximum 1.0 and 1.5, the single glass 6mm (Glazing1 and Glazing2) are selected since cooling is limited. For both internal and external walls (InWall1 and ExWall1), the thermal mass effect is not important in a climate that has a small temperature range between its minimum and maximum because in the Figure 8-21 shows that the inside temperature peak delays only two hours comparing to outside temperature peak.

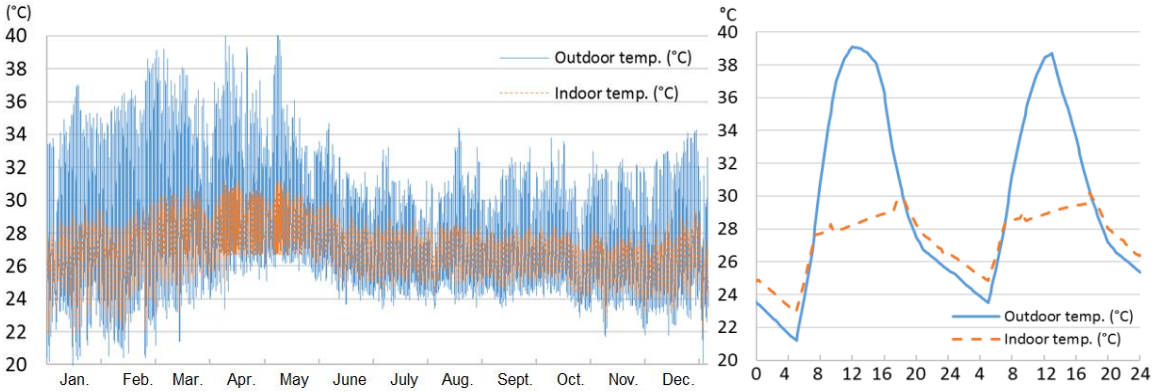

Figure 8-21 The indoor and outdoor temperature of a living room for one year and two days (2-3 March).

On building layout: the cost per m² of floor reaches a minimum when the width of a terraced unit reaches the value of 8m, since initial costs for street and infrastructure is a dominant factor and those costs are spread over more m² floor if the width is reduced for the same floor area. The minimal overhang depth of 0.5m proves to be enough to block strong direct solar beams. The window sizes affect solar gains as well as ventilation losses and the relation with the cost for comfort is not straight forward. The roof window can improve ventilation, but it can lead to important solar gains. The reflective glazing system has not been selected because of the high initial cost.

The **urban layout** influences the initial cost of both land and infrastructure, as well as energy use. The neighbouring buildings define the micro climate. They have an impact upon the natural ventilation (via wind pressure coefficients) and upon solar irradiation (due to shadows and reflectance). The front facade that faces to the South can capture higher wind

speeds and allow less solar gains due to the provided overhang. The following extreme values of the defined design space are on the Pareto-front: minimal street width, maximal block length, maximal building depth, minimal back garden) (Table 8-4). This proves that the definition of the design space is extremely important. Defining those limits is a challenge for designers, public authorities (in defining all kinds of regulations) and inhabitants (in expressing their requirements on views, openness, green space, etc.).

Table 8-4 Lowest LCC for the neighbourhood of the terraced house, based on optimization process.

Parameter	**Variable name**	**Unit**	Optimal value
Road width parallel building width	Rw	m	12
Road width parallel building length	Rl	m	12
Back garden	Bg	m	2
Height of all neighbour building	H	m	9.05
Orientation of front facade of building	Orientation	degree	180°
Length of building	L	m	120
Width of terraced building (row)	W	m	20
Width of terraced unit	Bw	m	8.0
Window1 width by 1.5 meter height	Ww1	m	2.75
Window2 width by 1.5 meter height	Ww2	m	3.0
Roof window width by 1.5 meter length	Wwr	m	0.5
Overhang depth of the front facade	Ov1	m	0.5
Overhang depth of the rear facade	Ov2	m	0.5

8.4.1.6 Sensitivity of parameters of terraced house

In the case of terraced house, 17 variables have been taken into consideration in the optimization process and in the sensitivity analyses. The sensitivity analysis was performed by using the results of 2000 random design options. The Standardized Regression Coefficient (SRC) of the input parameters of the terraced houses were sorted from the largest to the smallest, as shown in Figure 8-22 and Figure 8-23. The higher the absolute SRC is, the more influential the parameter is in the considered ranges. The positive or negative sign of the SRC indicates the proportional or inverse relationship between a variable and the LCC or energy cost (EC).

The variables were categorized into two groups, based on the sensitivity rankings of the SRC method: the highly influential group (absolute value of SRC > 0.1) and the less influential group (absolute value of SRC < 0.1). The Figure 8-22 shows that the absolute value of SRC of building width, terraced unit width, road width parallel the building length, back garden, building length, road width parallel the building width and type of external walls are larger than 0.1. These parameters are the most influential parameters for LCC. The

parameters related to infrastructure and land cost are high sensitive because their initial costs represent high percentage of the total initial cost.

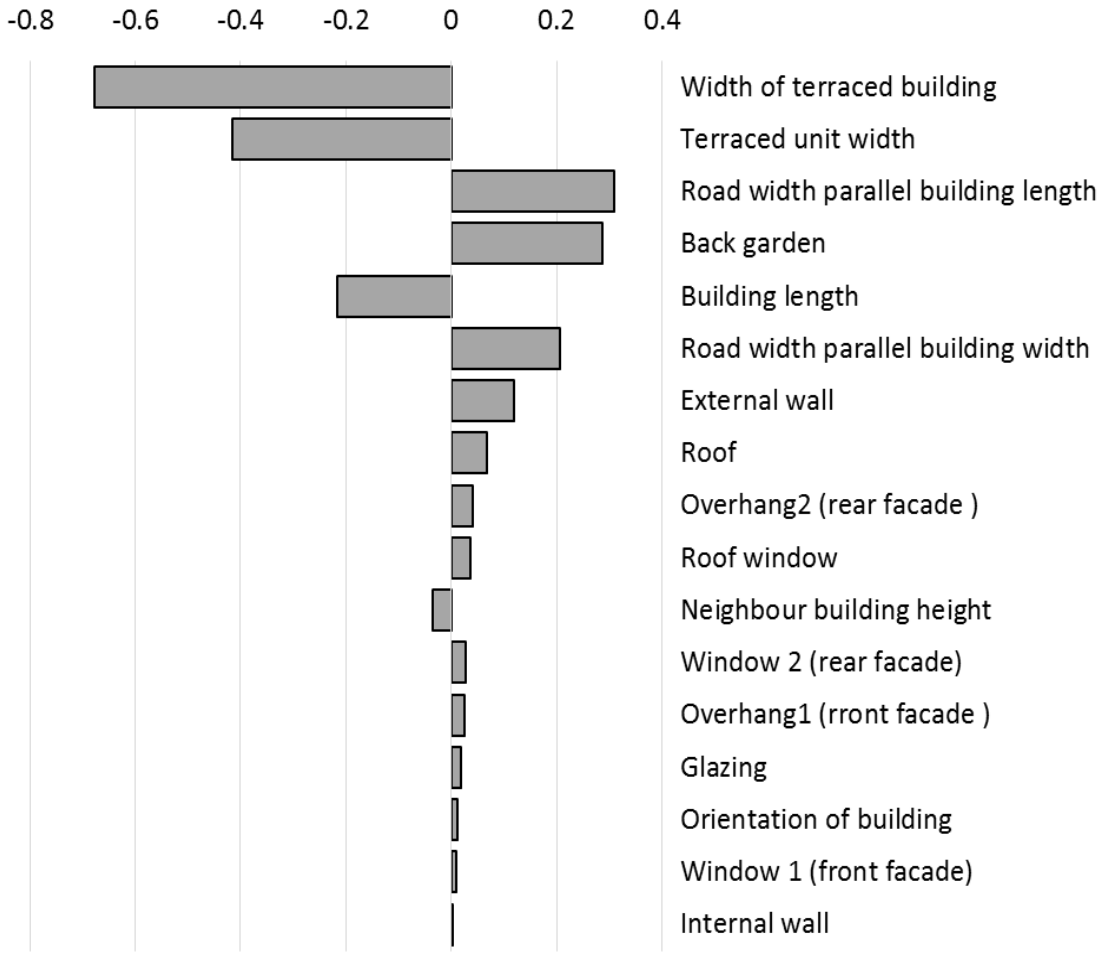

Figure 8-22 Sensitivity ranking via SRC – LCC of terraced house.

The Figure 8-23 shows that the absolute values of SRC larger than 0.1 of the terraced unit width are: width of terraced building, glazing, neighbour building height, and roof window. The parameters related to direct and indirect solar gain and natural ventilation. In some cases, if the road widths and the back garden are designed based on regulations or norms of cities, the glazing types, roof window should be considered to reduce the energy use. Moreover, the external wall, front overhangs and front windows are also significant to minimize the energy use.

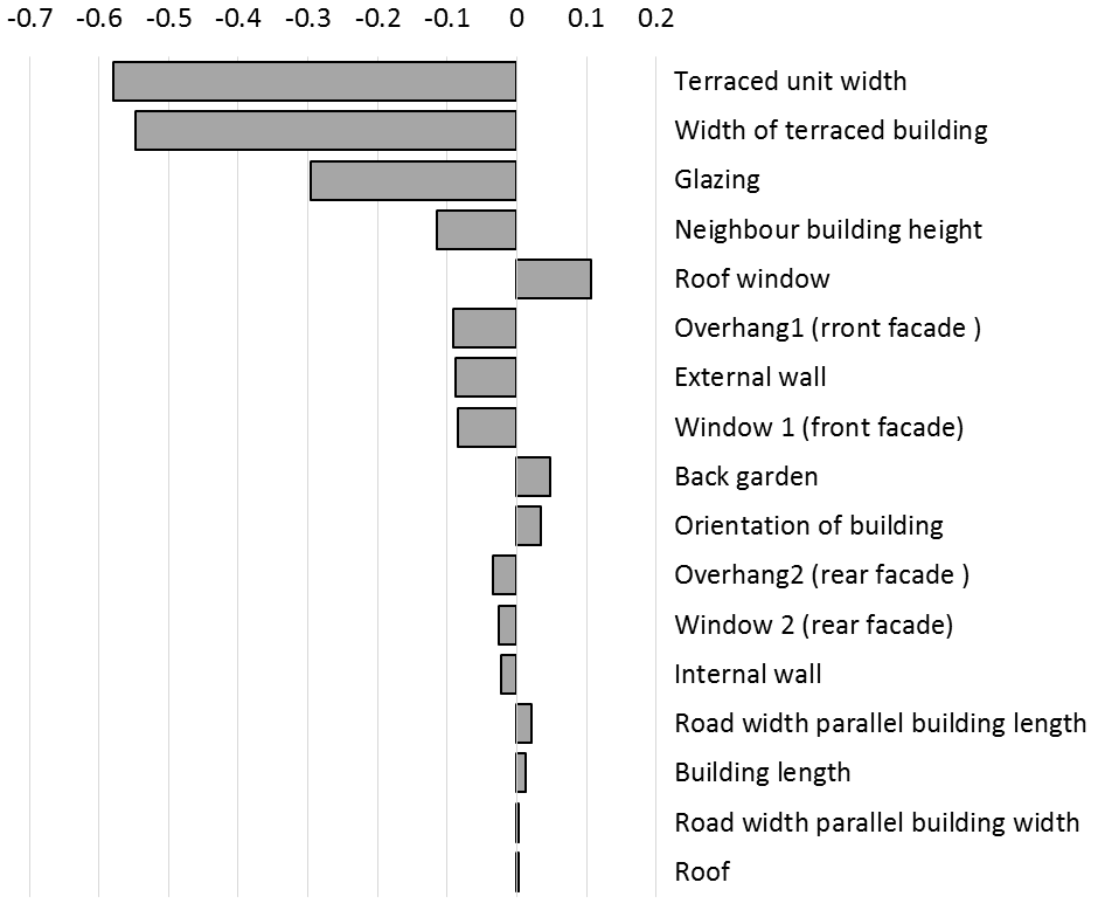

Figure 8-23 Sensitivity ranking via SRC – EC of terraced house.

8.4.2 Detached house: Parameters, results and discussions

8.4.2.1 Geometry and urban configuration

The geometries for the optimization process of the building and urban layout are visualized in Figure 8-24 and Table 8-5. The front facade of the building faces to the North orientation. When the orientation is changed during optimization the whole urban area is also rotated at the same time. The wind pressure coefficient model considers a larger urban area. The simplified geometries need to consider solar gain with impaction of the neighbouring buildings. The removed surfaces of the neighbouring building (see in Figure 8-24) do not generate the shadow on the studied building. Therefore, removing the surfaces can simplify the codes of the input definition file of EnergyPlus and the command file of GenOpt.

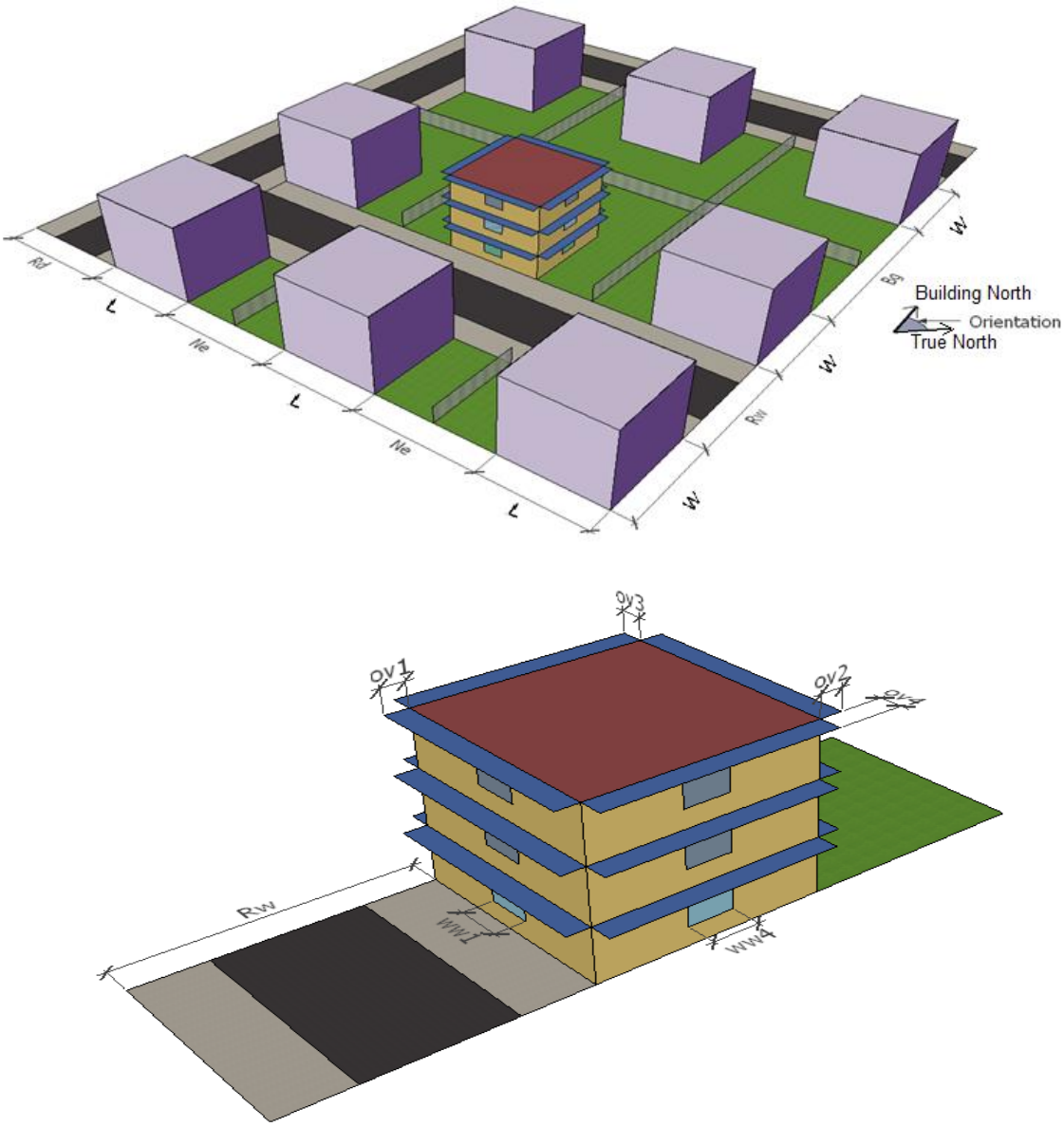

Figure 8-24 Geometry of detached houses and urban configuration.

Table 8-5 The urban and building geometry of the detached house.

Variable name	Parameter	Unit	Min	Max	Step
Urban pattern parameters					
Rw	Road width parallel building width	m	12	24	2
Rd	Road width parallel building depth	m	12	24	2
Bg	Back garden	m	20	30	2
Ne	Neighbour gap	m	12	20	2
Nbuild	Number of detached building a row	Building	10	50	10
Orientation	Orientation of building	degree	0°	360°	30°

Building geometry parameters					
L	Length of building	m	8	16	2
W	Width of building	m	6	12	2
ww1	Window1 width by 1.5 meter height of the front facade	m	1	5	1
ww2	Window2 width by 1.5 meter height of the rear facade	m	1	5	1
ww3	Window3 width by 1.5 meter height of the left facade	m	1	5	1
ww4	Window4 width by 1.5 meter height of the right facade	m	1	5	1
ov1	Overhang depth of the front facade	m	0.5	2	0.5
ov2	Overhang depth of the rear facade	m	0.5	2	0.5
ov3	Overhang depth of the left facade	m	0.5	2	0.5
ov4	Overhang depth of the right facade	m	0.5	2	0.5

8.4.2.2 Optimization

The minimal life cycle cost (including land cost and infrastructure cost) based on optimisation is reached for the following parameters (Table 8-6 and Table 8-7). Three parameters reach the maximum values of their designing ranges (length and width of the building and number of detached buildings per row) and six parameters (road width parallel to the building width and the building length, back gardens, neighbourhood gap and overhangs of both South and North orientations) reach their minimum values Table 8-6.

Table 8-6 Optimization result for the neighbourhood and building geometry of the detached house.

Variable name	Parameter	Unit	Optimal value
Urban pattern parameters			
Rw	Road width parallel building width	m	12
Rl	Road width parallel building length	m	12
Sb	Back garden	m	20
Ne	Neighbour gap	m	12
Nbuild	Number of detached building a row	Building	50
Orientation	Orientation of building	degree	0°(North)
Building geometry parameters			
L	Length of building	m	16
W	Width of building	m	12
w1	Window1 width by 1.5 meter height	m	3.75
ww2	Window2 width by 1.5 meter height	m	3.0
ww3	Window3 width by 1.5 meter height	m	4.0
ww4	Window4 width by 1.5 meter height	m	1.0
ov1	Overhang depth of the front facade	m	0.5
ov2	Overhang depth of the rear facade	m	0.5
ov3	Overhang depth of the left facade	m	1.875
ov4	Overhang depth of the right facade	m	1.875

The construction elements for optimal solutions are similar to in today's building practice (Table 8-7).

Table 8-7 Optimization results for the construction elements of detached house

Elements	Material layers
Roof	6mm asphalt; roof insulation, 10cm reinforced concrete; 1.5 cm ceiling mortar
External wall	1.5cm mortar; 10cm clay brick; 1.5cm mortar
Glazing	Clear glass 6mm

The Pareto fronts for the three predicted mean vote (PMV) ranges (0.0 to 0.5, 0.0 to 1.0, 0.0 to 1.5) values for the detached house provide different design alternatives that can be selected by designers or developers. The Pareto front covers a small range of LCC, EC. The small different values also come from the changing window and shading device sizes (Figure 8-25).

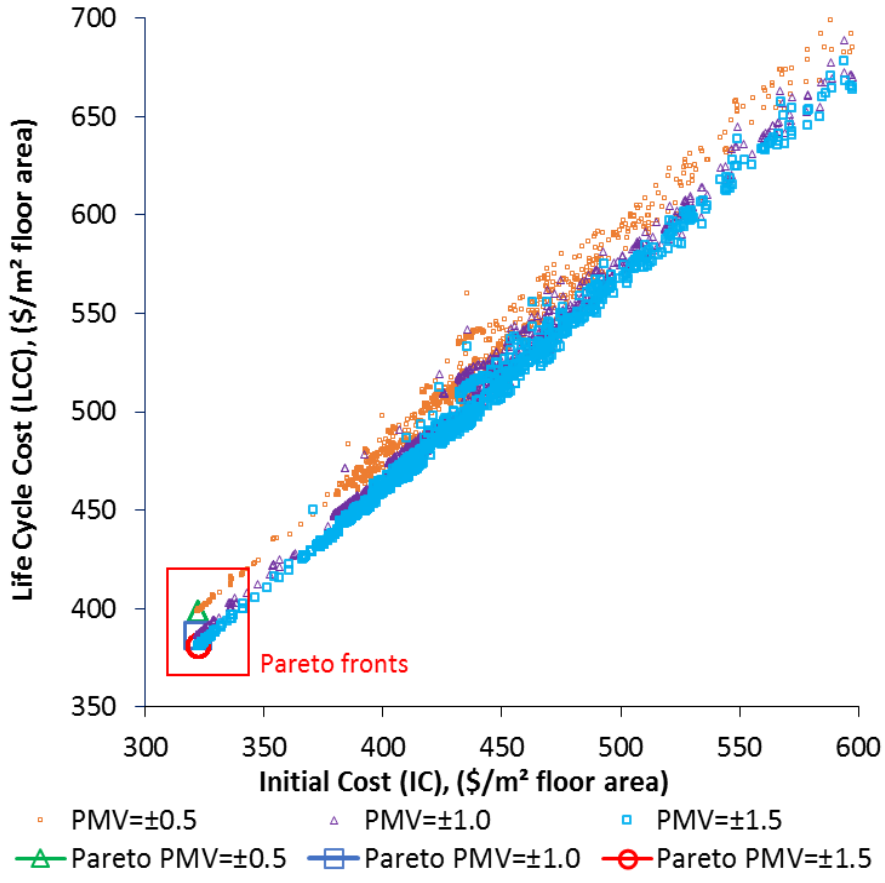

a)

b)

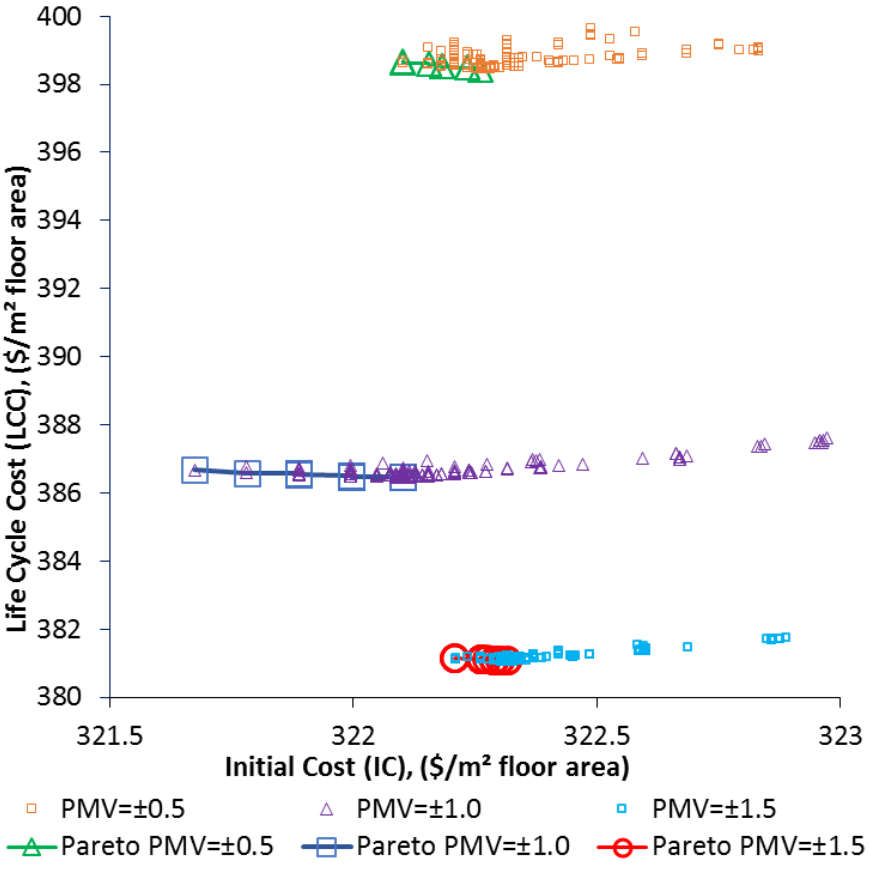

c)

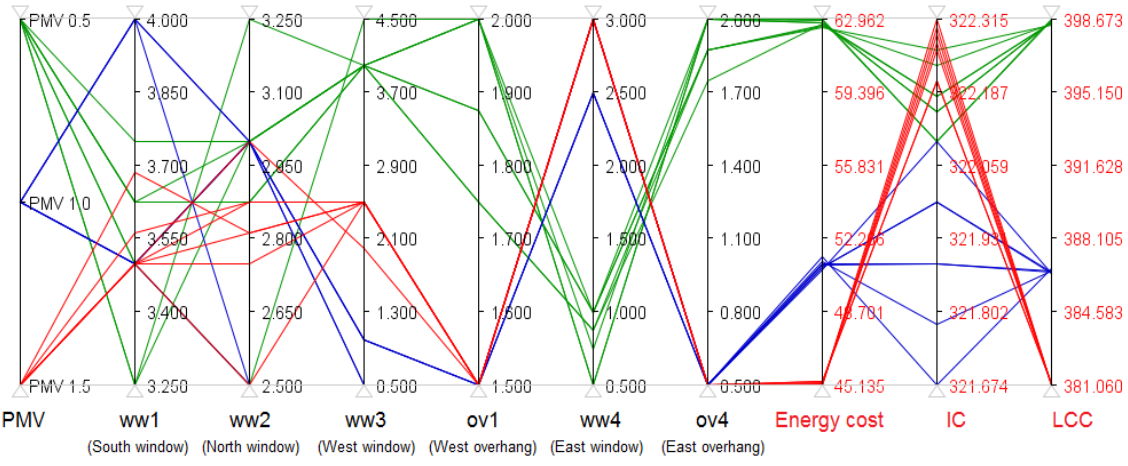

Figure 8-25 Detached houses, initial construction and land cost versus life cycle cost and land cost.

The reduction of the thermal comfort, PMV value ranges, from (0.0 to 0.5) to (0.0 to 1.0) and (0.0 to 1.5) can reduce the energy use from 18.8% to 27.9% Figure 8-26. So the

occupant behaviour is a crucial factor in energy saving in detached houses. The construction and infrastructure cost are also reduced which means that reductions cut energy use for fans and cooling systems, but only by reducing the initial cost by 1.8% to 2.1% of their initial cost via changing building geometry, Figure 8-27.

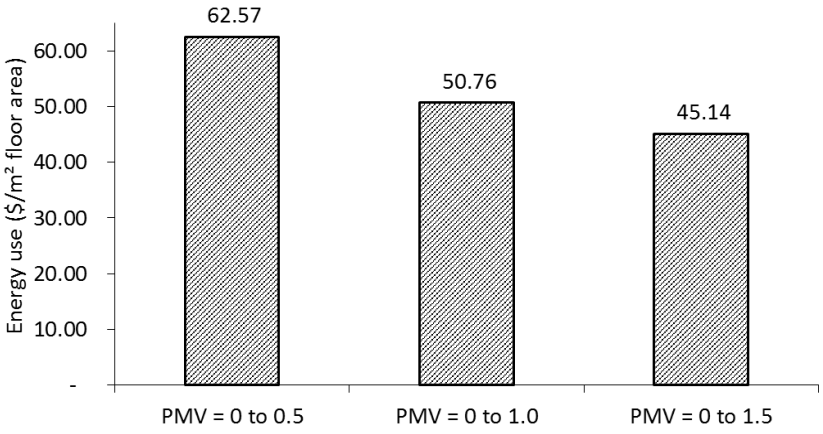

Figure 8-26 Energy saving for reducing thermal comfort ranges of detached houses, for 60 year period.

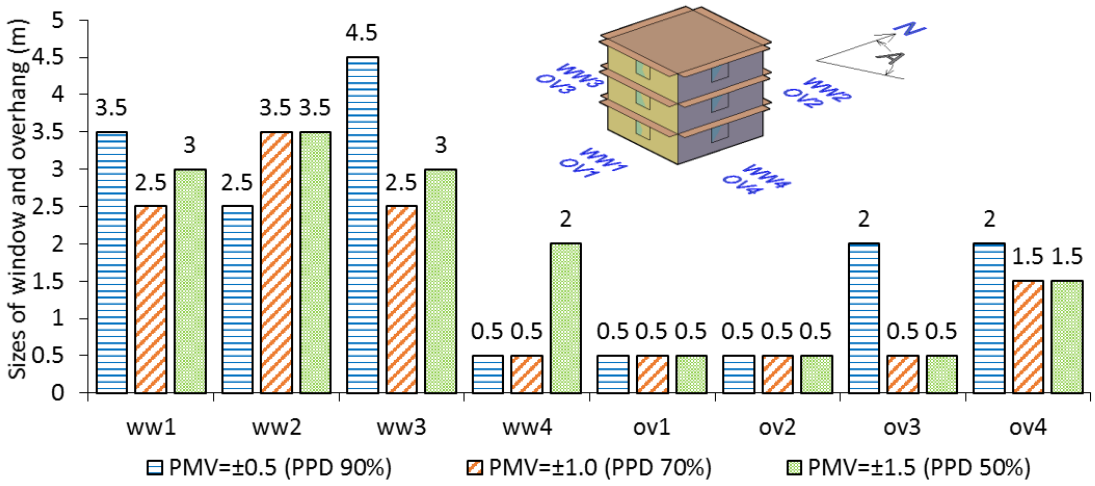

Figure 8-27 Window and overhang sizes of detached house of three PMV ranges. Their orientations are 0° for PMV=±0.5 and 300°.

8.4.2.3 Parallel coordinates solutions on Pareto front

The Pareto front is represented graphically (top) in Figure 8-28 together with the values of the design parameters of those solutions (bottom). For solutions on the Pareto front, several parameters fall on extreme values of the “design space”: minimal road widths

(RI and Rw) and maximal values of terraced building length (L), maximum length of the detached building (L = 16m) and maximal detached building depth (W = 12m). The variation of IC and LCC of the options on the Pareto front is the changes of the window size, the East and the West overhangs. Notably, the results will be changed for different PMV levels. Therefore, designers have other Pareto fronts for different thermal comfort settings.

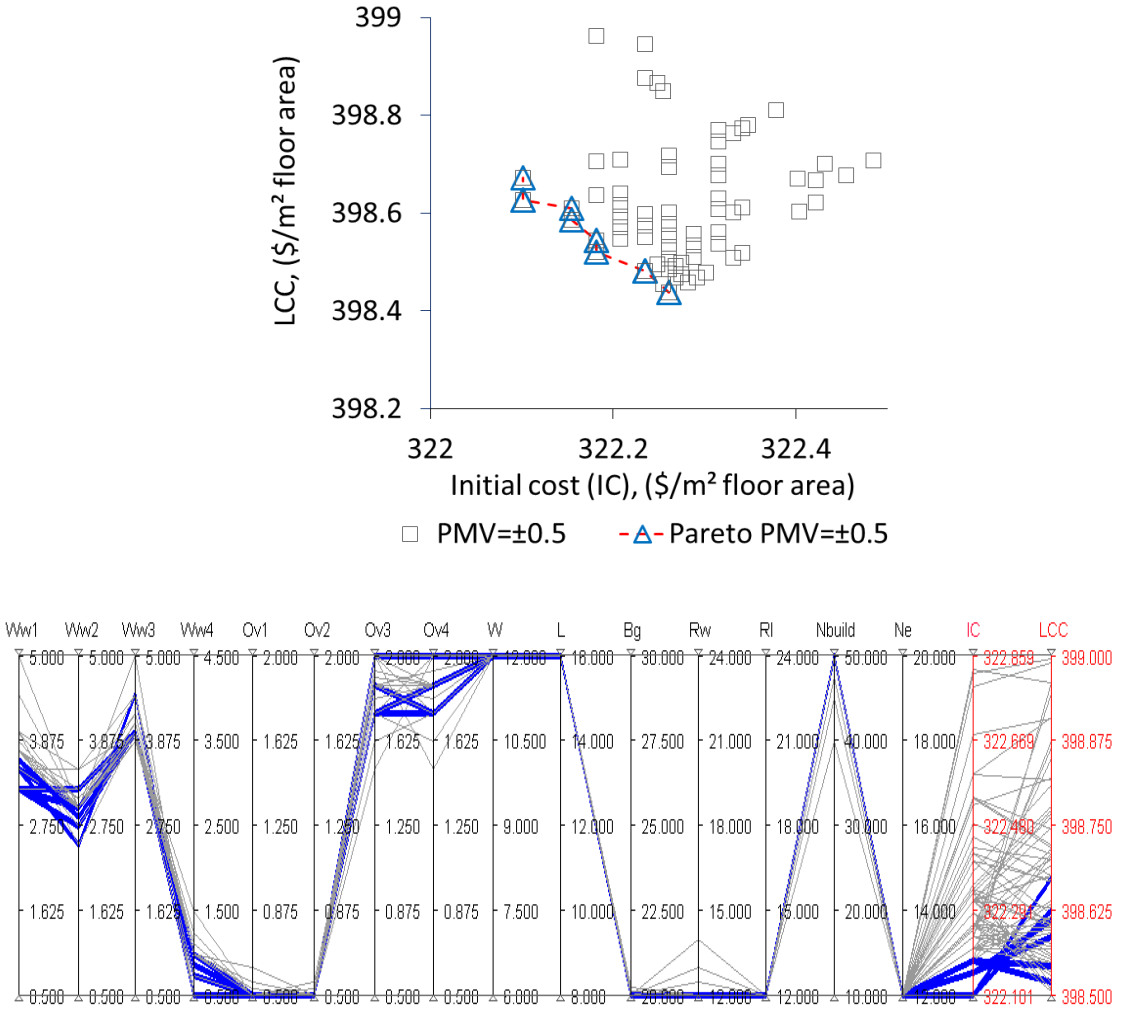

*Figure 8-28 the Pareto front and the p*arallel coordinate of the optimization results (with PMV maximum 0.5) balancing IC (Initial construction Cost) and LCC (Life Cycle Cost) of the detached house.

8.4.2.4 Patterns of the dynamic occupant behaviour of the detached house

The Figure 8-29 shows the average infiltration volume per hour of the detached house. The results indicate that duirng the night is the best period for the ventilation because the outdoor temperature is lower than the indoor temperature.

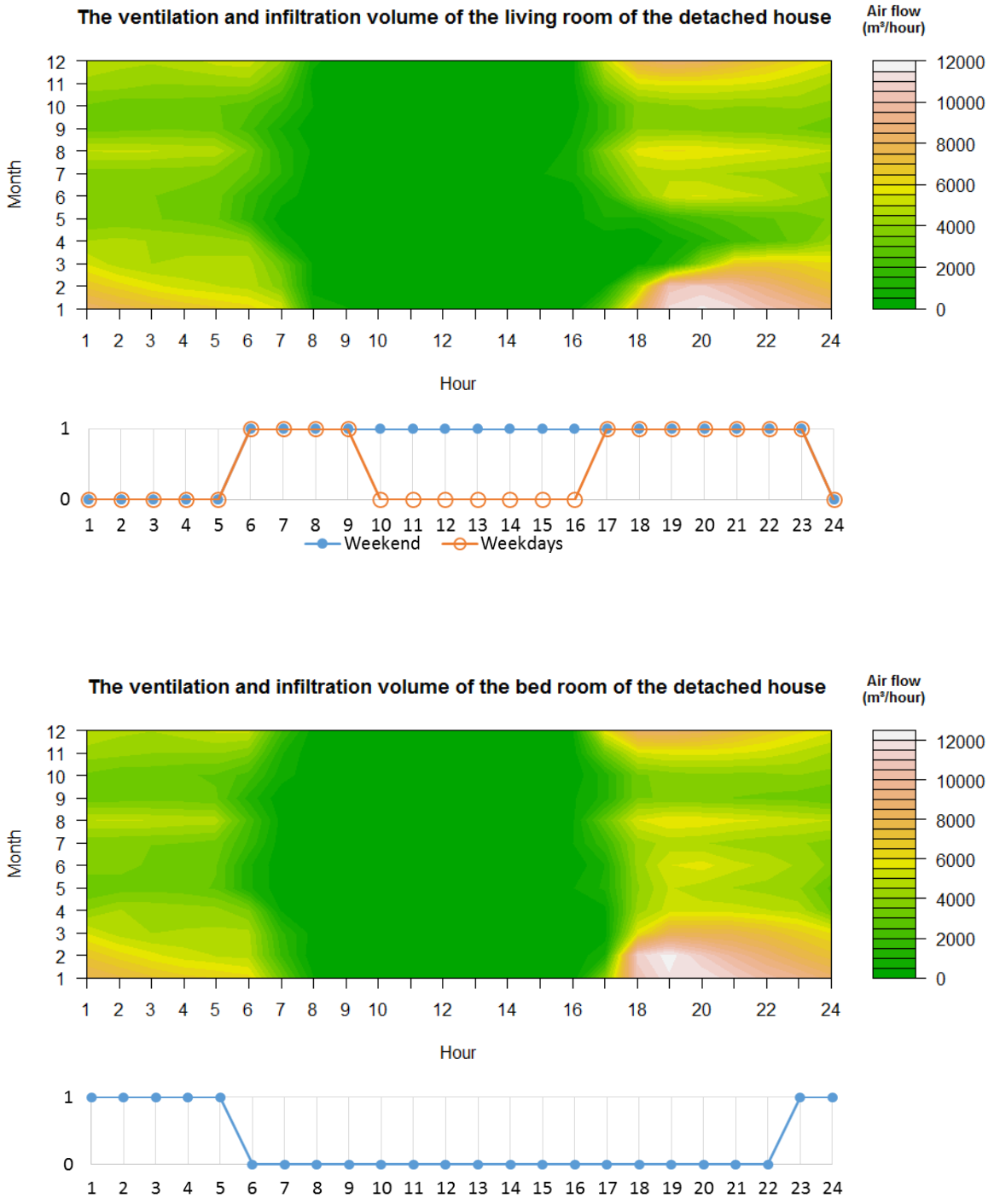

Figure 8-29 The ventilation and infiltration volume of the living room and the bed room of the detached house.

According to the simulation in the Figure 8-30, the average of the cooling and fan energy indicates that the occupants switch on the fan for occupying periods in the living room. The hot period from March to May is requirement the cooling.

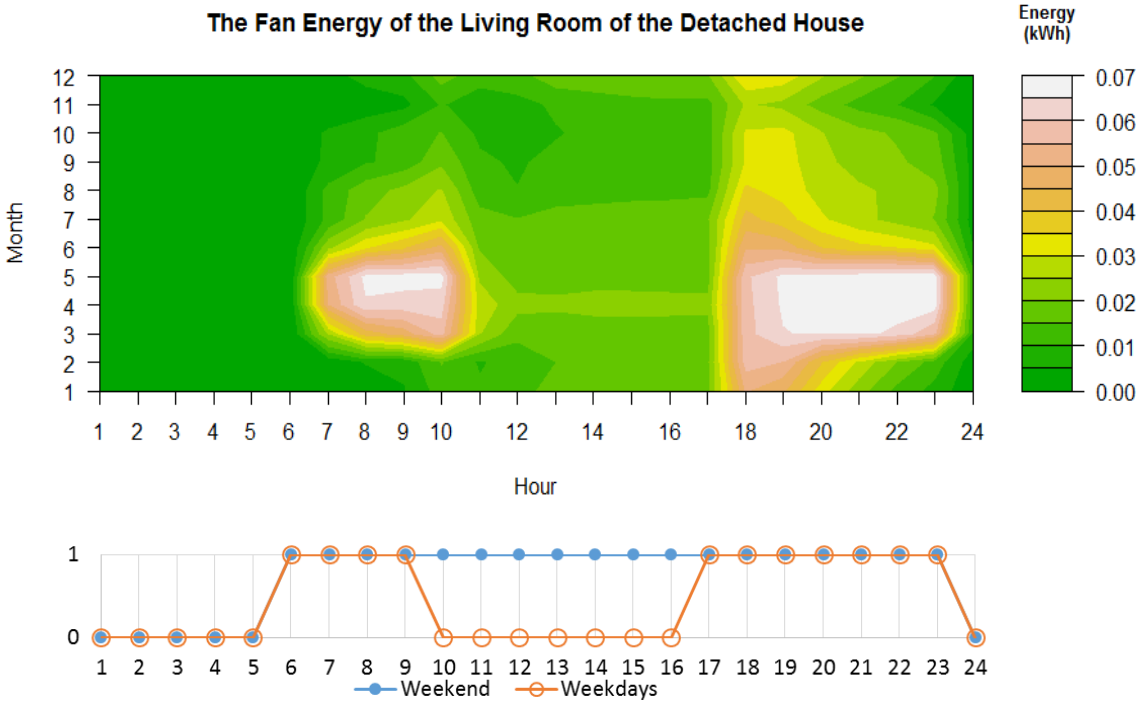
The Fan Energy of the Living Room of the Detached House
Energy (kWh)
0.07
0.06
0.05
0.04
0.03
0.02
0.01
0.00
Month
Hour
Weekend
Weekdays

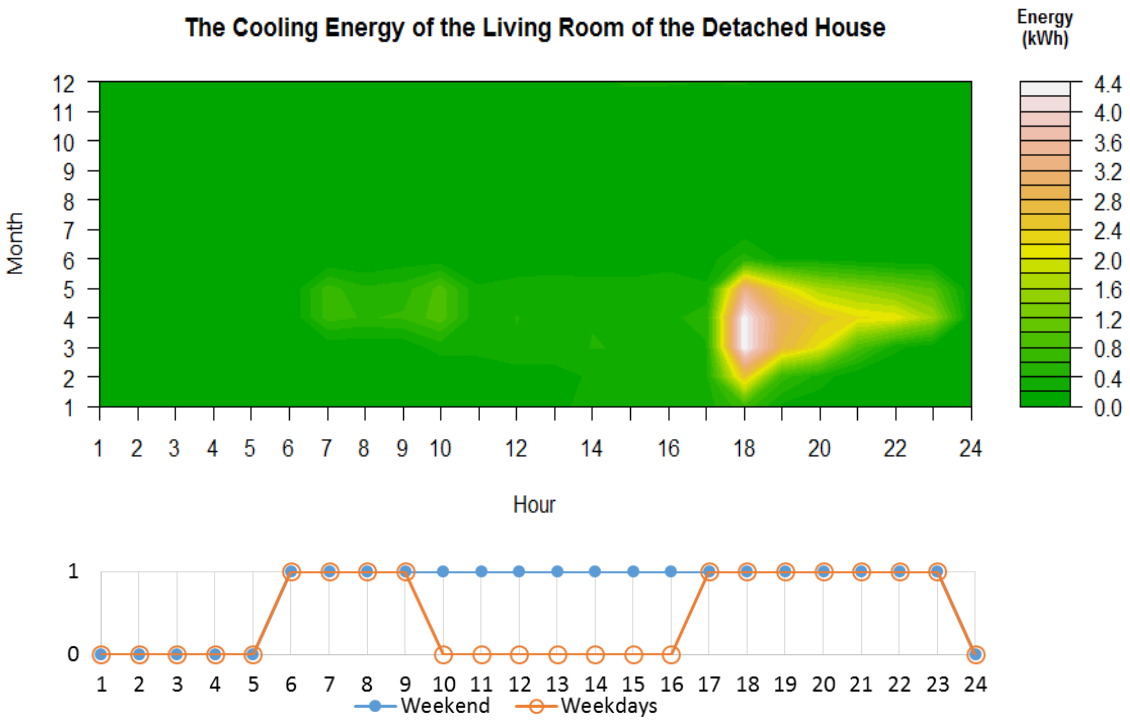
The Cooling Energy of the Living Room of the Detached House
Energy (kWh)
4.4
4.0
3.6
3.2
2.8
2.4
2.0
1.6
1.2
0.8
0.4
0.0
Month
Hour
Weekend
Weekdays

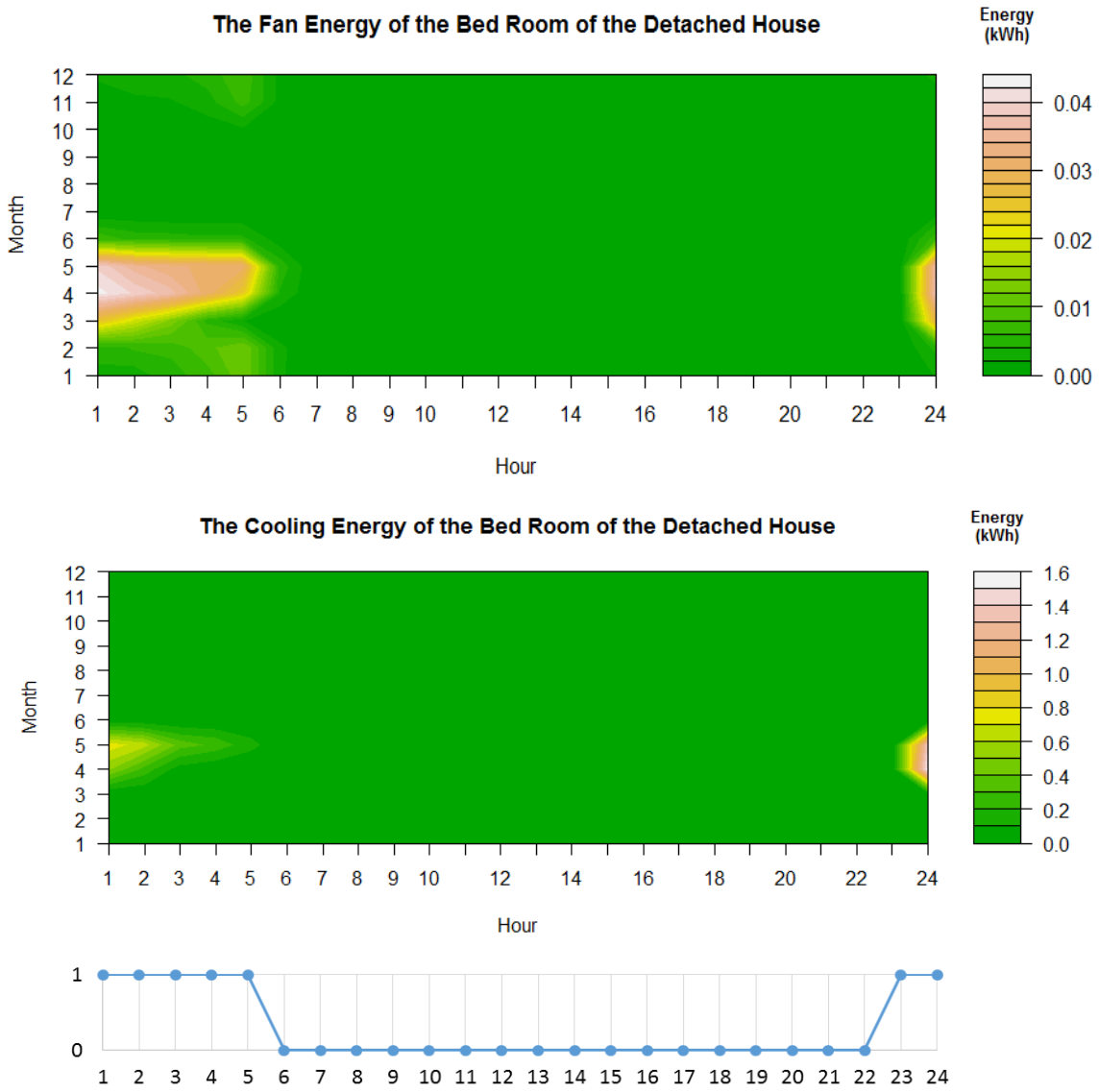

Figure 8-30 The energy use related to occupant behaviour during the year of the detached house.

8.4.2.5 Sensitivity of parameters of detached house

The sensitivity analysis was performed by using the 2000 random design combinations. In the case of detached houses, 19 variables were taken into consideration for the sensitivity analysis. The SRC was calculated based on same set of cases.

Based on the sensitivity rankings of the SRC method, the variables were categorized into two groups: the highly influential group (absolute value of SRC > 0.1) and the less influential group (absolute value of SRC < 0.1) Figure 8-31 and Figure 8-32. In the first

group, the width and length of the building, the width of the road parallel to the length of the building and the neighbouring gap are the most influential parameters of the total LCC (including land cost and infrastructure cost) due to the high unit cost of the infrastructure system (Figure 8-32).

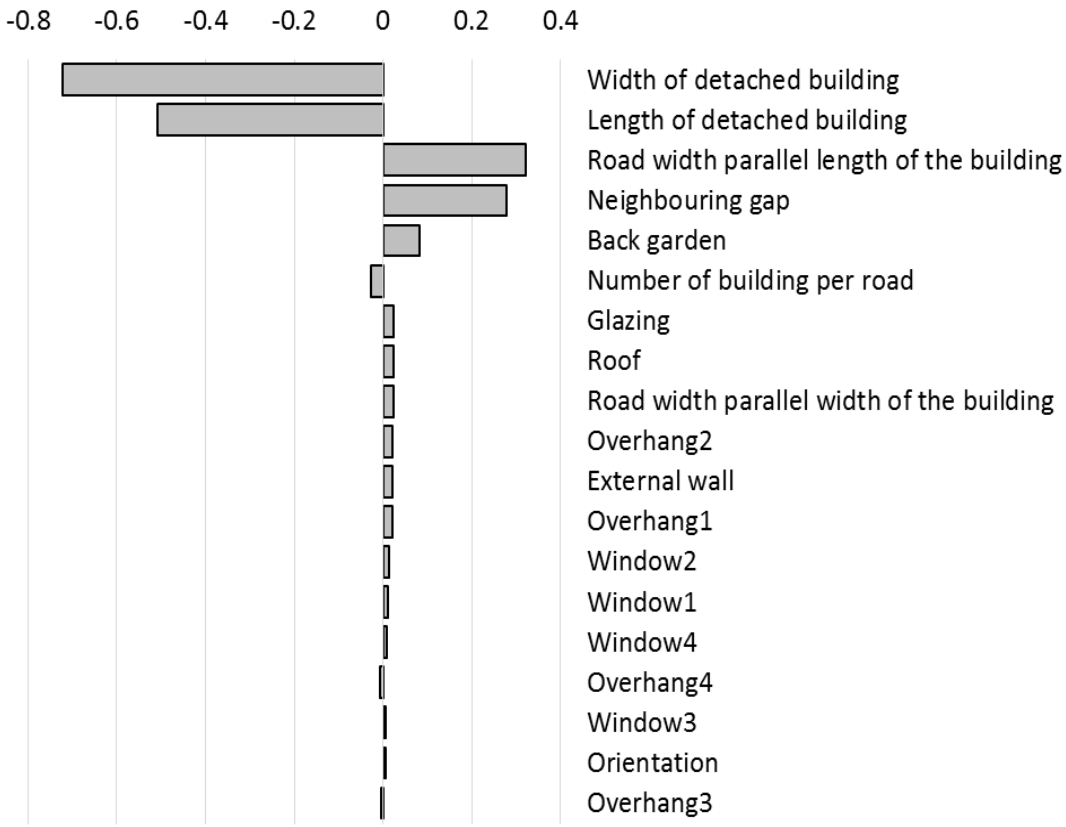

Figure 8-31 Sensitivity ranking via SRC – LCC including land cost and infrastructure cost.

Figure 8-32 shows that width and length of unit, type of external walls and the glazing of the building are the most influential parameters for energy use. The windows in the building North and building South orientations are much bigger than the others. They can reduce lighting energy the whole year round and also get less solar radiation due to the adjacent buildings. The orientation for this housing type has not a big effect on the energy consumption since there are four windows on the four facades.

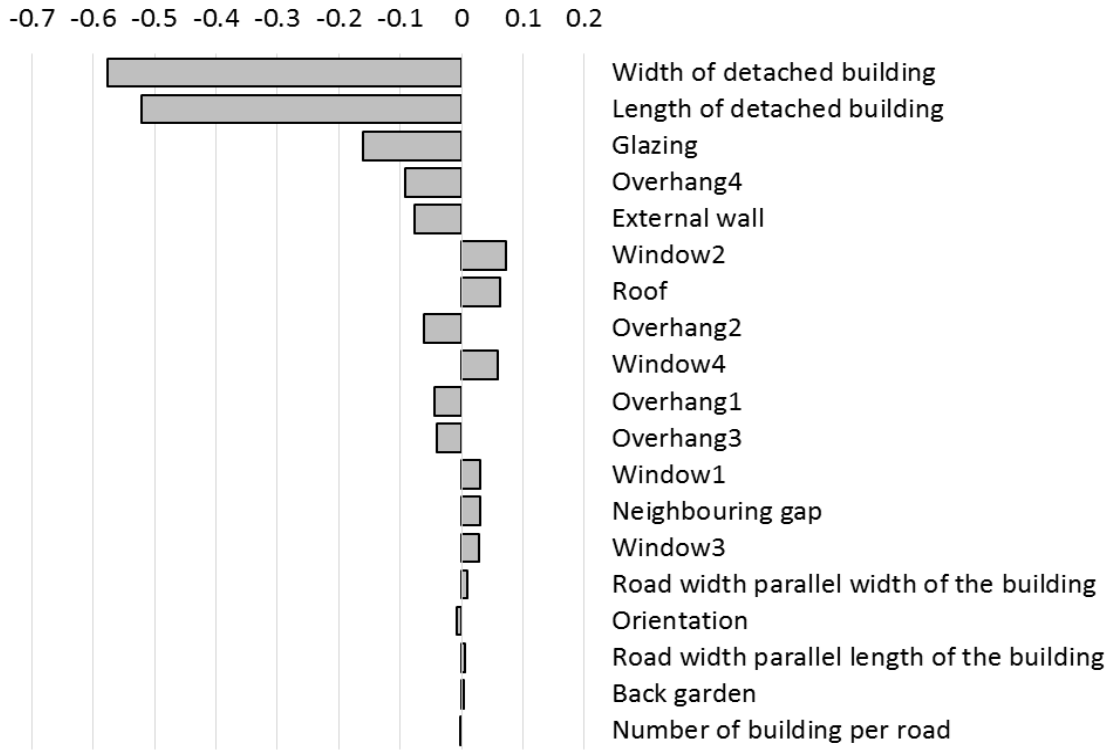

Figure 8-32 Sensitivity ranking via SRC – Energy use of a detached house.

8.4.3 Apartment: Parameters, Results and discussions

The geometries of the building and urban configuration considered for the optimization process are represented in Table 8-8 and Figure 8-33. The front facade of the building faces to the South (The orientation is 0°). The wind pressure coefficient model considers a larger urban area.

Table 8-8 The neighbourhood and building geometry of the apartment house.

Variable name	Parameter	Unit	Min	Max	Step
Urban pattern parameters					
Rw	Road width parallel building width	m	18	24	2
Rl	Road width parallel building length	m	16	24	2
Bg	Back garden	m	50	100	5
H	Height of apartment and neighbouring buildings	m	18	75	3
Ne	Neighbour gap	m	50	100	5
Nbuild	Number of apartment building per row	Building	4	10	2
Orientation	Orientation of building	degree	0°	360°	30°
Building geometry parameters					
L	Length of building	m	16	64	8
W	Width of building	m	8	16	2
ww1	Window1 width by 1.5 meter height	m	1	5	1
ww2	Window2 width by 1.5 meter height	m	1	5	1
ov1	Overhang depth of the rear facade	m	0.5	2	0.5

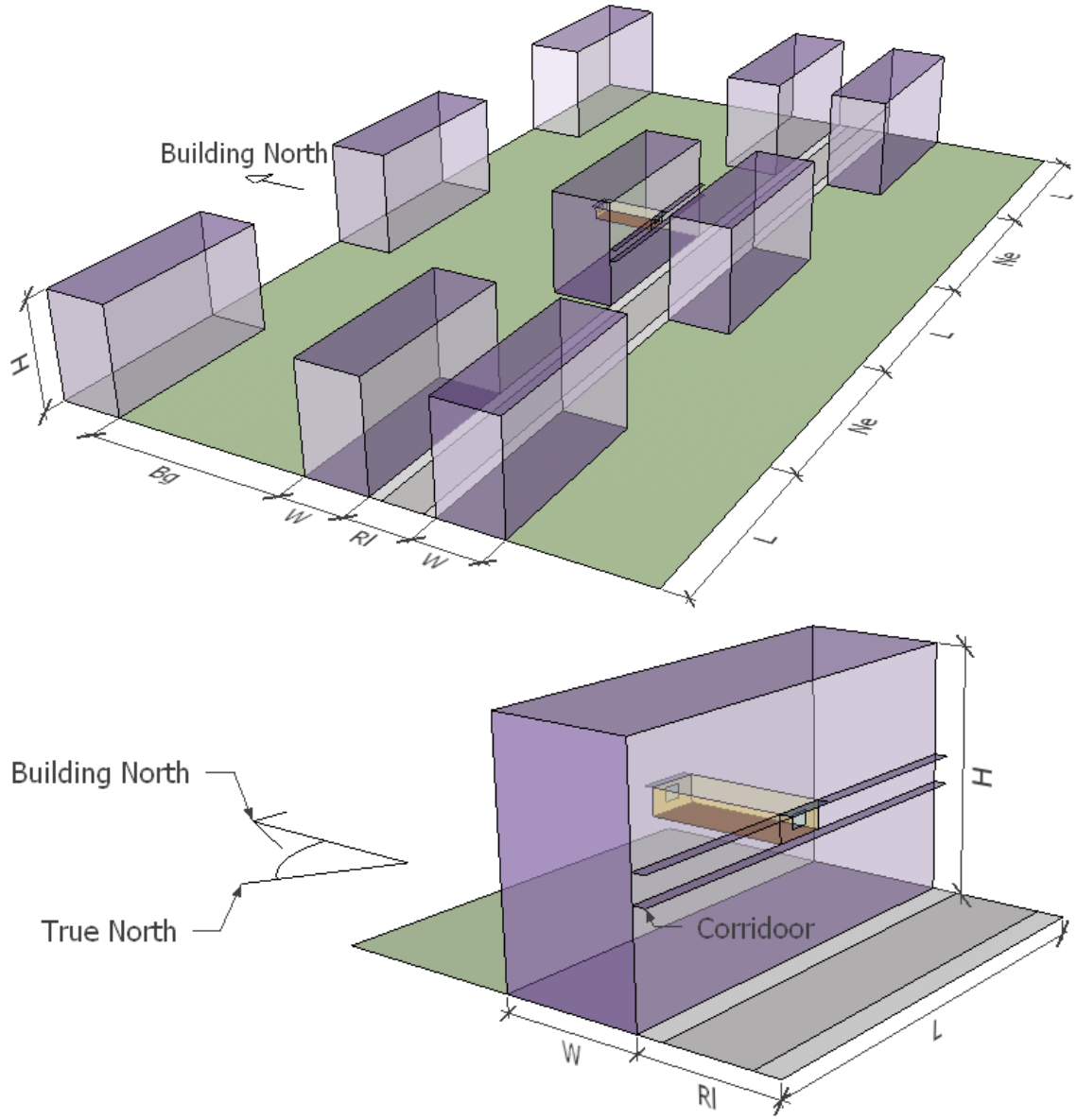

Figure 8-33 Apartment building urban pattern

8.4.3.1 Optimization results of the apartment

The optimal values of the building parameters are in the Table 8-9 and the Table 8-10. Four parameters reach maximum values for their designing range: length and width of the building and number of apartment buildings per row. Other seven parameters are near their minimum values: road width parallel to the building width and the building length, back garden, neighbouring gap and overhangs of both front and rear orientations Figure 8-35.

All parameters can be adapted for different orientations to reduce lighting energy, solar gains via radiation and maximum natural ventilation when inside temperature is higher than the temperature outside. Therefore, if some parameters are fixed, this model is able to deliver another optimal parameter set.

Table 8-9 Optimization results for the neighbourhood and building geometry of the apartment house.

Variable name	Parameter	Unit	Optimal value
Urban pattern parameters			
Rw	Road width parallel building width	m	18
Rl	Road width parallel building length	m	16
Sg	Back garden	m	50
H	Height of apartment and neighbour buildings	m	75
Ne	Neighbour gap	m	50
Nbuild	Number of apartment building per row	Building	10
Orientation	Orientation of building	degree	180°
Building geometry parameters			
L	Length of building	m	64
W	Width of building	m	16
ww1	Window1 width by 1.5 meter height	m	5.0
ww2	Window2 width by 1.5 meter height	m	4.5
ov1	Overhang depth of the rear facade	m	0.5

Table 8-10 Optimization results for the construction elements

Elements	Material layers
Roof	6mm asphalt; 10cm reinforced concrete; 1.5 cm ceiling mortar
Internal wall	1.5cm mortar; 10cm clay brick; 1.5cm mortar (high thermal mass)
External wall	1.5cm mortar; 10cm clay brick; insulation; clay brick ; 1.5cm mortar
Glazing	Clear glass 6mm
Floor	Floor tile; 1.5cm mortar; 10cm reinforced concrete; 1.5 cm ceiling mortar
Ground floor	Floor tile; 1.5cm mortar; 10cm reinforced concrete; soil (external layer)

The construction elements for optimal solution are similar to elements currently used in Vietnamese terraced houses today.

The Pareto fronts for three predicted mean vote (PMV) ranges (0.0 to 0.5), (0.0 to 1.0) and (0 to 1.5) for the apartment provide different design alternatives that can be selected by designers or developers. The Pareto front covers a small ranges of LCC due to the the changes of the window sizes.

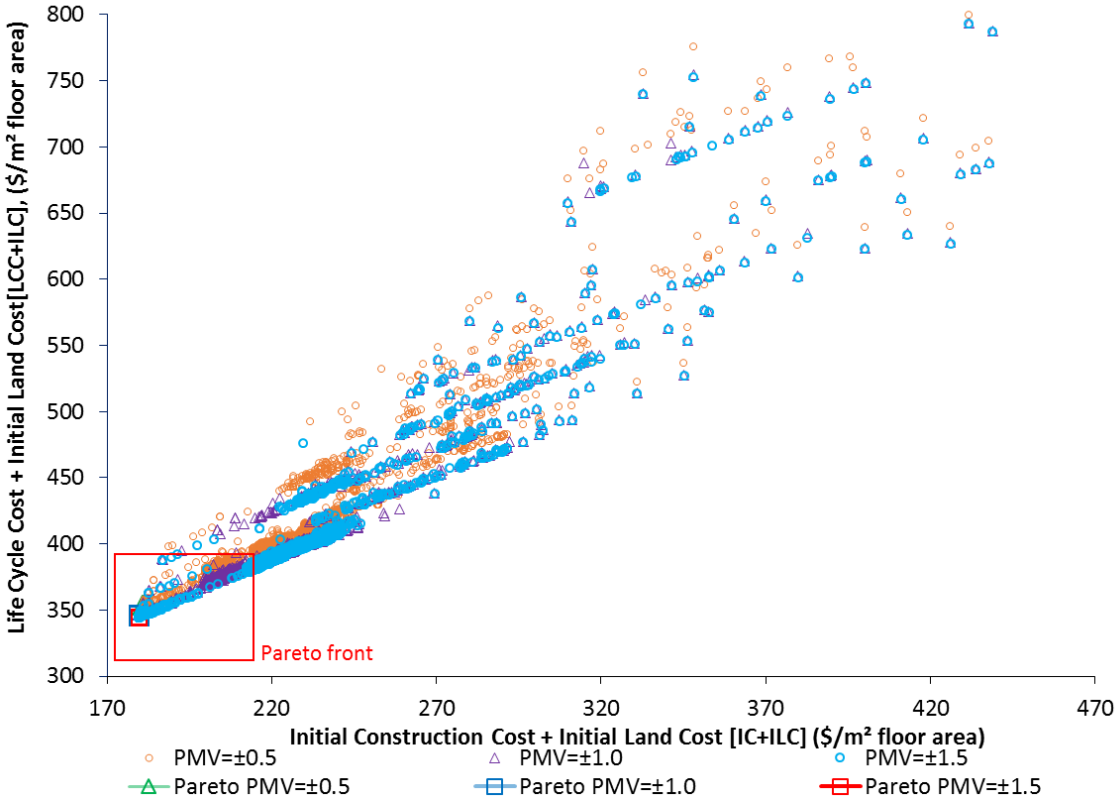
Life Cycle Cost + Initial Land Cost[LCC+ILC], ($/m² floor area)
800
750
700
650
600
550
500
450
400
350
300
Pareto front
170
220
270
320
370
420
470
Initial Construction Cost + Initial Land Cost [IC+ILC] ($/m² floor area)
PMV=±0.5
PMV=±1.0
PMV=±1.5
Pareto PMV=±0.5
Pareto PMV=±1.0
Pareto PMV=±1.5

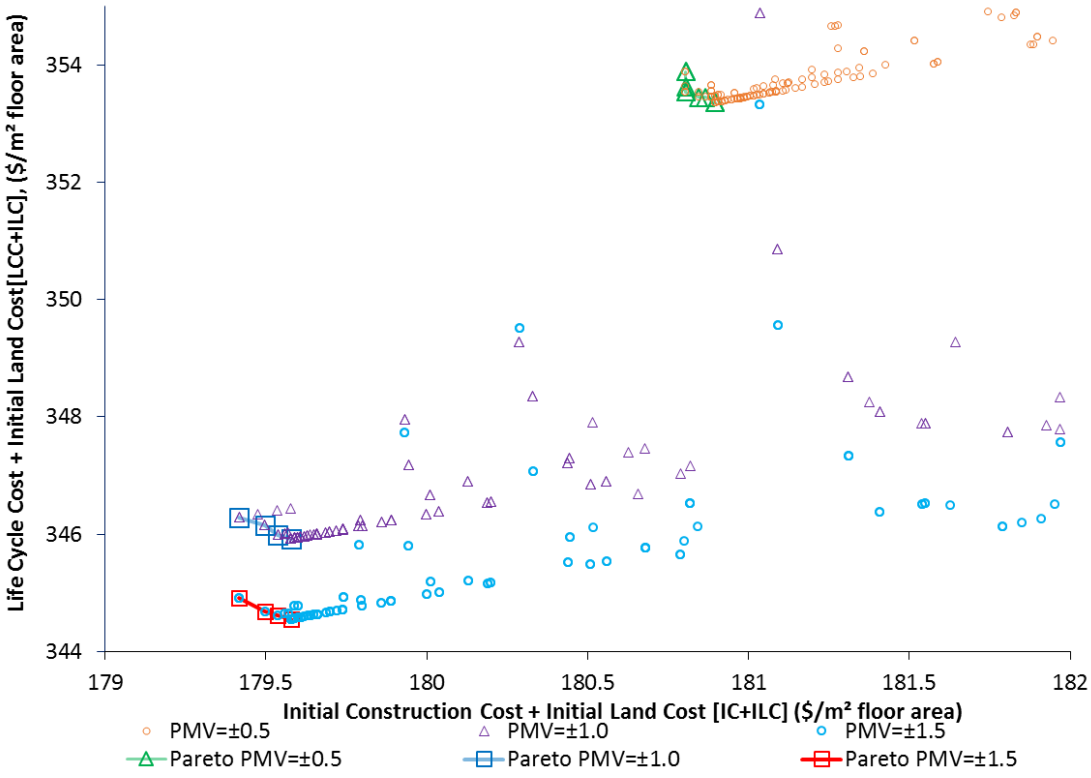
Life Cycle Cost + Initial Land Cost[LCC+ILC], ($/m² floor area)
354
352
350
348
346
344
179
179.5
180
180.5
181
181.5
182
Initial Construction Cost + Initial Land Cost [IC+ILC] ($/m² floor area)
PMV=±0.5
PMV=±1.0
PMV=±1.5
Pareto PMV=±0.5
Pareto PMV=±1.0
Pareto PMV=±1.5

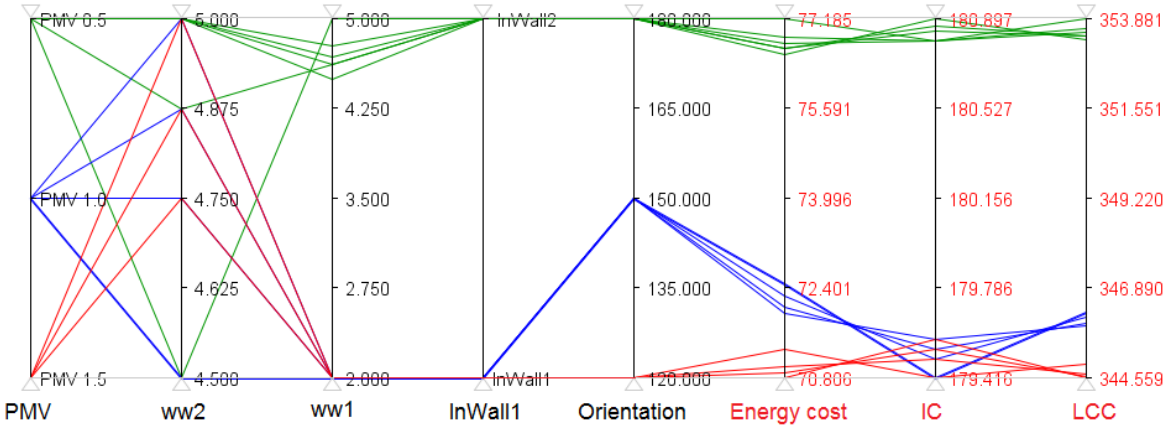

Figure 8-34 Apartment house, initial construction and land cost versus life cycle cost and land cost.

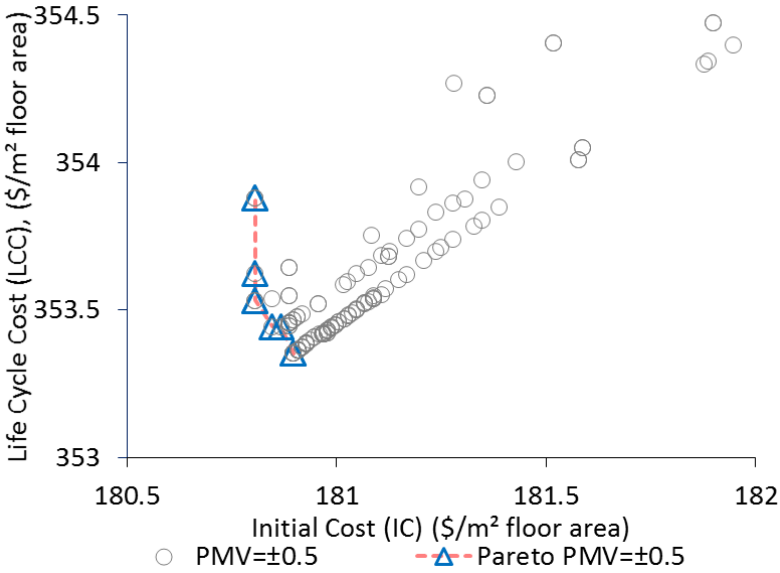

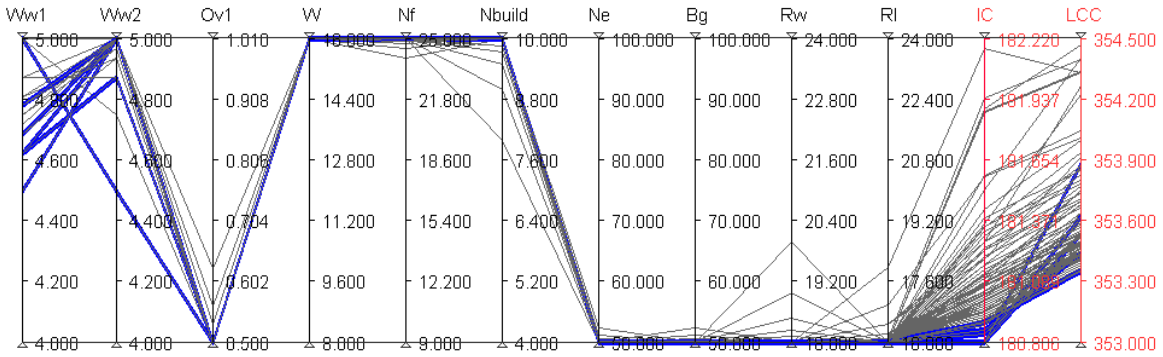

Figure 8-35 The Pareto front and the parallel coordinate of the optimization results of the apartment.

The reduction of thermal comfort acceptable PMV (0 to 0.5) to (0 to 1.0) and (0 to 1.5) can reduce energy use from 6.7% to 7.9%, Figure 8-36. These reductions of energy use are small because total energy for fans and cooling is about 10% of the total energy use based on analysis from chapter 7. Occupant behaviour is also crucial factor in energy saving for apartment buildings. The optimal design options become essential to minimize both initial and life cycle costs, Figure 8-37.

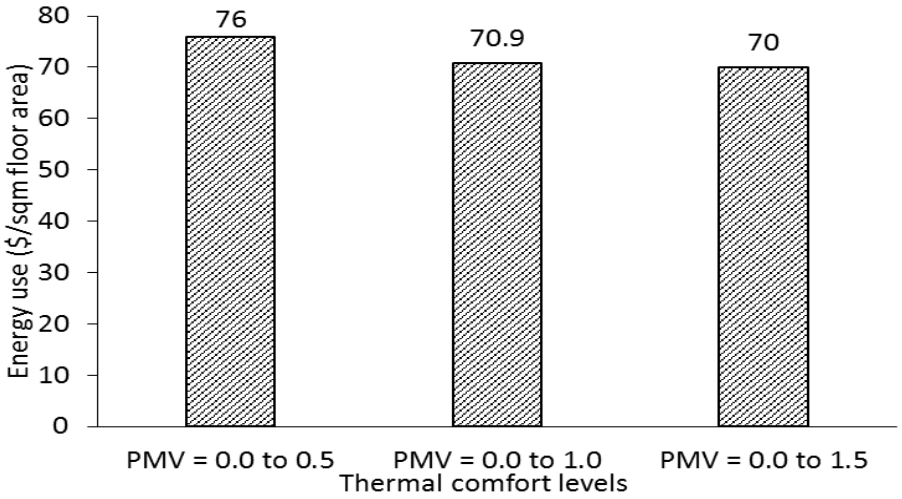

Figure 8-36 Energy saving for reducing thermal comfort ranges of apartments.

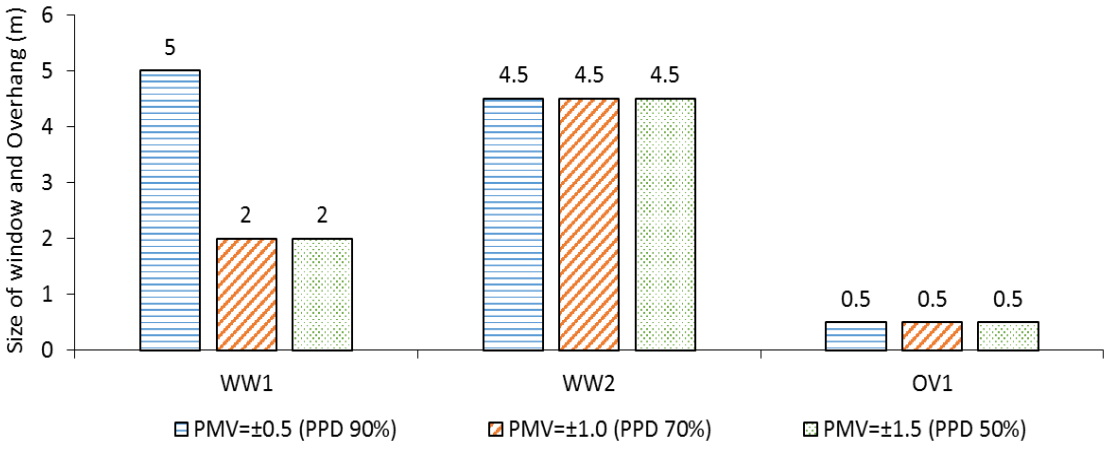

Figure 8-37 Window and overhang sizes of apartment of three PMV ranges of the optimal results.

8.4.3.2 Patterns of the dynamic occupant behaviour of the apartment

The Figure 8-38 shows the average infiltration volume per hour over the whole year of the apartment house. The results indicate that duirng the night is also the best period for the ventilation because the outdoor temperature is lower than the indoor.

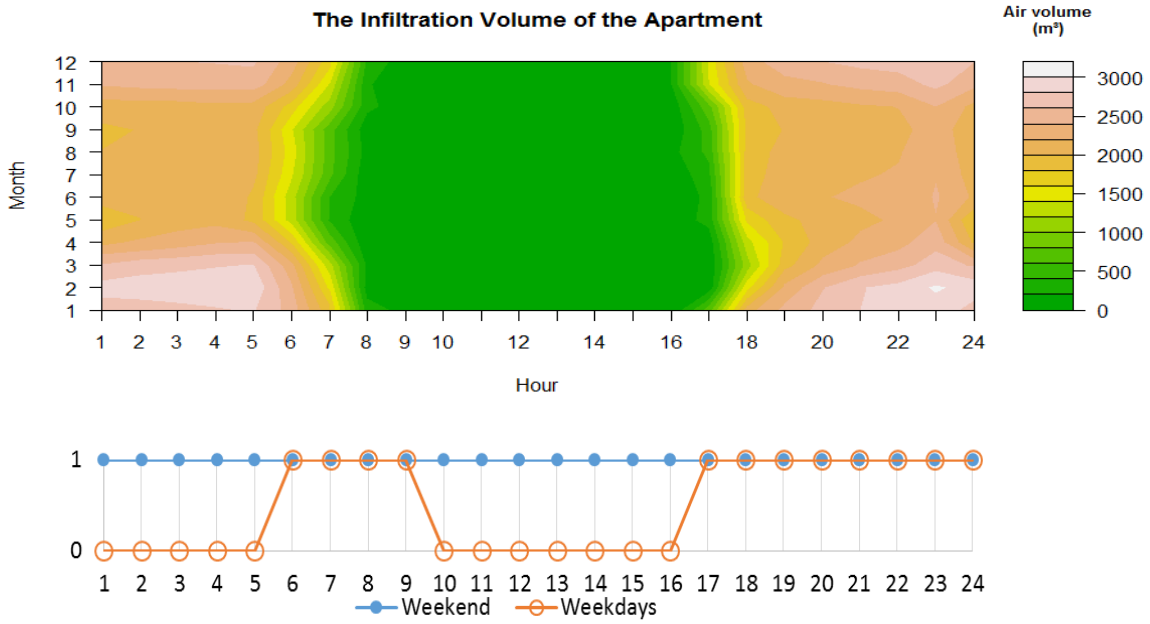

Figure 8-38 The infiltration volume of the living room and the bed room of the apartment.

According to the simulation represented in the Figure 8-39, the average of the cooling and fan energy indicates that the occupants switch on the fan from 23:30 to 5:00. The hot period from March to May requires a short period for cooling from 23:30 to 00:30).

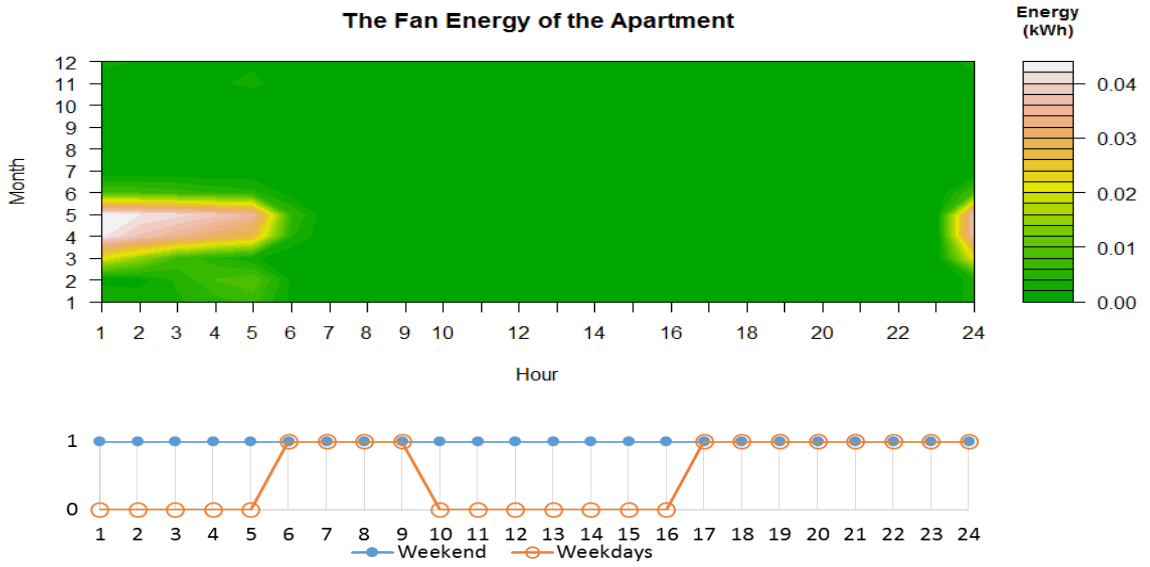

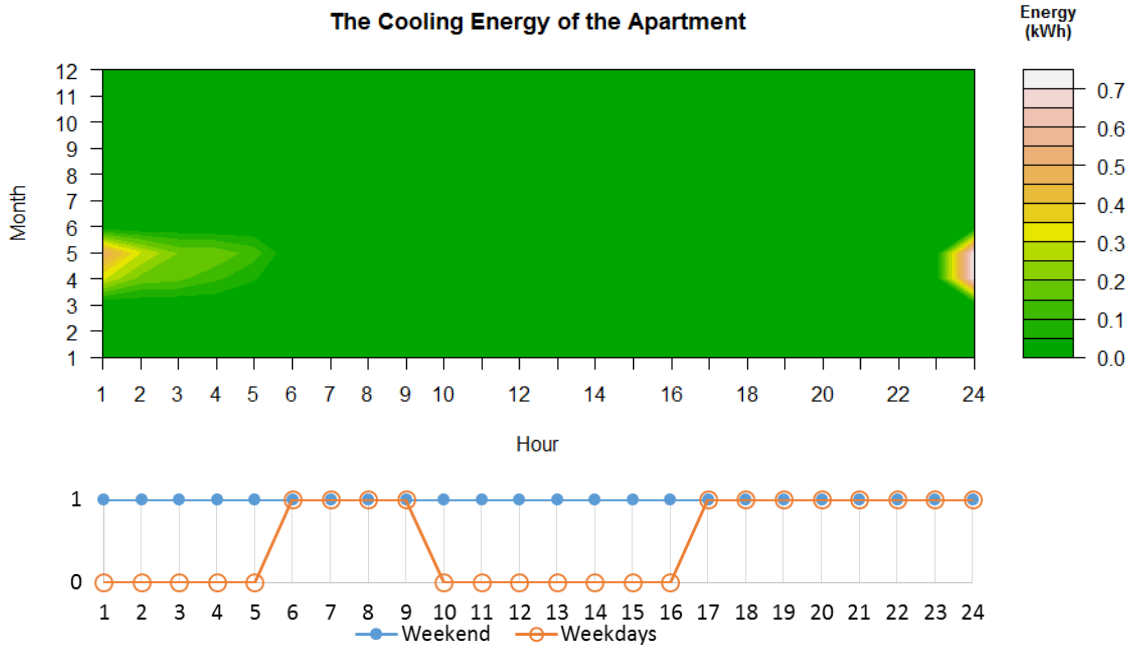

Figure 8-39 The energy use related to occupant behaviour during the year of the apartment.

8.4.3.3 Sensitivity of parameters of apartment

Design combinations are generated by using the random approach with 2000 combinations. In the apartment simulation, 17 variables were analysed for the sensitivity analysis. Based on the sensitivity ranking of SRC, Figure 8-40 and Figure 8-41, the variables were categorized into two groups: the highly influential group (absolute value of SRC > 0.1) and the less influential group (absolute value of SRC < 0.1). In the first group, the width and length of the apartment, number of floors (building height) and pile cost are the most influential parameters of the total LCC, due to the higher unit cost of the infrastructure system (Figure 8-40). Pile cost is the fourth sensitive parameter related to soil properties at different locations. The buildings' width or depth can reduce vertical load, generated by the wind and seismic loads, as examined previously. Although deep apartments limit natural ventilation and daylight, most apartments have been designed with a large depth in order to reduce foundation costs due to vertical or lateral loads.

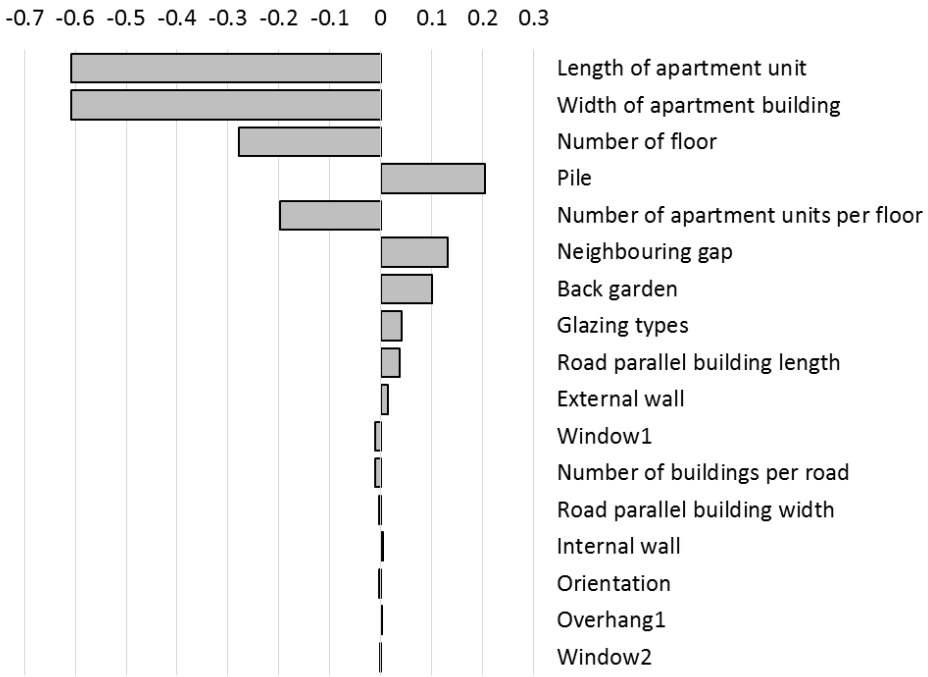

Figure 8-40 Sensitivity ranking via SRC – LCC and Land of apartment.

Considering energy Figure 8-41 shows that width (depth), length of apartment unit and window size are the most influential parameters in energy use. The height of the apartment building has an impact upon the lighting energy because of the shadow of apartment buildings in front of the building.

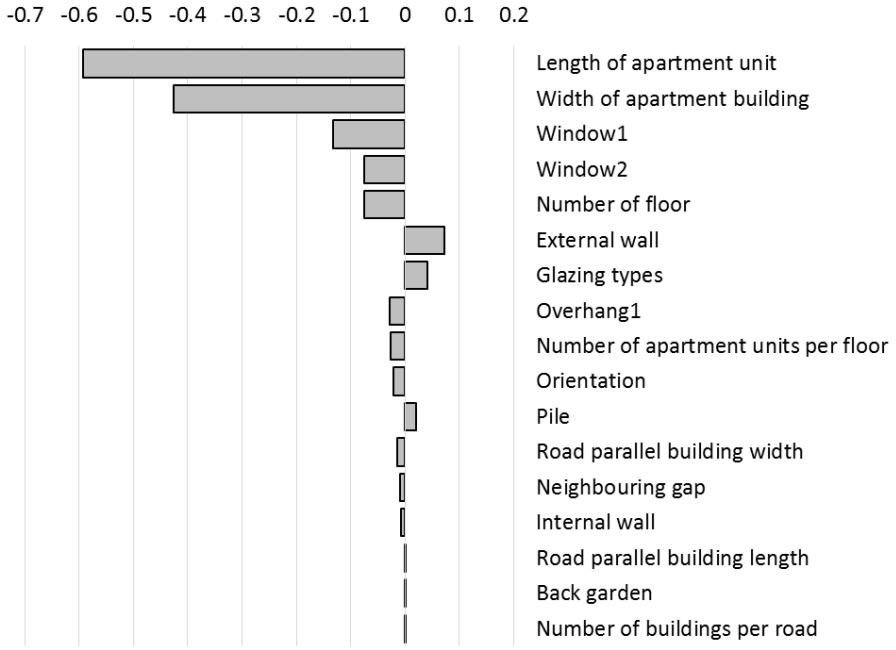

Figure 8-41 Sensitivity ranking via SRC – Energy use of apartment.

8.5 Comparison of the three housing types

For this comparison only the three types with the lowest LCC are considered and this only for a maximum acceptable PMV of 0.5 and optimal cases.

8.5.1 Comparison including land and infrastructure

The cost per square meter floor area of infrastructure and land generate a big difference between the three housing types (Figure 8-42). The detached house requires more land and road along the front facade. As a consequence, this type provides more green area and space for the wind flow between the buildings. In contrast, the apartment building with large number of floors reduces land and infrastructure cost per m² of floor area.

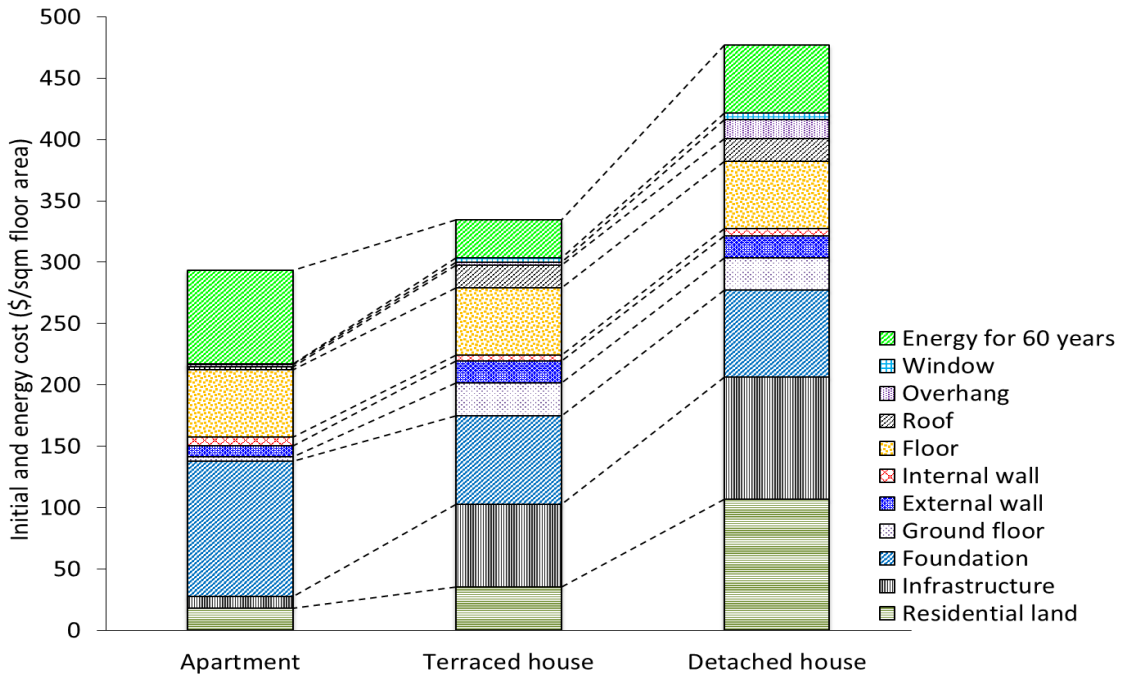

Figure 8-42 Costs of main components in three housing types.

8.5.2 Comparison without land and infrastructure

When only initial construction cost of the building and the present value of energy cost for period of 60 years are considered, for the apartment the foundation cost and the energy cost are the major components. For the apartment case, due to the wind and seismic loads in the soft soil condition, those costs are really more important compared to the detached and terraced house (Figure 8-43). For the other extreme, detached houses, land and infrastructure are the most important components. Terraced houses are situated in between.

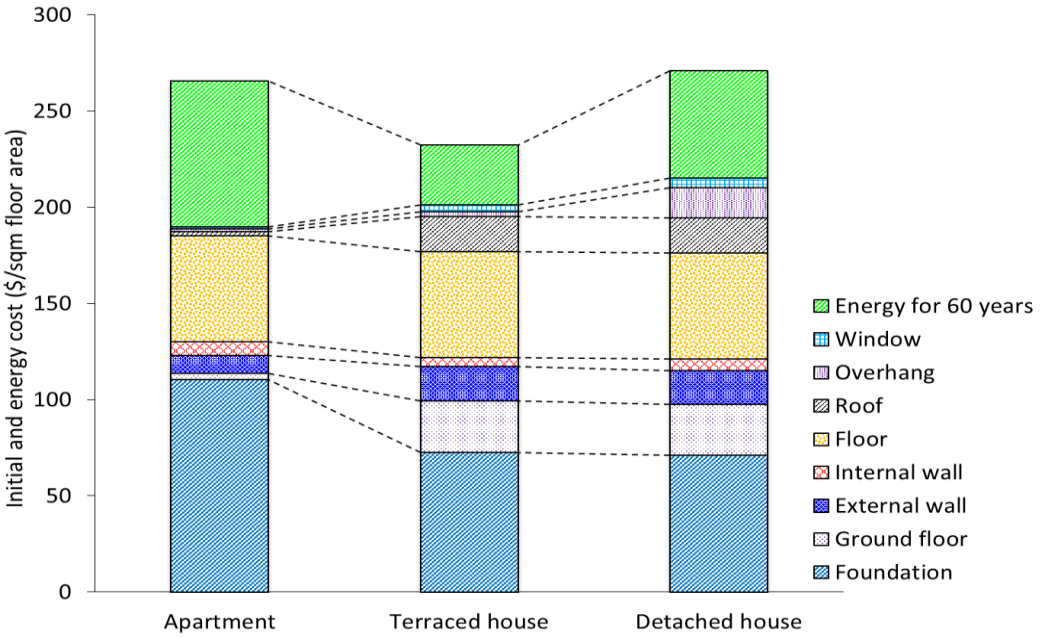

Figure 8-43 Life cycle cost without the infrastructure and the land use cost.

When excluding the present value of the energy cost, the difference between the initial cost per square meter floor area of three housing typologies (without land and infrastructure cost) is smaller. The cost of the roof and the ground floor of the apartment are nearly eight times smaller for the three floor high buildings compared to 25 floor apartment. We see the cost of the foundation is almost 50% of the initial cost of the apartment. Selecting appropriate building layout is, therefore, the key factor to influence the initial cost at the early design stages.

8.5.3 Comparison of energy use of three housing types

The energy use of three housing types is analysed in order to identify the major components. Energy cost per m² floor area of cooling, fans, light and cooking of three cheapest cases is shown in the Figure 8-44. However, for a good interpretation, one should be aware that the total floor area of three housing types is different: the apartment unit 128 m², the terraced house 468 m² and the detached house 576 m². For the apartment the area of the living room and the kitchen is nearly 70% of the total floor area. For the detached and terraced houses, the area of both living and kitchen is about 30% of the total floor area. Since energy use for cooking is fixed per dwelling unit, it is higher per m² of floor area for the apartment. The energy use for “light and cooking” together per square meter floor area in the apartment is about four times higher than the other types. In the contrary, the energy use per m² floor area of the fans and the cooling of the apartment is smallest due to a good natural ventilation.

The ratio of window area over facade area of the detached house is 10%, of the terraced house is 18%. Although the detached house has four facades that can receive daylight, since the windows size is small in order to reducing solar gain, a lot of artificial light is required. The light has to be switched on early in the day and to turn off late in the living and kitchen areas.

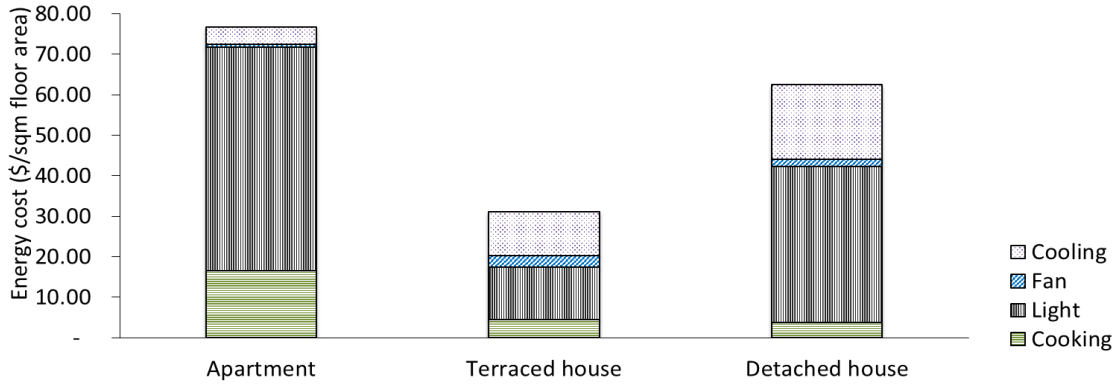

Figure 8-44 The energy cost per square meter floor area for 60 year period of different equipment.

8.5.4 Energy use for fans and cooling depending on acceptable PMV levels

The energy of fans and cooling for the different acceptable PMV levels is pictured in the Figure 8-45, Figure 8-46 and Figure 8-47. The cooling energy is in all cases much higher than the fan energy. The energy is reduced when increasing the acceptable PMV ranges. In the three housing types with an acceptable discomfort up a PMV 1.5, the cooling energy is nearly zero.

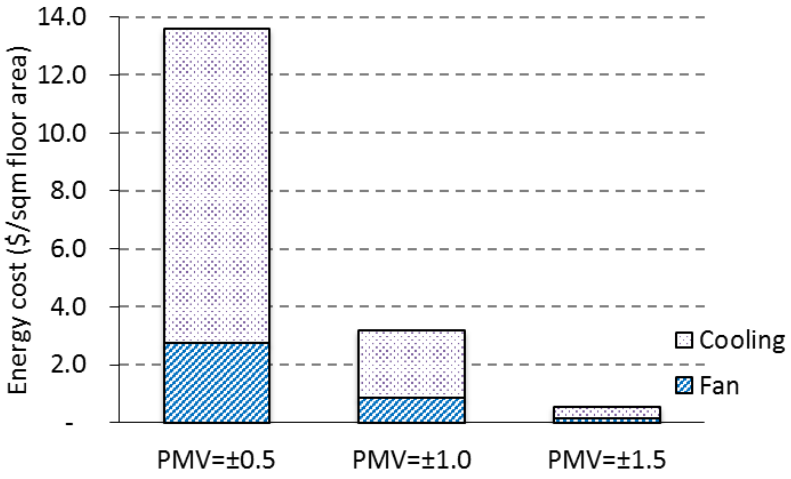

Figure 8-45 Energy use of the cooling and the fans of the terraced house

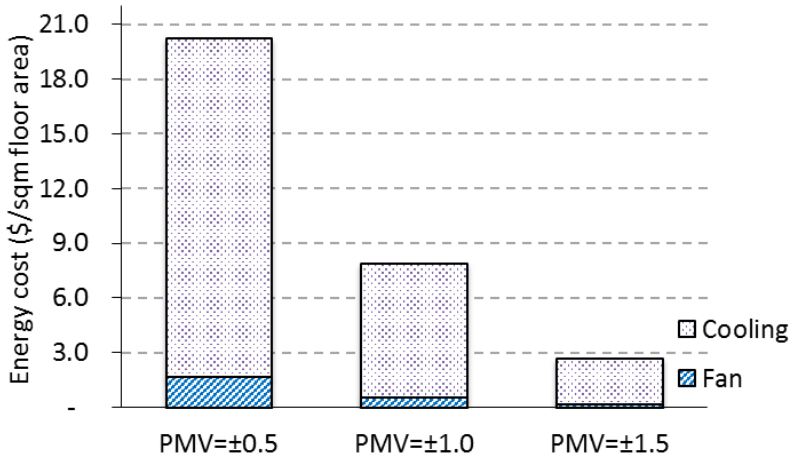

Figure 8-46 Energy use of the cooling and the fans of the Detached house

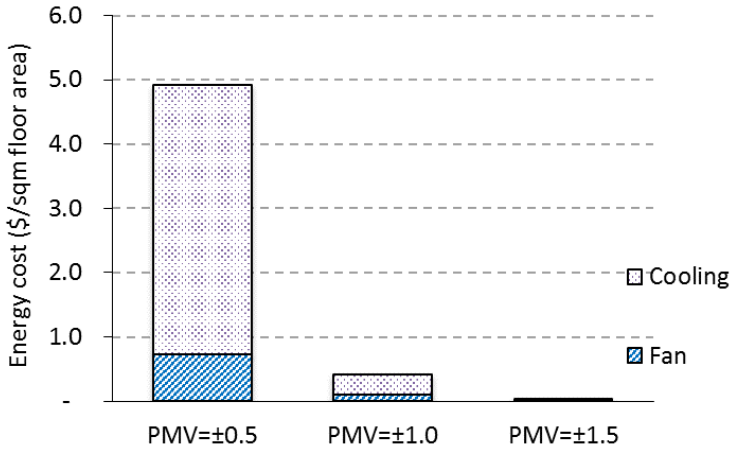

Figure 8-47 Energy use of the cooling and the fans of the apartment

8.5.5 Overhang, urban layout and orientations

The front facade of the terraced house and apartment faces to the South (180°) in order to minimise the solar gain and improve ventilation. According to optimization results, the front and rear overhangs reach the minimum values. The West and East overhangs of the detached house are near to the maximum ranges in order to reduce the solar gain.

The land and infrastructure have a significant impact on the life cycle cost of the terraced and detached buildings. The road widths and back garden are minimized in the cases with lowest LCC. The results show that the energy cost is not the most important

component of the LCC. Therefore, other aspects such as view from windows, green environment, setback defining the character of streets and water areas should be considered when elaborating regulations or norms.

8.6 Findings throughout three housing types

- **On the material and construction technology level**

The construction elements for the cost optimal solutions are similar to commonly used technology in today's building practice e.g. external walls: single hollow clay brick with two mortar layers; glazing: normal clear glass. The thermal mass of construction components is not important, due to the small variation between low and high temperature over a day and over the year in the studied location.

- **On the building level**

For **terraced house**, The South direction is the optimal orientation in order to have good natural ventilation. Windows should be about 15% to 25%of the facade areas and overhangs should be 0.5 m. Neighbouring buildings and overhangs can reduce direct solar gain during the day. The energy use can be reduced with 32% to 43% when thermal comfort limit is changed form the PMV = 0.5 to 1.0 and 1.5 respectively.

For the **detached house** type, the depth of overhangs of the East and West facades should be long enough to block direct solar radiation on windows and facades. The best orientation is the North. Every orientation can be selected by adapting overhang depths and window sizes. The energy use can be reduced with 19% to 28% when the acceptable PMV changes from 0.5 to 1.0 and to 1.5 respectively.

Regarding height, depth and length for **apartment block**, the maximum volumes leads to minimal costs. The cost for foundation and land is the main components affected when the number of floor increases. Larger apartment buildings reduce also the cost for infrastructure. In soft soil condition, high rise buildings should be higher than 10 floors. The exact number of floors depends on both soil properties and land cost. The orientation of apartment building should be North or South to reduce solar gains and improve natural ventilation. The energy use can be reduced with 7% to 8% when the thermal, acceptable levels (PMV) are reduced from 0.5 to 1.0 and to 1.5 respectively.

The ventilation and infiltration results of three dwelling types show that natural ventilation is provided in periods the indoor air temperature is higher than the outdoor air temperature. In fact, in warm and humid climates, natural ventilation in the buldings is also

required for the fresh air. The opening areas should allow manualy control or automaticaly steering to block the hot air from the outside and to get cool air from outside if required.

- **On urban level**

The urban layout effects directly the land and infrastructure cost. The optimization results show that the urban layout parameters reach to minimum values of the ranges in the design space in order to minimize the initial cost. This shows that on one hand, the optimization algorithms try to reduce the values of road widths, back garden, neighbouring gap in order to minimize the initial cost. On the other hand, smaller road, back garden and neighbouring gap increase energy use due to less natural ventilation. The cost per m² floor area of land and infrastructure is several times higher than the cost of energy use for fans and cooling system. Hence, the first priority to minimize LCC via the optimization algorithm is minimizing values of the urban layout parameters. The optimization model however does not include transportation issues for the large scale housing projects. Other aspects should be considered as well such as views, green areas, street characters and water surfaces.

8.7 Conclusions regarding the methodology

This model can be extended to other urban geometries, such as towers and urban street blocks, other energy management systems, other occupancy and activity schemes, other construction technologies and other economic scenarios (growth rate of energy and construction costs, interest rates and life span). The model also works well with different weather data and soil conditions.

Integration of sub-models: the work shows that LCC optimisation is possible including many different models: pile foundation optimisation, comfort strategy, meta-model for wind pressure and global layout.

Definition of design space: moreover the definition of the design space proved to be an essential point: often cost optimal points are situated on the extreme borders of the design space. As a consequence the definition of the design space is one of the most crucial steps. Running the optimisation can offer an important input for the actors: designers, developers, engineering consultants, end users and public authorities.

Sensitivity to values of input parameters: the research also proved that the results depend on the value of specific input parameter like soil properties, land prices, climate condition and occupant behaviour. Conclusions are only valid for the inputs of the model and one should not generalize.

Basic for interaction with designers: from the research it is clear that one should not look at the optimisation models as a straight forward way to pinpoint the optimal solution. They should be seen as a tool for the design process. Elaborating models and designing are complementary activities.

REFERENCES

[1] S. Attia, J.L.M. Hensen, L. Beltrán, A. De Herde, Selection criteria for building performance simulation tools: contrasting architects' and engineers' needs, J. Build. Perform. Simul. 5 (2012) 155–169.

[2] A.T. Nguyen, S. Reiter, P. Rigo, A review on simulation-based optimization methods applied to building performance analysis, Appl. Energy. 113 (2014) 1043–1058.

[3] S. Attia, Computational optimization zero energy building design: interviews with 28 international experts, 2012.

[4] J.H. Holland, Adaptation in Natural and Artificial Systems: An Introductory Analysis with Applications to Biology, Control and Artificial Intelligence, MIT Press, Cambridge, MA, USA, 1992.

[5] C.M. Fonseca, P.J. Fleming, Multiobjective optimization and multiple constraint handling with evolutionary algorithms. I. A unified formulation, IEEE Trans. Syst. Man Cybern. - Part Syst. Hum. 28 (1998) 26–37.

[6] R. Eberhart, J. Kennedy, A new optimizer using particle swarm theory, in: Proc. Sixth Int. Symp. Micro Mach. Hum. Sci. 1995 MHS 95, 1995: pp. 39–43.

[7] R.V. Mellaert, G. Lombaert, M. Schevenels, Global Size Optimization of Statically Determinate Trusses Considering Displacement, Member, and Joint Constraints, J. Struct. Eng. 142 (2016) 04015120.

[8] M. Wetter, GenOpt(R), Generic Optimization Program, User Manual, Version 3.1.0, (2011). http://SimulationResearch.lbl.gov.

[9] L.G. Caldas, L.K. Norford, Genetic Algorithms for Optimization of Building Envelopes and the Design and Control of HVAC Systems, J. Sol. Energy Eng. 125 (2003) 343.

[10] J.C. Vazquez, F. Valdez, Fuzzy logic for dynamic adaptation in PSO with multiple topologies, in: IFSA World Congr. NAFIPS Annu. Meet. IFSANAFIPS 2013 Jt., 2013: pp. 1197–1202.

[11] F. Marini, B. Walczak, Particle swarm optimization (PSO). A tutorial, Chemom. Intell. Lab. Syst. 149, Part B (2015) 153–165.

[12] A.A. El-Sawy, Z.M. Hendawy, M.A. El-Shorbagy, Reference Point Based TR-PSO for Multi-Objective Environmental/Economic Dispatch, 2013 (2013).

[13] A.A. El-Sawy, Z.M. Hendawy, M.A. El-Shorbagy, Reference Point Based TR-PSO for Multi-Objective Environmental/Economic Dispatch, Appl. Math. 04 (2013) 803–813.

[14] Z. Li-ping, Y. Huan-jun, H. Shang-xu, Optimal choice of parameters for particle swarm optimization, J. Zhejiang Univ. Sci. A. 6 (2005) 528–534. doi:10.1007/BF02841760.

[15] A.T. Nguyen, S. Reiter, Passive designs and strategies for low-cost housing using simulation-based optimization and different thermal comfort criteria, J. Build. Perform. Simul. 0 (2013) 1–14.

[16] T. Nguyen van, D. Trigaux, K. Allacker, F. De Troyer, Optimization for Passive Design of Large Scale Housing Projects for Energy and Thermal Comfort in a Hot and Humid Climate, in: CEPT UNIVERSITY PRESS, CEPT University, Ahmedabad, India, 2014.

[17] R. Hooke, T.A. Jeeves, “Direct Search” Solution of Numerical and Statistical Problems, J ACM. 8 (1961) 212–229.

[18] L. Tutelea, I. Boldea, Induction motor electromagnetic design optimization: Hooke Jeeves method versus genetic algorithms, in: 2010 12th Int. Conf. Optim. Electr. Electron. Equip. OPTIM, 2010: pp. 485–492.

[19] U.S. DOE, EnergyPlus Energy Simulation Software. U.S. Department of Energy | USA.gov, (2015). http://apps1.eere.energy.gov/buildings/energyplus/ (accessed December 8, 2015).

[20] M. Wetter, GenOpt (R) Generic Optimization Program, (2011). http://SimulationResearch.lbl.gov.

[21] J.H. Kämpf, M. Wetter, D. Robinson, A comparison of global optimization algorithms with standard benchmark functions and real-world applications using EnergyPlus, J. Build. Perform. Simul. 3 (2010) 103–120.

[22] R. Evins, P. Pointer, R. Vaidyanathan, S. Burgess, A case study exploring regulated energy use in domestic buildings using design-of-experiments and multi-objective optimisation, Build. Environ. 54 (2012) 126–136.

[23] L. Magnier, F. Haghighat, Multiobjective optimization of building design using TRNSYS simulations, genetic algorithm, and Artificial Neural Network, Build. Environ. 45 (2010) 739–746.

[24] A. Inselberg, B. Dimsdale, Parallel coordinates: a tool for visualizing multi-dimensional geometry, in: Proc. First IEEE Conf. Vis. 1990 Vis. 90, 1990: pp. 361–378.

[25] A. Inselberg, Xdat, Xdat. (2015). http://www.cs.tau.ac.il/~aiisreal/.

[26] B. De Meulder, K. Shannon, Water Urbanisms East, Park Books, Zurich, Switzerland, 2013.

CHAPTER 9 CONCLUSIONS AND FURTHER RESEARCH

This final chapter summarizes the main original contributions developed throughout the PhD study. It also outlines some limitations and possible future research into issues which could not be elaborated within the scope of this thesis.

Table of Contents

9.1	**Original contributions of the thesis**	**243**
9.1.1	Integration of sub models for cost and quality	243
9.1.2	Model for cost-optimal-pile foundations	243
9.1.3	Model predicting market value	244
9.1.4	Model predicting energy consumption	244
9.1.5	Model for life cycle costing including cost optimisation	245
9.2	**Limitations of the models in this thesis**	**245**
9.2.1	Limited integration of quality aspects	245
9.2.2	Limited to column and beam structures	245
9.2.3	Limitation of the thermal comfort model	246
9.2.4	Limitation of objective function	246
9.2.5	Future work	246

9.1 Original contributions of the thesis

9.1.1 Integration of sub models for cost and quality

The object of this PhD research is the development an open ended integrated quantitative approach to manage certain cost and certain quality aspects of large scale housing projects. First, sub models are elaborated starting from the state-of-the-art. Then, a global optimisation on multiple levels (from urban level, over building level, up to construction elements and material level) is developed. The integrated model provides insight into the cost reduction potential and the improvement of housing quality. Important sub-models are (1) the pile-foundation cost model for high rise apartments in soft soil condition applicable in first designing phase, (2) the model predicting market value and (3) the thermal comfort model, including artificial lighting when daylight is insufficient.

A methodology was elaborated to search for a design with minimal life cycle cost within comfort constraints. This methodology was applied to terraced units, detached units and to apartment blocks. The limitation to schematic urban layouts had to be included to allow the prediction of wind pressure for natural ventilation. The models were applied in the context of Cantho. Results can be used by designers, public decision makers and inhabitants. They can provide answers to questions: what comfort level can be reached only with natural ventilation without cooling? How does the regulation of urban layout affect on abilities of natural ventilation? How can the user behaviour affect the energy requirement in the same building?

9.1.2 Model for cost-optimal-pile foundations

In soft soil condition, pile foundation is required for high rise buildings. For a given layout an optimal pile size leading to minimal cost depends on the soil condition and pile type. The cost-optimal-pile model is based on existing theories. The existing approach was, however, developed for detailed design stage but it is reworked to generate information applicable in sketch design stage. The input data are soil characteristics, pile properties and construction cost of different pile types. The output is a pile foundation with minimal cost per ton capacity.

The model for deriving foundation costs contains different steps: first vertical loads on foundation are derived based on dead, live, wind and seismic loads. A simplified model for estimating how seismic and wind loads are transferred to vertical loads on pile foundation is elaborated. This model allows the designers to simulate the cost consequences of changing major layout options (e.g. number of floors and depth of building) and to integrate those costs with all other aspects in the decision makings during the design process.

9.1.3 Model predicting market value

A programme is elaborated to collect automatically technical characteristics and price information from advertising on the web. Although the available information for the context of Cantho is limited at present, the approach has possibilities for the future. The elaborated model allows project developers to search, starting from a basic investment, for the additional investment leading to the highest return. The same approach allows public authorities to select urbanistic rules to increase the quality for the users within a limited budget.

9.1.4 Model predicting energy consumption

The originality of the model lies in the integration of: (1) the estimation of wind driven natural ventilation in an urban environment and (2) user behaviour responding on the comfort sensation in every step of the dynamic energy calculation.

For the natural ventilation, meta-models are elaborated for estimating wind pressure for simplified neighbourhood layout in the case for detached houses, terraced house and apartment types. These models allow fast prediction of natural ventilation and the integration of natural ventilation in dynamic energy calculation for buildings.

For the comfort driven user behaviour, the model simulates following stepwise strategy for thermal comfort: (1) adapting clothing, (2) opening or closing windows, (3) switching on/off fans and stepwise increasing the fan speed and, as a last step, (4) closing windows and start cooling. The comfort sensation is affected by

parameters like clothing types, activities and wind speed. Therefore, this approach can be applied to various cultural habits and different climate conditions.

9.1.5 Model for life cycle costing including cost optimisation

The three models described above are integrated to analyse cost and quality consequences of the design decisions. In that way several scales are integrated: material selection, building element composition, building and urban layout. An optimization model searches for minimal life cycle cost (within constraints set by the designers).

9.2 Limitations of the models in this thesis

9.2.1 Limited integration of quality aspects

The challenge for design is, of course, not only to reduce cost but to find a balance between cost and qualities. The hypothesis is that people are willing to pay more for better quality. The model describing the “willingness to pay” based on major design parameters (percentage of open space, street width, etc.) is still limited but the principle is embedded in the approach. A procedure to look for the additional investments that generate the highest quality for users and possibly the highest returns for developers was implemented. However, the cultural, political, social and ecological context will evolve permanently but in all circumstances designers will have to make choices. Cantho is a young city where the housing preferences will change due to economic development and new population immigration. The procedure to collect and process the information can probably more easily be applied in future (since more information will be exchanged via the web) but limited data available at this moment and fluctuating prices, did not allow to come to reliable conclusion now. Other sources for land prices were not available or even less reliable.

9.2.2 Limited to column and beam structures

The foundation cost model is not appropriate for wall structures because of the distribution of axial forces. A finite element method is required to obtain proper fundamental frequency (building period) for calculating, in that case, vertical forces on foundation generated by seismic and wind loads.

9.2.3 Limitation of the thermal comfort model

The thermal comfort model has the following limitations in its present form:

(1) The urban heat island is not taken into account.

(2) Green areas and water surfaces can be beneficial for specific spots but only average climate conditions were analysed in this study.

(3) The 60-year life cycle cost estimation, used in the thesis, assumes that the climate remains the same during the 60 coming years. Other hypothesis may be integrated in the approach by extrapolating weather data to the future. Elaborating long term climate prediction was out of the scope of this work.

(4) The hypothesis regarding required light levels in the main rooms of the building will also strongly be influence the occupants comfort requirements and other evolutions can be integrated in the model.

9.2.4 Limitation of objective function

A single objective function (life cycle cost) is used for the optimization model, however optimization with other objective functions (like including environment cost, including social benefits or costs) can be considered in the future.

9.2.5 Future work

Fundamental for the approach is the “open ended” characteristic: sub-models can be replaced by more detailed ones, can be replaced by others models and or models can be added. This combination of models leads to a multi-level optimization of large scale housing projects with parameters of urban, building, element and material scale.

Finally, the main results of the study, from a scientific point of view, is the innovation concerning the optimisation of the life cycle costs via simulation. This approach is crucial for Vietnam, as well as for many other countries, but particularly for developing countries.

Appendix A

A.1 Data of the soil properties, Cai rang

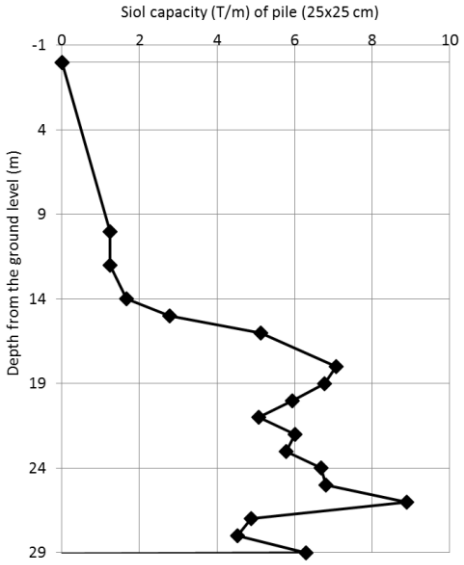

Figure A. 1 Soil capacity ton per running meter of pile 25 x 25 cm section.

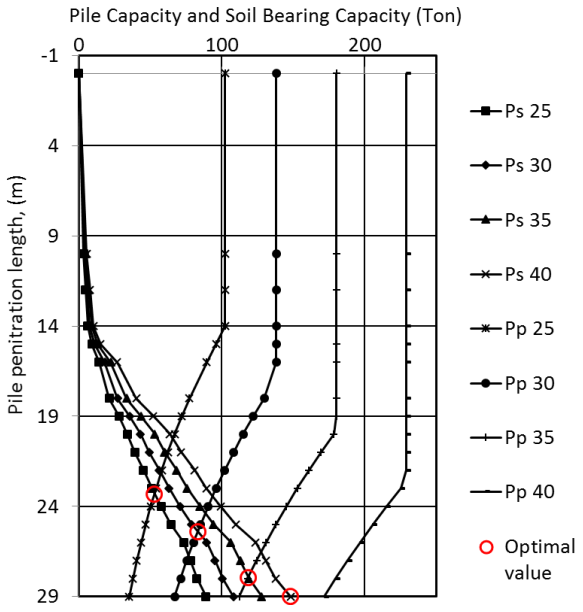

Figure A. 2 Optimal depth or capacity of different pile sections.

A.2 Hung Phu

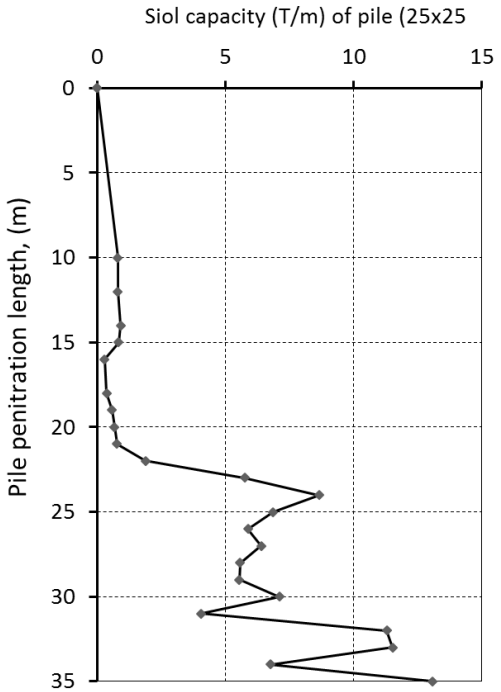

Figure A. 3 Soil capacity ton per running meter of pile 25 x 25 cm section.

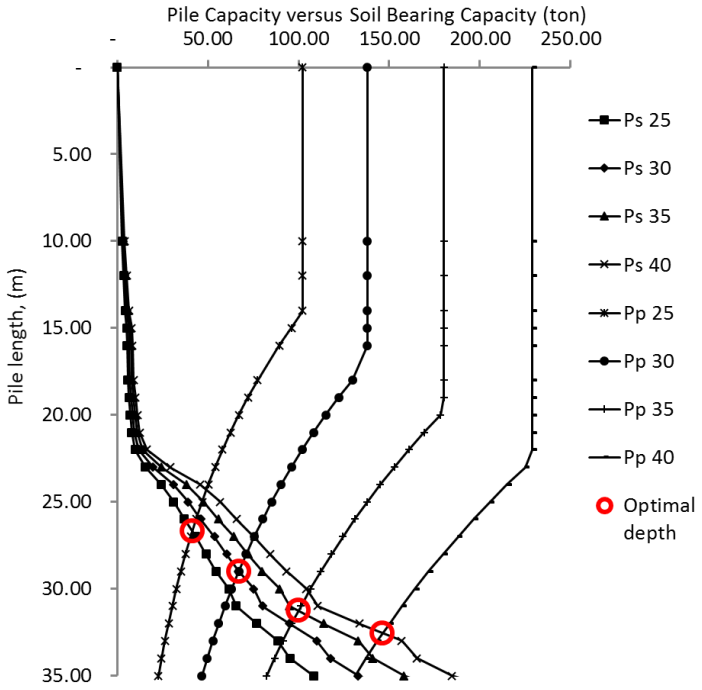

Figure A. 4 Optimal depth or capacity of different pile sections.

A.3 Ngan Thuan

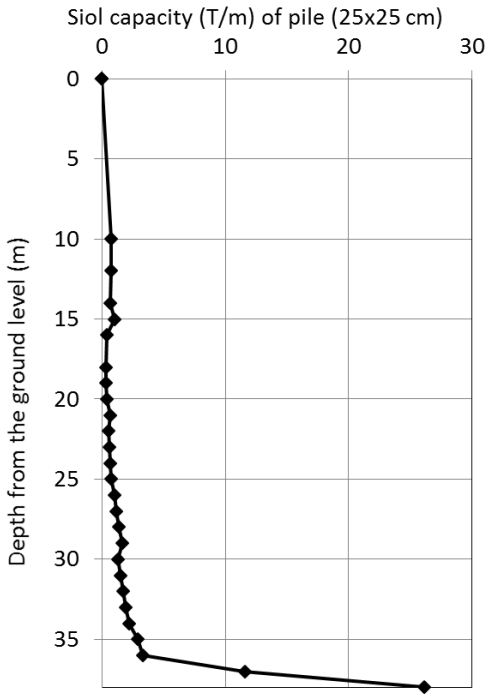

Figure A. 5 Soil capacity ton per running meter of pile 25 x 25 cm section.

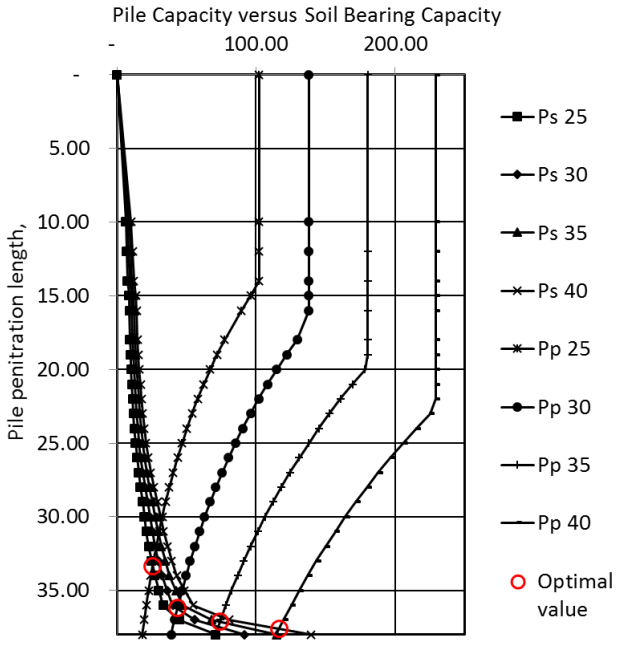

Figure A. 6 Optimal depth or capacity of different pile sections.

A.4 Hong Phat

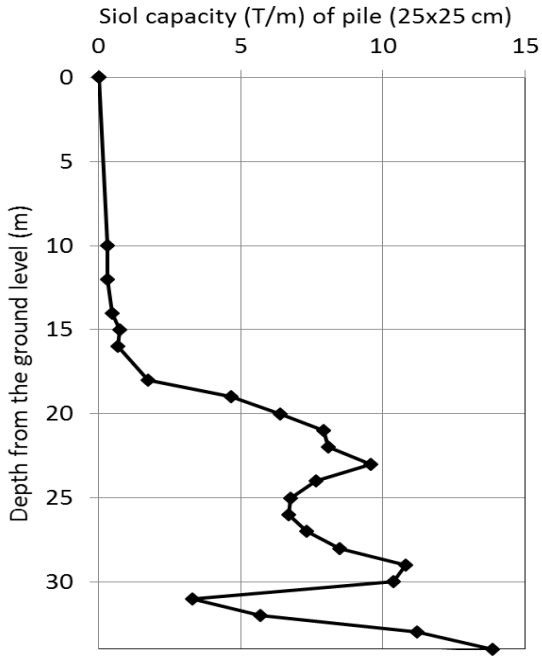

Figure A. 7 Soil capacity ton per running meter of pile 25 x 25 cm section.

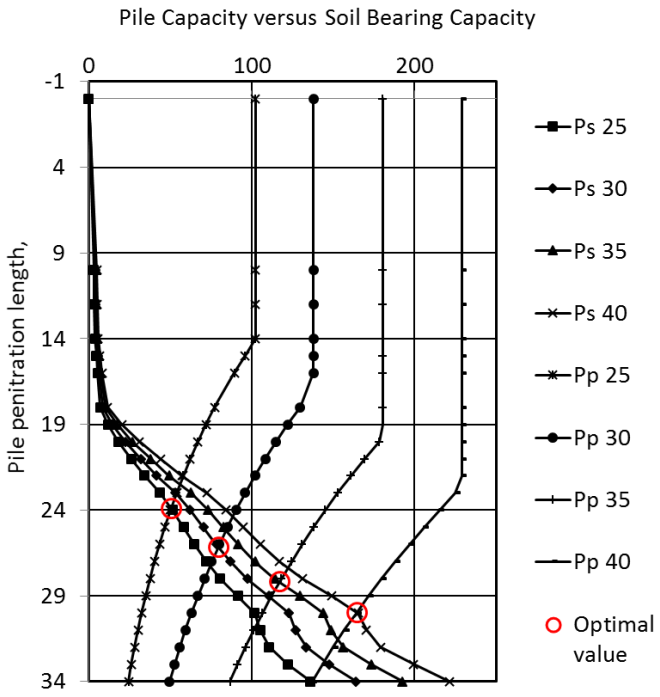

Figure A. 8 Optimal depth or capacity of different pile sections.

A.5 Binh Thuy

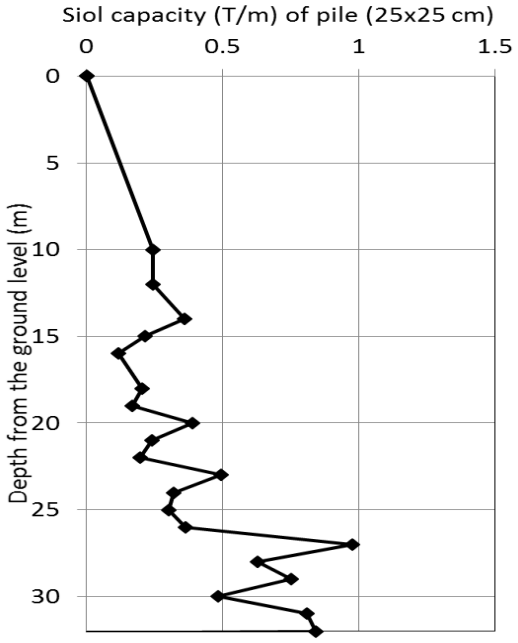

Figure A. 9 Soil capacity ton per running meter of pile 25 x 25 cm section.

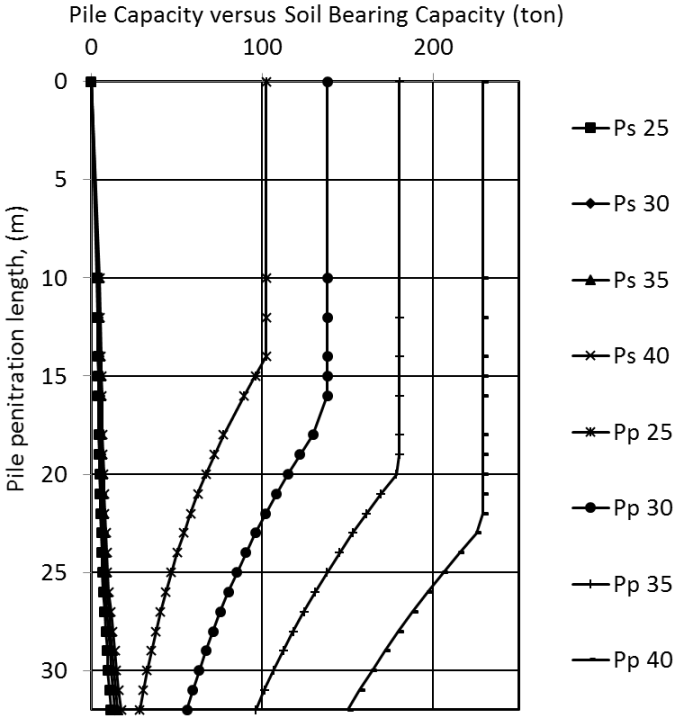

Figure A. 10 Optimal depth or capacity of different pile sections.

Appendix B

Regression functions based on Cp values of TNO Cp-Generator.

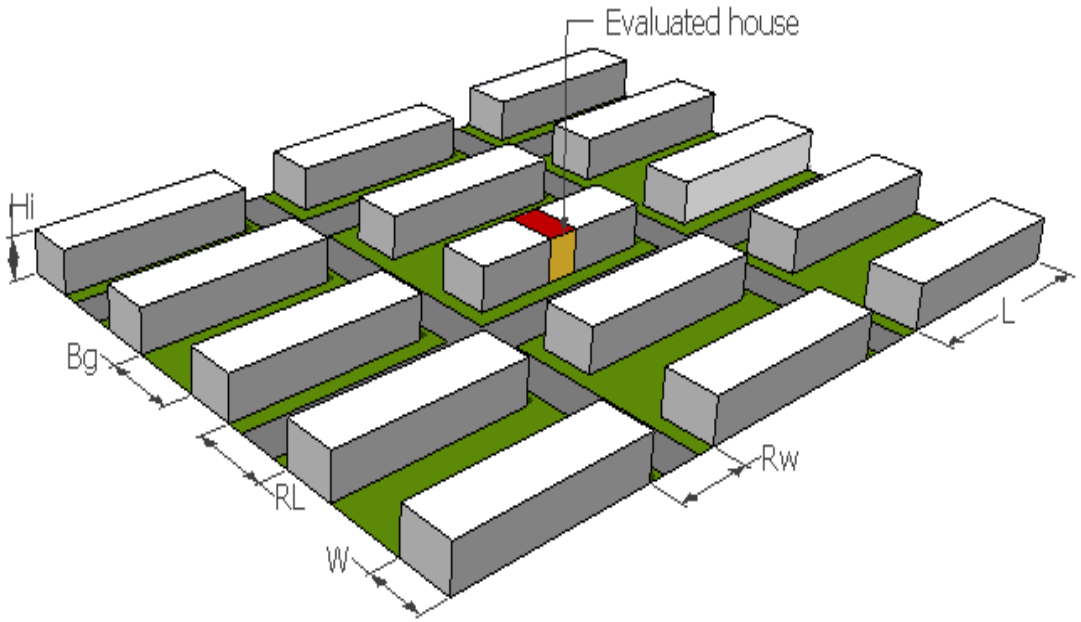

Cp of the front façade: $Cp_{front} = a_{f1}*H_1 + \ldots. a_{f14}*H_{14} + a_{f15}*L + a_{f16}*W + a_{f17}*Rw + a_{f18}*Rl + a_{f19}*Bg + intercept.$

Orientation	Intercept	H1	H2	H3	H4	H5	H6	H7	H8	H9
0	-2.06E-01	1.24E-04	5.15E-04	1.44E-04	-1.49E-04	-2.39E-03	2.38E-04	1.77E-04	2.63E-04	2.22E-04
10	-2.02E-01	8.97E-05	4.03E-04	1.28E-04	-1.44E-04	-2.21E-03	2.35E-04	1.44E-04	2.93E-04	2.24E-04
20	-1.91E-01	7.09E-05	2.21E-04	7.09E-05	-1.61E-04	-1.76E-03	2.04E-04	9.45E-05	3.13E-04	1.92E-04
30	-1.76E-01	1.40E-05	6.68E-05	2.56E-05	-1.38E-04	-1.19E-03	1.28E-04	7.31E-05	2.97E-04	1.13E-04
40	-1.55E-01	-1.18E-04	6.73E-05	1.61E-04	-1.52E-04	-6.12E-04	-3.28E-05	-6.38E-05	1.45E-04	-4.14E-07
50	-1.69E-01	-4.51E-05	2.00E-04	3.70E-04	-4.57E-05	-1.81E-04	4.96E-05	-1.08E-04	-4.07E-05	6.48E-05
60	-2.10E-01	1.02E-04	2.41E-04	2.96E-04	-1.70E-04	-1.25E-04	2.50E-04	-1.69E-04	-6.61E-05	1.04E-04
70	-2.13E-01	1.21E-04	2.07E-04	1.08E-04	-1.77E-04	1.06E-04	1.50E-04	-1.84E-04	-8.77E-05	1.10E-04
80	-2.21E-01	1.17E-04	2.08E-04	4.54E-05	-4.06E-05	1.26E-04	3.68E-05	-3.14E-05	7.54E-05	8.87E-06
90	-2.12E-01	8.58E-05	1.73E-04	-1.55E-05	4.54E-05	8.34E-05	-4.14E-05	1.47E-05	5.76E-06	-7.38E-05
100	-1.28E-01	8.56E-05	9.53E-05	-6.54E-05	4.58E-05	8.97E-05	-5.95E-05	-1.58E-05	-4.42E-05	-1.34E-04
110	-7.11E-02	-5.57E-05	1.24E-04	1.79E-04	7.22E-06	1.06E-04	-1.45E-04	-6.48E-05	6.38E-05	-1.67E-04
120	-4.51E-02	2.13E-04	4.70E-04	6.22E-04	-4.50E-04	9.95E-05	-4.27E-04	-3.36E-04	-7.09E-05	1.05E-04
130	2.37E-02	1.20E-04	7.62E-04	5.18E-04	-3.38E-04	2.35E-04	-3.54E-04	-3.91E-04	-2.53E-04	2.37E-04
140	8.53E-02	4.50E-05	3.32E-04	3.49E-04	-9.37E-05	2.10E-04	-3.65E-04	-1.78E-04	1.18E-04	5.14E-05
150	1.19E-01	2.01E-04	3.69E-05	6.98E-05	1.43E-04	-8.99E-05	-4.03E-05	7.69E-05	7.24E-05	-1.34E-04
160	1.00E-01	1.09E-04	1.27E-04	3.10E-04	2.60E-05	-1.74E-04	1.86E-04	2.21E-06	5.42E-05	-1.36E-04
170	7.39E-02	-1.47E-05	1.78E-04	5.73E-04	-4.85E-05	-1.79E-04	2.37E-04	-8.12E-05	6.17E-05	-1.08E-04
180	6.49E-02	-7.62E-05	2.08E-04	6.76E-04	-7.07E-05	-1.58E-04	2.13E-04	-1.22E-04	3.59E-05	-1.16E-04

Orientation	Intercept	H1	H2	H3	H4	H5	H6	H7	H8	H9
190	7.71E-02	-3.41E-06	1.68E-04	5.52E-04	-4.03E-05	-1.79E-04	2.39E-04	-7.62E-05	5.99E-05	-1.13E-04
200	1.06E-01	1.20E-04	1.12E-04	2.76E-04	2.63E-05	-1.62E-04	1.60E-04	1.86E-05	4.76E-05	-1.59E-04
210	1.21E-01	1.70E-04	5.39E-05	1.22E-04	2.62E-04	-1.21E-04	-2.45E-05	4.67E-06	1.48E-04	1.88E-05
220	8.66E-02	1.50E-04	4.25E-04	4.52E-04	-2.17E-04	2.04E-04	-2.91E-04	-1.43E-04	-7.18E-05	7.89E-05
230	-7.08E-03	-2.78E-04	5.10E-04	5.57E-04	-4.78E-04	1.74E-04	-1.78E-04	8.19E-05	-1.21E-06	-3.46E-04
240	-4.80E-02	-9.34E-05	1.59E-04	4.88E-04	-3.71E-04	-6.83E-05	-2.38E-04	1.62E-04	9.48E-05	-1.23E-03
250	-5.11E-02	1.06E-04	1.85E-04	1.35E-04	2.34E-05	-7.86E-05	-8.19E-05	-6.09E-06	-7.71E-06	-9.20E-04
260	-1.28E-01	8.60E-05	9.73E-05	-7.15E-05	3.68E-05	8.91E-05	-5.80E-05	-9.11E-06	-3.51E-05	-1.71E-04
270	-2.14E-01	9.09E-05	1.77E-04	-3.43E-06	4.20E-05	8.94E-05	-2.91E-05	7.76E-06	9.83E-06	-5.83E-05
280	-2.10E-01	-1.34E-05	1.97E-04	6.50E-05	-1.04E-04	-4.42E-06	-7.83E-06	8.26E-05	5.75E-05	5.32E-05
290	-2.23E-01	2.12E-05	2.79E-04	1.28E-04	-7.74E-05	-2.89E-05	8.59E-05	-1.44E-04	2.06E-05	4.53E-05
300	-1.92E-01	1.05E-04	1.63E-04	1.77E-04	3.90E-05	-7.21E-05	-1.90E-04	-9.17E-05	-8.87E-05	-8.35E-05
310	-1.60E-01	2.05E-04	1.21E-05	1.33E-04	-1.55E-04	-2.40E-04	-1.85E-04	-1.28E-05	4.54E-05	-7.32E-05
320	-1.65E-01	1.58E-04	-1.54E-05	7.50E-06	-1.61E-04	-6.58E-04	5.96E-05	8.94E-05	1.41E-04	4.68E-05
330	-1.76E-01	1.13E-04	5.76E-05	2.41E-06	-1.34E-04	-1.27E-03	1.60E-04	6.64E-05	2.52E-04	1.47E-04
340	-1.92E-01	7.08E-05	2.37E-04	7.94E-05	-1.64E-04	-1.82E-03	2.07E-04	1.04E-04	3.11E-04	1.97E-04
350	-2.02E-01	9.44E-05	4.21E-04	1.33E-04	-1.43E-04	-2.24E-03	2.36E-04	1.47E-04	2.88E-04	2.22E-04

Orientation	H10	H11	H12	H13	H14	W	L	RL	RW	Bg
0	5.45E-04	-9.71E-05	8.15E-05	1.86E-04	-4.95E-05	2.18E-03	-3.28E-05	-7.51E-04	1.68E-04	1.89E-03
10	4.87E-04	-1.18E-04	6.62E-05	1.83E-04	-1.96E-05	2.04E-03	-2.44E-05	-6.67E-04	2.12E-04	1.76E-03
20	3.56E-04	-1.47E-04	4.70E-05	1.27E-04	2.71E-05	1.86E-03	-3.34E-05	-4.82E-04	2.19E-04	1.48E-03
30	1.52E-04	-1.46E-04	9.69E-06	8.48E-05	7.16E-05	1.67E-03	-6.23E-05	-1.92E-04	1.64E-04	1.03E-03
40	-8.81E-05	-1.36E-04	4.41E-05	6.93E-05	1.06E-04	9.64E-04	-9.34E-05	2.09E-04	-1.17E-05	5.60E-04
50	-3.72E-04	-5.14E-05	1.01E-04	-1.26E-04	1.91E-04	4.00E-04	-1.72E-04	7.35E-04	4.88E-05	4.40E-04
60	-7.25E-04	-1.70E-04	8.78E-05	-8.29E-05	2.36E-04	3.90E-04	-2.08E-04	1.85E-03	5.16E-04	1.57E-04
70	-1.28E-03	-3.21E-04	8.05E-05	-1.05E-04	2.40E-04	2.64E-04	-2.65E-04	2.15E-03	4.82E-04	1.46E-05
80	-1.76E-03	-2.72E-04	9.60E-05	-1.86E-04	2.20E-04	-9.46E-05	-1.68E-04	2.11E-03	4.93E-04	3.60E-04
90	-1.88E-03	-1.48E-04	-5.71E-05	-2.20E-04	-4.75E-06	-7.89E-04	1.91E-04	1.49E-03	7.32E-05	4.79E-04
100	-1.00E-03	-1.20E-04	-1.03E-04	-1.29E-04	-1.71E-04	-4.98E-04	4.38E-04	5.10E-04	4.65E-05	4.16E-04
110	-2.42E-04	-8.02E-04	-1.70E-04	7.35E-05	4.05E-05	-4.58E-04	3.71E-04	1.03E-03	6.43E-04	4.36E-04
120	-9.35E-04	-1.63E-03	-1.09E-04	1.61E-04	-2.51E-04	1.27E-04	-7.91E-05	3.45E-03	2.22E-03	5.17E-04
130	-3.86E-03	-1.01E-03	1.94E-04	-3.51E-04	-3.38E-04	7.29E-05	-6.92E-04	6.02E-03	2.46E-03	3.26E-04
140	-7.50E-03	-5.51E-04	1.05E-04	-8.56E-04	-1.27E-04	6.09E-04	-1.10E-03	8.62E-03	1.35E-03	7.03E-04
150	-1.10E-02	-2.49E-04	-6.36E-05	-1.53E-03	1.33E-04	1.21E-03	-1.21E-03	1.04E-02	3.61E-04	1.18E-03
160	-1.33E-02	-2.99E-04	-1.02E-04	-3.01E-03	6.53E-05	1.48E-03	-7.90E-04	1.05E-02	7.12E-04	1.48E-03
170	-1.45E-02	-3.84E-04	-9.71E-06	-4.52E-03	-9.06E-05	1.59E-03	-2.57E-04	1.03E-02	7.81E-04	1.92E-03
180	-1.49E-02	-4.52E-04	3.69E-05	-5.10E-03	-1.41E-04	1.50E-03	-3.86E-05	1.01E-02	8.23E-04	2.15E-03

Orientation	H10	H11	H12	H13	H14	W	L	RL	RW	Bg
190	-1.44E-02	-3.74E-04	-1.96E-05	-4.39E-03	-7.39E-05	1.60E-03	-3.05E-04	1.03E-02	7.76E-04	1.87E-03
200	-1.31E-02	-2.79E-04	-8.70E-05	-2.85E-03	6.57E-05	1.43E-03	-8.50E-04	1.06E-02	6.67E-04	1.48E-03
210	-1.06E-02	-3.49E-04	-1.64E-04	-1.40E-03	1.59E-04	9.98E-04	-1.19E-03	1.01E-02	5.66E-04	7.62E-04
220	-7.09E-03	-6.04E-04	-3.34E-04	-7.34E-04	3.09E-04	8.16E-04	-1.15E-03	8.36E-03	1.39E-03	6.99E-04
230	-3.58E-03	-2.01E-04	-4.77E-04	-2.44E-04	6.16E-04	1.22E-03	-8.12E-04	6.12E-03	2.65E-03	6.65E-04
240	-9.85E-04	-1.35E-04	-5.01E-04	9.42E-05	3.43E-04	3.21E-04	-1.92E-05	3.41E-03	2.14E-03	3.39E-04
250	-3.06E-04	-6.50E-05	-1.23E-04	2.32E-05	-1.44E-04	-8.08E-04	4.28E-04	8.16E-04	3.35E-04	1.76E-04
260	-1.10E-03	-7.73E-05	-9.45E-05	-1.40E-04	-1.63E-04	-4.76E-04	4.16E-04	6.09E-04	4.26E-07	4.35E-04
270	-1.90E-03	-1.71E-04	-5.55E-05	-2.15E-04	1.90E-05	-7.55E-04	1.56E-04	1.58E-03	1.02E-04	4.79E-04
280	-1.61E-03	-1.31E-04	9.98E-05	-2.56E-04	2.59E-04	-1.91E-04	-2.00E-04	1.71E-03	7.39E-04	9.80E-05
290	-1.17E-03	-2.11E-04	2.32E-04	-8.06E-05	2.69E-04	4.05E-04	-2.25E-04	2.05E-03	6.54E-04	-2.39E-04
300	-6.26E-04	-2.20E-04	2.47E-04	5.56E-05	2.21E-04	-2.52E-04	-2.34E-04	1.98E-03	4.96E-04	-3.18E-05
310	-1.43E-04	-9.77E-05	1.18E-04	2.18E-05	1.86E-04	9.03E-06	-1.52E-04	8.17E-04	-3.07E-05	4.10E-04
320	-8.61E-06	-1.02E-04	4.77E-05	5.21E-05	1.62E-04	1.08E-03	-9.62E-05	2.71E-04	-9.05E-05	6.31E-04
330	1.76E-04	-1.42E-04	2.31E-05	7.08E-05	4.66E-05	1.68E-03	-7.15E-05	-1.43E-04	5.53E-05	1.14E-03
340	3.70E-04	-1.45E-04	4.99E-05	1.37E-04	2.52E-05	1.86E-03	-3.10E-05	-4.94E-04	2.24E-04	1.52E-03
350	4.98E-04	-1.18E-04	7.01E-05	1.82E-04	-2.31E-05	2.06E-03	-2.58E-05	-6.87E-04	2.13E-04	1.77E-03

Cp of the rear façade: $Cp_{front} = a_{f1}*H_1 + \ldots. a_{f14}*H_{14} + a_{f15}*L + a_{f16}*W + a_{f17}*Rw + a_{f18}*Rl + a_{f19}*Bg + intercept.$

Orientation	Intercept	H1	H2	H3	H4	H5	H6	H7	H8	H9
0	6.45E-02	-9.34E-04	-4.09E-03	-9.79E-04	-2.19E-04	-1.55E-02	2.42E-04	1.69E-04	-3.09E-04	-6.44E-04
10	7.46E-02	-9.25E-04	-3.40E-03	-9.47E-04	-1.92E-04	-1.51E-02	3.06E-04	2.17E-04	-3.25E-04	-5.90E-04
20	9.70E-02	-8.97E-04	-2.03E-03	-9.20E-04	-2.00E-05	-1.41E-02	3.57E-04	3.06E-04	-3.62E-04	-5.36E-04
30	1.10E-01	-8.43E-04	-8.58E-04	-1.03E-03	1.33E-04	-1.20E-02	3.39E-04	2.48E-04	-4.23E-04	-5.30E-04
40	1.00E-01	-6.42E-04	-1.55E-04	-1.24E-03	1.48E-04	-8.84E-03	2.83E-04	1.60E-04	-3.97E-04	-4.74E-04
50	6.36E-02	-3.22E-04	-1.06E-05	-1.24E-03	1.13E-04	-5.28E-03	9.55E-05	7.91E-05	-4.07E-04	-2.75E-04
60	-2.37E-02	-1.45E-04	-5.78E-05	-3.85E-04	-1.78E-04	-1.93E-03	-8.03E-04	2.36E-04	-2.25E-04	-4.29E-04
70	-7.49E-02	9.54E-05	1.20E-05	1.33E-04	-6.43E-05	-2.36E-04	-1.01E-03	1.95E-05	-1.51E-04	-1.25E-04
80	-1.32E-01	-6.89E-06	4.01E-05	-4.52E-05	-4.84E-05	-9.37E-04	-1.36E-04	-3.97E-06	-9.94E-05	-1.75E-04
90	-2.14E-01	-1.15E-04	8.61E-05	-1.83E-04	-6.61E-05	-2.14E-03	7.80E-06	-8.36E-06	-1.27E-04	-1.91E-04
100	-2.06E-01	-1.79E-04	5.94E-05	-3.20E-04	-8.33E-06	-2.17E-03	8.19E-05	-3.79E-05	-1.36E-04	-1.63E-04
110	-2.02E-01	2.94E-06	4.33E-05	-3.58E-04	-1.74E-05	-1.66E-03	1.45E-04	-1.90E-05	-2.39E-04	-8.05E-05
120	-1.93E-01	8.88E-05	8.27E-05	-2.35E-04	-7.33E-05	-1.15E-03	6.61E-05	7.50E-05	-2.01E-04	-9.19E-05
130	-1.75E-01	-4.16E-05	4.65E-05	-1.44E-05	-6.83E-05	-5.03E-04	-1.82E-05	-1.26E-05	-1.50E-04	6.73E-05
140	-1.62E-01	-7.40E-05	9.82E-06	-3.47E-05	3.16E-05	-4.33E-05	-8.71E-05	-2.68E-05	1.63E-05	8.74E-05
150	-1.50E-01	-4.81E-05	-5.11E-05	-7.03E-05	-5.44E-05	3.96E-04	-8.61E-05	-1.93E-05	3.75E-05	7.30E-06
160	-1.53E-01	-2.67E-05	-1.30E-04	-1.34E-04	-8.24E-05	7.68E-04	-1.28E-04	-3.43E-05	-1.79E-05	-2.91E-05
170	-1.58E-01	3.82E-05	-2.09E-04	-1.94E-04	-4.79E-05	1.01E-03	-1.61E-04	-2.31E-05	-4.36E-05	-6.68E-05
180	-1.60E-01	6.01E-05	-2.35E-04	-2.14E-04	-3.95E-05	1.09E-03	-1.77E-04	-2.54E-05	-6.85E-05	-9.24E-05

Orientation	Intercept	H1	H2	H3	H4	H5	H6	H7	H8	H9
190	-1.58E-01	3.34E-05	-2.05E-04	-1.91E-04	-5.61E-05	9.87E-04	-1.58E-04	-2.74E-05	-3.93E-05	-6.18E-05
200	-1.53E-01	-2.68E-05	-1.21E-04	-1.24E-04	-8.39E-05	7.29E-04	-1.29E-04	-3.03E-05	-1.11E-05	-2.62E-05
210	-1.52E-01	-3.58E-05	-2.30E-05	-7.00E-05	-8.28E-05	3.49E-04	-6.67E-05	-2.62E-05	4.38E-05	5.41E-07
220	-1.52E-01	2.07E-05	9.80E-06	-5.69E-05	-6.32E-05	1.09E-05	-5.26E-05	-1.44E-04	-2.48E-05	-1.50E-06
230	-1.62E-01	-4.74E-05	6.88E-05	4.62E-05	-1.67E-04	-5.34E-04	-7.34E-05	-1.07E-04	-7.75E-05	4.03E-05
240	-1.97E-01	-9.77E-05	5.41E-06	-1.08E-04	-8.34E-05	-1.07E-03	5.13E-05	9.79E-05	-8.58E-05	1.62E-04
250	-2.04E-01	-1.58E-04	8.48E-05	-3.39E-04	-2.39E-05	-1.84E-03	1.90E-04	4.92E-05	-1.09E-04	-2.80E-05
260	-2.00E-01	-2.44E-04	9.02E-05	-3.33E-04	-3.81E-05	-2.32E-03	9.08E-05	1.14E-04	-8.63E-05	-1.38E-04
270	-2.14E-01	-1.27E-04	7.09E-05	-1.68E-04	-6.81E-05	-2.05E-03	1.32E-06	-7.80E-06	-1.24E-04	-2.02E-04
280	-1.31E-01	2.04E-05	1.03E-07	-3.93E-05	-1.61E-04	-8.10E-04	-6.32E-05	5.92E-06	-9.78E-05	-1.70E-04
290	-8.25E-02	-9.61E-05	9.10E-05	2.08E-04	-1.12E-03	-2.27E-04	-1.72E-04	7.93E-05	-3.14E-04	-2.05E-04
300	-4.34E-02	-6.36E-04	1.58E-04	-2.88E-05	-1.24E-03	-2.06E-03	1.09E-04	1.98E-04	-4.11E-04	-2.84E-04
310	5.10E-02	-1.22E-03	1.91E-05	-7.37E-04	-3.67E-04	-5.56E-03	3.60E-04	1.16E-04	-3.22E-04	-3.04E-04
320	7.89E-02	-1.32E-03	-2.78E-04	-7.82E-04	-9.92E-05	-9.17E-03	3.50E-04	2.97E-04	-1.62E-04	-5.93E-04
330	9.63E-02	-9.67E-04	-9.07E-04	-9.40E-04	1.16E-04	-1.22E-02	3.90E-04	3.34E-04	-3.14E-04	-5.27E-04
340	9.51E-02	-8.59E-04	-2.18E-03	-9.47E-04	-2.33E-05	-1.42E-02	3.43E-04	2.75E-04	-3.86E-04	-5.30E-04
350	7.17E-02	-9.28E-04	-3.52E-03	-9.46E-04	-2.01E-04	-1.52E-02	2.96E-04	2.09E-04	-3.25E-04	-5.99E-04

Orientation	H10	H11	H12	H13	H14	W	L	RL	RW	Bg
0	-3.08E-04	2.32E-04	-6.08E-05	-3.95E-04	2.31E-04	2.67E-03	1.53E-04	2.34E-03	2.73E-05	1.12E-02
10	-2.18E-04	2.43E-04	-1.24E-05	-3.53E-04	3.38E-04	2.78E-03	-1.17E-04	2.28E-03	-9.36E-05	1.12E-02
20	-8.64E-05	2.33E-04	2.30E-06	-2.63E-04	4.96E-04	2.67E-03	-6.13E-04	2.08E-03	-2.15E-04	1.11E-02
30	-1.20E-05	1.89E-04	-6.09E-05	-2.55E-04	4.96E-04	2.41E-03	-8.92E-04	1.48E-03	1.22E-04	1.07E-02
40	3.34E-05	1.69E-04	-2.42E-05	-4.11E-04	5.47E-04	1.12E-03	-9.32E-04	8.51E-04	1.82E-04	1.04E-02
50	4.32E-06	8.81E-05	5.06E-05	-2.76E-04	3.46E-04	7.83E-04	-8.77E-04	1.85E-04	3.57E-04	9.25E-03
60	1.85E-05	-1.46E-04	-6.98E-06	-2.03E-04	2.04E-04	1.57E-03	-3.03E-04	-4.09E-05	1.26E-03	5.46E-03
70	-1.52E-05	-9.34E-05	5.30E-06	-1.82E-04	3.74E-05	-7.72E-05	3.72E-04	-3.05E-05	7.72E-04	1.73E-03
80	1.80E-05	-1.12E-04	3.29E-05	-1.54E-05	-1.69E-05	-6.77E-04	5.15E-04	1.40E-04	3.38E-04	3.99E-04
90	5.49E-05	-3.60E-05	5.96E-05	-9.72E-05	4.80E-05	-1.32E-03	4.13E-04	1.90E-04	3.96E-04	1.58E-03
100	-2.98E-05	-1.05E-04	4.09E-06	-1.42E-04	1.06E-04	-8.64E-04	8.78E-05	1.61E-04	2.94E-04	2.82E-03
110	-1.02E-04	-4.72E-05	-5.65E-05	-1.39E-04	7.11E-05	1.84E-04	-1.80E-04	-6.71E-05	3.43E-06	3.30E-03
120	-1.27E-04	2.27E-04	-7.14E-05	-1.38E-04	2.12E-04	6.23E-04	-2.93E-04	-1.36E-04	2.62E-05	3.18E-03
130	-1.70E-04	1.33E-04	-1.57E-05	-7.17E-05	3.87E-04	7.55E-04	-2.76E-04	2.41E-04	-1.31E-04	2.09E-03
140	-3.54E-04	4.41E-05	3.81E-05	-3.75E-05	3.25E-04	5.23E-04	-7.73E-05	6.39E-04	-5.87E-05	3.39E-04
150	-7.53E-04	1.21E-04	1.16E-04	7.56E-06	2.20E-04	4.95E-04	3.56E-05	7.95E-04	9.13E-05	-9.51E-04
160	-1.20E-03	1.87E-04	7.79E-05	1.33E-04	1.50E-04	6.79E-04	1.18E-04	1.08E-03	8.39E-05	-1.56E-03
170	-1.52E-03	2.81E-04	3.60E-05	3.04E-04	9.12E-05	8.58E-04	1.53E-04	1.35E-03	-4.34E-05	-1.97E-03
180	-1.63E-03	3.28E-04	2.26E-05	3.88E-04	6.62E-05	9.84E-04	1.58E-04	1.44E-03	-7.77E-05	-2.16E-03

Orientation	H10	H11	H12	H13	H14	W	L	RL	RW	Bg
190	-1.50E-03	2.72E-04	3.89E-05	2.91E-04	9.58E-05	8.47E-04	1.52E-04	1.32E-03	-3.12E-05	-1.94E-03
200	-1.15E-03	1.83E-04	8.24E-05	1.18E-04	1.55E-04	6.78E-04	1.12E-04	1.04E-03	9.40E-05	-1.52E-03
210	-6.91E-04	1.63E-04	1.61E-04	-2.32E-05	2.30E-04	5.02E-04	2.58E-05	7.02E-04	1.46E-04	-8.92E-04
220	-2.49E-04	1.13E-05	3.26E-04	-1.72E-04	2.16E-04	2.67E-04	-1.41E-04	5.59E-04	-2.09E-05	4.33E-04
230	-9.71E-05	-7.86E-05	2.01E-04	-1.57E-04	1.20E-04	4.51E-04	-2.87E-04	9.97E-05	-8.01E-05	2.09E-03
240	-2.12E-04	-1.24E-04	4.37E-05	-1.59E-04	1.78E-04	5.83E-04	-3.06E-04	-1.56E-04	2.53E-04	3.21E-03
250	-1.04E-04	-5.61E-05	-3.01E-05	-1.18E-04	1.42E-04	2.60E-04	-1.70E-04	-2.31E-04	2.25E-04	2.98E-03
260	6.56E-05	-6.98E-06	-2.74E-05	-1.79E-04	1.20E-04	-8.14E-04	9.37E-05	-1.77E-04	3.64E-04	2.57E-03
270	5.90E-05	-5.88E-05	5.97E-05	-9.05E-05	3.92E-05	-1.35E-03	4.41E-04	2.15E-04	4.05E-04	1.46E-03
280	4.22E-05	-1.11E-04	4.96E-05	1.65E-05	-2.88E-05	-7.18E-04	5.23E-04	6.95E-05	3.10E-04	3.80E-04
290	5.26E-05	-1.99E-04	4.83E-05	-2.26E-04	4.64E-05	-2.24E-04	3.90E-04	-1.23E-05	9.92E-04	2.25E-03
300	-1.21E-04	-1.50E-04	7.98E-05	-3.55E-04	4.56E-04	1.81E-03	-2.88E-04	2.58E-04	1.43E-03	5.54E-03
310	-1.16E-04	1.34E-04	5.34E-05	-3.27E-04	5.45E-04	1.57E-03	-8.51E-04	3.18E-04	6.73E-04	8.85E-03
320	1.65E-04	1.28E-04	3.68E-05	-3.69E-04	5.81E-04	1.84E-03	-9.32E-04	6.69E-04	6.34E-04	1.07E-02
330	2.77E-05	2.00E-04	-3.97E-05	-2.45E-04	6.05E-04	2.56E-03	-8.83E-04	1.46E-03	1.30E-04	1.08E-02
340	-1.06E-04	2.20E-04	-3.12E-06	-2.66E-04	4.60E-04	2.67E-03	-5.64E-04	2.13E-03	-2.36E-04	1.11E-02
350	-2.33E-04	2.40E-04	-1.60E-05	-3.58E-04	3.23E-04	2.77E-03	-7.12E-05	2.29E-03	-7.57E-05	1.12E-02

Cp of the roof: $Cp_{front} = a_{f1}*H_1 + \ldots. a_{f14}*H_{14} + a_{f15}*L + a_{f16}*W + a_{f17}*Rw + a_{f18}*Rl + a_{f19}*Bg + intercept.$

Orientation	Intercept	H1	H2	H3	H4	H5	H6	H7	H8	H9
0	-4.12E-01	3.93E-04	2.87E-03	5.90E-04	-2.61E-04	1.44E-03	3.33E-05	4.55E-04	4.66E-04	6.89E-04
10	-4.13E-01	3.62E-04	2.33E-03	5.01E-04	-2.68E-04	1.43E-03	-1.85E-05	3.76E-04	5.04E-04	5.81E-04
20	-4.24E-01	3.26E-04	1.39E-03	4.31E-04	-3.60E-04	1.35E-03	-6.55E-05	2.50E-04	5.50E-04	4.33E-04
30	-4.37E-01	3.20E-04	6.40E-04	5.01E-04	-3.54E-04	1.03E-03	-1.66E-04	2.13E-04	4.86E-04	2.97E-04
40	-4.39E-01	3.54E-05	1.60E-06	7.64E-04	-3.28E-04	7.36E-04	-1.24E-04	1.87E-05	4.07E-04	1.22E-04
50	-4.13E-01	9.46E-07	9.64E-06	7.78E-04	6.74E-05	5.49E-04	2.32E-04	-2.47E-04	1.44E-04	1.40E-04
60	-3.81E-01	1.20E-04	-2.14E-04	3.09E-04	8.63E-05	-2.69E-05	9.21E-04	-1.39E-04	7.04E-05	-2.19E-05
70	-3.32E-01	-3.46E-05	-9.61E-05	5.17E-05	-1.09E-04	-6.93E-05	5.05E-04	-1.40E-04	-6.10E-05	-1.50E-04
80	-2.17E-01	5.84E-05	6.02E-05	-7.24E-05	-9.33E-06	2.55E-05	5.05E-05	-6.45E-05	-1.83E-04	-7.15E-05
90	-2.04E-01	6.49E-05	5.81E-05	-1.60E-04	5.31E-05	2.75E-04	1.11E-04	-1.18E-04	-1.24E-04	-2.33E-05
100	-2.13E-01	6.11E-05	8.72E-05	-8.22E-05	4.61E-05	7.29E-05	-1.02E-05	-4.61E-05	-1.25E-04	-3.62E-05
110	-3.00E-01	-3.76E-05	-5.70E-05	-4.51E-05	2.83E-05	4.04E-05	-1.77E-04	-9.06E-05	-1.89E-04	-9.09E-05
120	-3.42E-01	-1.55E-04	-1.34E-04	-1.93E-04	3.61E-05	2.91E-05	-8.67E-05	4.40E-05	-2.23E-04	1.10E-04
130	-3.94E-01	-4.15E-04	-2.88E-04	-2.23E-04	2.26E-04	1.35E-05	1.21E-05	1.91E-04	3.63E-04	2.80E-04
140	-4.11E-01	-2.31E-04	-3.41E-04	-2.23E-04	-4.81E-05	-5.58E-05	7.14E-05	3.28E-04	3.03E-04	5.39E-05
150	-4.27E-01	-3.04E-04	-2.30E-04	-1.07E-04	-3.26E-04	-8.45E-05	-1.20E-04	2.09E-04	1.33E-04	1.35E-04
160	-3.95E-01	-2.66E-04	-3.89E-04	-2.88E-04	-3.86E-04	-4.11E-05	-3.63E-04	2.66E-04	1.23E-04	1.60E-04
170	-3.71E-01	-2.56E-04	-4.40E-04	-4.30E-04	-4.06E-04	-9.59E-05	-3.42E-04	3.16E-04	1.38E-04	1.60E-04
180	-3.65E-01	-2.70E-04	-4.36E-04	-4.62E-04	-4.20E-04	-1.39E-04	-2.81E-04	3.30E-04	1.92E-04	1.66E-04

Orientation	Intercept	H1	H2	H3	H4	H5	H6	H7	H8	H9
190	-3.74E-01	-2.55E-04	-4.43E-04	-4.22E-04	-4.07E-04	-8.91E-05	-3.47E-04	3.13E-04	1.35E-04	1.61E-04
200	-4.00E-01	-2.66E-04	-3.74E-04	-2.70E-04	-3.86E-04	-3.69E-05	-3.50E-04	2.52E-04	1.18E-04	1.68E-04
210	-4.32E-01	-3.15E-04	-2.32E-04	-1.61E-04	-3.87E-04	-7.08E-05	-1.13E-04	2.73E-04	1.60E-04	5.54E-05
220	-4.04E-01	-1.88E-04	-3.47E-04	-1.83E-04	7.84E-05	-2.38E-05	-2.67E-05	1.22E-04	2.67E-04	3.42E-05
230	-3.49E-01	1.29E-05	-1.48E-04	-8.90E-05	2.02E-04	-7.63E-05	5.59E-06	-3.92E-04	2.57E-05	3.94E-04
240	-3.75E-01	-8.53E-05	-2.02E-04	1.25E-04	1.82E-04	1.15E-04	-1.99E-04	-1.89E-04	-1.18E-05	8.76E-04
250	-3.07E-01	-1.64E-04	-6.81E-05	-9.13E-06	2.34E-05	1.63E-04	-1.02E-04	3.02E-06	-5.57E-05	3.88E-04
260	-2.11E-01	3.83E-05	9.71E-05	-8.07E-05	4.01E-05	4.76E-05	1.61E-05	-5.01E-05	-1.21E-04	-5.14E-05
270	-1.93E-01	-1.26E-04	3.52E-05	-8.72E-05	3.21E-06	-7.64E-06	2.67E-05	7.26E-05	-1.09E-04	1.15E-05
280	-2.22E-01	3.42E-05	7.72E-05	-6.31E-05	-3.78E-05	-4.68E-06	7.00E-05	-6.57E-05	-1.59E-04	-8.64E-05
290	-3.26E-01	-6.97E-05	-8.63E-05	-2.31E-05	4.31E-04	1.84E-05	-2.94E-05	-4.50E-05	-6.06E-05	-2.32E-04
300	-3.33E-01	4.37E-04	-4.87E-04	-1.88E-04	6.06E-04	-3.51E-05	-2.97E-04	1.05E-04	1.41E-04	-4.30E-04
310	-4.08E-01	8.48E-04	-1.94E-04	1.34E-04	7.81E-05	4.28E-04	-9.80E-05	1.58E-04	5.27E-04	-1.56E-05
320	-4.42E-01	7.71E-04	1.36E-04	2.86E-04	-9.78E-05	7.25E-04	1.08E-05	1.98E-04	4.99E-04	2.87E-04
330	-4.24E-01	4.47E-04	6.71E-04	4.01E-04	-3.36E-04	1.04E-03	-1.70E-04	1.46E-04	4.30E-04	3.30E-04
340	-4.21E-01	2.92E-04	1.48E-03	4.53E-04	-3.62E-04	1.37E-03	-5.27E-05	2.76E-04	5.48E-04	4.40E-04
350	-4.12E-01	3.69E-04	2.42E-03	5.14E-04	-2.60E-04	1.44E-03	-1.29E-05	3.88E-04	5.00E-04	5.99E-04

Orientation	H10	H11	H12	H13	H14	W	L	RL	RW	BG
0	1.50E-04	-3.34E-04	7.78E-05	-1.14E-05	-1.42E-04	3.95E-03	1.99E-04	-6.58E-04	1.04E-04	-2.26E-03
10	4.95E-05	-3.62E-04	1.05E-05	4.81E-05	-1.83E-04	4.15E-03	3.41E-04	-5.45E-04	1.72E-04	-2.39E-03
20	-5.67E-05	-3.47E-04	-1.80E-05	9.08E-05	-1.64E-04	4.84E-03	5.27E-04	-3.67E-04	2.59E-04	-2.47E-03
30	-3.36E-05	-2.56E-04	3.77E-05	6.83E-05	-4.15E-05	6.29E-03	4.88E-04	-1.13E-05	8.21E-05	-2.25E-03
40	-3.39E-05	-2.87E-04	6.31E-05	4.02E-05	7.51E-05	8.38E-03	3.32E-04	5.75E-04	-2.87E-05	-2.38E-03
50	-1.92E-04	-6.03E-05	5.22E-05	-9.15E-05	2.75E-04	8.35E-03	1.54E-04	4.17E-04	-6.50E-04	-1.27E-03
60	-1.27E-04	1.05E-04	-7.35E-05	-2.04E-04	9.70E-05	8.60E-03	-1.69E-04	2.61E-04	-4.23E-04	4.24E-04
70	-3.62E-05	-3.83E-05	-8.54E-05	-4.66E-05	1.43E-04	6.83E-03	1.42E-05	5.79E-04	2.71E-04	1.98E-04
80	-4.92E-05	-6.00E-05	-9.37E-06	-5.52E-05	-1.49E-05	5.63E-04	1.94E-04	2.41E-04	1.81E-04	3.98E-04
90	-1.76E-04	-1.75E-04	-1.00E-04	-1.05E-04	-2.62E-05	9.14E-04	6.63E-05	6.39E-05	6.11E-05	5.45E-04
100	-1.37E-04	-8.90E-05	-5.24E-06	-7.50E-05	-2.85E-05	6.37E-04	1.19E-04	-1.73E-06	2.11E-04	6.25E-04
110	-8.52E-05	4.62E-04	-6.68E-05	-1.34E-04	-5.16E-05	6.31E-03	-5.47E-06	-4.10E-04	-8.92E-05	9.15E-04
120	-3.93E-04	9.39E-04	8.46E-05	-2.96E-04	5.61E-04	8.52E-03	-2.13E-04	-5.39E-04	-7.49E-04	4.87E-04
130	-4.74E-05	5.51E-04	-1.35E-06	-4.91E-04	1.07E-03	9.05E-03	3.54E-05	-1.02E-03	-1.02E-03	6.86E-05
140	7.49E-04	2.51E-04	-3.01E-05	-1.39E-04	7.73E-04	8.16E-03	3.46E-04	-1.27E-03	-7.36E-04	-7.93E-04
150	1.31E-03	1.48E-04	-9.40E-05	4.47E-04	1.51E-04	7.20E-03	7.16E-04	-1.95E-03	-9.69E-05	-8.15E-04
160	1.73E-03	1.80E-05	-2.03E-04	1.30E-03	1.15E-05	5.73E-03	6.68E-04	-1.99E-03	-1.44E-04	-9.71E-04
170	1.92E-03	8.34E-05	-2.99E-04	2.27E-03	9.35E-05	5.28E-03	3.87E-04	-1.74E-03	-2.93E-04	-1.26E-03
180	1.98E-03	1.40E-04	-3.42E-04	2.69E-03	1.46E-04	5.28E-03	2.43E-04	-1.64E-03	-2.64E-04	-1.48E-03

Orientation	H10	H11	H12	H13	H14	W	L	RL	RW	BG
190	1.92E-03	7.58E-05	-2.87E-04	2.19E-03	8.35E-05	5.33E-03	4.13E-04	-1.77E-03	-2.92E-04	-1.23E-03
200	1.71E-03	2.62E-05	-2.21E-04	1.19E-03	3.12E-05	5.89E-03	6.90E-04	-2.00E-03	-1.15E-04	-1.01E-03
210	1.08E-03	2.50E-04	-4.51E-05	4.03E-04	1.35E-04	7.38E-03	7.15E-04	-1.80E-03	-1.50E-04	-6.59E-04
220	7.46E-04	2.57E-04	6.10E-04	-1.98E-04	2.71E-04	7.94E-03	3.24E-04	-1.21E-03	-8.82E-04	-7.98E-04
230	2.46E-04	-6.82E-05	1.04E-03	-2.87E-04	3.52E-05	8.35E-03	-1.03E-04	-8.43E-04	-1.58E-03	-4.07E-04
240	-1.57E-04	3.87E-05	3.97E-04	-4.01E-04	1.33E-04	8.70E-03	-2.88E-04	-4.94E-05	-6.24E-05	6.33E-04
250	-2.00E-04	-6.59E-05	-8.26E-05	-1.92E-04	2.77E-05	6.38E-03	-6.12E-05	-2.45E-04	6.78E-05	8.10E-04
260	-1.30E-04	-6.55E-05	-9.94E-06	-5.47E-05	-1.82E-05	6.15E-04	1.18E-04	-3.87E-05	2.16E-04	5.61E-04
270	6.45E-06	-3.96E-05	-9.90E-05	-1.58E-04	6.16E-05	8.24E-04	6.67E-05	-4.79E-04	3.31E-04	2.59E-04
280	-3.21E-05	-4.52E-05	5.62E-06	-4.92E-05	8.14E-07	5.85E-04	2.20E-04	2.74E-04	2.31E-04	3.56E-04
290	6.42E-05	-7.02E-05	1.12E-04	-1.12E-04	8.79E-05	6.59E-03	1.05E-05	7.47E-04	2.01E-05	4.46E-05
300	-4.57E-05	5.33E-05	8.96E-05	1.42E-04	-3.51E-05	7.36E-03	-1.94E-04	3.69E-04	-4.80E-04	-1.62E-04
310	1.77E-05	-5.16E-05	2.30E-05	4.99E-05	2.36E-06	8.03E-03	1.80E-04	2.84E-04	-8.98E-04	-1.12E-03
320	1.11E-05	-2.25E-04	-3.68E-05	1.99E-05	1.59E-04	7.83E-03	3.06E-04	5.65E-04	-4.57E-04	-2.23E-03
330	-9.81E-05	-2.63E-04	-7.73E-06	5.63E-05	-1.50E-04	6.02E-03	5.00E-04	3.75E-05	-8.43E-05	-2.28E-03
340	-5.99E-05	-3.44E-04	-1.10E-05	9.77E-05	-1.67E-04	4.72E-03	5.15E-04	-3.94E-04	2.72E-04	-2.47E-03
350	6.14E-05	-3.56E-04	1.68E-05	4.03E-05	-1.76E-04	4.09E-03	3.19E-04	-5.76E-04	1.65E-04	-2.37E-03

LIST OF TABLES AND FIGURES

LIST FIGURES

Figure 1.1	Typical Small private housing projects.	5
Figure 1.2	Typical large scale housing projects in Can Tho city.	6
Figure 1.3	The dissertation structure.	11
Figure 2-1	GDP per capita (current US$) of Vietnam which has an average growth rate of 13.3%, source of World Bank, 2015).	15
Figure 2-2	Total population of Vietnam. Source: World Bank, 2014.	16
Figure 2-3	Illustrating the urbanization progress of the South area of Cantho city using Google Earth from 2003 to 2017.	17
Figure 2-4	Map of household size by province in Vietnam, 2009 [2]	18
Figure 2-5	Household size by region in Vietnam, 2009, [1]	19
Figure 2-6	Typical structure of a new large scale housing project (Construction company Number 8 (CIC8) Viet Nam, http://cic8.com.	19
Figure 2-7	The win–win–win approach to public private partnerships.	21
Figure 2-8	Köppen-Geiger climate classification map of Asia [9]	23
Figure 2-9	Hourly temperature at Cantho city, relative humidity, radiation and Olgay' Comfort chart, TMY.	25
Figure 2-10	Bangkok's temperature hourly, relative humidity, radiation and Olgay' Comfort chart, TMY..	27
Figure 2-11	Hanoi's temperature hourly, relative humidity, radiation and Olgyay' Comfort chart, TMY.	29
Figure 2-12	Frequency of wind speed and wind direction per month, Cantho, Vietnam	31
Figure 2-13	Housing types in rural areas in Mekong Delta	32
Figure 2-14	Detached houses in Mekong Delta, [12]	33
Figure 2-15	Terraced houses in new urban areas at South Cantho and Cai Khe.	33
Figure 2-16	Detached house in urban areas, Khuong Island, Cantho	34
Figure 2-17	Front façade and section of Tay Nguyen Plaza Cantho, 2013	34
Figure 2-18	Five floor apartment 91B and public facilities, Ninh Kieu, Cantho.	35
Figure 2-19	Public space in the large scale housing projects, Nam Long, Cantho	36
Figure 2-20	Possible urban density on an 8,000 sqm-site dependent on building typology, [14]	36
Figure 2-21	Different cross sections of some road types in the large scale housing projects.	38

Figure 2-22	A large scale housing project at South Cantho city [16] p.156.	39
Figure 2-23	The cut and fill strategy, protection of sensitive eco-systems and creation of mineral platforms for urbanization need work carefully with the existing topography, soil and water conditions [16] p.78.	39
Figure 3-1	Hierarchical structural tree of building elements [3].	44
Figure 3-2	The element structure of a building [3]	45
Figure 3-3	Building elements of different levels [6]	46
Figure 3-4	Present value of 1,000 money units at moment tfor different discount rates.	48
Figure 3-5	Pareto set for maximization quality and minimization of costs	49
Figure 4.1	Small model of the large housing projects.	57
Figure 4.2	Representations depicting the process that large scale housing projects undergo.	58
Figure 4.3	Schematic graph of dwelling types (detached, terraced and apartment)	59
Figure 4.4	Typical example of street typology, setback and cross section of a terraced house	59
Figure 4.5	Real street pattern and building typology in the large scale housing project, named the 586 project, Cantho city [1]	60
Figure 4.6	Global impression of housing types: terraced, detached houses and apartments collected from different locations.	61
Figure 4.7	Cross section and view of typical terraced units in Cantho [1]	62
Figure 4.8	Typical detached unit (Nam Long, D2-26 Street 10, 510m^2)	62
Figure 4.9	Typical high rise (1,545sqm, 772m^2, 49.9% built-up density, 19 floors, 7.54 ratio between total floor area and residential area, 156 housing units, H=50m, 566 people)	62
Figure 4.10	Terraced houses in the large scale housing project 91B, Cantho.	63
Figure 4.11	a) Terraced houses do not have shared external walls because they were built at a different time. b) Terraces with external walls are shared by neighbours.	64
Figure 4.12	Urban form of terraced house, “Tube House” constructed at different times.	65
Figure 4.13	Characteristics of urban form of terraced house, “Tube House” constructed at different times.	66
Figure 4.14	Urban form of terraced houses which were constructed at the same time, (L=60m, D=20m, Rl=6m, Rw=8m).	66
Figure 4.15	Characteristics of urban forms of terraced houses which were constructed at the same time.	67
Figure 4.16	Five floor apartment in the large scale housing project 91B and apartment 21 floors at Cantho.	68
Figure 4.17	Urban form of apartment (5 floors, L=50m, W=18m, Rl = 12, Rw =16m); (Plot: W=30, L=70m)	68

Figure 4.18	Apartment with 5 floors.	69
Figure 4.19	Detached house in Nam Long project, Cantho	70
Figure 4.20	Urban form of detached houses.	70
Figure 4.21	A three-floor detached house.	71
Figure 4.22	Initial cost per m^2 floor area, including land and infrastructure systems	72
Figure 4.23	The large scale housing project, before and after [1].	72
Figure 4.24	Filled sand at a housing projects at Cantho [1]	73
Figure 5-1	Cost $ per square meter of gross floor area vs. height (Hong Kong) [3]	80
Figure 5-2	Small melaleuca wood piles. Melaleuca grows very fast in The Mekong Delta.	81
Figure 5-3	Installing reinforced concrete piles using the compression approach.	81
Figure 5-4	Large diameter pile foundations for heavy structures.	82
Figure 5-5	Structural systems categories [19].	83
Figure 5-6	Analysis procedure of the pile foundation cost model.	85
Figure 5-7	The optimal length pile based on soil capacity; P_{soil} 25 x 25 cm: the pile capacity based on soil properties for pile with section 25 x 25 cm; P_{pile} 25 x 25 cm: the pile capacity based on reinforced concrete piles with section 25 x 25 cm.)	86
Figure 5-8	Optimal depth or capacity of different pile sections. P_s 25: the pile capacity based on soil properties for pile with section 25 x 25 cm; P_p 25: the pile capacity based on reinforced concrete piles with section 25 x 25 cm.)	87
Figure 5-9	Here, α1 is the modification factor for span length, α2 is the modification factor for number of spans and α3 is the modification factor for amount of infill.	88
Figure 5-10	Three methods for estimating building periods related to their heights	89
Figure 5-11	Influence of exposure terrain on variation of wind velocity with height. Exposure D: Flat, unobstructed areas and water surfaces outside hurricane-pone regions; Exposure C: open terrain; Exposure B: urban and suburban terrain.	91
Figure 5-12	The wind load and vertical axial forces of columns at the ground floor with or without the shear lag phenomenon.	91
Figure 5-13	Key parameters in design response spectrum [33].	92
Figure 5-14	Recommended elastic response spectra for ground types A to E (5% damping), [28]. The circles on curve E are different natural periods of the different building heights, $T=0.075 * H^{\wedge 0.75}$, (Eurocode 8 [28].	94
Figure 5-15	Ground acceleration (m/s^2) zone map of Vietnam [35]. The study area is located in zone Imax = 7 and Imax ≤ 6.	95

Figure 5-16	The seismic load and vertical axial forces of columns at the ground floor with or without the shear lag phenomenon.	96
Figure 5-17	In the rigid frame, the axial force distribution under horizontal loads (right) is affected by shear lag phenomenon when the horizontal loads are transferred to vertical axial forces at the foundation level. D is the depth and W is the width of the building.	97
Figure 5-18	Distribution of axial forces from the lateral loads with and without shear lag effect. a) distribution axial forces from dead, live and lateral loads and total axial load; b) axial force of lateral loads without the shear lag effect; c) axial force of lateral loads with the shear lag effect, result from the finite element method.	98
Figure 5-19	The rigid frames are applied the horizontal loads in order to obtain correction factor for shear lag effect. Shear lag effect of 5 rigid bays, 25 floors, 6m bay and 3.6m floor height is analysed by a finite element method.	98
Figure 5-20	Shear lag effect of rigid 7 bays, 25 floors, 6m bay and 3.6m floor height. Axial forces of frame. Total loads with shear lag effect are smaller than total loads with true cantilever.	99
Figure 5-21	Correction factor for shear lag in the rigid frames: Y = 1.39 - 0.0075*X; X is the number of floors. The approximate calculation is selected on the safe side of the correction factors.	100
Figure 5-22	The optimal pile capacity based on both the soil and structural properties (Ps: soil bearing capacity of the pile, Pp: capacity of the pile based on reinforced concrete structure).	100
Figure 5-23	Cost of one ton capacity of the optimal pile foundation at Cantho.	101
Figure 5-24	Cost of one ton capacity of pile foundation at five places in Cantho.	101
Figure 5-25	The wind load generates the moment at the foundation level and the moment is converted to the vertical loads on piles of the building's width: 42m.	102
Figure 5-26	Moment of the seismic load at the foundation level. T_B and T_C are the lower and upper limit the period of the constant spectral acceleration branch. T_D value is the definition of the beginning of the constant displacement response range of the spectrum.	103
Figure 5-27	Vertical loads on foundation (kg/sq.m floor area) has	104
Figure 5-28	Total vertical load per square meter floor area (dead, live, wind and seismic loads) for different building depths and heights are appropriately calculated by the formula.	105
Figure 5-29	The cost of pile foundation per one square meter floor area is evaluated with the pile foundation cost 70$/ton capacity.	106
Figure 5-30	The cost of land and pile foundation per one square meter floor area. Land cost = 100$/sqm; Pile cost = 70$/ton.	106
Figure 5-31	Sensitivity analysis of four parameters.	107
Figure 5-32	Sensitivity of four parameters are ranked by using SimLab or R, the higher absolute value on the horizontal axis indicates the higher impact level of the parameter. A negative sign of the other	

	parameters means that when we increase the parameter, the outputs decreases. Sensitivity values are dimensionless and vary between -1 to 1.	108
Figure 6.1	Price of land versus width of plot, utility function: $y = \sum a * x^b + e$ and $(0<b<1)$; or $\ln(y) = \sum(\ln(a) + b * \ln(x)) + e$.	116
Figure 6.2	Selling price of land is related to width and depth of plot by a power function.	117
Figure 6.3	Cost and profit of residential plots.	117
Figure 6.4	Graphical representation of price and cost with two parameters: width and depth of plot.	118
Figure 6.5	Decision based on preferences and designs flowchart	119
Figure 6.6	Comparison between predicted price and actual prices of two utility functions, (1$ = 20,000 VNĐ). Two regression functions are almost the same R-squared values.	124
Figure 6.7	Profit maximizations with two Pareto fronts. Alternative E brings the highest profit to the developers, (1$ = 20,000 VNĐ).	125
Figure 6.8	Layout properties, Multi-Objective maximizations of the Pareto sub optimal points.	126
Figure 6.9	Land price and profit of two Pareto fronts, (1$ = 20,000 VNĐ).	126
Figure 6.10	Subsidy is a tax reductions, subsidy or provisions of infrastructure to improve profit for the developers, (1$ = 20,000 VNĐ).	127
Figure 8-1	The increased trend of the number of optimization studies in building science [2].	186
Figure 8-2	Use frequency of different optimization algorithms, the result was derived from more than 200 building optimization studies [2].	187
Figure 8-3	Depiction of the velocity and position updates in PSO modified from[12].	189
Figure 8-4	Flow diagram illustrating the particle swarm optimization algorithm	190
Figure 8-5	The pattern search (Hooke-Jeeves) looks for local optimal solution after PSO algorithm within smaller steps after identifying the global best with the initial parameter steps.	191
Figure 8-6	The hybrid algorithm is capable of working efficiently since it performs a global search by the particle swarm optimization and the Hooke–Jeeves algorithm then searches for a local optimization.	192
Figure 8-7	The optimization results of the terraced house with the thermal comfort limit PMV = 0.5.	193
Figure 8-8	The optimization results of the detached house with the thermal comfort limit PMV = 0.5.	193
Figure 8-9	The optimization results of the apartment building with the thermal comfort limit PMV = 0.5.	194
Figure 8-10	Seven trails of the optimization processes using the terraced house model.	195

Figure 8-11	Link between different sub-models, models with "(*)" have been developed or extended by the author.	196
Figure 8-12	Pareto set for the maximization of quality and for the minimization of costs	199
Figure 8-13	Pareto front visualization for solution and parallel coordinates.	200
Figure 8-14	Urban form or terraced house type	201
Figure 8-15	Optimization effectiveness using the particle swarm optimization and Hooke-Jeeves algorithms and Pareto front based on optimization results.	203
Figure 8-16	Deferent design alternatives of three thermal comfort levels (Maximum PMV = 1.5, 1.0 and 1.5)	204
Figure 8-17	Energy use for thermal comfort requirements in case of the terraced house.	204
Figure 8-18	*Parallel coordinates of the optimization results (with PMV maximum 0.5) balancing IC (Initial construction Cost) and LCC (Life Cycle Cost).*	205
Figure 8-19	The ventilation and infiltration volume of the living room and the bed room of the terraced house.	207
Figure 8-20	The energy use related to occupant behaviour during the year of the terraced house. User behaviour schedules as tool to be included in the optimization	208
Figure 8-21	The indoor and outdoor temperature of a living room for one year (2-3 March).	209
Figure 8-22	Sensitivity ranking via SRC – LCC of terraced house.	211
Figure 8-23	Sensitivity ranking via SRC – EC of terraced house.	212
Figure 8-24	Geometry of detached houses and urban configuration.	213
Figure 8-25	Detached houses, initial construction and land cost versus life cycle cost and land cost.	216
Figure 8-26	Energy saving for reducing thermal comfort ranges of detached houses, for 60 year period.	217
Figure 8-27	Window and overhang sizes of detached house of three PMV ranges. Their orientations are 0° for PMV=±0.5 and 300°.	217
Figure 8-28	the Pareto front and the parallel coordinate of the optimization results (with PMV maximum 0.5) balancing IC (Initial construction Cost) and LCC (Life Cycle Cost) of the detached house.	218
Figure 8-29	The ventilation and infiltration volume of the living room and the bed room of the detached house.	219
Figure 8-30	The energy use related to occupant behaviour during the year of the detached house.	221
Figure 8-31	Sensitivity ranking via SRC – LCC including land cost and infrastructure cost.	222
Figure 8-32	Sensitivity ranking via SRC – Energy use of a detached house.	223

Figure 8-33	Apartment building urban pattern	224
Figure 8-34	Apartment house, initial construction and land cost versus life cycle cost and land cost.	227
Figure 8-35	The Pareto front and the parallel coordinate of the optimization results of the apartment.	227
Figure 8-36	Energy saving for reducing thermal comfort ranges of apartments.	228
Figure 8-37	Window and overhang sizes of apartment of three PMV ranges of the optimal results.	228
Figure 8-38	The infiltration volume of the living room and the bed room of the apartment.	229
Figure 8-39	The energy use related to occupant behaviour during the year of the apartment.	230
Figure 8-40	Sensitivity ranking via SRC – LCC and Land of apartment.	231
Figure 8-41	Sensitivity ranking via SRC – Energy use of apartment.	231
Figure 8-42	Costs of main components in three housing types.	232
Figure 8-43	Life cycle cost without the infrastructure and the land use cost.	233
Figure 8-44	The energy cost per square meter floor area for 60 year period of different equipment.	234
Figure 8-45	Energy use of the cooling and the fans of the terraced house	234
Figure 8-46	Energy use of the cooling and the fans of the Detached house	235
Figure 8-47	Energy use of the cooling and the fans of the apartment	235

LIST OF TABLES

Table 1.1	Distribution of employment by sector, 2000 - 2007 (%)	4
Table 4.1	Input parameters of terraced house without shared walls	64
Table 4.2	Input parameters of terraced houses with shared walls.	65
Table 4.3	Input parameters of apartment.	68
Table 4.4	Input parameters of detached house.	70
Table 5-1	Slenderness ratio of piles, M. Jacobson	86
Table 5-2	The values of S, T_B, T_C and T_D of the elastic response spectra	94
Table 6.1	Attributes of residential land for detached and terraced housing unites	122
Table 6.2	Attribute selection by using multiple linear regression method	122
Table 6.3	Descriptive statistics of the land attributes	123
Table 7-1	Six factors take into consideration when designing for thermal comfort	136
Table 7-2	non-air conditioned buildings in warm climates	137
Table 7-3	Predicted Mean Vote sensation scale, the recommended acceptable PMV range for thermal comfort from ASHRAE 55 is between -0.5 and +0.5 for an interior space.	137
Table 7-4	Numerical variables and their design options for urban layout (continuous variables).	144
Table 7-5	Input template text file for Cp Generator TNO	145
Table 7-6	Numerical variables and their design options of urban forms.	148
Table 7-7	Numerical variables and their design options for urban layout (continuous variables).	156
Table 7-8	Range of input parameters of Cp model.	158
Table 7-9	Factors of 12 regression formulas of 30° orientations of the detached and semi-detached houses.	158
Table 7-10	Range of input parameters of Cp model.	160
Table 7-11	Factors of 12 regression formulas of 30° orientations of apartment buildings.	160
Table 7-12	Other costs and fees	163
Table 7-13	Design options and strategies (discrete variables).	164
Table 7-14	Numerical variables and their design options (continuous variables).	165
Table 7-15	Parameter values of detached house	165
Table 8-1	Optimization programs are applied to building performance optimization based on [3].	186
Table 8-2	Setting in the Command File of the GenOpt	197

Table 8-3	The neighbourhood and building geometry of the terraced house.	202
Table 8-4	Lowest LCC for the neighbourhood of the terraced house, based on optimization process.	210
Table 8-5	The urban and building geometry of the detached house.	213
Table 8-6	Optimization result for the neighbourhood and building geometry of the detached house.	214
Table 8-7	Optimization results for the construction elements of detached house	215
Table 8-8	The neighbourhood and building geometry of the apartment house.	223
Table 8-9	Optimization result for the neighbourhood and building geometry of the apartment house.	225
Table 8-10	Optimization results for the construction elements	225

Publications

Articles in internationally reviewed academic journals

Nguyen Van, T., Nguyen Hieu, T., De Troyer, F. (2016). Managing Pile Foundation and Land Cost for High Rise Buildings in the Early Design Stages. Architectural Engineering and Design Management, 12 (3), 151-169.

Papers at international scientific conferences and symposia, published in full in proceedings

Miyamoto, A., Trigaux, D., **Nguyen Van, T**., Allacker, K., De Troyer, F. (2016). *Support tool for energy efficient design: from a simple tool in the early design phase to dynamic simulations in a later design stage. SBE16, Sustainable Built Environment: Expanding Boundaries: Systems Thinking in the Built Environment, Zurich 13–17 June 2016.*

Miyamoto, A., **Nguyen Van, T**., Trigaux, D., Allacker, K., De Troyer, F. (2015). *Visualisation tool to estimate the effect of design parameters on heating demand in the early design phases*. 31th International PLEA Conference Passive Low Energy Architecture at Bologna, Italy, 09-11 September 2015.

Nguyen Van, T., Trigaux, D., Allacker, K., De Troyer, F. (2014). *Optimization for Passive Design of Large Scale Housing Projects for Energy and Thermal Comfort in a Hot and Humid Climate*. In Rawal, R. (Ed.), Manu, S. (Ed.), Khadpekar, N. (Ed.), Sustainable habitat for developing societies: Vol. 1 (1).30th International PLEA Conference. Ahmedabad, 16-18 December 2014 (pp. 21-21). Ahmedabad, India: CEPT UNIVERSITY PRESS.

Nguyen Van, T., Miyamoto, A., Trigaux, D., & De Troyer, F. (2014). *Cost and comfort optimisation for buildings and urban layouts by combining dynamic energy simulations and generic optimisation tools*. Eco-Architecture V (pp. 81–92). Presented at the ECO-ARCHITECTURE V, Harmonisation Between Architecture and Nature, SIENA, Italy: WIT Press.

Nguyen Van, T., De Troyer, F. (2013). *Deriving Housing Preferences from advertising on the web for improving decision making by Economic and Social actors*. (ISBN: 9789078862062). RC43 conference 2013, "At home in the housing market". Amsterdam University, 10-12 July 2013 (pp. 104-114).

Meeting abstracts, presented at other scientific conferences and symposia, published or not published in proceedings or journals

Miyamoto, A., **Nguyen Van, T**., Trigaux, D., Allacker, K., De Troyer, F. (2015). Parallel coordinates visualization of energy demand estimation in the early design stages. DS2BE. Brussels, 29-30 April 2015.

Nguyen Van T., Trigaux D., Allacker K., De Troyer F. (2014). Optimization for Passive Design of Large Scale Housing Projects for Energy and Thermal Comfort in a Hot and Humid Climate. Sustainable habitat for developing societies: vol. 1 (1). 30th International PLEA Conference. Ahmedabad, 16-18 December 2014, 21-21.

Meeting abstracts, presented at other scientific conferences and symposia, published or not published in proceedings or journals

Miyamoto A., **Nguyen Van T**., Trigaux D., Allacker K., De Troyer F. (2015). Parallel coordinates visualization of energy demand estimation in the early design stages. DS2BE. Brussels, 29-30 April 2015.

Miyamoto, A., **Nguyen Van, T**., De Troyer, F. (2014). The effect of parameters and its interrelationship in dynamic energy simulation. Architectural Engineering seminar. Leuven, 9 December 2014.

Nguyen Van, T. (2011). *Managing cost and quality in large scale housing projects via public partnerships*. Doctoral Seminars CAAD, Design & Building Methodology. Leuven, 15 February 2011.

Nguyen Van, T., De Troyer, F. (2011). *Including cost of pile foundation for high-rise buildings in soft soil condition from the early design decisions on - Case study in Mekong Delta, Vietnam*. ASRO seminar. Leuven, 14 December 2011.

Hoang Vi Minh, **Nguyen Van Tam**, Ngo Van Anh (2002), Small wood pile foundation for soft soil condition in Mekong Delta Area - Vietnam, Conference on Structure of Foundation on soft soil in Cantho city, Vietnam.

Tam NGUYEN VAN (NGUYỄN VĂN TÂM)

Education

PhD Student at Division of Architectural Engineering, Department of Architecture, Urbanism and Planning, KU Leuven, 2017.

M.Sc., Engineering in Construction, Engineering and Infrastructure Management (CEIM), Asian Institute of Technology (AIT), Thailand, 2009.

B.Sc., Civil Engineering for Rural Development, Cantho University, Vietnam, 1997.

Research areas

Life cycle cost; Life cycle assessment; Architectural Engineering; Optimization energy use and initial cost Large scale housing projects; Foundation in soft soil condition; Building material; Quality assessment in construction; Construction management; Project Financing and Project Performance; Occupational Safety and Health Management in Construction; Construction Law; Sustainable construction.

Teaching subjects

Construction engineering, Building material, Construction Machine, Construction structure experiment, integrated project planning and control, Information Technology in construction management and Soil mechanics.

Experiences

Construction Verify Structural test; Construction design: building, bridge and retaining wall and water treatment system design; Construction management; Project financial management, construction cost estimating; Specialist on Construction verify and consultant from 1998 to 2008; Landscape urbanism; Architecture urbanism.